Dissertation zur Erlangung des Doktorgrades
der Fakultät für Chemie und Pharmazie
der Ludwig-Maximilians-Universität München

The novel MKL1/2 dependent target gene myoferlin modulates expansion and senescence of hepatocellular carcinoma

Constanze Gloria Maria Mittermeier, geb. Hermanns
aus
Herdecke

2017

I Erklärung

Diese Dissertation wurde im Sinne von § 7 der Promotionsordnung vom 28. November 2011 von Herrn Prof. Dr. Thomas Gudermann betreut und von Herrn PD Dr. Dietmar Martin von der Fakultät für Chemie und Pharmazie vertreten.

Eidesstattliche Versicherung

Diese Dissertation wurde eigenständig und ohne unerlaubte Hilfe erarbeitet.

München, den 18.12.2017

.....

Constanze Mittermeier

Dissertation eingereicht am 24.10.2017

1. Gutachter: PD Dr. Dietmar Martin

2. Gutachter: Prof. Dr. Thomas Gudermann

Mündliche Prüfung am 14.12.2017

Table of Contents

1 Summary

The two homologous proteins Megakaryoblastic Leukemia 1 and 2 (MKL1 and MKL2 or MRTF-A and MRTF-B) are transcriptional coactivators of the transcription factor serum response factor (SRF) that are essential for fundamental biological processes like cell migration, cell proliferation, cell differentiation as well as actin cytoskeleton organization. Depletion of MKL1/2 was shown to reduce the proliferative, migratory and invasive capacity of HuH7 hepatocellular carcinoma (HCC) cells and also *in vivo* the HCC tumor growth of nude mice in a xenograft model was significantly reduced due to the systematic treatment of polyethylenimine (PEI)-complexed siRNA directed against MKL1 and MKL2 by inducing oncogene-induced senescence.

A DNA microarray analysis of MKL1/2 depleted HuH7 cells versus HuH7 control cells revealed several novel MKL1/2 dependent target genes that were potential mediators of the MKL1/2 dependent induction of oncogene-induced senescence. In this context, we identified the transmembrane protein myoferlin (MYOF) as a novel MKL1/2 and SRF dependent target gene responsible for the effects of MKL1/2 on the characteristics of tumor cells. We could show that depletion of MYOF in HCC cells resulted in reduced cell proliferation and cell invasion as well as the sustained activation and phosphorylation of the epidermal growth factor receptor (EGFR). As a consequence, the loss of MYOF also activated the Ras/Raf/MEK/ERK signaling pathway and finally ended up in senescence induction, revealed by β-galactosidase staining and the increased expression of the senescence messaging secretome factors CXCL10 and TNFSF10. In this work, we additionally provided evidence that the mRNA and protein expression of MYOF was increased *in vivo* in the premalignant nodule tissue and even stronger increased in the tumor tissue of mice conditionally expressing SRF-VP16 in hepatocytes in comparison to the non-tumorous control tissue showing no MYOF expression. Furthermore, we could confirm the results obtained *in vitro* in HCC cell lines also *ex vivo* in liver tumor cells derived from SRF-VP16 expressing mice and figured out that MYOF depletion also leads to the oncogene-induced senescence response by activating the EGFR and the Ras/Raf/MEK/ERK pathway.

In conclusion, in this thesis we pointed out that MYOF is a novel MKL1/2 dependent target gene that mediates the tumor inhibiting properties of an MKL1/2 knockdown by the induction of oncogene-induced senescence. This way, MYOF serves as a promising therapeutical target for HCC patients by a senescence inducing strategy.

2 Introduction

2.1 The transcription factor Serum Response Factor (SRF)

2.1.1 Structure and biological functions

Transcription factors are proteins that bind to DNA sequences and thereby control gene expression in response to intra- and extracellular signals. Well coordinated transcription requires transcription factors acting alone or in concert with coregulators, like coactivators or corepressors. The highly conserved Serum Response Factor (SRF) is a ubiquitously expressed transcription factor that belongs to the family of MADS-box proteins. The MADS-box itself, named after its founding members MCM1, Agamous, Deficiens and SRF, is a conserved structure motif in the DNA binding domain being characteristic for all proteins of the MADS-box family (Pellegrini et al., 1995). Since the N-terminus of the MADS-box is responsible for the specific DNA binding of SRF to the Serum Response Element (SRE) of target genes, the C-terminus enables the dimerization of two SRF monomers (Treisman, 1986 and Shore & Sharrocks, 1995). A schematic structure of the SRF protein containing the MADS-box and the transcription activation domain (TAD) is shown in Fig. 1.

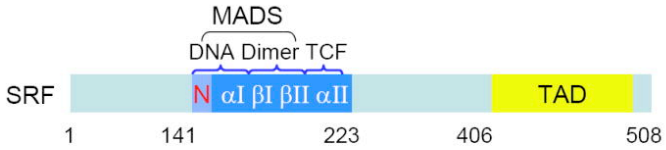

Figure 1: Schematic structure of human SRF. Shown are the MADS-box domain and the transcription activation domain (TAD) of the transcription factor SRF (Niu et al., 2007).

For control of transcription and induced expression of SRF dependent target genes SRF binds the DNA at the SRE or also named CArG box with the conserved palindromic $CC(A/T)_6GG$ consensus sequence that is found in many promoter regions of known SRF target genes (Treisman, 1986). This DNA consensus sequence is recognized by SRF and subsequently bound by an SRF homodimer (Treisman, 1986 and Sun et al., 2006). Recently, 160 different target genes directly regulated by SRF are found (Pipes et al., 2006). A majority of these target genes are so called immediate early genes (IEG) due to their rapid transcriptional activation by stimulation with serum or growth factors within only few minutes (Winkles, 1998). SRF regulates via its target genes essential biological processes in the cell,

like actin cytoskeleton organization, cell proliferation, migration and differentiation (Knoll & Nordheim, 2009 and Olson & Nordheim, 2010). Already well characterized and established SRF target genes are c-fos (Shaw et al., 1989), the connective tissue growth factor (CTGF) (Muehlich et al., 2007), integrin alpha-5 (Itga5) (Leitner et al., 2011 and Muehlich et al., 2012) and Transgelin (TAGLN/SM22) (Olson & Nordheim, 2010).

2.1.2 Signaling pathways of SRF activation

The induction of SRF activity occurs by two independent but in parallel proceeding signaling pathways involving the Ras/MAPK/TCF cascade as well as the Rho/actin signaling pathway (Fig. 2).

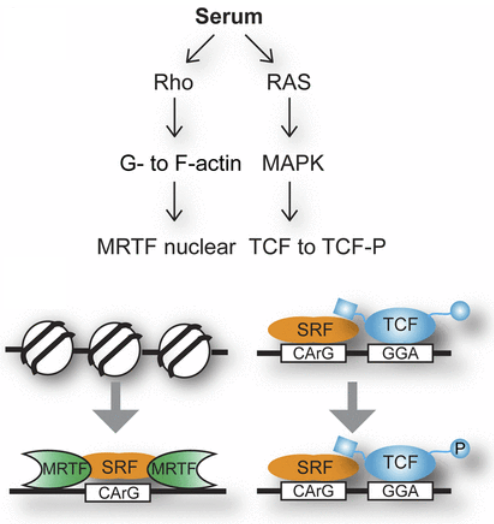

Figure 2: Model of SRF activation by two different pathways. SRF becomes activated upon serum stimulation resulting in activation of the Rho or Ras signaling pathway (Clark and Graves, 2014).

First, the ternary complex factor (TCF) dependent signaling pathway is activated by extracellular stimuli, like serum, lysophosphatidic acid (LPA) or growth factors. The subsequent activation of the small GTPase Ras then leads to phosphorylation and therefore activation of the mitogen activated protein kinases (MAPK). As a consequence, the TCFs were phosphorylated by the three MAPK subfamilies extracellular signal regulated kinase (ERK), c-Jun N-terminal kinase (JNK) and p38 (Whitmarsh et al., 1997). The activated TCFs consisting of Elk-1, SAP-1 and SAP-2/Net that all belong to a subgroup of the Ets family of transcription factors recognize and bind an Ets Binding Site (EBS) in proximity to a CArG box (Janknecht & Nordheim, 1993, Treisman, 1994 and Treisman, 1995). This way, TCFs bind

SRF and act as transcriptional coactivators for induction of target gene expression. The activation of SRF by the TCF-dependent signaling pathway is shown in Fig. 3.

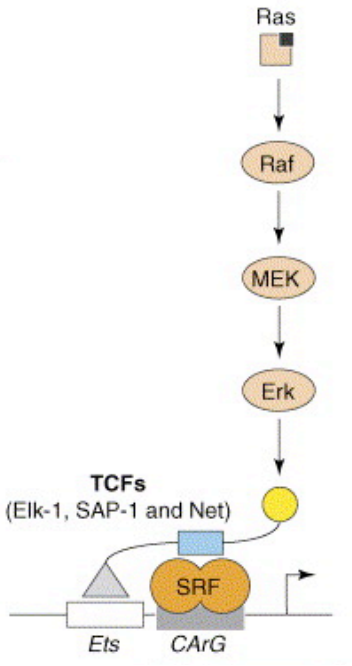

Figure 3: Model of the TCF-dependent SRF activation. TCFs were phosphorylated by the Ras/Raf/MAPK pathway and then activate SRF to trigger target gene expression (Posern & Treisman, 2006).

Second, the TCF-independent signaling pathway is also activated by extracellular stimuli, like serum, LPA or growth factors. This stimulation leads to activation of RhoA, a member of the Rho family of small GTPases resulting in altered actin dynamics (Hill et al., 1995 and Wang & Olson, 2004). In more detail, RhoA leads to an enhanced polymerization of unpolymerized globular G-actin monomers into the formation of polymerized filamentous F-actin. The decrease of G-actin in the cytoplasm delivers the transcriptional coactivator Megakaryoblastic Leukemia 1 (MKL1/MRTF-A) from bound G-actin resulting in nuclear translocation of MKL1. MKL1 itself subsequently binds SRF and activates it leading to target gene expression (Miralles et al., 2003 and Muehlich et al., 2008). This pathway shown in Fig. 4 regulates the activity of SRF and target gene induction also by the phosphorylation status of MKL1 in the nucleus. After phosphorylation of MKL1 by ERK1/2 G-actin binds to MKL1 that in consequence leads to nuclear export of MKL1 and therefore prevents activation of SRF and target genes (Muehlich et al., 2008).

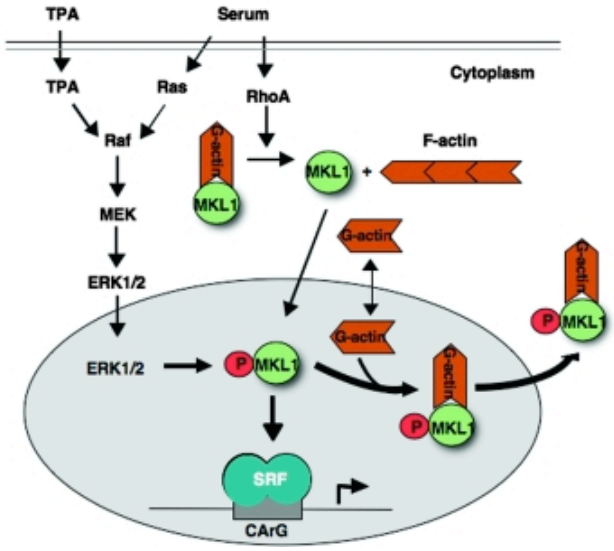

Figure 4: Model of SRF activation by MKL1 regulation. Activation of RhoA leads to an increased formation of F-actin and a decrease of G-actin that shuttles MKL1 into the nucleus where it binds and activates SRF. Inhibition of target gene expression is achieved by phosphorylation of MKL1 by ERK1/2 and the subsequent nuclear export of the phosphorylated MKL1 bound to G-actin (Muehlich et al., 2008).

2.2 The transcriptional coactivators Megakaryoblastic Leukemia 1 and 2 (MKL1 and MKL2)

2.2.1 Structure and biological functions

The two proteins Megakaryoblastic Leukemia 1 and 2 (MKL1 and MKL2) are transcriptional coactivators of the transcription factor serum response factor (SRF). Before identifying them myocardin that is specifically expressed in cardiac and smooth muscle cells was initially discovered by performing a screening to find cardiac-specific genes and thus, myocardin was described as transcriptional coactivator of SRF (Wang et al., 2001). Later in 2002, MKL1 and MKL2 were identified in mammalian species and due to its function as myocardin analoga they were also called myocardin related transcription factors A and B (MRTF-A/B) (Wang et al., 2002). In contrast to the cell type specific expression of myocardin, MKL1 and MKL2 are ubiquitously expressed proteins acting as transcriptional coactivators in a variety of different tissues (Du et al., 2004). As shown in Fig. 5 the functional domains within the proteins of the MRTF family, the cardiac and the smooth muscle isoform of myocardin, MRTF-A (MKL1) and MRTF-B (MKL2), are homologous and evolutionary conserved (Pipes et al., 2006 and Olson & Nordheim, 2010).

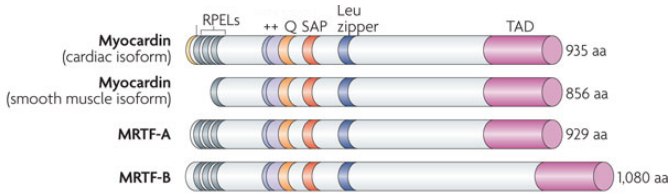

Figure 5: Homology of the functional domains within the proteins of the myocardin family. The structures and different domains of the two myocardin isoforms, MRTF-A (MKL1) and MRTF-B (MKL2) as well as the number of amino acids are shown (Olson & Nordheim, 2010).

Sharing the same functional regions in all proteins of the myocardin family (Fig. 5), the different domains will be described closer in the following exemplified for the MKL1 protein shown in Fig. 6. The RPEL domain located at the N-terminus of the protein consists of three distinct RPEL motifs and is named after its amino acid sequence of Arg-Pro-X-X-X-Glu-Leu (Miralles et al., 2003). This sequence in the proteins of the MRTF family serves as binding domain for monomeric G-actin thus maintaining MKL1 in unstimulated cells in the cytoplasm (Miralles et al., 2003 and Posern et al., 2004). The association of the transcriptional coactivators and their transcription factor SRF occurs at the basic region (B) and the glutamine-rich region (Q) (Wang et al., 2001 and Muehlich et al., 2008). Another important domain for the myocardin family is the SAP domain, named after SAF-A/B, Acinus and Pias, that is relevant for the interaction with other transcription factors (Pipes et al., 2006). It is suggested that the SAP domain is also involved in the regulation of apoptosis as well as chromosomal dynamics and DNA metabolism (Aravind & Koonin, 2000 and Wang et al., 2001). The conserved leucine zipper domain (LZ) mediates the homo- and heterodimerization of the members of the myocardin family (Wang et al., 2001 and Miralles et al., 2003). At the C-terminus myocardin and the MRTFs contain the transcriptional activation domain (TAD) that is required for the stimulation and activation of SRF activity (Cen at al., 2003).

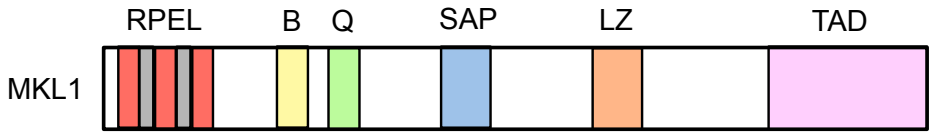

Figure 6: Schematic representation of the MKL1 structure. Shown are the RPEL domain, the basic region (B), the glutamine-rich region (Q) as well as the SAP domain and a leucine zipper region (LZ) of MKL1.

Looking at the biological function of MKL1 and MKL2 in the cell, both proteins function, as previously described, as transcriptional coactivators of SRF and activate by association with SRF in the nucleus target genes involved in essential biological processes, like cell growth or

cell differentiation (Pipes et al., 2006). This way, they act in an interface between two essential signaling pathways, the MAPK and the RhoA pathway, that are involved in tumorigenesis, described by a RhoA overexpression that was found in different tumors (Kohno et al., 2006). Another important role of MKL1 is its requirement for skeletal muscle differentiation and muscle growth (Selvaraj & Prywes, 2003). As much as known about the physiological and cellular processes MKL1 is involved in, the role of MKL1 and MKL2 in embryogenesis and development was also investigated by a great number of MKL1 and/or MKL2 knockout mice studies. Since a knockout of MKL1 mostly revealed viable and fertile mice, the female MKL1 knockout mice failed to nurse their offspring due to defects in the mammary gland epithelial cell differentiation affecting the milk ejection (Li et al., 2006 and Sun et al., 2006a). Further studies also showed that depletion of MKL1 in a small number of mice resulted in dead MKL1 null embryos because of cardiac abnormalities (Sun et al., 2006a). Another important outcome is that the megakaryocyte maturation and platelet formation is affected by a parallel knockout of both MKL1 and MKL2 and also of MKL1 alone displaying a reduced number of platelets and also a decreased amount of mature megakaryocytes (Cheng et al., 2009 and Smith et al., 2012). However, MKL2 depletion in mice always led to embryonic lethality due to cardiovascular effects and defects in the smooth muscle differentiation suggesting a crucial role for MKL2 in the development of mice (Oh et al., 2005). Medjkane et al. (2009) pointed out that the presence of MKL1 and MKL2 is necessary for tumor cell invasion and metastasis, because depletion of MKL1/2 in human breast carcinoma and mouse melanoma cells using specific siRNA eliminated cell adhesion, motility and invasion. In a more recent study of Hampl and colleagues MKL1 displayed also migratory as well as proliferative effects in hepatocellular carcinoma (HCC) cells monitored by several cell-based assays (Hampl et al., 2013). In further studies a very important result was obtained from HCC xenograft models in which human liver carcinoma cells were transplanted into nude mice and the developed tumors were treated with polyethylenimine (PEI)-complexed control or MKL1+2 siRNA. This depletion of MKL1 and MKL2 inhibited the tumor growth suggesting a role of evading tumorigenesis by MKL1 and MKL2 knockdown (Hampl et al., 2013).

2.2.2 The novel MKL1 binding partner Filamin A (FLNa)

In a recent study of Kircher and colleagues Filamin A (FLNa), a protein of the filamin family, was found to interact with MKL1 and to act as novel MKL1 binding partner (Kircher et al., 2015). The FLNa protein is a homodimer consisting of two large subunits, which form a V-shaped structure (van der Flier & Sonnenberg, 2001) since at each of the monomers an actin binding domain is located at the N-terminus (Gorlin et al., 1990). Whereas Filamins in general are actin-binding proteins that are essential for crosslinking of actin filaments and also for linking actin filaments to proteins localized in the cell membrane, FLNa specifically is the most potent protein among the filamin family for actin filament crosslinking underlined by the fact that only one FLNa homodimer per actin filament is sufficient for induction of actin-based gelation, the ability of FLNa for efficiently gathering actin filaments into a three-dimensional gel *in vitro* by crosslinking actin filaments (Hartwig et al., 1980; Bennett et al., 1984 and Ito et al., 1992). Since FLNa is a multifunctional protein acting on a variety of different proteins and therefore signaling complexes, the most noteworthy features of cells expressing FLNa are the providing of cell stability as well as the possibility of cell motility (Stossel et al., 2001 and Small et al., 2002). Confirming these properties, M2 cells lacking FLNa expression show an unstable surface and are not able to undergo locomotion (Cunningham et al., 1992 and Dai & Sheetz, 1999). M2 cells also display so-called blebs, a phenomenon that arises because the cell cortex is unable to withstand hydrostatic pressure within the cell and results from a weakened actin structure, because the blebs contain predominantly monomeric G-actin and not filamentous F-actin (Cunningham, 1995). There is also an increasing evidence for FLNa to be directly involved in cell signaling and transducing gene expression via an interaction of FLNa and its targets (Stossel et al., 2001). Referring to this, the filamins bind a variety of different molecules and thus 20 binding partners are known so far (Stossel et al., 2001). Several studies provide evidence that FLNa has an important role in the nucleus by directly interacting with transcription factors and nuclear proteins, like FOXC1 and proteins of the SMAD family as well as with the tumor suppressor BRCA1/2 (Sasaki et al., 2001; Yuan et al., 2001 and Berry et al., 2005). Due to its association with the RNA polymerase I FLNa is able to suppress the ribosomal RNA (rRNA) transcription (Deng et al., 2012). FLNa is also known to bind to Rho GTPases and their cofactors involved in the regulation of actin assembly and to play an important role in signal transduction by transducing stress signals to the actin cytoskeleton (Glogauer et al., 1998 and Bishop & Hall, 2000). Additionally, Kircher *et al.* found FLNa to directly interact with the transcriptional coactivator MKL1 in different cell lines proved by immunoprecipitation and showed the novel MKL1-FLNa complex by immunofluorescence (Kircher et al., 2015). Some functional studies also revealed a positive effect for FLNa presence on target gene expression and promoter activity, thus suggesting a role for FLNa in the activation of SRF by MKL1 as shown in Fig. 7.

Therefore, in the following the extended model of SRF and target gene activation described under 2.1.2 and the localization of MKL1 will be specified. Generally, the subcellular localization and the transcriptional activity of MKL1 is regulated by Rho/actin signaling whereas the actin sensitivity of SRF is mediated by the MKLs (Miralles et al., 2003). In unstimulated cells, like in NIH 3T3 fibroblasts, MKL1 is located in the cytoplasm and exists in a repressive complex bound to monomeric G-actin (Miralles et al., 2003 and Posern et al., 2004). After stimulation with serum or LPA, the G-actin monomers polymerize into filamentous F-actin resulting in the release of MKL1 from the G-actin-MKL1 complex and therefore in a translocation and accumulation of MKL1 in the nucleus where it can bind SRF and induce target gene expression (Miralles et al., 2003 and Vartiainen et al., 2007). Baarlink and his group additionally showed that the nuclear actin polymerization triggered by serum stimulation enhances SRF activation mediated by released MKL1, whereas another result of cell stimulation is the ERK1/2 dependent phosphorylation of MKL1 at serine 454 that serves as a stimulus for MKL1-G-actin binding (Muehlich et al., 2008 and Baarlink et al., 2013). Besides the existing repressive complex of MKL1 and G-actin also an activating MKL1-FLNa complex exists (Fig. 7) in which the bound FLNa impairs the MKL1 phosphorylation and enhances the formation of F-actin resulting in active SRF and further target gene expression (Kircher et al., 2015).

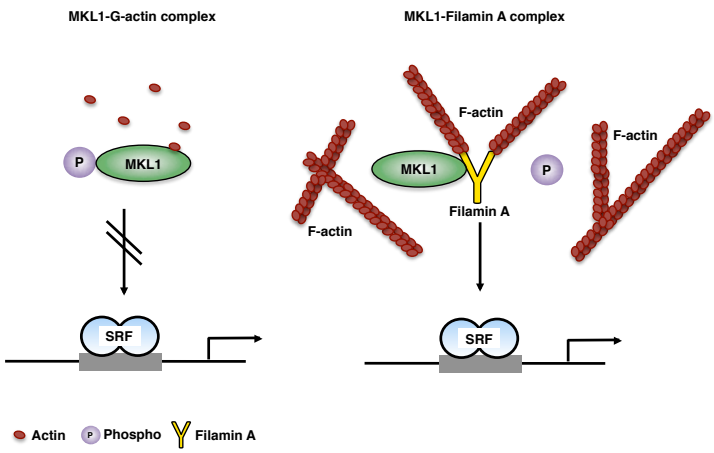

Figure 7: Model of the activating MKL1-FLNa complex. MKL1 is in a repressive state bound to G-actin (left) or in an activating state bound to FLNa (right) thereby impairing MKL1 phosphorylation and enhancing formation of F-actin (Kircher et al., 2015).

2.3 The novel MKL target gene myoferlin

2.3.1 Structure and biological functions

Myoferlin, abbreviated MYOF and also named Fer-1-like protein 3 (FER1L3), is a protein of the evolutionary conserved ferlin family of proteins. The first discovered member of the ferlin family is represented by dysferlin, a protein that was identified in patients with Miyoshi myopathy and limb girdle muscular dystrophy type 2B arising from diverse mutations in the dysferlin gene (Liu et al., 1998 and Weiler et al., 1999). A database and BLAST searching with the dysferlin sequence revealed a novel protein that was called myoferlin due to its high homology over nearly the whole length of the dysferlin gene and its strong preferential expression in cardiac and skeletal muscles (Davis et al., 2000). All proteins of the ferlin family, consisting of dysferlin, myoferlin, fer-1 and otoferlin, share a very similar structure and nearly the same functional domains. In Fig. 8 the schematic structure of MYOF with its essential domains is shown and described in greater detail in the following. Based on its structural properties and its single-pass transmembrane domain (TM), MYOF was characterized as type II transmembrane protein with an intracellular N-terminus and a C-terminal membrane-spanning domain (Davis et al., 2000). The large cytoplasmic domain consists of six C2 domains (A-F) that are known for playing a role in signal transduction and in the capability of Ca^{2+}, phospholipid and lipid bilayer binding and thus especially for involvement in calcium-mediated membrane fusion or membrane repair (Davletov & Sudhof, 1993). Another important domain of MYOF is the SH3 domain specifically recognizing prolin-rich amino acid regions and therefore interacting with tyrosine kinases and adaptor proteins and participating in signaling pathways (Yu et al., 1992).

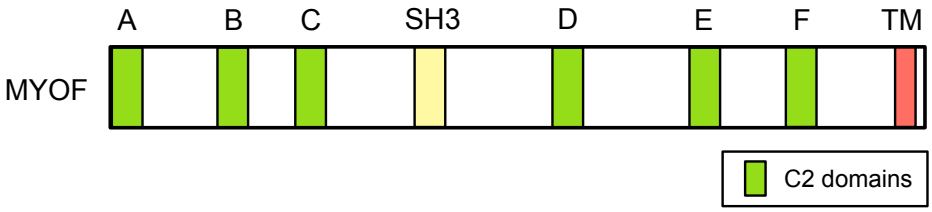

Figure 8: Schematic representation of the MYOF structure. The C2, SH3 and transmembrane (TM) domains of MYOF are shown.

Since the expression of MYOF was restricted to cardiac and skeletal muscle cells at the beginning of its discovery, several novel studies substantiate a broader MYOF expression also in other cell tissues and cell types, like endothelial and breast cancer cells (Bernatchez et al., 2007 and Eisenberg et al., 2011). Within the cell, it was shown that MYOF was

associated with the plasma membrane as well as with the nuclear membrane (Davis et al., 2000). On a cellular level, a potential modifying function of MYOF for muscular dystrophy and cardiomyopathy was assessed in two different mouse models with muscular dystrophy (Davis et al., 2000). Doherty and colleagues demonstrated convincingly a requirement of MYOF for normal myoblast fusion (Doherty et al., 2005). Therefore, they generated MYOF null mice exhibiting no alteration in fertility, viability and longevity but still showing a significantly smaller body mass compared to the wildtype control mice. Concerning the myoblasts, visible effects of MYOF loss were detected, namely the MYOF null mice revealed smaller muscles with strongly reduced mean myofiber size and MYOF null mice muscles additionally failed to regenerate completely after injury than wildtype mice did (Doherty et al., 2005). This data confirmed a crucial role for MYOF in the maturation of myotubes and also in the further formation of large myotubes arising from the myoblast fusion to multinucleate myotubes. Another fundamental impact of MYOF is its influence on the stability and function of diverse receptor tyrosine kinases. Thus, silencing of MYOF in vascular endothelial cells was shown to result in instability and also rapid degradation of the vascular endothelial growth factor receptor 2 (VEGFR-2) (Bernatchez at al., 2007). Demonbreun and colleagues demonstrated a decline in insulin growth factor 1 receptor (IGFR) and a receptor accumulation in vesicles upon MYOF knockdown, whereas Yu and colleagues also reported an effect of MYOF on the angiogenic tyrosine kinase receptor (Tie-2) (Demonbreun et al., 2010 and Yu et al., 2011). Beside these important cellular characteristics, MYOF takes also part in a variety of essential cellular processes, such as endocytosis, membrane repair and vesicular transport (Bernatchez et al., 2009 and Sharma et al., 2010).

2.3.2 MYOF and its role in cancer

Regarding the Human Protein Atlas and the publications of the last years, a strong MYOF expression in different cancer types, like breast, ovarian and liver cancer for example, was observed (Adam et al., 2003; Labhart et al., 2005 and Ponten et al., 2008). Beyond the direct effect of MYOF on cancer cells by its strong upregulation it is indispensible to give a deeper insight into the association of MYOF and cancer and thus to additionally have a look at the more indirect involvement of MYOF by showing its cancer cell specific attributes. One very important characteristic of cancer cells is their invasive capacity that is affected by MYOF expression compellingly demonstrated by Eisenberg et al. (2011). They used the breast cancer cell line MDA-MB 231 and compared the invasive behavior of control cells and cells with a stable lentiviral-based knockdown of MYOF achieving the result that the MYOF depleted cells revealed a strongly reduced invasivity compared to the control cells

(Eisenberg et al., 2011). Thus, MYOF seems to play an important role in promoting the invasive behavior of cancer cells. The MDA-MB 231 breast cancer cells likewise exhibited a more epithelial-like morphology upon MYOF depletion than the fibroblastic shape and more mesenchymal appearance of the control cells, referring to a mesenchymal-epithelial transition (MET) in accordance to the known epithelial-mesenchymal transition (EMT) known as characteristic for tumor cells (Li et al., 2012). A good correlation between the visible morphologic shift and the downregulation of the corresponding EMT markers, like fibronectin and vimentin, as well as the upregulation of the epithelial marker E-cadherin at the molecular level in MYOF knockdown cells was shown (Li et al., 2012). In addition, silencing of MYOF via intratumoral injections of MYOF siRNA decreased the tumor growth of mouse Lewis Lung carcinoma (LLC) cells *in vivo* (Leung et al., 2013). There was also evidence for MYOF dependent regulation of cell proliferation because depletion of MYOF decreased the proliferation rate of the LCC tumors *in vivo* as well as *in vitro* in cultured LCC cells (Leung et al., 2013). Recently in 2013, MYOF was initially characterized as a specific, negative regulator of the epidermal growth factor receptor (EGFR) in human breast cancer cells (Turtoi et al., 2013). In the absence of myoferlin, the EGFR gets activated due to a block of the phosphorylated EGFR degradation and therefore activates the EGFR signaling pathway leading to inhibition of migration of the breast cancer cells (Turtoi et al., 2013). Concluding, MYOF is strongly overexpressed in a variety of different cancer cell lines and plays an important role in mediating cancer cell specific properties. Thus, it seems very indispensable and promising to investigate the underlying mechanisms of MYOF acting on tumorigenesis and MYOF itself serves as a potential therapeutic target to prevent cancer development and progression.

2.4 Senescence

2.4.1 Hallmarks of cancer

More than 100 different types of cancers exist and the developed tumors can be found in a plenty of specific organs, giving rise to the need of a better understanding of the process of tumorigenesis and the progressive transformation of normal cells into tumorigenic cells. In contrast to somatic cells, cancer cells display a multitude of alterations on the histological level visible under the microscope as well as on the cellular level. This way, cancer cells often have an enlarged and irregular shaped nucleus or actually multiple nuclei accompanied by smaller amounts of cytoplasm and the nucleoli are more prominent

(Hanahan & Weinberg, 2000 and Baba & Câtoi, 2007). Besides the morphological changes, a malignant cell is amongst others characterized by prolonged proliferation, uncontrolled mitotic divisions, a tissue invasive and metastatic behavior and also an acceleration of the cell cycle due to circumventing the cell cycle restriction points (Hanahan & Weinberg, 2000 and Baba & Câtoi, 2007). For a better understanding and classification of cancer cells and the process of a malignant cell transformation, Hanahan and Weinberg defined a variety of distinct capabilities that tumorigenic cells acquire as the six hallmarks of cancer shown in Fig. 9 (Hanahan & Weinberg, 2000). In 2011, they expanded their model by two further hallmarks, the reprogramming of energy metabolism and the evading of immune destruction of transforming cells (Hanahan & Weinberg, 2011). These principals shared by all cancers impressingly demonstrate that cells develop several tumor evasion strategies that are circumvented by tumor cells resulting in metastatic cancer. The fact that tumor development occurs relatively rare in a human lifespan compared to the enormous number of cells in the human body, suggests also for very effective cancer evading strategies. One very prominent mechanism is the apoptosis pathway, a naturally occurring programmed cell death that influences the malignant phenotype (Wyllie et al., 1980 and Lowe & Lin, 2000). Due to the complexity of tumor diseases and their development, even more programs for bypassing tumorigenesis have to exist. In contrast to apoptosis, the non-apoptotic form of programmed cell death is represented by cellular senescence, a mechanism of cell cycle arrest described in greater detail in the following chapter (Wynford-Thomas, 1999).

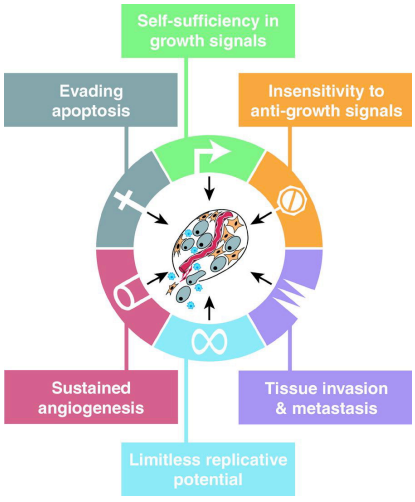

Figure 9: Hallmarks of cancer. The six acquired features of cancer cells are shown (Hanahan & Weinberg, 2000).

2.4.2 Cellular senescence

The word senescence goes back to *senex*, the latin origin that means “old man” or “old age” and therefore is used interchangeably with ageing. In this context, the term cellular senescence was initially described in 1961 by Hayflick and Moorhead pointing out that normal somatic cells have a limited ability to proliferate in culture and thus a finite number of replicative cycles (Hayflick & Moorhead, 1961 and Hayflick, 1964). The so-called Hayflick limit therefore says that normal mitotic cells undergo only approximately 50 cell divisions before they become senescent and die. Among the limited life span of human cells, three phases of cell growth in a cell’s life are described. Phase one is characterized as the primary culture, whereas phase two is defined as the period of proliferation and exponential replication of the subcultivated cells. At least, cells reach phase three specified by decreased cell growth and cell division and remain in this senescent state until they die (Hayflick & Moorhead, 1961). Hayflick and colleagues also showed that the non-dividing cells remained viable and metabolically active, but failed to proliferate (Hayflick & Moorhead, 1961). The initially discovered underlying molecular mechanism of cellular senescence was the phenomenon of telomere shortening explaining the ceased division of cells in culture (Harley et al., 1990 and Harley, 1991). As depicted in Fig. 10, telomeres, the characteristic repetitive DNA sequences at the end of chromosomes, were shortened with each cell doubling resulting in the loss of telomeric DNA and a threshold telomere length causing senescence, by this reason also termed replicative senescence. This replication end problem naturally occurs due to the inability of the DNA polymerase to replicate the lagging strand of the DNA in the 3’ to 5’ direction (Harley et al., 1990 and D’Adda di Fagagna et al., 2004). The telomere shortening can be efficiently circumvented by the enzyme named telomerase exhibiting a reverse transcriptase activity that was discovered for the first time in 1985 (Greider & Blackburn, 1985; Greider & Blackburn, 1987 and Lingner et al., 1997). Telomerases are predominantly active in highly proliferative cells, like stem cells or germline cells and a majority of cancer cells, since they are not or only modestly expressed in most normal somatic cells explaining why the telomerase activity in these cells is only low (Wright et al., 1996 and Shay & Bacchetti, 1997). The cellular function of the telomerase is the elongation of the telomers by *de novo* synthesis of telomeric DNA and its addition directly to the chromosome ends counteracting the telomere shortening and senescence induction (Greider & Blackburn, 1987 and Collins & Mitchell, 2002). Mechanistically, an RNA component associated with the reverse transcription subunit of the telomerase serves as template for the extending of the telomeric DNA strand (D’Adda di Fagagna et al., 2004). In 1998, Bodnar and colleagues introduced a telomerase into normal human epithelial cells and fibroblasts and provided evidence for the concept of antagonizing reduction of telomere length and entering senescence by telomerase activity displayed by an extension of life-span

in the telomerase expressing cells due to telomere lengthening (Bodnar et al., 1998). The regulation of telomere shortening and telomere elongation depending on the telomerase activity and the resulting fate of different cell types is illustrated in Fig. 10.

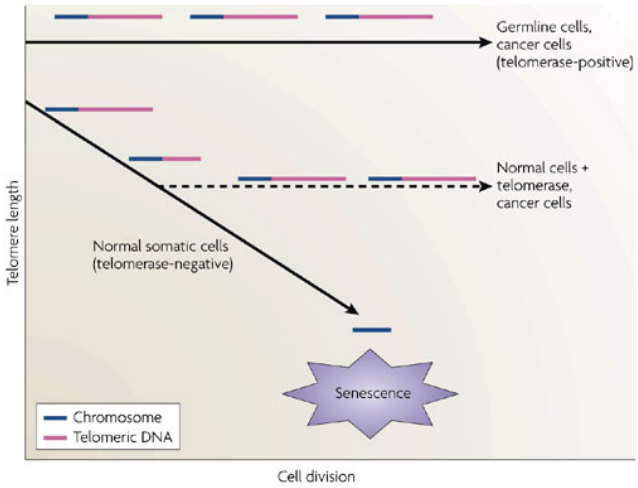

Figure 10: Telomerase-dependent cellular senescence. Telomeres (pink) are located at the end of each chromosome (blue) in order to protect them. Since germline cells and many cancer cells express a telomerase and thus telomere length is maintained, normal somatic cells mostly lack the expression of a telomerase resulting in shortened telomeres and therefore in senescence (Campisi & D'Adda di Fagagna, 2007).

Besides the telomerase-dependent replicative senescence, the irreversible growth arrest of cultured cells can additionally arise by various stress stimuli and is thus referred to as stress-induced premature senescence (SIPS), whereas the term premature is due to the fact that the stress-induced senescence occurs prior to the state at which it is induced by telomere shortening (Collado & Serrano, 2006 and Kuilman et al., 2010). It was shown that oxidative stress induced a proliferation arrest in cultured human cells and that this type of senescence results from inadequate culturing conditions, such as abnormal nutrient and growth factor concentrations (Packer & Fuehr, 1977; Yuan et al., 1995 and Sherr & DePinho, 2000). In agreement with these findings, it is also reported that an activation of premature senescence independently of telomere shortening senescence also occurs in mouse cells that have longer telomeres than humans and that express telomerases (Kipling & Cooke, 1990 and Prowse & Greider, 1995). Confirming this, several studies also revealed that mouse embryonic fibroblast (MEF) cells also undergo senescence after a restricted number of passages in culture and that an elongated life-span of cells is only accomplished by culturing cells in serum-free medium and a defined composition of growth factors as well as by culturing under physiological conditions (Loo et al., 1987 and Parrinello et al., 2003). Concluding, immortalization of cells requires also optimal culture conditions and not only telomere maintenance (Ramirez et al., 2001 and Herbert et al., 2002).

2.4.3 Oncogene-induced senescence (OIS)

In contrast to the replicative and premature senescence, in 1997 a novel form of senescence induction, known as oncogene-induced senescence (OIS), was described by Serrano and colleagues (Serrano et al., 1997). This oncogene-induced senescence reflected by a cell cycle arrest was shown to be provoked by the overexpression of active forms of oncogenes or by the loss of anti-mitogenic tumor suppressor genes (Braig et al., 2005; Chen et al., 2005 and Michaloglou et al., 2005). The first evidence for the existence of OIS was provided by the group of Serrano demonstrating that the overexpression of an active form of H-Ras (H-Ras^{V12}) resulted in a senescent like growth and cell cycle arrest when introduced into normal human fibroblasts that were accompanied by an upregulation of the tumor suppressor proteins p16^{Ink4a}, p53 and p21 (Serrano et al., 1997). In addition, the overexpression of not only oncogenic H-Ras but also of the oncogenic versions of the members of the Ras signaling pathway, like Raf, Mek and Braf, caused an oncogene-induced senescence response (Lin et al., 1998; Zhu et al., 1998 and Michaloglou et al., 2005). The fact that normal cells respond to the activation of a variety of oncogenes by undergoing senescence is underscored by studies in 2001, where some rodent cells are not able to replicatively senesce in serum-free medium suggesting that an excessive mitogenic stimulation is required for their senescence (Mathon et al., 2001 and Tang et al., 2001). The multitude of mitogenic signals is also shown in consideration of the fact that about 50 oncogenes are known that are able to induce oncogene-induced senescence (Gorgoulis & Halazonetis, 2010). A hallmark in the field of oncogene-induced senescence was published by Michaloglou and colleagues in 2005, when they figured out that benign naevi in human skin contain cells expressing oncogenic BRAF (BRAF^{E600}) and are senescent (Michaloglou et al., 2005). They pointed out that the sustained expression of the oncogenic BRAF^{E600} in human melanocytes resulted in a senescence-like phenotype exhibiting a stable growth arrest, the induction of p16^{Ink4a} and a senescence-associated β-galactosidase (SA-β-Gal) activity, explaining the phenomenon that naevi normally remain in a growth arrested state for a long time and only few of them progress into malignant melanoma (Bennett, 2003 and Michaloglou et al., 2005). This way oncogene-induced senescence serves as tumor suppressor mechanism *in vivo*. Several studies also attached importance to the *in vivo* relevance of OIS occurring during the early stages of tumorigenesis both in mice and in humans indicating that oncogene-induced senescence maintains the tumor in a premalignant, non-aggressive state and therefore restricts the further growth of oncogenically stressed cells, whereas cells lacking OIS progress to a malignant state (Braig et al., 2005; Collado et al., 2005 and Collado & Serrano, 2010).

Pointing out the delimitation of the oncogene-induced senescence to the replicative senescence, the overexpression of the human telomerase catalytic subunit (hTERT) in

normal human lung fibroblasts revealed no bypassing of senescence, confirming its independence from telomere shortening (Wei et al., 1999).
This way, the concept of oncogene-induced senescence emerged as a potential tumor suppressor mechanism depending on different effector mechanisms and several pathways are involved in, described in more detail in the following section.

2.4.4 Pathways affected by senescence

The complexity of senescence is driven by multiple oncogenic and senescence-activating pathways and a number of senescence triggers and various stimuli. The variety of proteins involved in senescence induction can be distinguished in those that are oncogenes itself and those that act upstream or downstream of the oncogenes. As depicted in Fig. 11, the shown pathways are leading to senescence when they are aberrantly activated, since the oncogenes and tumor suppressor genes shown in red, like Ras, Raf, PTEN or Akt, directly induce sensescence when they are mutated. The proteins functioning upstream and therefore controlling oncogenes are the phosphatase and tensin homolog (PTEN), von Hippel-Lindau (VHL), neurofibromin 1 (NF1) and the retinoblastoma (Rb) protein, which activity is necessary to prevent the induction of oncogene-induced senescence (Collado & Serrano, 2010). On the other hand, there are the proteins p53, INK4a and ARF that only inducibly function when the oncogenic signaling is activated and that way they all act downstream of oncogenes (Collado & Serrano, 2010). Several studies revealed the involvement of many different factors playing a crucial role in senescence activation *in vitro* and *in vivo* and among the mostly described and best characterized role of p53 or p16/Rb, also the loss of the VHL or of PTEN was shown to trigger senescence (Young et al., 2008 and Alimonti et al., 2010).

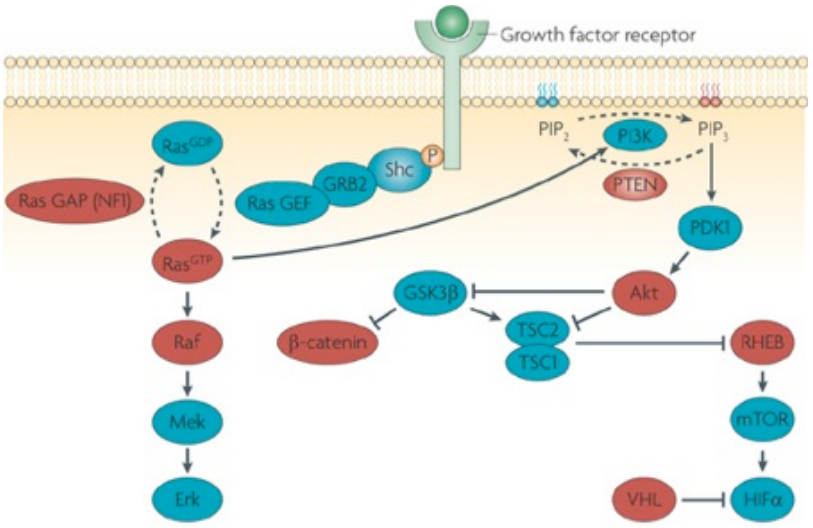

Figure 11: Pathways of oncogene-induced senescence. The pathways leading to induced senescence when they are activated are shown, since the tumor suppressors and oncogenes are red and the effector and substrate proteins are blue (Collado & Serrano, 2010).

Having a look at the multitude of studies on oncogene-induced senescence, the one hallmark and common feature shared by all cells undergoing senescence is the involvement of the p53 and p16/Rb pathways (Ben-Porath & Weinberg, 2005 and Campisi, 2005). All described pathways by which the oncogenic stimuli are signaled often activate p53 and nearly all of them converge in the activation of the cyclin dependent kinase (CDK) inhibitors, such as p15, p16, p21 and p27 (Campisi & D'Adda di Fagagna, 2007). The INK4A/ARF locus is under physiological conditions only expressed at low levels in most tissues of young organisms but becomes activated with ageing (Krishnamurthy et al., 2004). These two key tumor suppressors were also shown to be responsible for a cell cycle arrest and to be upregulated in oncogenically stressed cells, since INK4A activates proteins of the Rb family whereas ARF activates p53 (Lowe et al., 2004). As shown in Fig. 12, in the following a more detailed description of the two most essential pathways inducing senescence is given. Firstly, for the p53 pathway Serrano and colleagues postulated 20 years ago an increased transcriptional activity of the tumor suppressor p53 upon accumulation of cell doublings and stress stimuli (Serrano et al., 1997). The stability and expression levels of the tumor suppressor p53 are regulated by ARF via its inactivation of the p53-degrading E3 ubiquitin protein ligase Mdm2/Hdm2 disabling the ubiquitinylation and therefore forcing the activation of p53 (Kim & Sharpless, 2006). ARF itself becomes activated by senescence inducing signals and then blocks the Mdm2/Hdm2 mediated p53 degradation (Levine & Oren, 2009). In consequence, p53 activates its transcriptional target, the CDK inhibitor protein p21 that leads to the senescence response (Brown et al., 1997). In accordance to the senescence induction upon p21 activation and its accumulation in senescent cells, a loss of p21 was

shown to result in life-span extension (Tahara et al., 1995 and Brown et al., 1997). p21 additionally inhibits the cyclin E/CDK2 complex and thus p16 and p21 act in concert to ensure that Rb becomes not phosphorylated indicating a crosslink between the p53 and the second important p16/Rb pathway (Serrano et al., 1997). Already in 1998, the p16/Rb or also termed Raf/MEK/ERK pathway downstream of the small GTPase Ras was revealed as the most relevant pathway for senescence induction (Lin et al., 1998 and Zhu et al., 1998). The CDK inhibitor protein $p16^{Ink4a}$ inhibits CDK4/6 by binding and therefore inhibiting their kinase activity and since implicated in the regulation of the G1 to S phase transition, activated $p16^{Ink4a}$ forces a G1 cell cycle arrest (Hara et al., 1996 and Serrano et al., 1997). Several studies also revealed remarkably increased levels of $p16^{Ink4a}$ RNA and protein levels when normal human fibroblasts underwent senescence (Hara et al., 1996 and Serrano et al., 1997). These highly overexpressed $p16^{Ink4a}$ levels prevent the phosphorylation of Rb and this way contribute to the Rb maintenance in its activated, hypophosphorylated state serving as crucial component for induction of senescence (Futreal & Barrett, 1991 and Chicas et al., 2010). Consequently, the hypophosphorylated form of Rb associates with the transcription factor E2F and inhibits the transcription of its target genes cyclin A and cyclin E which are required for the G1 to S phase transition and thus results in senescence (Serrano et al., 1997 and Burkhart & Sage, 2008). Summing up, both pathways can proceed independently or interact with each other at different stages for an alteration of the cell cycle progression. The contribution of mechanisms that ultimately lead to senescence depends on the cell strain and may depend on the cell type as well as on the conditions.

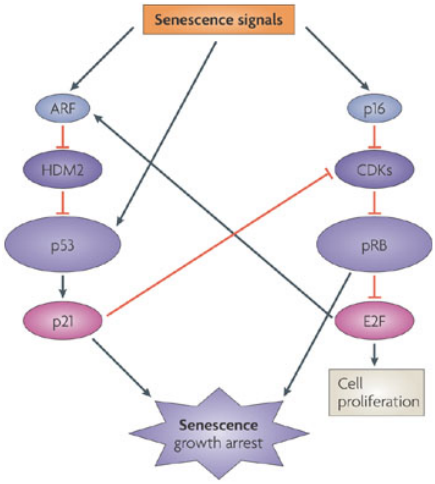

Figure 12: Senescence controlled by the p53 and p16/Rb pathway. Senescence signals trigger the ARF pathway and thereby active p53 or the p16/Rb pathway leading to a growth arrest designated as senescence (Campisi & D'Adda di Fagagna, 2007).

2.5 Hepatocellular carcinoma (HCC)

The hepatocellular carcinoma (HCC) is a malignant cancer, directly developed from healthy liver cells, and the most common type of liver cancer as well as the fifth most common cancer worldwide, representing 7 % of all cancers in the world (Jemal et al., 2011 and He et al., 2015). Since the 1980s the HCC's incidence has significantly increased and also in the western countries additionally to the developing countries an increasing incidence was documented (Jemal et al., 2011 and Binder-Fouard et al., 2014). With 745 000 registered deaths per year HCC is the second common cause of cancer deaths worldwide (Jemal et al., 2011 and Ferlay et al., 2015). HCC is more common in the male population than in the female one, with a ratio of 4:1 and is a result of hepatitis B and hepatitis C viral infections, chronic alcohol consumption, liver cirrhosis as well as alfatoxin-contaminated food in Asian and African countries, whereas HCC arises in the developed countries to a greater extend from type 2 diabetes and obesity, metabolic disorders and non-alcoholic fatty liver diseases (NAFLD) (Farazi & DePinho, 2006; Yang et al., 2015; Reeves et al., 2016 and Trojan et al., 2016). Despite its rising incidence and its role as one of the most predominant malignancies, the reasons for HCC development are far from being fully understood and the underlying mechanisms driving the conversion of healthy hepatic cells into malignant tumor cells are still nebulous. Clarifying the underlying mechanisms turned out to be very complicated due to the formation of HCC being a complex and multistep process that involves several different accumulations of genetic as well as epigenetic alterations in important regulatory genes and the deregulation of multiple signaling pathways. Since the genetic changes of the cell are irreversible, the epigenetic changes, like DNA methylations or histone modifications that are attributed to initiation and progression of HCC by enhancing proliferation, invasion etc. are reversible (Ma et al., 2014). Therefore the epigenetic mechanisms open up the development of novel therapeutic biomarkers and drugs that reverse the epigenetic alterations serve as promising target for HCC treatment.

Regarding all these described facts, the molecular mechanisms underlying the HCC formation remain to be enlightened and it also remains to be investigated how tumorigenesis and especially the development and progression of HCC can be efficiently limited and which molecules or proteins serve as promising therapeutic targets.

3 Aim of the thesis

In previous studies of our group we could show that MKL1/2 depletion inhibits hepatocellular carcinoma (HCC) xenograft growth by inducing oncogene-induced senescence (OIS) (Hampl et al., 2013). For further insights into the mechanism of HCC regression and senescence induction, the aim of this thesis was to search for MKL1/2 dependent target genes that mediate the effect of MKL1/2. Therefore, a microarray analysis with HuH7 cells stably expressing a control shRNA and HuH7 cells stably expressing MKL1/2 shRNA (MKL1/2 KD) was performed. Taken a threshold at the 2.5-fold reduced expression of the MKL1/2 KD cells compared to the control cells, we identified 8 MKL1/2 dependent target genes, amongst those 2 of them, Transgelin/SM22 and myosin heavy chain 9 (MYH9), were already known. The other 6 novel identified genes were glioma pathogenesis-related 1 **(**GLIPR1), calponin 1 (CNN1), transforming growth factor beta 1 (TGFß1), vestigial-like family member 3 (VGLL3), microtubule-associated protein 1B (MAP1B) and myoferlin (MYOF). These genes, except for VGLL3, were also downregulated *in vivo* in a xenograft model upon treatment of the mice with MKL1+2 siRNA.

Based on these findings, the first aim of this thesis was to validate the MKL1/2 dependency of the above mentioned target genes and to characterize their regulation by the Rho/actin signaling pathway in different HCC cell lines.

The second issue to address in this thesis was the dependency of the novel target genes on Filamin A (FLNa), the newly identified binding partner of MKL1 (Kircher et al., 2015) and the relevance of FLNa for target gene expression.

Finally, the third aim was to characterize the novel MKL target gene myoferlin regarding its involvement in tumor development and senescence induction in hepatocellular carcinoma cell lines and its significance as potential therapeutic target in HCC patients.

4 Materials

4.1 Cell culture

4.1.1 Cell lines

Table 1: Cell lines and their culture medium

cell line	origin / cell type	culture medium	provider
A7	human melanoma cell line stably expressing FLNa	MEM	Prof. Thomas P. Stossel, Harvard Medical School, Boston, MA, USA
HEK293T	human embryonic kidney cell line	DMEM	Anna-Lena Forst, Ludwig-Maximilians-University Munich, Munich, Germany
HepG2	human hepatocellular carcinoma cell line	RPMI	Dr. Stephan Singer, Ruprecht-Karls-University Heidelberg, Heidelberg, Germany
HepG2 MLC	human hepatocellular carcinoma cell line with empty vector	RPMI	Dr. Scott Lowe, Cold Spring Harbor, New York, NY, USA
HepG2 shRNA DLC1	human hepatocellular carcinoma cell line with stable DLC1 knockdown	RPMI	Dr. Scott Lowe, Cold Spring Harbor, New York, NY, USA
HLF	human hepatocellular carcinoma cell line	RPMI	Dr. Stephan Singer, Ruprecht-Karls-University Heidelberg, Heidelberg, Germany
HuH6	human hepatocellular carcinoma cell line	DMEM	Dr. Stephan Singer, Ruprecht-Karls-University Heidelberg, Heidelberg, Germany Heidelberg, Germany
HuH7	human hepatocellular carcinoma cell line	DMEM	Dr. Stephan Singer, Ruprecht-Karls-University Heidelberg, Heidelberg, Germany
LT	liver tumor cells derived from SRF-VP16 expressing mice	DMEM	Prof. Alfred Nordheim, Eberhard Karls university Tuebingen, Tuebingen, Germany
M2	human melanoma cell line lacking expression of FLNa	MEM	Prof. Thomas P. Stossel, Harvard Medical School, Boston, MA, USA
MDA-MB 468	human breast carcinoma cell line	DMEM	Dr. Ramon Parsons, Mount Sinai Hospital, New York, NY, USA
NIH 3T3	mouse embryonic fibroblast cell line	DMEM	ATCC, Wesel, Germany

4.1.2 Cell culture media

Table 2: Cell culture media and their supplements

medium	supplement	manufacturer
DMEM (Dulbecco's Modified Eagle's Medium)	10 % (v/v) FBS 5 % (v/v) penicillin/streptomycin	Sigma-Aldrich, Taufkirchen, Germany
MEM (Minimum Essential Medium)	10 % (v/v) FBS 5 % (v/v) penicillin/streptomycin	Sigma-Aldrich, Taufkirchen, Germany
Opti-MEM	/	Gibco® Invitrogen, Karlsruhe, Germany
RPMI (RPMI 1640 medium)	10 % (v/v) FBS 5 % (v/v) penicillin/streptomycin	Sigma-Aldrich, Taufkirchen, Germany

4.1.3 Transfection reagents

Table 3: Transfection reagents

reagent	manufacturer
GenJet™ DNA In Vitro Transfection Reagent	SignaGen Laboratories, Rockville, USA
Lipofectamine® 2000 Reagent	Invitrogen, Karlsruhe, Germany
Lipofectamine® RNAiMAX™ Reagent	Invitrogen, Karlsruhe, Germany

4.2 Antibodies

4.2.1 Primary antibodies for immunoblotting

Primary antibodies were diluted as indicated in TBS-T and enriched with a spatula tip BSA and a 2 % sodium azide solution (0.02 % final concentration) for conservation.

Table 4: Primary antibodies used for immunoblotting and their dilution

antibody	dilution	manufacturer
anti-EGFR (rabbit)	1:500	Cell Signaling Technology, Danvers, MA, USA
anti-Erk1/2 (p44/42 MAPK) (rabbit)	1:10000	Cell Signaling Technology, Danvers, MA, USA
anti-GAPDH (rabbit)	1:1000	Sigma-Aldrich, Taufkirchen, Germany
anti-GLIPR1 (rabbit)	1:500	Thermo Fisher Scientific, Schwerte, Germany

anti-HA (3F10) (mouse)	1:1000	Santa Cruz Biotechnology, Santa Cruz, CA, USA
anti-HSP90 (mouse)	1:500	Santa Cruz Biotechnology, Heidelberg, Germany
anti-MKL1 (rabbit)	1:500	*Muehlich et al., 2008*
anti-MKL2 (rabbit)	1:500	*Muehlich et al., 2008*
anti-Myoferlin (rabbit)	1:250	Sigma-Aldrich, Taufkirchen, Germany
anti-$p16^{INK4a}$ (goat)	1:250	R&D Systems, Wiesbaden, Germany
anti-phospho EGFR (Tyr1173) (rabbit)	1:1000	Cell Signaling Technology, Danvers, MA, USA
anti-phospho-p44/42 MAPK (Erk1/2) (Thr202/Tyr204) (rabbit)	1:1000	Cell Signaling Technology, Danvers, MA, USA
anti-pRb (mouse)	1:500	BD Biosciences, Heidelberg, Germany
anti-Ras (mouse)	1:500	Cell Signaling Technology, Danvers, MA, USA
anti-SM22 (rabbit)	1:1000	GeneTex, Inc., Irvine, CA, USA
anti-VP16 (rabbit)	1:300	Abcam, Cambridge, UK
monoclonal Anti-Flag® M2 (mouse)	1:1000	Sigma-Aldrich, Taufkirchen, Germany

4.2.2 Secondary antibodies for immunoblotting

Table 5: Secondary antibodies used for immunoblotting and their dilution

antibody	dilution (in TBS-T)	manufacturer
anti-goat IgG, HRP-linked antibody	1:50000	Santa Cruz Biotechnology, Santa Cruz, CA, USA
anti-mouse IgG, HRP-linked antibody	1:10000	Cell Signaling Technology, Frankfurt, Germany
anti-rabbit IgG, HRP-linked antibody	1:10000	Cell Signaling Technology, Frankfurt, Germany

4.2.3 Antibodies for ChIP assay

Table 6: Antibodies used for pulldown in ChIP assay

antibody	manufacturer
anti-FLNa (mouse)	Merck Millipore, Darmstadt, Germany
anti-MKL1 (goat)	Santa Cruz Biotechnology, Santa Cruz, CA, USA

4.3 Nucleic acids

4.3.1 Plasmids

Table 7: Plasmids and their expressing vectors

plasmid DNA	vector	provider
EGFR-GFP	pEGFP-N1	Prof. Alexander Sorkin, University of Pittsburgh, PA, USA
Flag GFP Dia1 ct (mDiact)	pEF	Prof. Guido Posern, Martin Luther university, Halle, Germany
Mig6 (pCMV-Flag gene 33)	pCMV5	Prof. John Kyriakis, Woburn, MA, USA
Myc-FLNa wt	pcDNA 3	Prof. John Blenis, Weill Cornell Medical College, New York, NY, USA
Myoferlin promoter 200bp	pGL2	Prof. Elizabeth M. McNally, Northwestern university, Chicago, IL, USA
Myoferlin promoter 400bp	pGL2	Prof. Elizabeth M. McNally, Northwestern university, Chicago, IL, USA
Myoferlin promoter 500bp	pGL2	Prof. Elizabeth M. McNally, Northwestern university, Chicago, IL, USA
Myoferlin promoter 900bp	pGL2	Prof. Elizabeth M. McNally, Northwestern university, Chicago, IL, USA
Myoferlin promoter 1500bp	pGL2	Prof. Elizabeth M. McNally, Northwestern university, Chicago, IL, USA
Myoferlin promoter Δ304-363 bp	pGL2	*Hermanns et al., 2017*
P3 x Flag MKL1 N100	pCin4	Prof. Ron Prywes, Columbia University New York, NY, USA
P3 x Flag MKL1 S454A	pCin4	Prof. Ron Prywes, Columbia University New York, NY, USA
P3 x Flag MKL1 wt	P3 x Flag-CMV™-7.1	Prof. Ron Prywes, Columbia University New York, NY, USA
P3 x Flag MKL1 Δ301-310	P3 x Flag-CMV™-7.1	*Kircher et al., 2015*
P3 x Flag MKL1 Δ301-342	P3 x Flag-CMV™-7.1	*Kircher et al., 2015*
pcDNA 3.1 empty vector	pcDNA3.1	Prof. Konstanze F. Winklhofer, Ludwig-Maximilians-University Munich, Munich, Germany
Renilla luciferase SV40	pSV	Prof. Ron Prywes, Columbia University New York, NY, USA
SRF-VP16	pMLV	Prof. Margarete Goppelt-Strübe, Friedrich-Alexander-University Erlangen-Nürnberg, Erlangen, Germany

4.3.2 Primers

4.3.2.1 Human primers for qRT-PCR

Table 8: Human primers for qRT-PCR and their sequence

primer	sequence	manufacturer
18S rRNA Fw 18S rRNA Rv	5'-TCG AGG CCC TGT AAT TGG AAT-3' 5'-CCC TCC AAT GGA TCC TCG TTA-3'	Sigma-Aldrich, Taufkirchen, Germany
CNN1 Fw CNN1 Rv	5'-GCT GTC AGC CGA GGT TAA GA-3' 5'-CCC TCG ATC CAC TCT CTC AG-3'	Metabion, Martinsried, Germany
CTGF Fw CTGF Rv	5'-TTG GCA GGC TGA TTT CTA GG-3' 5'-GGT GCA AAC ATG TAA CTT TTG G-3'	Metabion, Martinsried, Germany
CXCL10 Fw CXCL10 Rv	5'-CCC CAC GTT TTC TGA GAC AT-3' 5'-TGG CAG TTT GAT TCA TGG TG-3'	Metabion, Martinsried, Germany
EGFR Fw EGFR Rv	5'-TTC CTC CCA GTG CCT GAA-3' 5'-GGG TTC AGA GGC TGA TTG TG-3'	Metabion, Martinsried, Germany
FLNa Fw FLNa Rv	5'-TCG CTC TCA GGA ACA GCA-3' 5'-TTA ATT AAA GTC GCA GGC ACC TA-3'	Metabion, Martinsried, Germany
GLIPR1 Fw GLIPR1 Rv	5'-TCT TTC CAA TGG AGC ACA TTT-3' 5'-TCT TAT ATG GCC AAG TTG GGT AA-3'	Metabion, Martinsried, Germany
MAP1B Fw MAP1B Rv	5'-GAC GCT TTG TTG GAA GGA AA-3' 5'-CTG AGT CAT GAG TTG GGA TCA G-3'	Metabion, Martinsried, Germany
Mig6 Fw Mig6 Rv	5'-ACC CAC TGA AGT AGC TCA TCG-3' 5'-TTC CAT CTG AGT CTA ACG TAC CC-3'	Sigma-Aldrich, Taufkirchen, Germany
MKL1 Fw MKL1 Rv	5'-CCC AAT TTG CCT CCA CTT AG-3' 5'-CCT TGG CTC ACC AGT TCT TC-3'	Metabion, Martinsried, Germany
MKL2 Fw MKL2 Rv	5'-CTT ACC CCC TCT GAA CGA AA-3' 5'-CTC TCG TCC TCC TTT GTT GC-3'	Metabion, Martinsried, Germany
MYH9 Fw MYH9 Rv	5'-TGG AGG ACC AGA ACT GCA A-3' 5'-GGT TGG TGG TGA ACT CAG CTA-3'	Metabion, Martinsried, Germany
MYOF Fw MYOF Rv	5'-CCA TTA CTG GCT TCT AAG CTG AC-3' 5'-TTC CCC TGA GGA AGC ATA AA-3'	Metabion, Martinsried, Germany
SM22 Fw SM22 Rv	5'-GGC CAA GGC TCT ACT GTC TG-3' 5'-CCC TTG TTG GCC ATG TCT-3'	Metabion, Martinsried, Germany
SRF Fw SRF Rv	5'-AGC ACA GAC CTC ACG CAG A-3' 5'-GTT GTG GGC ACG GAT GAC-3'	Metabion, Martinsried, Germany
TGFβ1 Fw TGFβ1 Rv	5'-ACT ACT ACG CCA AGG AGG TCA C-3' 5'-TGC TTG AAC TTG TCA TAG ATT TCG-3'	Metabion, Martinsried, Germany
TNFSF10 Fw TNFSF10 Rv	5'-TTC ACA GTG CTC CTG CAG TC-3' 5'-GCC ACT TTT GGA GTA CTT GTC C-3'	Metabion, Martinsried, Germany
VGLL3 Fw VGLL3 Rv	5'-TCC CAG TAT CTG CCC AAC C-3' 5'-TGC TGA ATA CCG CTA ACT TCT TC-3'	Metabion, Martinsried, Germany
Random Hexamers	5'-NNN NNN-Wobbles-3'	Metabion, Martinsried, Germany

4.3.2.2 Mouse primers for qRT-PCR

Table 9: Mouse primers for qRT-PCR and their sequence

primer	sequence	manufacturer
CNN1 Fw CNN1 Rv	5'-CGG CTT GTC TGC TGA AGT AA-3' 5'-ACC CCC TCA ATC CAC TCT CT-3'	Metabion, Martinsried, Germany
CTGF Fw CTGF Rv	5'-TGA CCT GGA GGA AAA CAT TAA GA-3' 5'-AGC CCT GTA TGT CTT CAC ACT G-3'	Metabion, Martinsried, Germany
CXCL10 Fw CXCL10 Rv	5'-GCT GCC GTC ATT TTC TGC-3' 5'-TCT CAC TGG CCC GTC ATC-3'	Sigma-Aldrich, Taufkirchen, Germany
EGFR Fw EGFR Rv	5'-CAA CAA AGA AAT CCT TGA CGA A-3' 5'-GGA CAG TGG AGG TCA GAC AGA-3'	Sigma-Aldrich, Taufkirchen, Germany
FLNa Fw FLNa Rv	5'-GAC CTC AGC CTG AAG ATT CCT-3' 5'-ATG GGT CTT GCC TGA TGG-3'	Metabion, Martinsried, Germany
GLIPR1 Fw GLIPR1 Rv	5'-TGC CCT AAT GGA GCA AAT TTT A-3' 5'-TTA TAT GGC CAC GTT GGG TAA-3'	Metabion, Martinsried, Germany
ITGA5 Fw ITGA5 Rv	5'-CAC CAT TCA ATT TGA CAG CAA-3' 5'-TCC TCT CCC TTG GCA CTG TA-3'	Metabion, Martinsried, Germany
MAP1B Fw MAP1B Rv	5'-CCT GGA TGC CTT GTT GGA-3' 5'-GGA GTC ATG TGT CGG AAT CA-3'	Metabion, Martinsried, Germany
MYOF Fw MYOF Rv	5'-TGA AGA TCC ATC TGT GGT AGG A-3' 5'-ATC CGG CAA GGG GTA GAT-3'	Sigma-Aldrich, Taufkirchen, Germany
p16 Fw p16 Rv	5'-GAC AGG AAA GGA ATT GCA TGA-3' 5'-TTA AAC AAT CCA GCC ATT ATT CC-3'	Sigma-Aldrich, Taufkirchen, Germany
SRF Fw SRF Rv	5'-CTG ACA GCA GTG GGG AAA C-3' 5'-GCT GGG TGC TGT CTG GAT-3'	Metabion, Martinsried, Germany
SM22 Fw SM22 Rv	5'-CCT TCC AGT CCA CAA ACG AC-3' 5'-GTA GGA TGG ACC CTT GTT GG-3'	Metabion, Martinsried, Germany
TNFSF10 Fw TNFSF10 Rv	5'-GCT CCT GCA GGC TGT GTC-3' 5'-CCA ATT TTG GAG TAA TTG TCC TG-3'	Sigma-Aldrich, Taufkirchen, Germany

4.3.2.3 Primers for ChIP qRT-PCR

Table 10: Primers for ChIP qRT-PCR and their sequence

promoter	sequence	manufacturer
Actin	5'-AGG GTC TTC CCA GGC TGG CTT TGA-3' 5'-CAA GAC TCC ATG TGC CAC AGA GGA T-3'	Sigma-Aldrich, Taufkirchen, Germany
CTGF	5'-GGA GTG GTG CGA AGA GGA TA-3' 5'-GCC AAT GAG CTG AAT GGA GT-3'	Sigma-Aldrich, Taufkirchen, Germany
GAPDH	5'-CGG GAT TGT CTG CCC TAA TTA T-3' 5'-GCA CGG AAG GTC ACG ATG T-3'	Sigma-Aldrich, Taufkirchen, Germany
MYOF	5'-TAG ATT CCA ACC TAT GGA ACT GA-3' 5'-TTC CTC ATT AAA GGC ATT CCA-3'	Sigma-Aldrich, Taufkirchen, Germany
MYOF-1167 (neg. control)	5'-TCT GAC TTT CCT GAG ACA TTT GAA-3' 5'-TTT TTG CTT CTG ACA TAC AAC CA-3'	Sigma-Aldrich, Taufkirchen, Germany
α-SMA	5'-AGC AGA ACA GAG GAA TGC AGT GGA AGA GAC-3' 5'-CCT CCC ACT CGC CTC CCA AAC AAG GAG C-3'	Sigma-Aldrich, Taufkirchen, Germany

4.3.3 siRNAs

Table 11: siRNAs and their sequence

siRNA	**sequence** (sense und antisense)	**manufacturer**
scrambled (neg. control)	5'-CGUACGCGGAAUACUUCGA[dt][dt]-3' 5'-UCGAAGUAUUCCGCGUACG[dt][dt]-3'	Sigma-Aldrich, Taufkirchen, Germany
EGFR (human)	5'-GCUGCUCUGAAAUCUCCUUUA[dt][dt]-3' 5'-UAAAGGAGAUUUCAGAGCAGC[dt][dt]-3'	Sigma-Aldrich, Taufkirchen, Germany
FLNa (human)	5'-GCACAUGUUCCGUGUCCUA[dt][dt]-3' 5'-UAGGACACGGAACAUGUGC[dt][dt]-3'	Dharmacon, Lafayette, CO, USA
FLNa (mouse)	5'-GGUACACAAUCCUCAUCAATT[dt][dt]-3' 5'-UUGAUGAGGAUUGUGUACCGG[dt][dt]-3'	Qiagen, Hilden, Germany
Mig6 (human)	5'-CUACACUUUCUGAUUUCAA[dt][dt]-3' 5'-UUGAAAUCAGAAAGUGUAG[dt][dt]-3'	Sigma-Aldrich, Taufkirchen, Germany
MKL1 (human)	5'-GAAUGUGCUACAGUUGAAA[dt][dt]-3' 5'-UUUCAACUGUAGCACAUUC[dt][dt]-3'	Sigma-Aldrich, Taufkirchen, Germany
MKL1 V2 (human)	5'-GUGUCUUGGUGUAGUGUAA[dt][dt]-3' 5'-UUACACUACACCAAGACAC[dt][dt]-3'	Sigma-Aldrich, Taufkirchen, Germany
MKL1/2 (human)	5'-AUGGAGCUGGUGGAGAAGAA[dt][dt]-3' 5'-UUCUUCUCCACCAGCUCCAU[dt][dt]-3'	Sigma-Aldrich, Taufkirchen, Germany
MKL2 (human)	5'-GUAACAGUGGGAAUUCAGC[dt][dt]-3' 5'-GCUGAAUUCCCACUGUUAC[dt][dt]-3'	Sigma-Aldrich, Taufkirchen, Germany
MKL2 V2 (human)	5'-AAGAGCTCGACTAGCAGATGA[dt][dt]-3' 5'-TCATCTGCTAGTCGAGCTCTT[dt][dt]-3'	Sigma-Aldrich, Taufkirchen, Germany
MYOF (human)	5'-CCCUGUCUGGAAUGAGA[dt][dt]-3' 5'-UCUCAUUCCAGACAGGG[dt][dt]-3'	Sigma-Aldrich, Taufkirchen, Germany
MYOF (mouse)	5'-AACCCUGUCUGGAAUGAGAUU[dt][dt]-3' 5'-AAUCUCAUUCCAGACAGGGUU[dt][dt]-3'	Sigma-Aldrich, Taufkirchen, Germany
MYOF V2 (human)	5'-CGGCGGAUGCUGUCAAAUA[dt][dt]-3' 5'-UAUUUGACAGCAUCCGCCG[dt][dt]-3'	Sigma-Aldrich, Taufkirchen, Germany

4.4 Antibiotics

Table 12: Antibiotics

antibiotic	**manufacturer**
ampicillin	Gibco® Invitrogen, Karlsruhe, Germany
G418 (Geneticin disulphate)	Carl Roth, Karlsruhe, Germany
kanamycin	Gibco® Invitrogen, Karlsruhe, Germany
penicillin/streptomycin	Sigma-Aldrich, Taufkirchen, Germany

4.5 Enzymes

Table 13: Enzymes

enzyme	manufacturer
Proteinase K	Sigma-Aldrich, Taufkirchen, Germany
RNase A	Thermo Scientific, Schwerte, Germany
SuperScript® II Reverse Transcriptase	Invitrogen, Karlsruhe, Germany
Trypsin-EDTA solution 0.05 %	Sigma-Aldrich, Taufkirchen, Germany

4.6 Stimulants and inhibitors

Table 14: Stimulants and inhibitors and their final working concentration

reagent	final concentration	manufacturer
Actinomycin D	1 µg/mL	AppliChem, Darmstadt, Germany
Cytochalasin D	2 µM	Sigma-Aldrich, Taufkirchen, Germany
FBS	20 %	Life Technologies, Darmstadt, Germany
Jasplakinolide	0.5 µM	CalBiochem, Darmstadt, Germany
Latrunculin B	0.3 µM	Merck, Darmstadt, Germany
LPA	10 µM	Sigma-Aldrich, Taufkirchen, Germany
MG132	10 µM	Sigma-Aldrich, Taufkirchen, Germany
SOS SH3 domain inhibitor	20 µM	Santa Cruz Biotechnology, Santa Cruz, CA, USA
Tyrphostin AG1478	10 µM	Sigma-Aldrich, Taufkirchen, Germany

4.7 Ladders

Table 15: DNA and protein ladders

ladder	manufacturer
100 bp DNA ladder	Invitrogen, Karlsruhe, Germany
Spectra™ Multicolor Broad Range Protein Ladder	Thermo Scientific, Schwerte, Germany
Spectra™ Multicolor High Range Protein Ladder	Thermo Scientific, Schwerte, Germany

4.8 Kits

Table 16: Kits

kit	manufacturer
Active Ras Detection Kit	Cell Signaling Technology, Danvers, MA, USA
Dual-Luciferase® Reporter Assay System	Promega, Mannheim, Germany
GenElute™ HP Plasmid Midiprep Kit	Sigma-Aldrich, Taufkirchen, Germany
MinElute PCR Purification Kit	Qiagen, Hilden, Germany
Q5® Site-Directed Mutagenesis Kit	New England Biolabs GmbH, Frankfurt am Main, Germany
QIAquick PCR Purification Kit	Qiagen, Hilden, Germany
Senescence β-Galactosidase Staining Kit	Cell Signaling Technology, Danvers, MA, USA

4.9 Buffers und solutions

4.9.1 Agarose gels

Table 17: Buffers used for agarose gel electrophoresis

50x TAE buffer		
	242.0 g	Tris
	57.1 mL	acetic acid (100%)
	100.0 mL	0.5 M EDTA, pH 8.0
		ad **1 L $H_2O_{ultrapure}$**
1x TAE buffer		
	100 mL	50x TAE buffer
		ad **5 L $H_2O_{ultrapure}$**

4.9.2 Bacteria cultivation

Table 18: LB agar and LB medium used for bacteria cultivation

LB agar		
	10 g	tryptone
	5 g	yeast extract
	10 g	NaCl
	15 g	agar
		ad **1 L $H_2O_{ultrapure}$, pH 7.5**

		-> autoclave
optionally:	100 µg/mL	antibiotic
LB medium		
	10 g	tryptone
	5 g	yeast extract
	10 g	NaCl
		ad **1 L $H_2O_{ultrapure}$, pH 7.5**
		-> autoclave

4.9.3 Calcium phosphate transfection

Table 19: Solutions used for calcium phosphate transfection

2x HBS		
	8.0 g	NaCl
	0.2 g	Na_2HPO_4 x 7 H_2O
	6.5 g	HEPES
		ad **500 mL $H_2O_{ultrapure}$, pH 7.0**
2.5 M $CaCl_2$		
	87.6 g	$CaCl_2$ x 6 H_2O
		ad **200 mL $H_2O_{ultrapure}$**
		-> sterile filtration

4.9.4 cDNA synthesis and qRT-PCR

Table 20: Reagents used for cDNA sytnthesis and qRT-PCR

reagent	**manufacturer**
5x First-Strand Buffer	Invitrogen, Karlsruhe, Germany
Deoxynucleoside triphosphates (dNTPs) (10 mM)	Invitrogen, Karlsruhe, Germany
LightCycler® 480 SYBR Green I Master	Roche, Penzberg, Germany

4.9.5 ChIP assay

Table 21: Buffers used for ChIP assay

Farnham Lysis buffer		
	0.76 g (5 mM)	PIPES, pH 8.0
	3.17 g (85 mM)	KCl
	2.50 mL (0.5%)	NP-40
		ad **500 mL $H_2O_{ultrapure}$**
Lysis buffer 0,1%		
	5.00 mL (10 mM)	1 M Tris, pH 7.5
	1.00 mL (1 mM)	0.5 M EDTA
	5.00 mL (0.1%)	10% SDS
		ad **500 mL $H_2O_{ultrapure}$**
LiCl Wash buffer		
	50.00 mL (100 mM)	1 M Tris, pH 7.5
	10.60 g (500 mM)	LiCl
	5.00 mL (1%)	NP-40
	5.00 g (1%)	sodium deoxycholate
		ad **500 mL $H_2O_{ultrapure}$**
IP buffer		
	6.70 g (56.25 mM)	HEPES
	4.60 g (157.5 mM)	NaCl
	1.00 mL (1 mM)	0.5 M EDTA
	5.625 mL (1.125%)	Triton X-100
	0.5625 g (0.1125%)	sodium deoxycholate
		ad **500 mL $H_2O_{ultrapure}$**
IP Elution buffer		
	50.00 mL (1%)	10% SDS
	4.20 g (100 mM)	$NaHCO_3$
		ad **500 mL $H_2O_{ultrapure}$**
TE buffer		
	5.00 mL (10 mM)	1 M Tris, pH 7.5
	1.00 mL (1 mM)	0.5 M EDTA
		ad **500 mL $H_2O_{ultrapure}$**
Sonication buffer		
	5.00 mL (10 mM)	1 M Tris, pH 7.5
	1.00 mL (1 mM)	0.5 M EDTA
	20.00 mL (0.4%)	10% SDS
		ad **500 mL $H_2O_{ultrapure}$**

4.9.6 Immunoblotting

Table 22: Buffers used for immunoblotting

5x transfer buffer		
	7.25 g	Tris
	3.65 g	glycine
	0.47 g	SDS
	200 mL	methanol
		ad **1 L $H_2O_{ultrapure}$**
10x TBS		
	60.55 g	Tris
	85.20 g	NaCl
		ad **1 L $H_2O_{ultrapure}$**, **pH 7.6** with HCl
1x TBS-T		
	500 mL	10x TBS
	5 mL	Tween 20
		ad **5 L $H_2O_{ultrapure}$**

4.9.7 Immunoblotting detection

Table 23: Reagents and solutions used for immunoblotting detection

Luminol stock solution		
	5 mL	1 M HEPES, pH 7.4
	3 mL	5 M NaCl
	1 mL	100 % Triton X-100
	0.2 mL	0.5 M EDTA, pH 8.0
	10 mL	100 % glycerin
		ad **100 mL $H_2O_{ultrapure}$**
add freshly to 1 mL:	2 µL	0.25 M PMSF
	4 µL	0.25 M DTT
	10 µL	10x Protease Inhibitor
stabilizer solution		
	2 mL	1 M Tris/HCl, pH 8.0
	2.92 g	NaCl
	0.5 mL	1 M imidazole
		ad **100 mL 8 M Urea**, **pH 7.9**

S1 solution		
	80.0 mL	$H_2O_{ultrapure}$
	10.0 mL	1 M Tris/HCl, pH 8.5
	1.00 mL	luminol stock solution
	0.44 mL	stabilizer solution
		ad **100 mL $H_2O_{ultrapure}$**
S2 solution		
	80 mL	$H_2O_{ultrapure}$
	10 mL	1 M Tris/HCl, pH 8.5
	60 µL	30 % H_2O_2
		ad **100 mL $H_2O_{ultrapure}$**
working solution		
	1:1	S1 solution:S2 solution

reagent	**manufacturer**
Roti®-Lumin 1+2	Carl Roth, Karlsruhe, Germany
SuperSignal™ West Femto Chemiluminescent Substrate	Thermo Scientific, Schwerte, Germany

4.9.8 Immunofluorescence

Table 24: Solution used for immunofluorescence

4% PFA		
	250 mL	$H_2O_{ultrapure}$
		-> 60 °C
	20 g	PFA
	50 µL	10 M NaOH
	50 mL	10x PBS
		ad **500 mL $H_2O_{ultrapure}$**

4.9.9 Invasion assay

Table 25: Solutions used for invasion assay

Staining Solution		
	40 mL	1x PBS
	8 mL (20%)	methanol
	0.04 g (0.1%)	crystal violet
Destaining Solution		
	40 mL	1x PBS
	8 mL (20%)	methanol

4.9.10 Protein isolation and purification

Table 26: Buffer and solution used for protein isolation and purification

Kralewski lysis buffer		
	5 mL	1 M HEPES, pH 7.4
	3 mL	5 M NaCl
	1 mL	100 % Triton X-100
	0.2 mL	0.5 M EDTA, pH 8.0
	10 mL	100 % glycerin
		ad **100 mL $H_2O_{ultrapure}$**
add freshly to 1 mL:	2 µL	0.25 M PMSF
	4 µL	0.25 M DTT
	10 µL	10x Protease Inhibitor
0.25 M PMSF		
	435.5 mg	PMSF
	10 mL	isopropanol

4.9.11 SDS-PAGE

Table 27: Buffers used for SDS-PAGE

4x SDS sample buffer		
	8 mL	1 M Tris, pH 8.8
	16 mL	20 % SDS
	16 mL	glycerin
	320 µL	0.5 M EDTA
	4 mg	bromophenol blue
add freshly to 960 µL:	40 µL	β-mercaptoethanol
10x SDS-PAGE running buffer		
	30.26 g	Tris
	10.00 g	SDS
	143.20 g	glycine
		ad **1 L $H_2O_{ultrapure}$**

4.9.12 Washing and dilution solutions

Table 28: PBS used for washing and dilutions

10x PBS		
	2 g	KCl
	2 g	KH_2PO_4
	80 g	NaCl
	21.6 g	Na_2HPO_4 x 7 H_2O
		***ad* 1 L $H_2O_{ultrapure}$, pH 7.4**

Table 29: DEPC H_2O used for RNA resuspension

DEPC H_2O		
	0.5 g	DEPC
	500 mL	$H_2O_{ultrapure}$
		1 h, 37 °C
		-> autoclave

4.10 Gels

Table 30: Composition of running and stacking gels used for SDS-PAGE

5 % running gel		
	8.50 mL	$H_2O_{ultrapure}$
	2.50 mL	30 % acrylamide
	3.75 mL	1.5 M Tris, pH 8.8
	0.150 mL	10 % SDS
	0.200 mL	10 % APS
	0.012 mL	TEMED
10 % running gel		
	3.97 mL	$H_2O_{ultrapure}$
	3.33 mL	30 % acrylamide
	2.50 mL	1.5 M Tris, pH 8.8
	0.100 mL	10 % SDS
	0.100 mL	10 % APS
	0.004 mL	TEMED
12 % running gel		
	4.80 mL	$H_2O_{ultrapure}$
	6.00 mL	30 % acrylamide
	3.90 mL	1.5 M Tris, pH 8.8
	0.150 mL	10 % SDS
	0.150 mL	10 % APS
	0.006 mL	TEMED

5 % stacking gel		
	5.40 mL	$H_2O_{ultrapure}$
	1.34 mL	30 % acrylamide
	2.00 mL	1.0 M Tris, pH 6.8
	0.080 mL	10 % SDS
	0.080 mL	10 % APS
	0.008 mL	TEMED

4.11 Bacterial strains

Table 31: Bacterial strains

strains	manufacturer
E. coli DH5α	Takara Bio, Kyoto, Japan
NEB® 5-alpha competent *E. coli*	New England Biolabs GmbH, Frankfurt am Main, Germany

4.12 Chemicals

Table 32: Chemicals

chemical	manufacturer
16% Formaldehyde (w/v), methanol-free	Thermo Fisher Scientific, Schwerte, Germany
6x DNA loading dye	Thermo Fisher Scientific, Schwerte, Germany
Agar	Carl Roth, Karlsruhe, Germany
Ammonium peroxodisulfate (APS)	Carl Roth, Karlsruhe, Germany
Bovine Serum Albumin (BSA)	Carl Roth, Karlsruhe, Germany
Bromophenol blue	Carl Roth, Karlsruhe, Germany
$CaCl_2$ x 6 H_2O	Carl Roth, Karlsruhe, Germany
Chloroform	Emsure® Merck, Darmstadt, Germany
Crystal violet	Merck Millipore, Darmstadt, Germany
Diethyl dicarbonate (DEPC)	Carl Roth, Karlsruhe, Germany
Dimethyl sulfoxide (DMSO)	Carl Roth, Karlsruhe, Germany
Dithiothreitol (DTT)	Invitrogen, Karlsruhe, Germany
Dynabeads® Protein G	Thermo Fisher Scientific, Schwerte, Germany
ECM matrigel from Engelbreth-Holm-Swarm murine sarcoma	Sigma-Aldrich, Taufkirchen, Germany
Ethanol	Emsure® Merck, Darmstadt, Germany
Ethylenediaminetetraacetic acid (EDTA)	Carl Roth, Karlsruhe, Germany
FBS (Fetal Bovine Serum)	Gibco® Invitrogen, Karlsruhe, Germany
Fluoromount	Sigma-Aldrich, Taufkirchen, Germany
Glycerin	Carl Roth, Karlsruhe, Germany
Glycine	Carl Roth, Karlsruhe, Germany
HEPES	Carl Roth, Karlsruhe, Germany

Hydrochloric acid (HCl)	Merck, Darmstadt, Germany
Imidazole	Carl Roth, Karlsruhe, Germany
Immersion oil Immersol 518 F	Carl Zeiss AG, Oberkochen, Germany
Isopropyl alcohol	Carl Roth, Karlsruhe, Germany
Lithium chloride	Merck Millipore, Darmstadt, Germany
Low fat milk powder	Heirler, Radolfzell, Germany
Methanol	Carl Roth, Karlsruhe, Germany
N,*N*-Dimethylformamide (DMF)	Sigma-Aldrich, Taufkirchen, Germany
N,N,N',N'- Tetramethylethylenediamine (TEMED)	Carl Roth, Karlsruhe, Germany
Nonidet P-40 (NP-40)	Sigma-Aldrich, Taufkirchen, Germany
Nuclease free H_2O	Thermo Scientific, Schwerte, Germany
Paraformaldehyde (PFA)	Carl Roth, Karlsruhe, Germany
peqGold universal agarose	Peqlab Biotechnology GmbH, Erlangen, Germany
phenylmethylsulfonyl fluoride (PMSF)	Calbiochem, Darmstadt, Germany
Piperazine-N,N′-bis(2-ethanesulfonic acid) (PIPES)	Carl Roth, Karlsruhe, Germany
Potassium chloride (KCl)	Carl Roth, Karlsruhe, Germany
Potassium dehydrogen phosphatase (KH_2PO_4)	Carl Roth, Karlsruhe, Germany
Propidium iodide	Sigma-Aldrich, Taufkirchen, Germany
Protease Inhibitor Cocktail Set III, Animal-Free	Merck Millipore, Darmstadt, Germany
Roti®-Quant	Carl Roth, Karlsruhe, Germany
Roti®-Safe GelStain	Carl Roth, Karlsruhe, Germany
Rotiphorese® Gel 30 (37.5:1) (30% acrylamide)	Carl Roth, Karlsruhe, Germany
Sodium azide	Carl Roth, Karlsruhe, Germany
Sodium chloride (NaCl)	Carl Roth, Karlsruhe, Germany
Sodium deoxycholate	Carl Roth, Karlsruhe, Germany
Sodium dodecyl sulfate (SDS)	Carl Roth, Karlsruhe, Germany
Sodium hydrogen carbonate ($NaHCO_3$)	Carl Roth, Karlsruhe, Germany
Sodium hydrogen phosphate (Na_2HPO_4)	Carl Roth, Karlsruhe, Germany
Sodium hydroxide (NaOH)	Carl Roth, Karlsruhe, Germany
Tris	Carl Roth, Karlsruhe, Germany
Triton X-100	Carl Roth, Karlsruhe, Germany
TRIzol® Reagent	Invitrogen, Karlsruhe, Germany
Tryptone	Carl Roth, Karlsruhe, Germany
Tween® 20	Carl Roth, Karlsruhe, Germany
Urea	Carl Roth, Karlsruhe, Germany
Yeast extract	Carl Roth, Karlsruhe, Germany
β-Mercaptoethanol	Serva, Heidelberg, Germany

4.13 Consumables

Table 33: Consumables

consumable	manufacturer
24-well hanging cell culture inserts, 8.0 µm	Merck Millipore, Darmstadt, Germany
Cell culture dishes, 6 cm, 10 cm and 6well plates	Sarstedt, Nümbrecht, Germany
Cell scraper	Sarstedt, Nümbrecht, Germany
Cover slips 20x20 mm	Carl Roth, Karlsruhe, Germany
Cryovials CryoPure 1.6 mL	Sarstedt, Nümbrecht, Germany
Falcon tubes, 15 mL and 50 mL	Sarstedt, Nümbrecht, Germany
Glas pearls	Carl Roth, Karlsruhe, Germany
LightCycler® 480 Multiwell Plate 96	Roche, Penzberg, Germany
LightCycler® 480 Sealing Foil	Roche, Penzberg, Germany
Microscope slides 76x26 mm	Carl Roth, Karlsruhe, Germany
Multiply®-Pro tubes, 0.2 mL	Sarstedt, Nümbrecht, Germany
Pasteur pipettes, 230 mm	Carl Roth, Karlsruhe, Germany
PVDF membrane	Millipore, Schwalbach, Germany
Reaction tubes SafeSeal, 1.5 mL and 2.0 mL	Sarstedt, Nümbrecht, Germany
Serological pipettes, 2 mL, 5 mL, 10 mL and 25 mL	Sarstedt, Nümbrecht, Germany
Tube with ventilation cap, 13 mL	Sarstedt, Nümbrecht, Germany
UV-transparent cuvettes	Sarstedt, Nümbrecht, Germany
Whatman paper 0.8 mm	Optilab, München, Germany

4.14 Technical devices

Table 34: Technical devices

tool	manufacturer
Analytical balance	Acculab, Sartorius Group, Göttingen, Germany
BioPhotometer plus	Eppendorf, Hamburg, Germany
Blotting equipment Mini Protean® Tetra Cell	Bio-Rad, Munich, Germany
Centrifuge 5424	Eppendorf, Hamburg, Germany
Centrifuge 5424R	Eppendorf, Hamburg, Germany
Chemi-Smart™ 5100 (chemiluminescent imager)	Peqlab Biotechnology GmbH, Erlangen, Germany
DynaMag™-2 magnet	Thermo Fisher Scientific, Schwerte, Germany
Electrophoresis equipment	Peqlab Biotechnology GmbH, Erlangen, Germany
Electrophoresis Power Supply EPS 301	GE Healthcare GmbH, Freiburg, Germany
FlexCycler²	Analytik Jena AG, Jena, Germany
Freezer (-20 °C)	Liebherr, Biberach an der Riss, Germany
Fridge	Liebherr, Biberach an der Riss, Germany
HERAcell® 240 incubator	Thermo Scientific, Schwerte, Germany
Heraeus™ Biofuge™ Stratos	Thermo Scientific, Schwerte, Germany

Heraeus™ Labofuge™ 400	Thermo Scientific, Schwerte, Germany
Incubator MaxQ 6000	Thermo Scientific, Schwerte, Germany
Infinity 3026 WL/26 MX gel documentation system	Peqlab Biotechnology GmbH, Erlangen, Germany
Laminar flow HERASafe KS18	Kendro, Langenselbold, Germany
LightCycler® 480 II	Roche, Penzberg, Germany
Lumat³ LB 9508 Single Tube Luminometer	Berthold Technologies Bio & Co.KG, Bad Wildbad, Germany
Microscope Axiovert 135M	Carl Zeiss AG, Oberkochen, Germany
Microscope Axiovert 40 CFL	Carl Zeiss AG, Oberkochen, Germany
Microscope CKX41	Olympus, Hamburg, Germany
Neubauer cell counting chamber (0.1 mm)	Marienfeld, Lauda-Königshofen, Germany
pH meter Lab850	Schott Instruments, SI Analytics, Mainz, Germany
Pipetus	Hirschmann, Eberstadt, Germany
Power Supply EV231	Peqlab Biotechnology GmbH, Erlangen, Germany
Power supply peqPOWER 300	Peqlab Biotechnology GmbH, Erlangen, Germany
SDS-PAGE equipment	Bio-Rad, Munich, Germany
Shaker Polymax 1040	Heidolph, Schwabach, Germany
sonicator	MSE, London, UK
Thermomixer compact	Eppendorf, Hamburg, Germany
Vortex-Genie™	Bender & Hobein AG, Zürich, Switzerland
Water bath	Memmert, Schwabach, Germany

4.15 Software

Table 35: Software programs

software	manufacturer
ChemiCapt™ Software	Peqlab Biotechnology GmbH, Erlangen, Germany
EndNote X8	Thomson Reuters, New York, NY, USA
Excel 2011	Microsoft, Redmond, WA, USA
ImageJ 1.43u	Wayne Rasband, National Institutes of Health, Bethesda, MD, USA
InfinityCapt 14.2	Vilber Lourmat Deutschland GmbH, Eberhardzell, Germany
LightCycler® 480 Software	Roche, Penzberg, Germany
Loading Calculator	Dr. Susanne Muehlich, Walther-Straub-Institut, Munich, Germany
NEBaseChanger™	New England Biolabs GmbH, Frankfurt am Main, Germany
Powerpoint 2011	Microsoft, Redmond, WA, USA
Prism 5	GraphPad Software, La Jolla, CA, USA
Word 2011	Microsoft, Redmond, WA, USA
ZEN	Carl Zeiss AG, Oberkochen, Germany

5 Methods

5.1 Cell culture methods

5.1.1 Cultivation of cell lines

All cell lines were cultured as monolayers in the appropriate medium containing 10 % (v/v) fetal bovine serum (FBS) and 1 % (v/v) penicillin/streptomycin in 10 cm cell culture dishes until a confluence of 80-100 %. Cells were cultured at 37 °C and 5 % CO_2. For passaging, adherent cells were washed with 5 mL prewarmed 1x phosphate-buffered saline (PBS) and detached with 2 mL Trypsin-EDTA. After incubation at 37 °C for 4 min, 8 mL prewarmed medium was added and cells were resuspended. A defined volume of the cell suspension was added to a new 10 cm culture dish with fresh medium containing FBS and penicillin/streptomycin. Cells were usually splitted in a range from 1:2 to 1:20. Cell lines and their culture medium are listed in table 1.

5.1.2 Thawing cells

Cells frozen in liquid nitrogen for long-term storage were thawed by gently shaking the cryovials in a 37 °C water bath. Cell suspension was transferred to a falcon tube with 5 mL of the relevant prewarmed medium and centrifuged for 5 min at 1000 rpm and room temperature. The pellet was resuspended in 1 mL medium and given in a culture dish with the adequate amount of prewarmed medium. The thawed cells were cultivated in an incubator at 37 °C and 5 % CO_2.

5.1.3 Freezing cells

For long-term storage, cells were frozen in liquid nitrogen. Therefore, cells were washed with PBS, trypsinized and resuspended in 3 mL of the appropriate medium. Cell suspension was centrifuged for 5 min at 1000 rpm and room temperature and cell pellet was resuspended in 900 µL ice-cold FBS and 100 µL DMSO. Cell suspension was aliquoted in 3 cryovials and placed in a cryofreezing box containing isopropanol for slow cooling to -80 °C. After 1 month,

cells were stored in liquid nitrogen.

5.1.4 Serum stimulation

Before serum stimulation, cells were washed twice with PBS and then serum-starved by adding the appropriate medium containing 0.2 % FBS for 16 h. After starvation, cells were stimulated for 2 h with 20 % FBS by directly adding the FBS to the starvation medium.

5.1.5 Drug treatment

Stimulants and inhibitors listed in table 14 were directly added to the medium of the seeded cells in the appropriate amount to obtain the final working concentration and the cells were incubated with the reagents for the adequate period of time.

5.1.6 Transient siRNA mediated knockdown by Lipofectamine® RNAiMAX™

For transient knockdown of target gene expression by RNA interference (RNAi), cells were transfected with Lipofectamine® RNAiMAX™ by reverse transfection according to the manufacturer's instructions. Briefly, in a 6 cm cell culture dish, 50 nM negative control or 50 nM gene-specific small-interfering RNA (siRNA) and 10 µL Lipofectamine® RNAiMAX™ were incubated in 1 mL OptiMEM for 20 min at room temperature. Meanwhile, cells were trypsinized and pelleted by centrifugation for 5 min at 1000 rpm and room temperature. Cell pellet was resuspended in 10 mL OptiMEM and an adequate number of cells was diluted in 3 mL OptiMEM and then added to the siRNA/RNAiMAX™ mix. Cells were incubated at 37 °C and 5 % CO_2 overnight. The next day, transfection medium was removed and fresh culture medium containing FBS and antibiotics was added. Analysis of the target gene knockdown was assessed by quantitative real-time PCR (qRT-PCR) or western blot 48 h or 5 days post transfection for senescence experiments. Used siRNAs are listed in table 11.

5.1.7 Transient transfection by Lipofectamine® 2000

For transient overexpression of plasmids, all cell lines, except for HepG2, were transfected with Lipofectamine® 2000 according to the manufacturer's instructions. Therefore, cells were seeded in 6 cm culture dishes with culture medium without antibiotics 24 h before transfection. 4 µg of plasmid DNA and 5 µL Lipofectamine® 2000 were each incubated in 250 µL OptiMEM for 5 min at room temperature. Then both transfection solutions were mixed and incubated for 20 min at room temperature. Transfection mix was added to cells and incubated at 37 °C and 5 % CO_2. After 4-6 h, medium was replaced by fresh medium containing FBS and antibiotics. Cells were cultivated and further experiments were done 24 h post transfection.

5.1.8 Transient transfection by GenJet™ transfection reagent

For transient transfection of HepG2 cells, the GenJet™ transfection reagent was used according to the manufacturer's instructions. Thus, cells were seeded in 6 cm culture dishes 24 h before transfection in culture medium and 60 min before transfection, medium was replaced by fresh medium. Plasmid DNA and GenJet™ transfection reagent in a ratio of 1:3 were each diluted in 250 µL medium without serum and then mixed. Transfection cocktail was added to cells and incubated at 37 °C and 5 % CO_2. After 16 h, medium was replaced by fresh medium containing FBS and antibiotics.

5.1.9 Calcium phosphate transfection method

Cells were transfected with the calcium phosphate transfection method for transient transfection and overexpression of proteins. The day before transfection, cells were seeded and medium was replaced by fresh medium supplemented with FBS but without antibiotics 2 h before transfection. For each 6-well, 2 µg of plasmid DNA and 3.5 µL $CaCl_2$ (2 M) were mixed with sterile H_2O for a total volume of 62.5 µL. This cocktail was added dropwise to an eppendorf tube with 62.5 µL 2x HBS while vortexing. After 5 min incubation at room temperature, cocktail was added to cells in 6-well plates. The next day, medium was replaced by fresh medium containing FBS and antibiotics.

5.1.10 Cell proliferation assay

For cell proliferation assays, 2.4 x 10^5 HepG2 cells or 1.2 x 10^5 of all other cell lines were seeded in 6-well plates and cultured at 37 °C and 5 % CO_2. Cell number was counted at 24 h intervals for 4 to 6 days.

5.1.11 Cell invasion assay

Performing the cell invasion assay, cell culture inserts were placed in a 24-well plate and 100 µL ECM matrigel solution (diluted 1:2 with cold DMEM) was placed into the inserts. After incubation of the plate at 37 °C for around 1 h, 600 µL DMEM with 10 % FBS were laid in the lower chamber, whereas 4 x 10^4 cells in 200 µL DMEM supplemented with 1 % FBS were placed into the upper chamber. Cells were allowed to invade through the matrigel due to the concentration gradient for around 24 h at 37 °C. The next day, invaded cells were stained by incubating the cell inserts in a crystal violet staining solution for 5 min, washing them with PBS and holding them afterwards into the destaining solution. Non-invasive cells were removed from top of the matrigel with cotton swabs. Images were taken at the Zeiss Axiovert 40 CFL microscope and quantification of cells was carried out by counting the invasive, magenta-colored cells using the ZEN software.

5.1.12 Senescence-associated ß-Galactosidase staining

Cellular senescence was determined by using the Senescence ß-Galactosidase staining kit according to the manufacturer's instructions. Cells were seeded and incubated at 37 °C and 5 % CO_2 for 5 days. Then cells were stained with staining solution and X-Gal and incubated overnight at 37 °C and 0 % CO_2. The number of blue cells per 100 cells was counted and the percentage of SA-β-gal-positive cells was calculated.

5.2 Methods of protein analyses

5.2.1 Protein isolation

Adherent cells were washed twice with ice-cold 1x PBS and harvested with 80-150 µL Kralewski lysis buffer per 6 cm culture dish depending on the cell density. Cells were scrapped by a cell scraper and transferred to an eppendorf tube. Cells were lysed on ice for 15 min. After centrifugation at 12700 rpm for 15 min at 4 °C, the clear supernatant was transferred to a new eppendorf tube. Lysates were kept on ice for further treatment or frozen at -20 °C.

5.2.2 Measurement of protein concentration by Bradford assay

For determination of the cell lysates protein concentration, 2 µL of the lysate or 2 µL of the Kralewski lysis buffer as control were given to 1 mL 1x Roti®-Quant. Solutions were incubated at room temperature for 5-10 min. Measurement was performed in UV-transparent cuvettes at the BioPhotometer at 595 nm. The amount of cell lysate for 10-30 µg protein for SDS-PAGE loading was calculated.

5.2.3 SDS polyacrylamide gel electrophoresis (SDS-PAGE)

SDS-PAGE was used for separating proteins in an electric field according to their molecular weight and their electrophoretic mobility. Determined amounts of cell lysates and 1/4 of the volume of 4x Laemmli SDS sample buffer were boiled at 95 °C for 10 min for protein denaturation. Samples were centrifuged at 12700 rpm for 1 min and then together with a protein ladder loaded onto a polyacrylamide gel. Protein separation was performed with 1x running buffer at 100 V constant for around 1:45 h until the dye front reached the end of the running gel.

5.2.4 Immunoblotting

By SDS-PAGE resolved proteins were transferred to a polyvinylidene fluoride (PVDF) membrane, which was activated by methanol and equilibrated in transfer buffer before. The immunoblotting was performed at 350 mA constant for 1:15 h in transfer buffer while the blotting chamber was cooled with ice. Membrane was blocked in 5 % milk powder solution in TBS-T for 1 h for avoiding unspecific antibody binding and then 3 times washed with TBS-T for 5 min. Specific primary antibody in the appropriate dilution was added to the membrane and incubated at 4 °C overnight. The next day, membrane was washed 3 times with TBS-T for 15 min, incubated with the secondary antibody for 1 h at room temperature and then washed again 3 times with TBS-T for 5 min. TBS-T was replaced by TBS and membrane was incubated with 1.5 mL of each detection solution S1 and S2 for 1 min. Detection of proteins was performed via chemiluminescene at the luminescent imager Chemi-Smart™ 5100. Analysis was done with the ChemiCapt™ and the ImageJ software.

5.2.5 Agarose gel electrophoresis

By using an agarose gel electrophoresis, DNA fragments were separated by size in an electric field. For a 1 % agarose gel, 1.5 g agarose were solved in 150 mL 1x TAE buffer while boiling the solution in a microwave. 7.5 µL Roti®-Safe GelStain and the agarose solution were added to the electrophoresis chamber. After curing of the gel, the chamber was filled with 1x TAE buffer and 1 µg DNA mixed with 6x DNA loading dye and also an appropriate ladder mixed with 6x DNA loading dye were filled in the slots. Gel was running at 100 V for 1 h. For visualization of the DNA bands, the gel was photographed at the Infinity gel documentation imager and the bands were made visible with the Infinity software.

5.2.6 Ras assay

Ras activation indicated by the level of GTP-bound Ras was analysed by using the Active Ras Detection Kit according to the manufacturer's instructions. Cells were seeded and after 5 days, cells were harvested and lysed under nondenaturing conditions. Glutathione resin, the fusion protein GST-Raf1-RBD that binds the activated GTP-bound Ras and the cell lysate were added to a spin column and incubated at 4 °C for 1 h. After washing, activated

Ras was eluted with SDS buffer and heated for 5 min at 95 °C. Ras activation levels were determined by western blotting using a specific Ras antibody.

5.2.7 Chromatin Immunoprecipitation (ChIP)

4.5 x 10^6 cells per ChIP were seeded in cell culture flasks. The next day, adherent cells were cross-linked with 1% methanol-free formaldehyde and quenched with 0.125 M glycine. Nuclei were pelleted and lysed for 10 min on ice. After washings, lysates were sonicated four times for 30 sec into DNA fragments of 200-2000 bp. Sheared chromatin was immunoprecipitated with 15 µg anti-MKL1 or anti-FLNa antibody coupled to Dynabeads Protein G overnight at 4 °C. A fraction (1%) of sonicated chromatin was set aside as input without antibody. After washings of immune complexes and elution of DNA of both input and ChIP samples using the MinElute PCR Purification Kit, qRT-PCR was performed using specific primers for target gene and GAPDH promoters for normalization.

5.2.8 Immunofluorescence

Cells were seeded on coverslips in 6-well plates and incubated at 37 °C and 5 % CO_2 for 48 h. Then cells were washed 3 times with 1 mL 1x PBS and fixed with 700 µL of 4% paraformaldehyde (PFA) in PBS for 10 min at room temperature. Cells were washed again 3 times with 1 mL 1x PBS and mounted with Fluoromount on a slide. After drying, coverslips were sealed with nail polish. Slides were stored at 4 °C in the dark until images were taken at the microscope.

5.3 Methods of nucleic acids analyses

5.3.1 RNA isolation using TRIzol® reagent

Adherent cells were washed twice with 5 mL 1x PBS and scrapped by a cell scraper after addition of 500 µL TRIzol® reagent. Cell suspension was transferred to an eppendorf tube, homogenized by pipetting up and down and incubated for 5 min at room temperature. 200 µL chloroform were added and suspension was shaken for 15 sec and incubated for 3 min at

room temperature. After centrifugation at 13000 rpm for 15 min at 4 °C, the upper clear phase that contains the RNA was transferred to a new eppendorf tube and 250 µL isopropanol were added. The solution was mixed, incubated for 15 min at room temperature and centrifuged at 13000 rpm for 15 min at 4 °C. The pellet was resuspended in 1 mL ethanol and centrifuged at 12000 rpm for 5 min at 4 °C. The supernatant was discarded and the pellet was dried for 10 min at room temperature, resuspended in 15 µL DEPC-H_2O and heated to 55 °C for 10 min. RNA was stored at -80 °C.

5.3.2 cDNA synthesis

For transcribing RNA into cDNA, 1 µg RNA was mixed with 1 µL random hexamers (50 µM) and fulfilled with nuclease free H_2O to 5 µL. Incubation took place at 70 °C for 5 min and then on ice for 5 min. Meanwhile, the following mix (table 36) was pipetted, added to the incubated solution and cDNA synthesis was performed in the FlexCycler^2 using the SuperScript® II Reverse Transcriptase under the following conditions (table 37).

Table 36: Mix for cDNA synthesis

cDNA mix	
4 µL	5x First Strand Buffer
2 µL	DTT (0.1 M)
1 µL	dNTPs (10 mM)
1 µL	SuperScript® II Reverse Transkriptase
ad **15 µL**	nuclease free H_2O

Table 37: Reaction conditions for cDNA synthesis

temperature	**time**
25 °C	5 min
42 °C	60 min
70 °C	5 min

All pipetting steps were performed on ice. cDNA was stored at -20 °C.

5.3.3 Quantitative real-time polymerase chain reaction (qRT-PCR)

For amplification and quantification of nucleic acids, a quantitative real-time polymerase chain reaction (qRT-PCR) was performed. 6 µL cDNA in a 1:10 dilution were placed in a 96-well plate and 14 µL of the following qRT-PCR mix (table 38) with the respective target gene primers were added. mRNA expression was normalized to the endogenous housekeeping control gene 18S rRNA. Therefore, cDNA was diluted 1:100 before placing in the multiwell plate. The gene specific primers used for amplification are listed in tables 8 and 9.

Table 38: Mix for qRT-PCR

qRT-PCR mix	
10 µL	LightCycler® 480 SYBR Green I Master
1 µL	primer forward (10 µM)
1 µL	primer reversed (10 µM)
ad **14 µL**	nuclease free H_2O

The qRT-PCR was carried out at the LightCycler® 480 II under the following reaction conditions (table 39):

Table 39: Reaction conditions and temperature profile for qRT-PCR

step	temperature	time	cycles
preincubation	42 °C	5:00 min	1
denaturation amplification elongation	95 °C 55 °C 72 °C	0:10 min 0:10 min 0:10 min	50
melting curve analysis	95 °C 60 °C 95 °C	0:30 min 1:00 min 0:10 min	1
cooling	4 °C	0:30 min	1

Analyses of the measurements were done by the LightCycler® 480 Software. The statistical evaluations and also the graphic illustrations were performed with GraphPad Prism 5.

5.3.4 Transformation of DNA into bacteria

DNA was transformed into bacteria via the heatshock method. First, competent bacteria, that were stored at -80 °C, were thawed on ice for 15 min and 50 µL bacteria suspension per reaction were transferred to a precooled eppendorf tube. 1 µL plasmid DNA was added and suspension was incubated 30 min on ice while thoroughly tipping the tube every 5 min. Heatshock was performed by holding the tube into a 42 °C waterbath for 90 sec and then for 2 min on ice. 0.9 mL prewarmed LB medium was added and transferred to a tube with ventilation cap for incubation at 37 °C and 150 rpm for 1 h. Then 150 µL of the suspension were plated onto a LB plate with antibiotic before incubating the plate at 37 °C overnight for colony growing.

5.3.5 Plasmid preparation

16 h before plasmid preparation, one bacteria colony grown on an agar plate was added with a pipette tip in an Erlenmeyer flask with 50 mL LB medium and 50 µL of the appropriate antibiotic (50 mg/ml), ampicillin or kanamycin, and incubated at 37 °C and gentle agitation. The next day, plasmid DNA was isolated by using the GenElute™ HP Plasmid Midiprep Kit according to the manufacturer's instructions. Briefly, the overnight culture was centrifuged at 3500 rpm for 10 min at 4 °C. The pellet was resuspended, lysed and neutralized. After washing of the binding column, bacteria solution was added to the binding column, washed and finally eluted with 800 µL elution solution. Plasmid DNA was transferred to a precooled eppendorf tube and put on ice immediately. Plasmids were stored at -20 °C.

5.3.6 Generation of MKL1 and myoferlin (MYOF) mutants

The MKL1 Δ301-310 bp deletion mutant and the MYOF Δ304-363 bp promoter deletion mutant were generated by using the Q5® Site-Directed Mutagenesis Kit according to the manufacturer's instructions. Therefore, the P3x Flag MKL1 wt plasmid was used as template for the MKL1 deletion mutant and the 1500 bp myoferlin promoter construct expressed in pGL2 vector was used for the MYOF promoter deletion mutant. The mix shown in table 40 containing the specific deletion primer pair was prepared. The amplification was carried out in the FlexCycler^2 under the following conditions (table 41).

Table 40: Mix for mutagenesis PCR

Q5® site-directed mutagenesis mix	
12.5 µL	Q5® Hot Start High-Fidelity 2x Master Mix
1.25 µL	primer forward (10 µM)
1.25 µL	primer reversed (10 µM)
1.00 µL	template DNA (20 ng/µL)
9.00 µL	nuclease free H_2O

Table 41: Reaction conditions for PCR

step	temperature	time	cycles
initial denaturation	98 °C	0:30 min	1
denaturation amplification elongation	98 °C 58 °C 72 °C	0:10 min 0:20 min 3:00 min	25
final extension	72 °C	2:00 min	1
cooling	4 °C	∞	1

The PCR product was prepared for the KLD digest with the following reagents and incubated for 5 min at room temperature (table 42). 5 µL of the KLD mix were transformed into NEB® 5-alpha competent *E. coli* bacteria by heatshock method and bacteria colonies were grown on LB plates with ampicillin at 37 °C overnight.

Table 42: Mix for KLD digest

KLD digest	
1 µL	PCR product
5 µL	2x KLD Reaction Buffer
1 µL	10x KLD Enzyme Mix
3 µL	nuclease free H_2O

5.4 Luciferase assay

For reporter gene assays, the Dual-Luciferase® Reporter Assay System was used according to the manufacturer's instructions. Cells were transfected with 500 ng of a myoferlin promoter construct, 1 µg of an empty vector (pcDNA), the SRF-VP16 or the MKL1-N100 plasmid and 250 ng of the *Renilla* luciferase simian virus 40 (SV40) plasmid as internal control. Cells were washed twice with 1x PBS and harvested with 70 µL 1x Passive Lysis Buffer 24 h post transfection. Cells were lysed on ice for 15 min and centrifuged for 1 min at top speed and 4 °C. 5 µL of the supernatant was transferred to a glass tube. 20 µL LAR II and 20 µL Stop&Glo were added consecutively to the sample while the luciferase assay was performed at the Lumat³ LB 9508 Single Tube Luminometer.

5.5 Statistical analysis

Statistical analysis among two groups was performed using Student's unpaired t-test. Unless otherwise indicated, data were analysed from three independent experiments and values are presented as mean and standard deviation (mean ± SD). P-values are *p<0.05, **p<0.01 and ***p<0.001.

6 Results

6.1 MKL1/2 target gene expression in HCC cells

6.1.1 Newly identified target genes are MKL1 and MKL2 dependent

6.1.1.1 Transient knockdown of MKL1/2

The first aim of this thesis was the validation of a performed microarray in HuH7 hepatocellular carcinoma (HCC) control cells versus HuH7 cells with a stable MKL1/2 knockdown and the verification of the newly found MKL1/2 dependent target genes by qRT-PCR.

By transfecting HuH7 HCC cells with MKL1/2 siRNA that is directed against MKL1 and MKL2 at once, we obtained a knockdown efficiency of about 80% for MKL1 and around 65% for MKL2 (Fig. 13, top). For almost all newly in the microarray identified target genes, GLIPR1, TGFβ1, MAP1B and MYOF, but not for CNN1, we observed a strongly reduced mRNA expression upon transient knockdown of MKL1/2 (Fig. 13). The already known MKL1 and MKL2 target genes SM22 and MYH9 were also highly significantly downregulated, serving as a positive control of our experimental RNA interference (RNAi) approach.

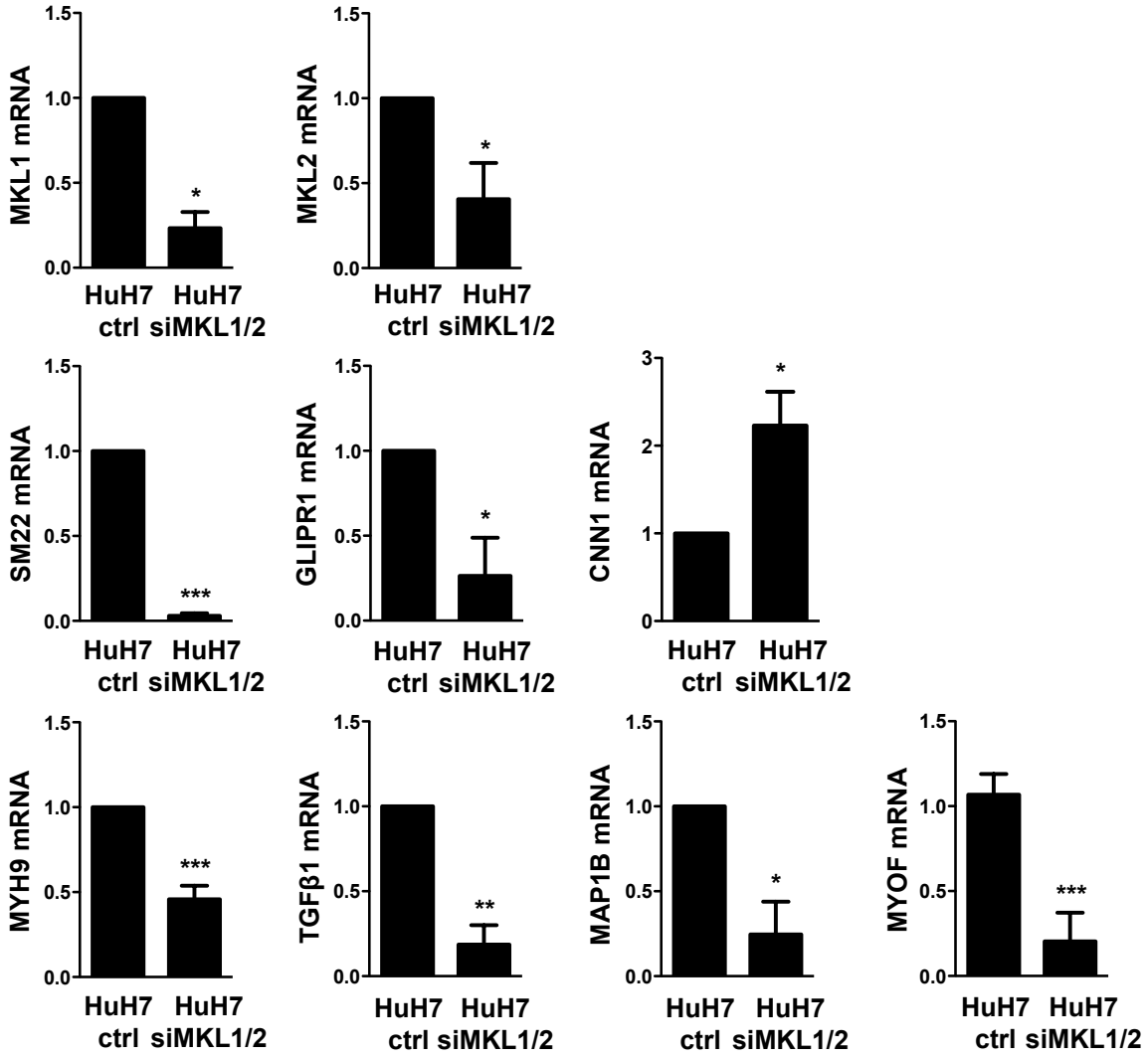

Figure 13: Target gene expression upon transient MKL1/2 knockdown. HuH7 cells were transfected with negative control (ctrl) or MKL1/2 siRNA. mRNA expression was assessed by qRT-PCR using the respective gene specific primers and 18S rRNA primers for normalization. Values are mean ± SD (n=3); *p<0.05, **p<0.01, ***p<0.001.

The same transient knockdown using MKL1/2 siRNA was performed in HuH6 (Fig. 14A) and HepG2 (Fig. 14B) hepatocellular carcinoma cells. In both cell lines, the MKL1 expression was reduced by around 70% in the MKL1/2 knockdown cells compared to the control cells. The new target genes GLIPR1 and CNN1 and also the known target genes SM22 and MYH9 as positive controls were significantly downregulated upon MKL1/2 knockdown. This way, we could show that the expression of the target genes found by microarray analysis are also MKL1/2 dependent in HuH6 and HepG2 cells concluding that this dependency is not only cell line specific but rather a general finding in HCC cell lines.

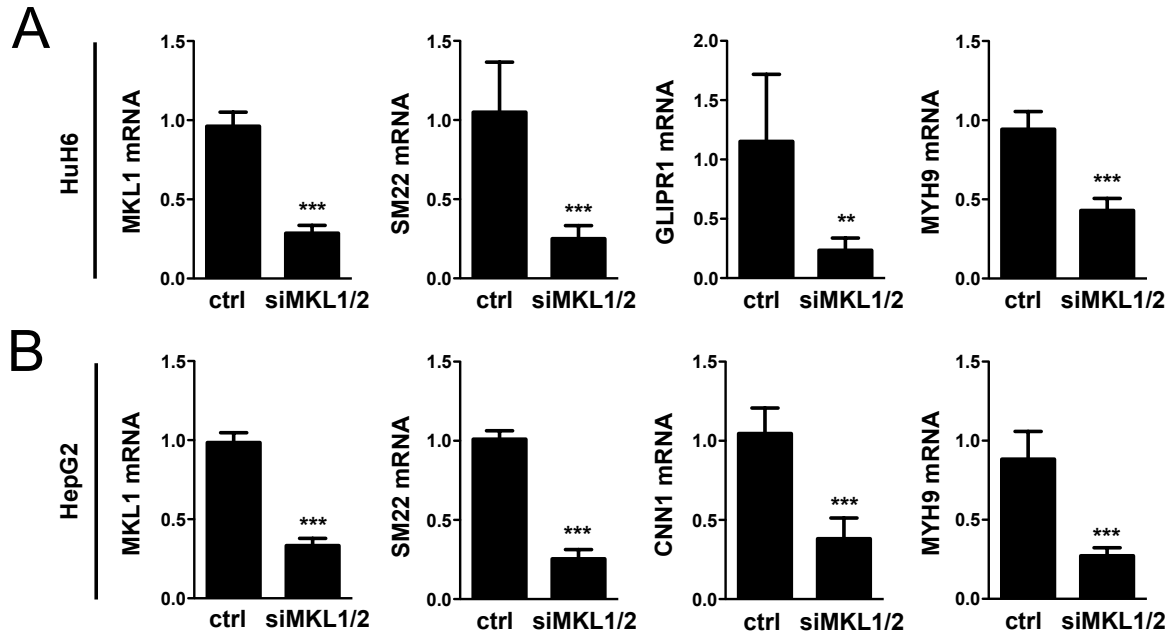

Figure 14: Target gene downregulation upon MKL1/2 depletion in HuH6 and HepG2 cells. mRNA expression of the indicated target genes in **(A)** HuH6 and **(B)** HepG2 ctrl and siMKL1/2 cells was measured by qRT-PCR. Values are mean ± SD (n=3); **p<0.01, ***p<0.001.

6.1.1.2 Knockdown of MKL1 or MKL2 alone or in combination

Next, we investigated the role of MKL1 and MKL2 siRNA alone or in combination in HuH7 cells. The MKL1 siRNA had a knockdown efficiency of nearly 90% and the MKL2 siRNA of 80% (Fig. 15A, top). All target genes, except for TGFβ1, showed a strongly reduced mRNA expression upon a single MKL1 knockdown and also all genes a reduced mRNA expression upon a single MKL2 knockdown (Fig. 15A). The expression levels of the genes after single siRNA treatment were comparable to those of the combined knockdown of both MKL1 and MKL2 siRNA. The mRNA expression of SRF as target gene of MKL1/2 itself was also affected by MKL1 and MKL2 siRNA (Fig. 15A). Furthermore, we also observed a significant reduction of GLIPR1 protein expression in HuH7 siMKL1 and HuH7 siMKL2 single knockdown and also in HuH7 siMKL1+2 cells compared to control cells (Fig. 15B). Regarding these results, we could show for the first time that MKL1 and MKL2 siRNA alone are very efficient and sufficient for target gene downregulation and that a double knockdown of both MKL1 and MKL2 is not necessary.

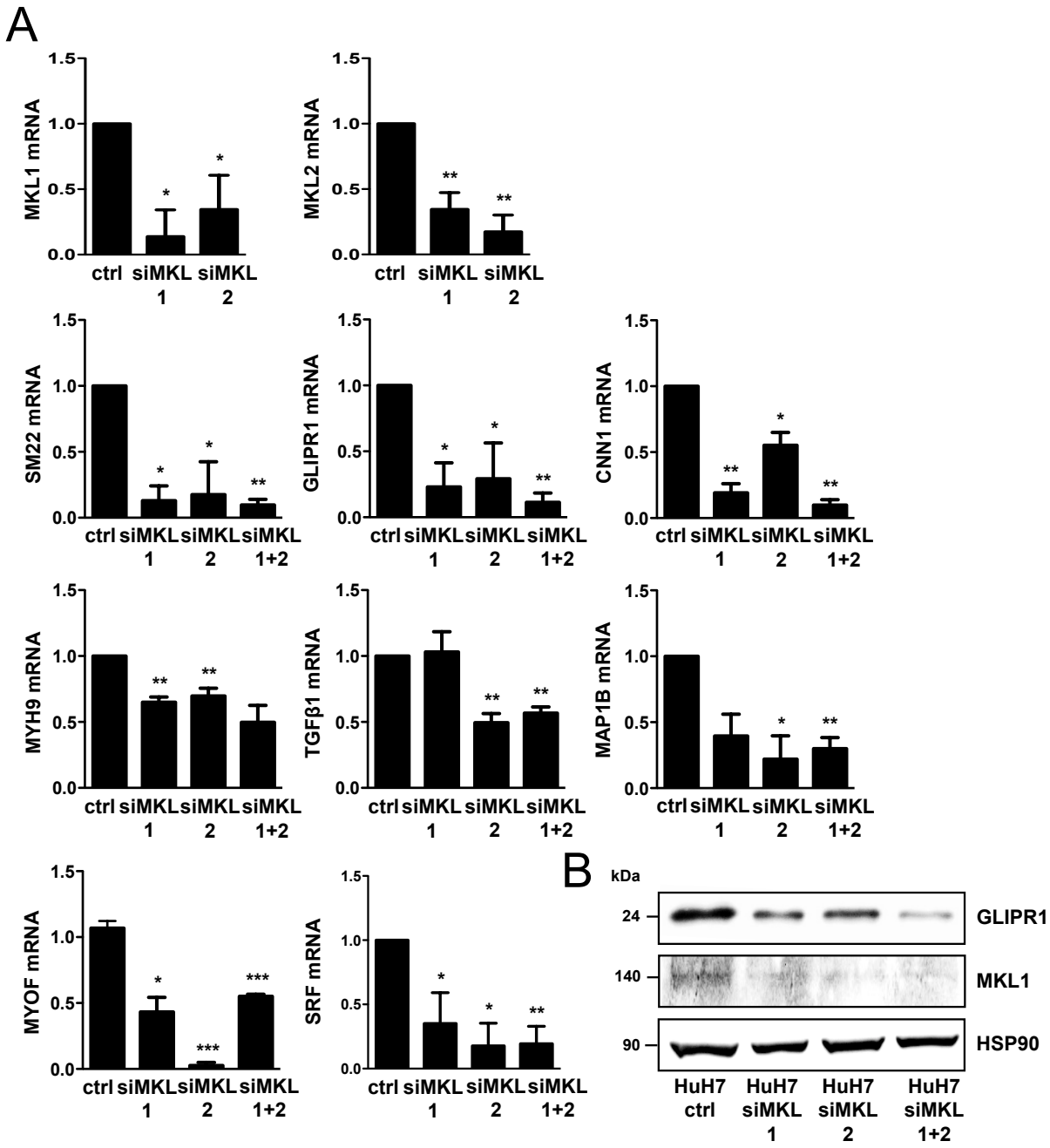

Figure 15: MKL1 or MKL2 knockdown is sufficient for target gene downregulation. (A) HuH7 cells were transfected with negative control (ctrl), MKL1, MKL2 or the combination of MKL1 and MKL2 siRNAs. mRNA expression of target genes was analysed by qRT-PCR using the respective gene specific primers and 18S rRNA primers for normalization. Values are mean ± SD (n=3); *p<0.05, **p<0.01, ***p<0.001. **(B)** Lysates of HuH7 cells transfected as in (A) were immunoblotted with anti-GLIPR1, anti-MKL1 and anti-HSP90 antibodies as loading control.

6.1.2 Mutual dependence of MKL1 and MKL2 in HCC cell lines

Since siRNA mediated knockdown of MKL1 led to a significant reduction of MKL2 mRNA and also a knockdown of MKL2 resulted in a strongly reduced MKL1 mRNA expression in HuH7

cells (Fig. 15A, top), we tried to confirm these findings in HuH6 (Fig. 16A) and HepG2 (Fig. 16B) cells. In both cell lines, we could observe the same result as in HuH7 cells. The MKL1 knockdown resulted in reduced protein (Fig. 16A) and mRNA (Fig. 16B) expression levels of MKL2 and the other way around. This result explains also why a single knockdown of MKL1 or MKL2 was sufficient for target gene downregulation and no combination of both siRNAs was needed.

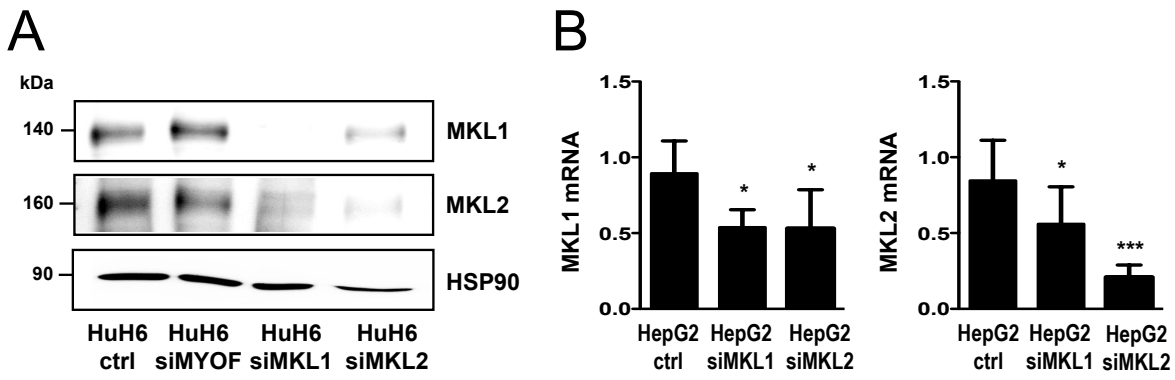

Figure 16: Mutual dependence of MKL1 and MKL2 in HCC cells. (A) HuH6 cells were transfected with negative control, MKL1 or MKL2 siRNA. Lysates were immunoblotted with anti-MKL1, anti-MKL2 and anti-HSP90 antibodies as loading control. **(B)** MKL1 and MKL2 mRNA expression of HepG2 cells transfected as in (A) was determined by qRT-PCR. Values are mean ± SD (n=3); *p<0.05, ***p<0.001.

In order to demonstrate that the given results of MKL1/2 target gene downregulation and mutual dependence of MKL1 and MKL2 in HCC cell lines are not only an effect of unspecific binding and a crossreactivitiy of the used siRNAs, we used second variants of MKL1 and MKL2 siRNAs that are directed against another sequence of MKL1 and MKL2 mRNA. The siRNA mediated silencing of MKL1 or MKL2 in HuH7 cells with these second variants of siRNA (siRNA V2) showed a good knockdown efficiency and also a mutual dependence of MKL1 and MKL2 where MKL1 knockdown reduced the MKL2 mRNA expression and vice versa (Fig. 17A). We also observed a downregulation of the new target genes, like GLIPR1 and CNN1 upon MKL1 knockdown and a downregulation of SM22 and MYOF upon MKL2 knockdown (Fig. 17B). Summing up the results of the RNAi experiments described above and the demonstration of the specificity of MKL1 and MKL2 downregulation, we can postulate the discovery of 6 new MKL1 and MKL2 dependent target genes functioning as possible mediators of the effects of MKL1/2 on HCC growth arrest and senescence induction (Hampl et al., 2013).

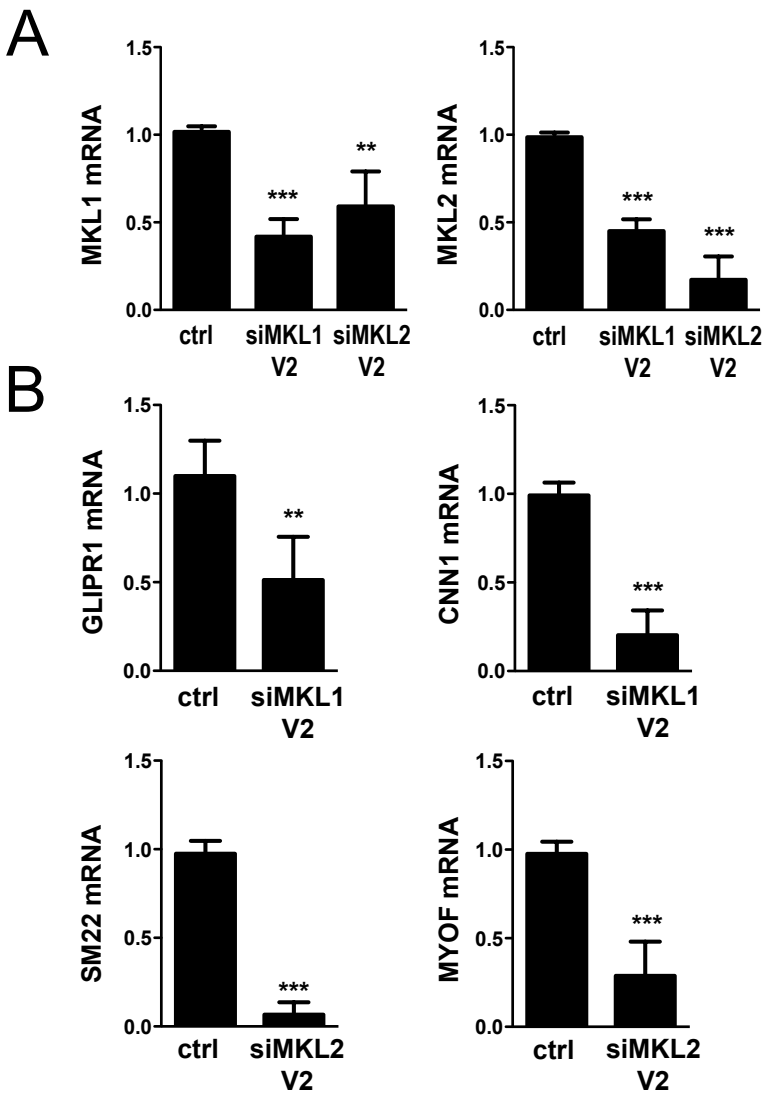

Figure 17: MKL1 or MKL2 knockdown by second variants of MKL1 and MKL2 siRNA. HuH7 cells were transfected with negative control or a second variant of MKL1 or MKL2 siRNA. Knockdown efficiency of MKL1 and MKL2 **(A)** and mRNA expression of GLIPR1, CNN1, SM22 and MYOF **(B)** were subjected to qRT-PCR. Values are mean ± SD (n=3); **p<0.01, ***p<0.001.

6.1.3 Regulation of newly identified target genes upon stimulant or inhibitor treatment

After demonstrating the dependency of the target genes on MKL1 and MKL2, we next focused our interest on the influence of stimuli or inhibitors on gene expression of the newly identified target genes. Since MKL1 is activated via the Rho/actin signaling axis (Miralles et al., 2003 and Muehlich et al., 2008), we wanted to focus our next experiments on the direct effect of stimulating or inhibiting reagents on the target gene level.

6.1.3.1 Inhibition of target genes upon LatB treatment

The first extracellular inhibitor whose role on target gene expression we investigated was Latrunculin B (LatB). LatB is still known as an actin polymerization inhibitor and prevents filamentous F-actin polymerization from monomeric G-actin by binding to G-actin monomers (Yarmola et al, 2000). Performing qRT-PCR analysis, we found a significantly reduced gene expression of the transcription factor SRF and also of the MKL1/2 target genes SM22, CNN1, GLIPR1, MYH9 and MYOF upon LatB treatment of the cells (Fig. 18).

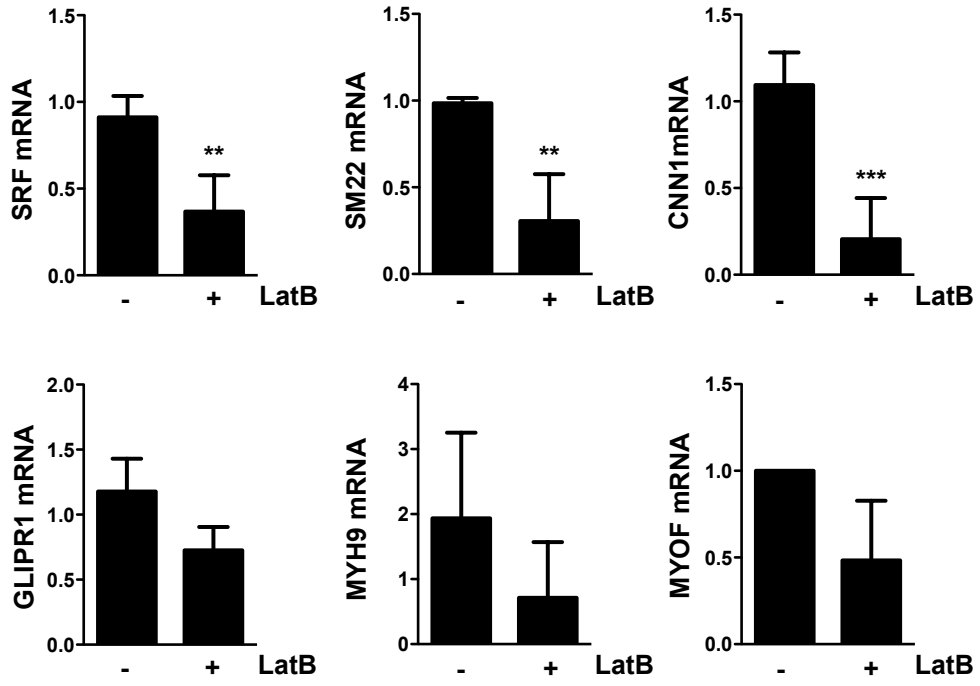

Figure 18: Downregulation of target genes upon LatB treatment. SRF and target gene mRNA expression of A7 cells treated with or without 0.3 µM LatB for 45 min was analysed by qRT-PCR with SRF, SM22, CNN1, GLIPR1, MYH9, MYOF and 18S rRNA primers for normalization. Values are mean ± SD (n=3 for SRF, SM22 and CNN1); **p<0.01, ***p<0.001.

6.1.3.2 Stimulation of target genes upon serum (FBS) treatment

In contrast to the LatB induced target gene inhibition we next assessed the role of serum, in detail fetal bovine serum (FBS) treatment on gene expression. Serum acting on the Rho/actin signaling pathway has been shown to increase the actin polymerization from monomeric G-actin to filamentous F-actin leading to nuclear localization of MKL1 (Miralles et al., 2003). As expected, FBS treatment of NIH 3T3 fibroblast and HepG2 hepatocellular

carcinoma cells having cytoplasmic MKL1 under unstimulated conditions showed a stimulatory effect on gene expression (Fig. 19). SRF itself, SM22 and CNN1 expression is induced in NIH 3T3 (Fig. 19A) and HepG2 (Fig. 19B) cells upon serum stimulation confirming the known mechanism of MKL1 translocation into the nucleus, its activation of SRF and therefore enhanced target gene transcription.

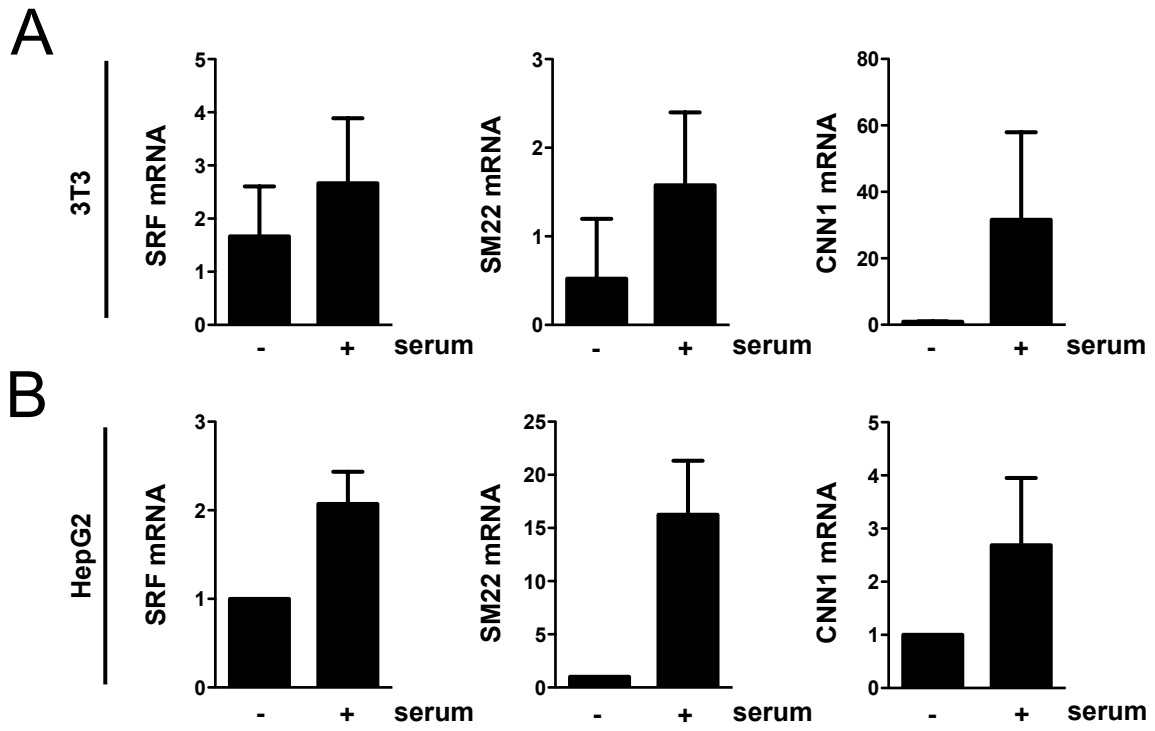

Figure 19: Increased target gene expression upon serum (FBS) stimulation. NIH 3T3 **(A)** and HepG2 **(B)** cells were serum-starved for 16 h and then stimulated with 20% FBS for 2 h. mRNA expression of SRF, SM22 and CNN1 was analysed by qRT-PCR.

6.1.3.3 Stimulation of target genes upon LPA treatment

As additional stimulation of cells and as an active component of serum we analysed the role of lysophosphatidic acid (LPA) on gene expression. LPA is a potent signaling molecule involved in the alteration of many cellular processes and enhances, similar to serum, actin polymerization into F-actin filaments (Muehlich et al., 2004 and Lin et al., 2010). In this experiment, we found SRF and many target genes upregulated by LPA stimulation in HepG2 (Fig. 20A) and MCF7 cells (Fig. 20B) and also in human primary fibroblasts (Fig. 20C) all showing MKL1 in the cytoplasm in an unstimulated status.

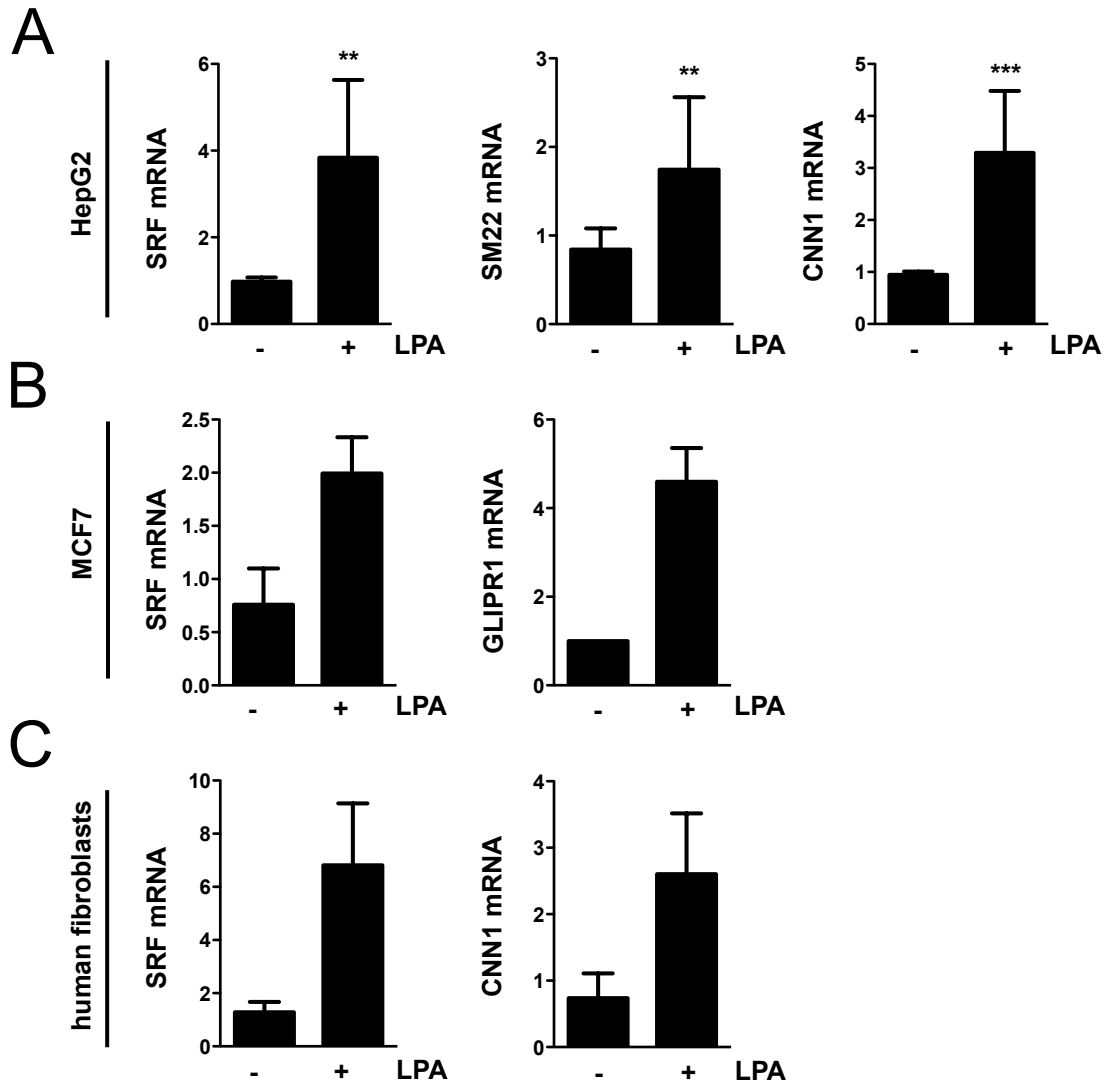

Figure 20: Upregulation of target genes upon LPA treatment. HepG2 **(A)**, MCF7 **(B)** and primary human fibroblasts **(C)** were serum-starved for 16 h and then stimulated with 10 µM LPA for 2 h. mRNA expression of the indicated genes was analysed by qRT-PCR. Values are mean ± SD (n=3 for HepG2); **p<0.01, ***p<0.001.

6.1.3.4 Stimulation of target genes upon CytoD treatment

Following the target gene inhibition by LatB and the stimulation by FBS and LPA, we next focused on the gene expression alteration due to Cytochalasin D (CytoD) treatment. Performed qRT-PCR analyses revealed a strong stimulatory effect on target gene mRNA expression in different cell lines, namely NIH 3T3, HepG2, HLF and MCF7 (Fig. 21A-D), all having MKL1 in the cytoplasm under untreated conditions.

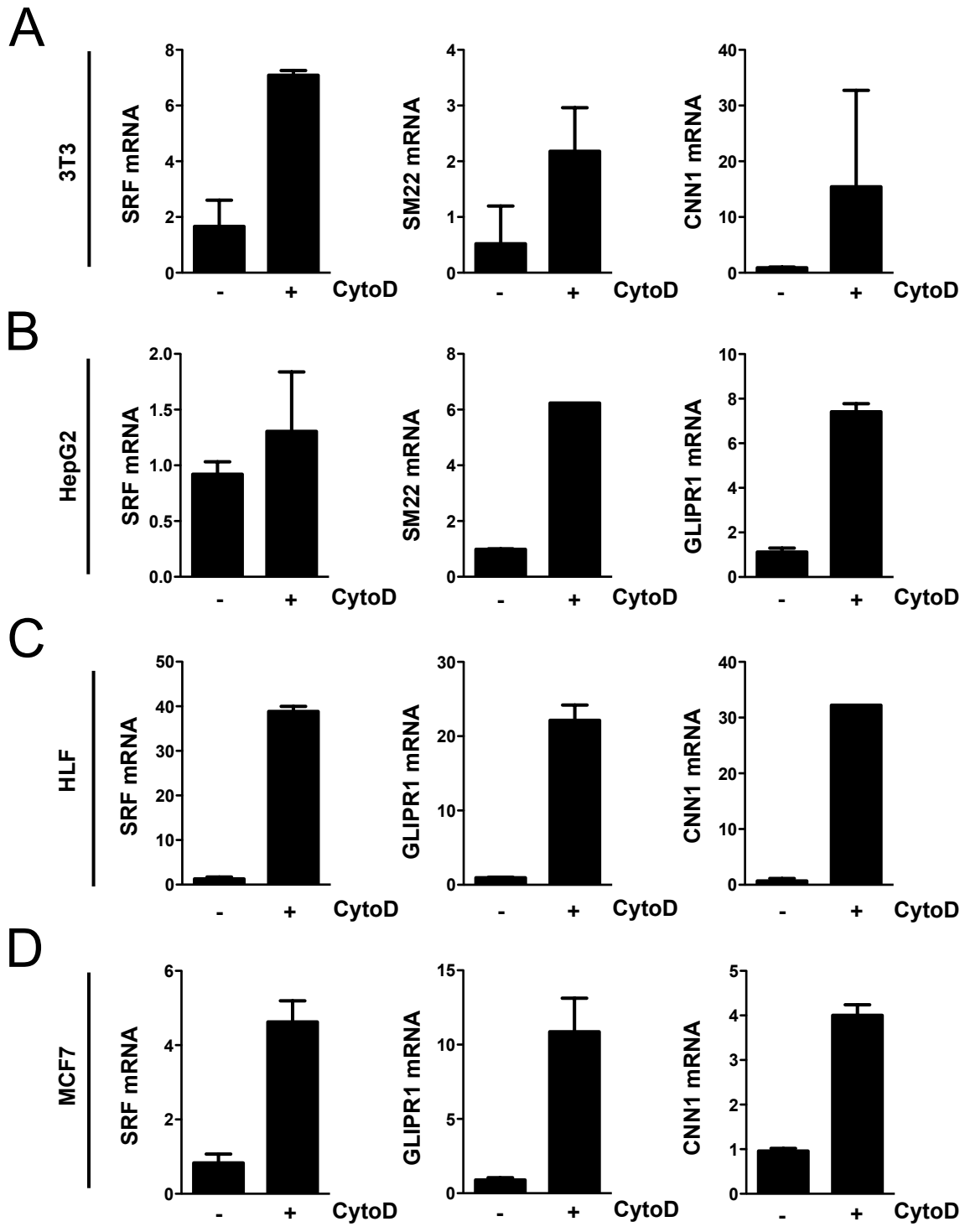

Figure 21: Upregulation of target gene expression upon CytoD treatment in cell lines with cytoplasmic MKL1. NIH 3T3 **(A)**, HepG2 **(B)**, HLF **(C)** and MCF7 **(D)** cells were treated with 2 µM CytoD for 2 h and mRNA expression of the indicated genes was determined by qRT-PCR using the gene specific primers and 18S rRNA primers for normalization.

In contrast to the shown stimulating effect of CytoD, treatment of HuH7 and MDA-MB 468 cells with CytoD revealed no or only modest effects on target gene expression (Fig. 22A-B). These two cell lines still own nuclear MKL1 due to their deficiency in DLC1 (Muehlich et al., 2012) and therefore have activated SRF and constant high levels of target gene expression explaining why stimulation with CytoD doesn't result in enhanced gene expression.

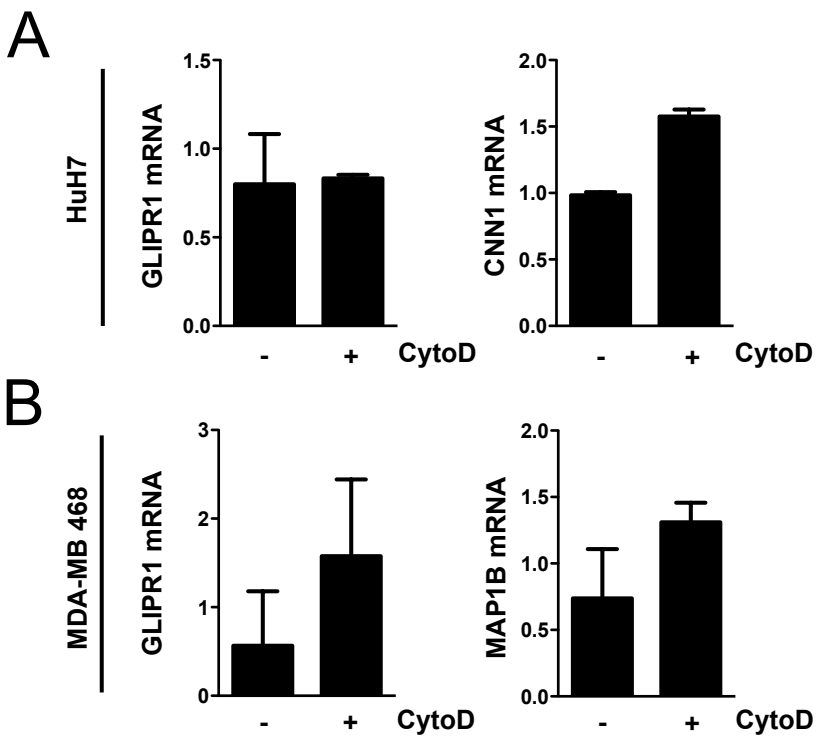

Figure 22: CytoD treatment has nearly no effect on target gene expression in cell lines with nuclear MKL1. HuH7 **(A)** and MDA-MB 468 **(B)** cells were treated with 2 µM CytoD for 2 h. mRNA expression of the indicated genes was analysed by qRT-PCR.

6.2 FLNa as novel binding partner of MKL1

In a recent study of our group, we identified a new interaction partner for MKL1, the Filamin A (FLNa) protein (Kircher et al., 2015). We therefore analysed the requirement of the MKL1-FLNa interaction for the expression of the newly identified target genes and tested the dependency of the novel MKL1/2 target genes on FLNa.

6.2.1 The effect of MKL1/2 in A7 cells

We performed all the following experiments in A7 melanoma cells constitutively expressing FLNa or in FLNa deficient M2 melanoma cells. Both cell lines were dominantly used for experiments showing the interaction of FLNa and MKL1 in the study of Kircher *et al.* (2015) and thus we first investigated the role of MKL1/2 in A7 cells expressing FLNa additionally to the experiments in HCC cell lines shown above.

6.2.1.1 MKL1/2 target gene downregulation upon MKL1/2 knockdown in A7 cells

We first focused on the MKL1/2 dependent target genes and looked for their responsiveness to MKL1/2 knockdown in A7 melanoma cells. qRT-PCR experiments revealed a good knockdown efficiency for MKL1 and MKL2 and also a strong downregulation of the target genes SM22, GLIPR1, CNN1, MAP1B and MYH9 (Fig. 23). Also the expression of FLNa, the novel binding partner of MKL1, was strongly decreased (Fig. 23) showing the direct influence of MKL1/2 on the FLNa expression.

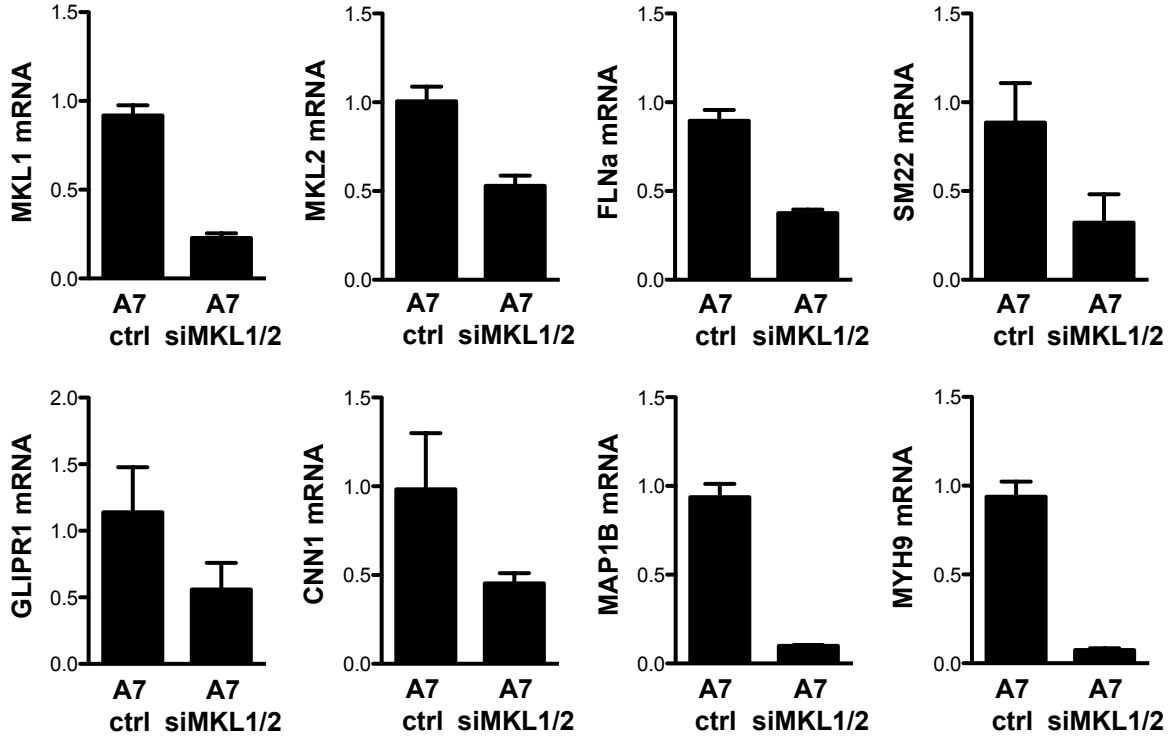

Figure 23: Downregulation of FLNa and MKL1/2 target genes upon MKL1/2 knockdown in A7 cells. A7 cells were transfected with negative control or MKL1/2 siRNA and mRNA expression was measured by qRT-PCR using the gene specific primers. Values are mean ± SD (n=2).

Additionally, we assessed the role of a single MKL1 knockdown on target gene regulation. We obtained a good knockdown efficiency by using MKL1 siRNA and also observed reduced MKL2 and FLNa mRNA levels in the knockdown cells (Fig. 24, top). Here we found the same phenomenon like in HCC cells showing a mutual dependence of MKL1 and MKL2 where a depletion of MKL1 results also in decreased MKL2 expression. The FLNa mRNA expression was also strongly reduced after the single MKL1 knockdown demonstrating the relevance of MKL1 expression for FLNa once again (Fig. 24, top). Also the target genes MAP1B and an already known and characterized target gene of MKL1, the connective tissue growth factor (CTGF) (Muehlich et al., 2007), were downregulated by MKL1 depletion (Fig. 24, bottom) pointing out an important role for MKL1 in the regulation of target genes in melanoma cells. We also looked for the endogenous expression levels of MKL1 and MKL2 in A7 cells and observed much higher mRNA expression levels of MKL1 compared to MKL2 mRNA expression (Fig. 24 bottom, right) also explaining that a single MKL1 knockdown suffices for target gene downregulation and that a knockdown of both MKL1 and MKL2 is not required in A7 cells.

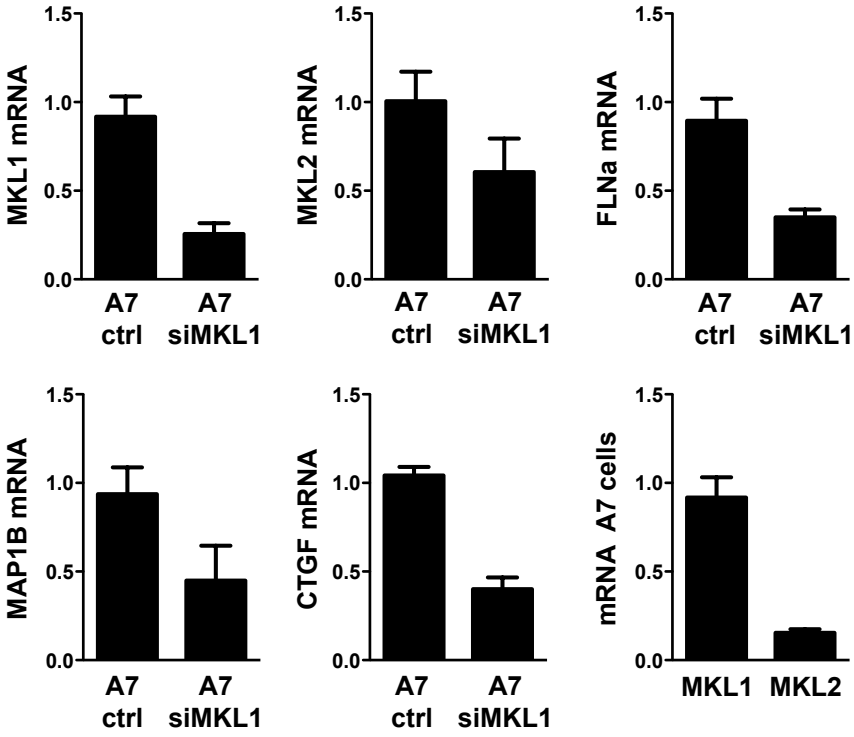

Figure 24: Downregulation of FLNa, MAP1B and CTGF upon MKL1 knockdown in A7 cells. MKL1 knockdown efficiency and MKL2, FLNa, MAP1B and CTGF mRNA expression of A7 ctrl and A7 siMKL1 were analysed by qRT-PCR. Values are mean ± SD (n=2). Also the mRNA expression levels of MKL1 and MKL2 in A7 cells were investigated by qRT-PCR.

6.2.1.2 Knockdown of MKL1/2 leads to proliferation arrest and senescence in A7 cells

After showing a dependence of the target gene expression on MKL1 and MKL2 in A7 melanoma cells, we also performed a proliferation assay for further characterization of A7 cells. We therefore transiently depleted MKL1/2 via RNAi and compared the proliferation properties of A7 control and A7 siMKL1/2 cells. This assay revealed a strongly inhibited cell proliferation of cells lacking MKL1/2 expression (Fig. 25).

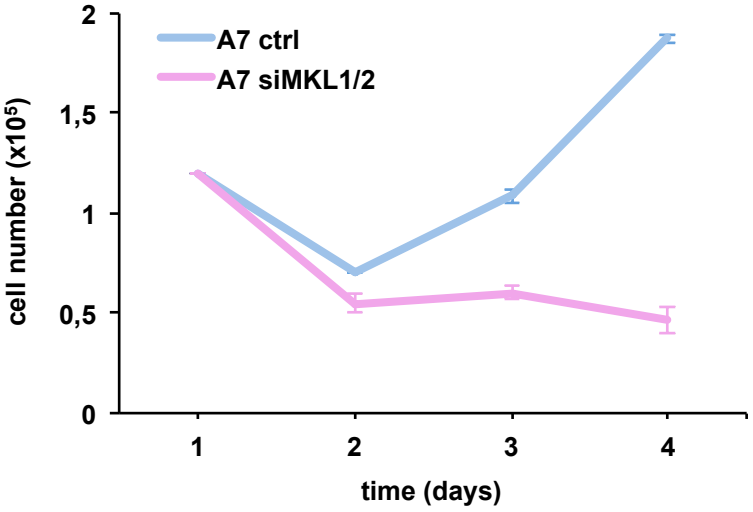

Figure 25: MKL1/2 siRNA leads to proliferation arrest in A7 cells. A7 cells were transfected with negative control or MKL1/2 siRNA and counted daily for 4 days.

Since in MKL1+2 depleted HCC cells the reduced proliferation rates were due to oncogene-induced senescence, we also tested the senescence induction of A7 cells with MKL1+2 knockdown. Performing senescence associated β-galactosidase staining, we observed a potent increase of senescent A7 cells upon MKL1+2 knockdown (Fig. 26, left). Also a single knockdown of MKL1 alone was sufficient for senescence induction in A7 cells very similar to the amount of senescent cells with a knockdown of both MKL1 and MKL2 (Fig. 26, right).

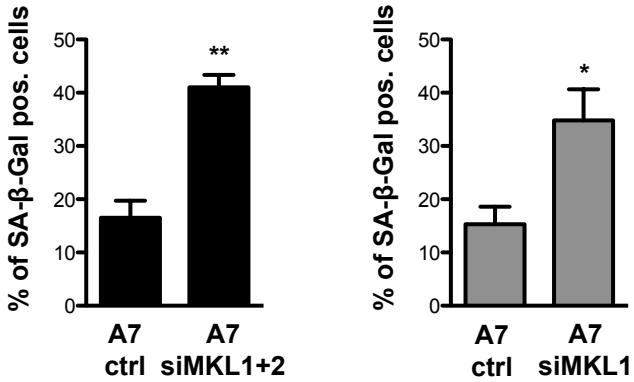

Figure 26: Senescence induction upon MKL1+2 and MKL1 siRNA in A7 cells. Senescence associated β-galactosidase staining was performed in A7 ctrl and A7 siMKL1+2 (left) and siMKL1 (right) cells. Numbers of SA-β-gal positive cells were counted. Values are mean ± SD (n=3); *p<0.05, **p<0.01.

Based on these results that MKL1 and/or MKL2 contribute to cell proliferation and senescence induction also in melanoma cells thereby recapitulating the results shown in HCC cells above we could demonstrate that senescence induction is a general phenomenon.

6.2.2 Impact of FLNa on target gene expression

6.2.2.1 Newly identified target genes are FLNa dependent

Another aim of this thesis was to demonstrate the dependency of the newly identified MKL1/2 target genes on FLNa in different cell lines. Therefore, we introduced FLNa siRNA into HepG2 hepatocellular carcinoma cells, MDA-MB 468 mammary carcinoma cells, A7 melanoma cells and NIH 3T3 fibroblasts (Fig. 27A-D) and found strongly reduced target gene mRNA expressions as well as a good knockdown efficiency of FLNa itself. We can conclude that the MKL1/2 dependent target genes are not only MKL1/2 dependent but also FLNa dependent and thus, FLNa was shown to be essential for MKL1 transcriptional activity.

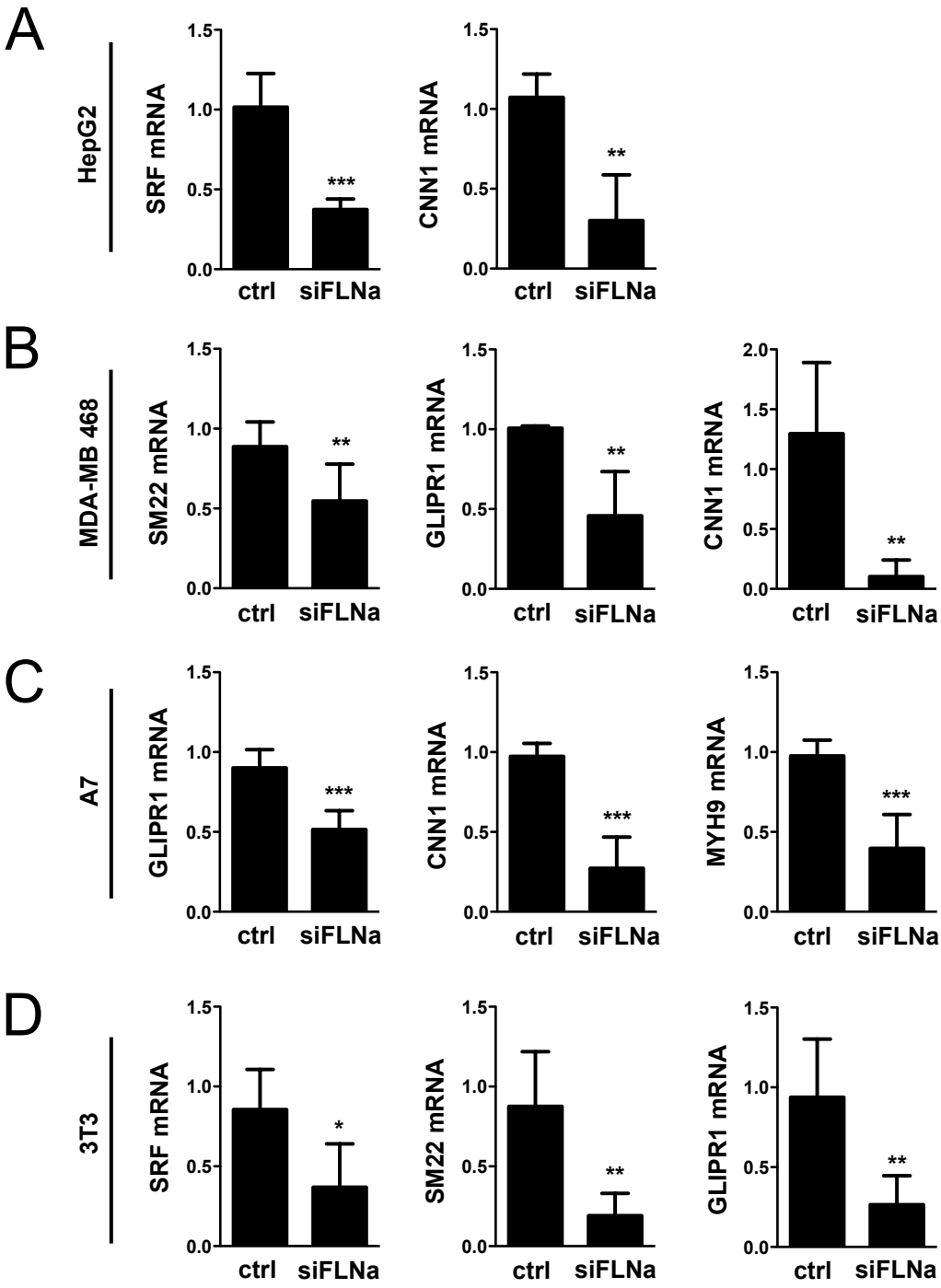

Figure 27: Target gene downregulation upon FLNa knockdown in different cell lines. HepG2 **(A)**, MDA-MB 468 **(B)**, A7 **(C)** and NIH 3T3 **(D)** cells were transfected with negative control or FLNa siRNA. Knockdown efficiency of FLNa and mRNA expression of the indicated genes were analysed by qRT-PCR and normalized to 18S rRNA expression levels. Values are mean ± SD (n=3); *p<0.05, **p<0.01, ***p<0.001.

6.2.2.2 Target gene upregulation upon MKL1 S454A expression

To give further mechanistic insights into the activation of target genes by MKL1 and the influence of FLNa expression, we transfected A7 cells with MKL1 wt or the MKL1 S454A plasmid, bearing a mutation in the phosphorylation site of MKL1 preventing MKL1 from being phosphorylated. This way, we found increased SRF and GLIPR1 expression levels upon MKL1 wt expression compared to the endogenous levels of MKL1 in A7 cells (Fig. 28). Furthermore, we still observed an even stronger induction of SRF and GLIPR1 expression upon MKL1 S454A mutant overexpression (Fig. 28) suggesting that MKL1 becomes constitutively active due to reduced phosphorylation and therefore stronger activates the target gene expression. The same effect of increased target gene expression with the MKL1 S454A mutant compared to the MKL1 wt expression was detectable in A7 cells silenced of FLNa by siRNA, in which however the total amount of SRF and GLIPR1 expression was much less than in the FLNa expressing cells (Fig. 28) suggesting an important role for FLNa also in the presence of activated MKL1.

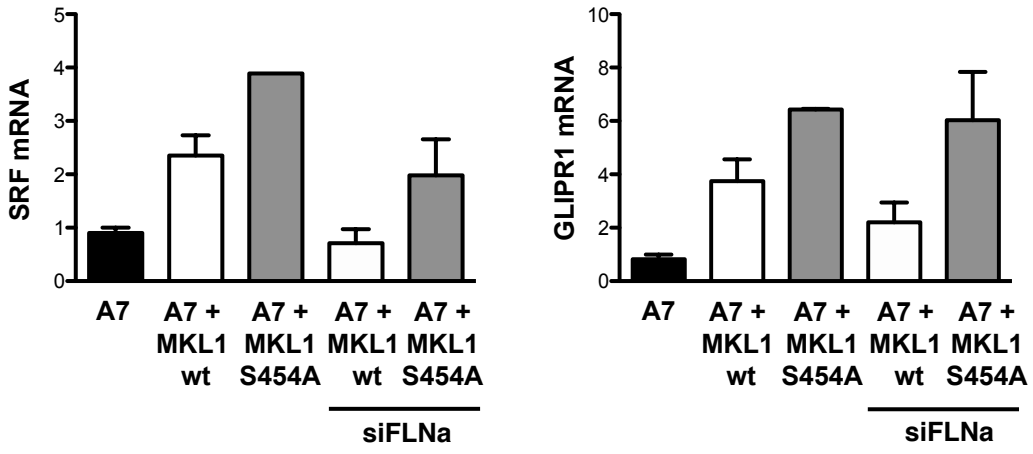

Figure 28: Increased mRNA expression of SRF and GLIPR1 upon MKL1 S454A overexpression. A7 ctrl and A7 siFLNa cells were transfected with MKL1 wt or the MKL1 S454A mutant. SRF and GLIPR1 mRNA expression was assessed by qRT-PCR.

6.2.2.3 Enhanced target gene expression upon constitutive active MKL1 in the presence of FLNa

Beside the described important role of FLNa existence for a stronger target gene upregulation, also in the context of constitutively active MKL1, we further wanted to analyze the FLNa dependency of MKL1-induced target gene expression. For comparing the effects obtained by FLNa presence or absence, we used the FLNa expressing cell line A7 and the FLNa deficient cell line M2. We overexpressed the MKL1 wildtype (wt) or a constitutively active and siRNA resistant form of MKL1, the MKL1 N100 mutant, in A7 control cells and A7 cells with FLNa knockdown (siFLNa) and also in M2 cells and verified the mRNA expression levels of the target genes SM22 and GLIPR1 by qRT-PCR analysis. SM22 as well as GLIPR1 expressions were significantly upregulated upon constitutive active MKL1 expression in A7 control cells (Fig. 29). In contrast, the induction of SM22 and GLIPR1 upon MKL1 N100 overexpression in FLNa lacking cells showed only modest effects compared to the MKL1 wt expression and also compared to the strong gene induction in A7 control cells (Fig. 29). This experiment underscores the importance of FLNa presence for MKL1/2 dependent target gene expression.

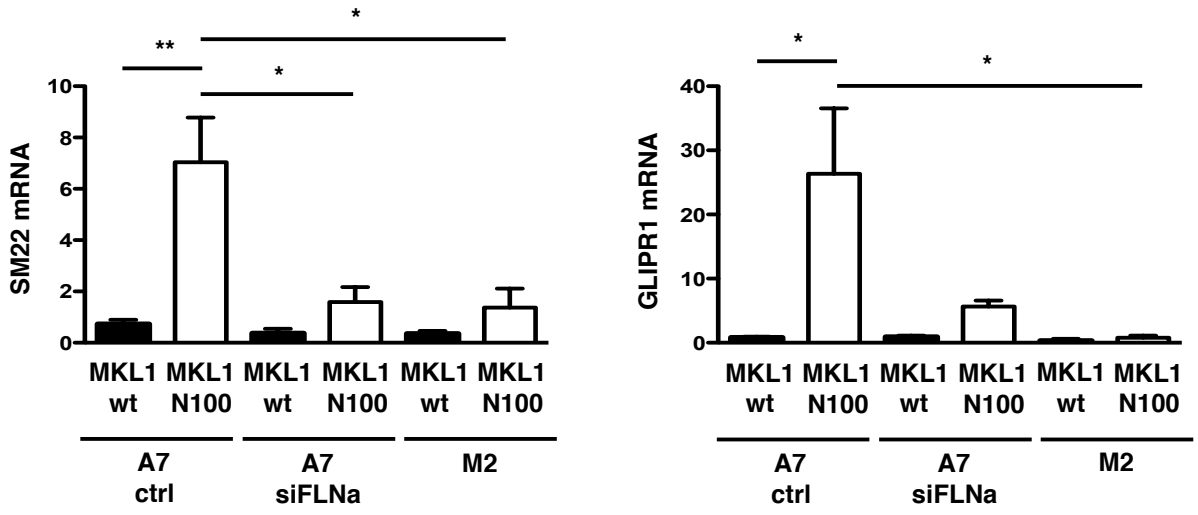

Figure 29: Target gene downregulation in FLNa deficient cells upon MKL1 N100 overexpression. SM22 and GLIPR1 mRNA expressions in A7 ctrl, A7 siFLNa and M2 cells either transfected with MKL1 wt or MKL1 N100 mutant were analysed by qRT-PCR using SM22, GLIPR1 and 18S rRNA primers. Values are mean ± SD (n=3); *p<0.05, **p<0.01.

6.2.3 Generation of MKL1 mutants lacking FLNa binding

After confirming the relevance of FLNa presence for MKL1 activation and subsequently target gene expression, we wanted to figure out the effect of FLNa nonbinding mutants on MKL target gene expression. By a recent study of our group, the MKL1 mutant lacking the amino acids 301-342 (MKL1 Δ301-342) was found to be essential for FLNa binding (Kircher et al., 2015). To prove the effect of this mutant on the target gene induction, we performed qRT-PCR analysis in A7 control cells and A7 cells overexpressing the MKL1 wt and the MKL1 Δ301-342 mutant. Beside a strong MKL1 induction upon overexpression of MKL1 wt, SM22 and GLIPR1 were, as expected, strongly upregulated in cells expressing the MKL1 wt plasmid (Fig. 30). However, mRNA expression of SM22 and GLIPR1 in A7 cells with overexpressed MKL1 Δ301-342 was significantly reduced compared to the cells expressing MKL1 wt (Fig. 30) showing that FLNa binding to MKL1 is essential for target gene expression.

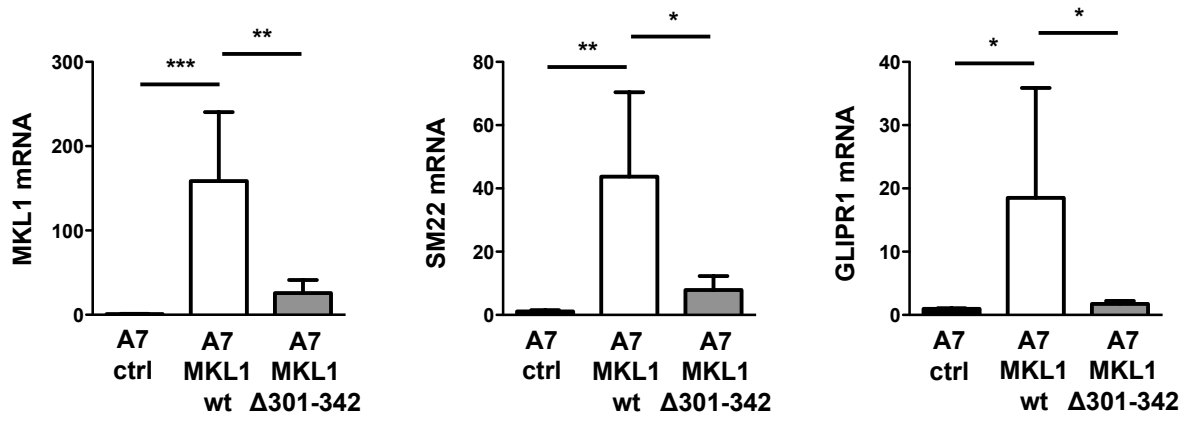

Figure 30: Reduced target gene expression upon overexpression of MKL1 deletion mutant Δ301-342. A7 cells were transfected with empty vector (ctrl), MKL1 wt or the MKL1 deletion mutant Δ301-342 for 24 h. mRNA expression of MKL1, SM22 and GLIPR1 was measured by qRT-PCR with MKL1, SM22, GLIPR1 and 18S rRNA primers for normalization. Values are mean ± SD (n=3); *p<0.05, **p<0.01, ***p<0.001.

For postulating a more precise binding site sequence of FLNa on MKL1, we generated MKL1 mutants deleted of only the amino acids 301-310 and overexpressed this mutant or the MKL1 wt in A7 cells. Again, we found strongly increased levels of MKL1, SM22 and CTGF expression in A7 cells with overexpressed MKL1 wt (Fig. 31) but overexpression of MKL1 Δ301-310 strongly decreased the induced mRNA expression of target genes observed upon MKL1 wt expression.

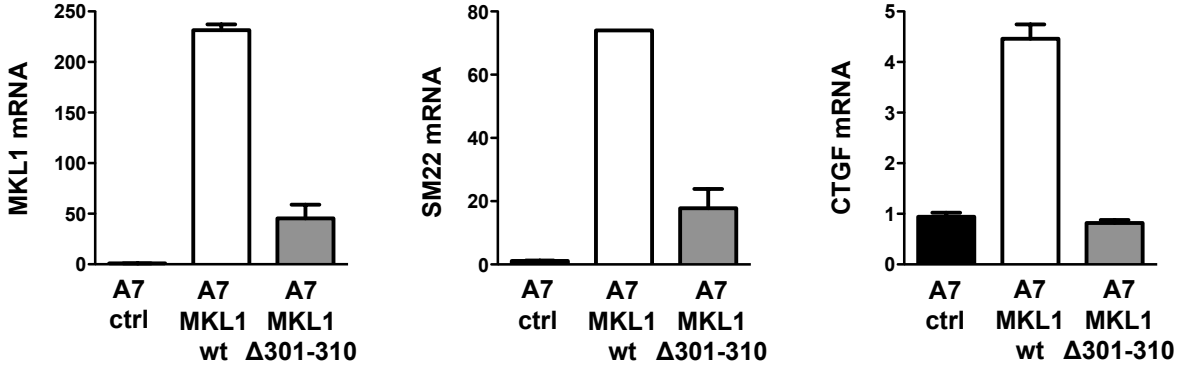

Figure 31: Reduced target gene expression upon overexpression of MKL1 deletion mutant Δ301-310. mRNA expression of MKL1, SM22 and CTGF in A7 cells overexpressing an empty vector (ctrl), MKL1 wt or the MKL1 deletion mutant Δ301-310 was analysed by qRT-PCR as described above. Values are mean ± SD (n=2).

6.2.4 Direct recruitment of FLNa to promoters

To further investigate the role of FLNa in activating target genes, we performed chromatin immunoprecipitation (ChIP) analysis with a specific FLNa antibody for pulldown in both A7 and M2 cells. CTGF and actin promoters were strongly amplified from FLNa immunoprecipitates whereas GAPDH serving as negative control doesn't show induced promoter occupancy in A7 cells (Fig. 32). This enrichment of CTGF and actin was only observable in A7 but not in M2 cells (Fig. 32) concluding that FLNa directly controls the target gene and actin expression by binding to its promoters.

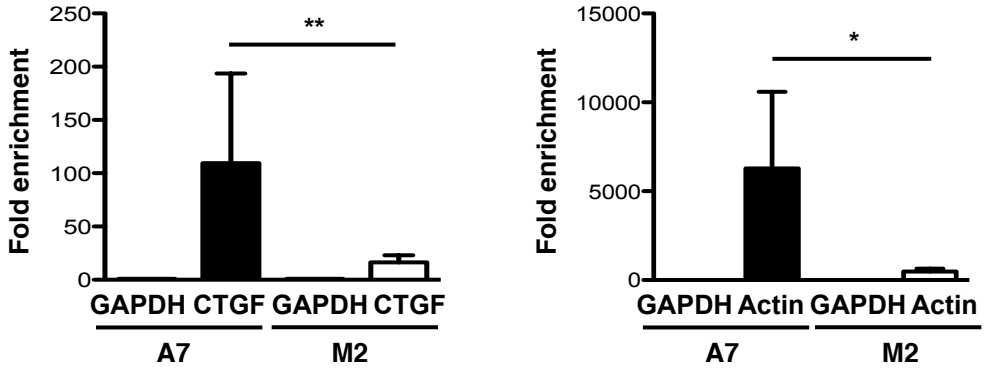

Figure 32: FLNa recruitment to the CTGF and actin promoters. ChIP was performed using a specific FLNa antibody for immunoprecipitation in FLNa-expressing A7 and FLNa-deficient M2 cells and specific primers for CTGF (left), actin (right) and GAPDH promoters for qRT-PCR. Values are mean ± SD (n=3); *p<0.05, **p<0.01.

6.2.5 Influence of actin expression

6.2.5.1 Increased target gene expression upon mDiact expression

In the last part of this chapter, we further analysed the impact of actin on FLNa and thus the target gene expression. We overexpressed for the following approaches the FLNa wt and/or mDiact, a protein of the formin family and Rho effector that is a constitutively active variant of mDia1 being predominantly located in the nucleus, in M2 or A7 cells and monitored gene expression by qRT-PCR analysis. Since mDiact interacts with the barbed ends of actin it accelerates the actin nucleation and elongation of G-actin into F-actin (Watanabe et al., 1999 and Baarlink et al., 2013). M2 cells with overexpressed FLNa showed, as expected, a strong induction of FLNa and GLIPR1 (Fig. 33) but a much stronger induction of GLIPR1 expression was obtained by transfection with FLNa wt and mDiact in parallel (Fig. 33).

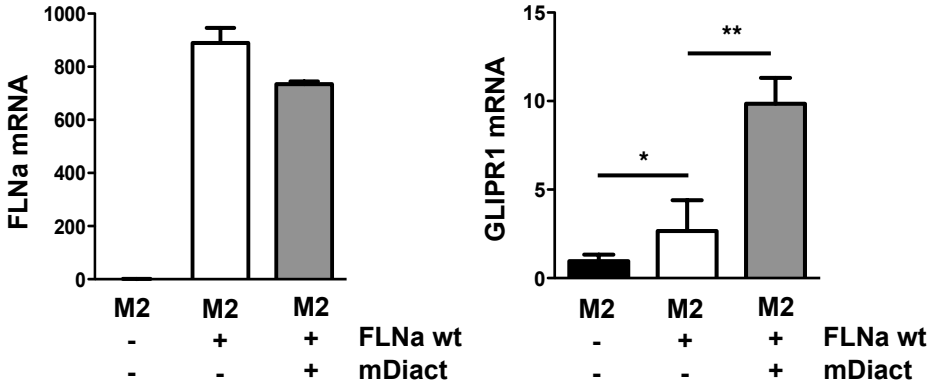

Figure 33: Increased GLIPR1 mRNA expression upon FLNa and mDiact overexpression. M2 cells were transfected with mDiact and/or FLNa wt. mRNA expression of FLNa and GLIPR1 was determined by qRT-pCR. Values are mean ± SD (n=3 for GLIPR1); *p<0.05, **p<0.01.

Similar to the experiments performed in M2 cells, we overexpressed mDiact in A7 cells still expressing FLNa and observed higher mRNA expression rates of the transcription factor SRF and the target genes SM22, GLIPR1 and CTGF (Fig. 34). Underlying these results, mDiact seems to provoke enhanced mRNA expression by actin nucleation and F-actin formation in the presence of FLNa.

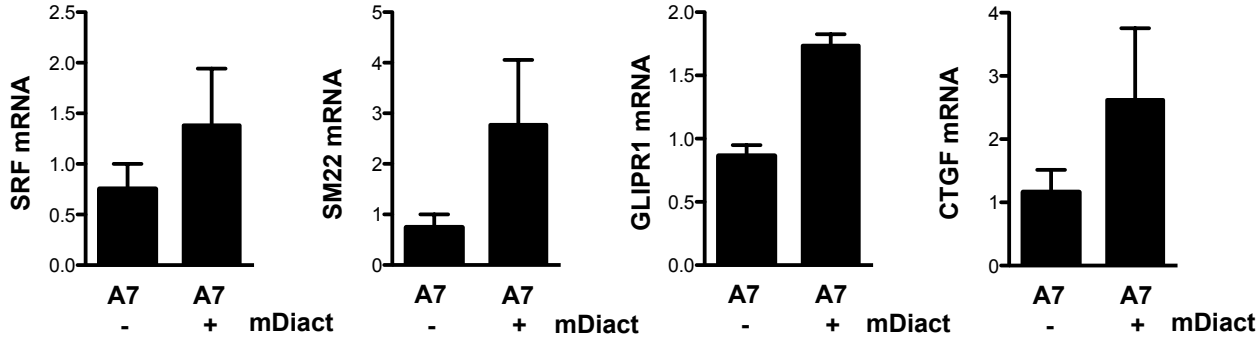

Figure 34: Increased target gene expression upon mDiact overexpression. mRNA expression of A7 cells transfected with or without mDiact was analysed by qRT-PCR. Values are mean ± SD (n=2).

6.3 The target gene myoferlin

Based on the performed microarray and the identified 8 target genes strongly depending on MKL1/2 expression, we had to choose one of these genes that may mediate the effects of MKL1/2 on reduction of tumorigenesis and senescence induction. The identified target gene myoferlin (MYOF) showed the strongest downregulation in HCC xenografts after MKL1/2 siRNA treatment (Hermanns et al., 2017) and also plays an important role in mammary carcinoma cells as reported in a recent study (Turtoi et al., 2013). We therefore focused in this thesis on the transmembrane protein myoferlin to get a deeper insight into the mechanism of the MKL1/2 mediated effects on cell signaling pathways and essential biological processes, such as cell proliferation, cell migration and cell invasion.

6.3.1 Characterization of myoferlin

First of all, we had to characterize myoferlin in greater detail especially in the context of hepatocellular carcinoma and had a look at the signaling pathways of myoferlin activation and regulation. In Fig. 13 and Fig. 15 we demonstrated that MYOF is directly depending on the MKL1 and MKL2 expression levels where a knockdown of MKL1 and/or MKL2 resulted in strongly reduced levels of MYOF mRNA expression.

6.3.1.1 Myoferlin expression is enhanced upon stimulation

To show that MYOF is regulated by the RhoA-actin signaling pathway, we serum-starved HuH7 and MDA-MB 468 cells for 16 h and then stimulated them with FBS (serum), lysophosphatidic acid (LPA), Cytochalasin D or Jasplakinolide. In both cell lines we found increased myoferlin expression levels upon treatment with the mentioned stimulants (Fig. 35) indicating that MYOF is directly regulated by this agents and activated by the RhoA signaling pathway.

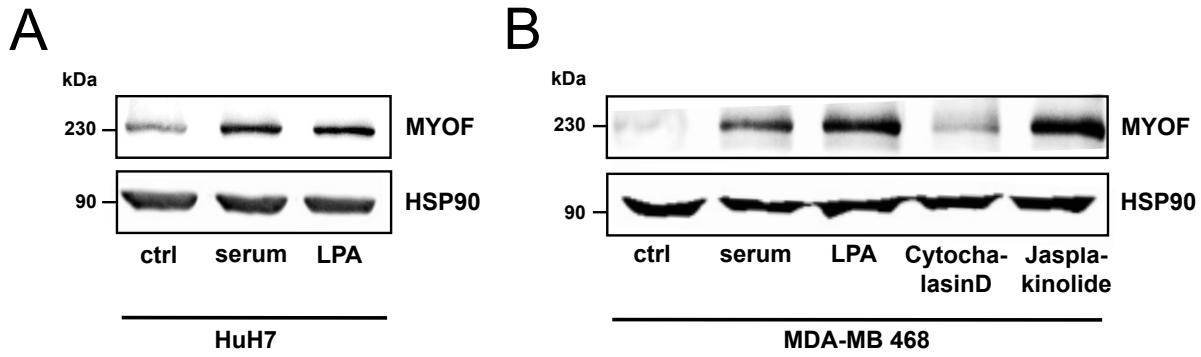

Figure 35: Myoferlin expression is upregulated upon stimulants. HuH7 cells were serum-starved for 16 h and then stimulated with 20 % FBS (serum) or 10 µM LPA for 2 h **(A)** and MDA-MB 468 cells were treated with 20 % FBS (serum), 10 µM LPA, 2 µM Cytochalasin D or 0.5 µM Jasplakinolide **(B)**. Lysates were immunoblotted with anti-MYOF and anti-HSP90 antibodies.

6.3.1.2 MKL1 and SRF bind to the myoferlin promoter

Next, we generated various MYOF promoter constructs and investigated the role of MKL1 and SRF on MYOF expression as direct transcriptional regulators and performed reporter gene assays with these different MYOF promoter constructs (Fig. 36A). The activity of the indicated MYOF promoter constructs was measured due to the overexpression of the constitutively active forms of SRF, SRF-VP16, and MKL1, MKL1 N100. The activity of the 900 bp promoter construct but not of the 200 bp promoter construct was increased by expression of SRF-VP16 and also MKL1 N100 (Fig. 36B). We also generated a promoter deletion mutant that lacks a CArG box between the basepairs 304-363 (MYOF Δ304-363) and found that the activity of this promoter construct was not activated by MKL1 N100 expression anymore. This way, we can assume that MYOF is directly activated by either SRF or MKL1 and that SRF and MKL1 bind the CArG box of the myoferlin promoter between the 200 - 900 bp segment.

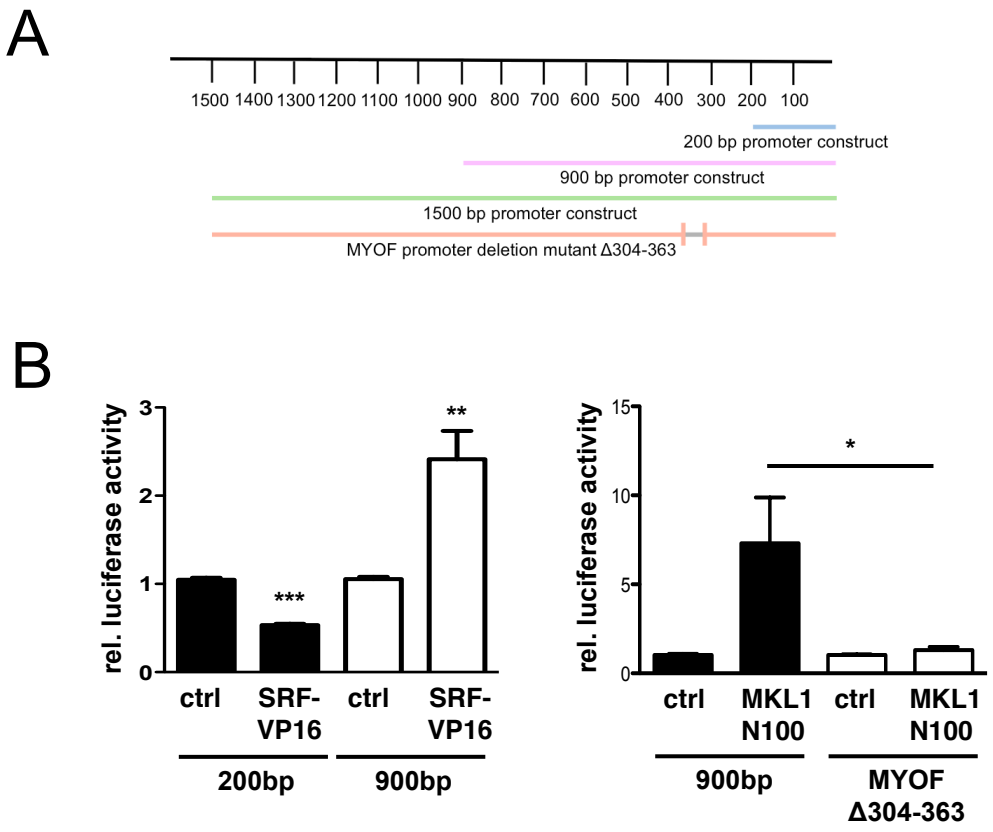

Figure 36: The 900 bp promoter construct of myoferlin is activated by SRF and MKL1. (A) Promoter constructs of MYOF used in reporter gene assays. **(B)** Luciferase assays in HEK293T cells transfected with empty vector (ctrl), SRF-VP16 or MKL1-N100 vector together with a 200 bp, a 900 bp or a MYOF promoter deletion construct (Δ304-363) and a pRLSV40 Renilla luciferase construct. Values are mean ± SD (n=3); *p<0.05, **p<0.01, ***p<0.001.

To validate this concept of MYOF activation we performed a chromatin immunoprecipitation (ChIP) assay with MKL1 pulldown. The α-smooth muscle actin (α-SMA) promoter that serves as positive control and the MYOF promoter itself were strongly amplified by MKL1 as compared to the control GAPDH promoter (Fig. 37A, left). Also the other negative control, an upstream site in the MYOF promoter (MYOF 1167), showed no enrichment by MKL1 (Fig. 37A, left). Next, we tested whether the MYOF promoter amplification was inducible by stimulation. Here we found that the MYOF promoter was stronger amplified by MKL1 upon LPA treatment of the cells (Fig. 37A, right), being in accordance to the results obtained in Fig. 35. We also investigated the role of FLNa, the novel MKL1 interaction partner, on the MYOF promoter occupancy. Thus, we performed the ChIP assay additionally in FLNa expressing A7 and FLNa-deficient M2 cells with FLNa pulldown and observed that the MYOF promoter was only amplified in A7 but not in M2 cells compared to the GAPDH control promoter (Fig. 37B). Based on these experiments we could show the direct recruitment of MKL1 and FLNa to the MYOF promoter and therefore the direct transcriptional regulation of MYOF.

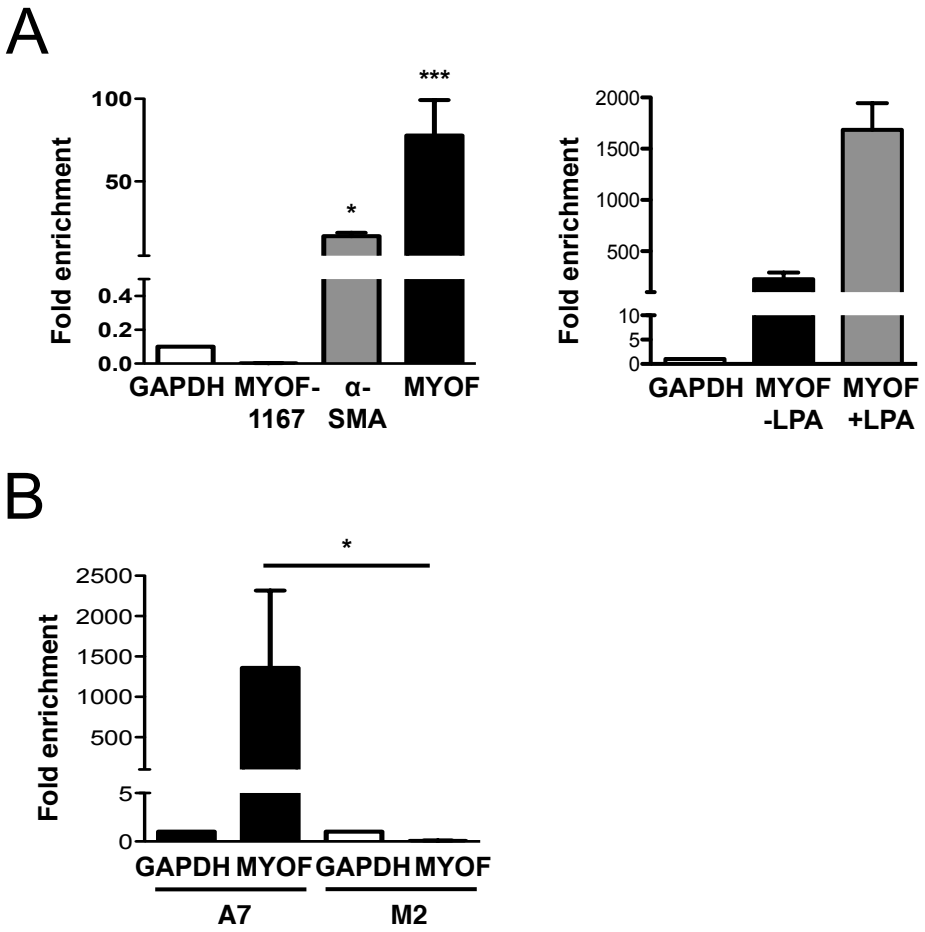

Figure 37: MKL1 and FLNa recruitment to the myoferlin promoter. (A) ChIP was performed using a specific antibody against MKL1 for immunoprecipitation and specific primers for α-SMA, MYOF and GAPDH promoters for qRT-PCR. As an additional negative control, primers spanning an upstream site in the myoferlin promoter (MYOF 1167) were used (left). Values are mean ± SD (n=3); *p<0.05, ***p<0.001. ChIP was also performed in serum-starved and LPA (10 µM) stimulated cells for 2 h (right). **(B)** ChIP assay with a specific FLNa antibody in FLNa-expressing A7 and FLNa-deficient M2 cells. Values are mean ± SD (n=3); *p<0.05.

6.3.2 Myoferlin expression *in vivo*

In order to show also the *in vivo* contribution of MYOF in hepatocellular carcinoma, we thankfully obtained RNA samples and protein lysates isolated from SRF-VP16^{iHep} mice (Ohrnberger et al., 2015) from Prof. Alfred Nordheim (University of Tuebingen, Tuebingen, Germany). These mice express the constitutively active SRF-VP16 in hepatocytes resulting in hyper proliferative premalignant nodules that rapidly develop to lethal HCC tumors. Importantly, MYOF mRNA (Fig. 38A) and protein (Fig. 38B) expression was upregulated in the nodule tissue and even stronger upregulated in the tumor tissue indicating an important role for MYOF in HCCs and the *in vivo* relevance of MYOF.

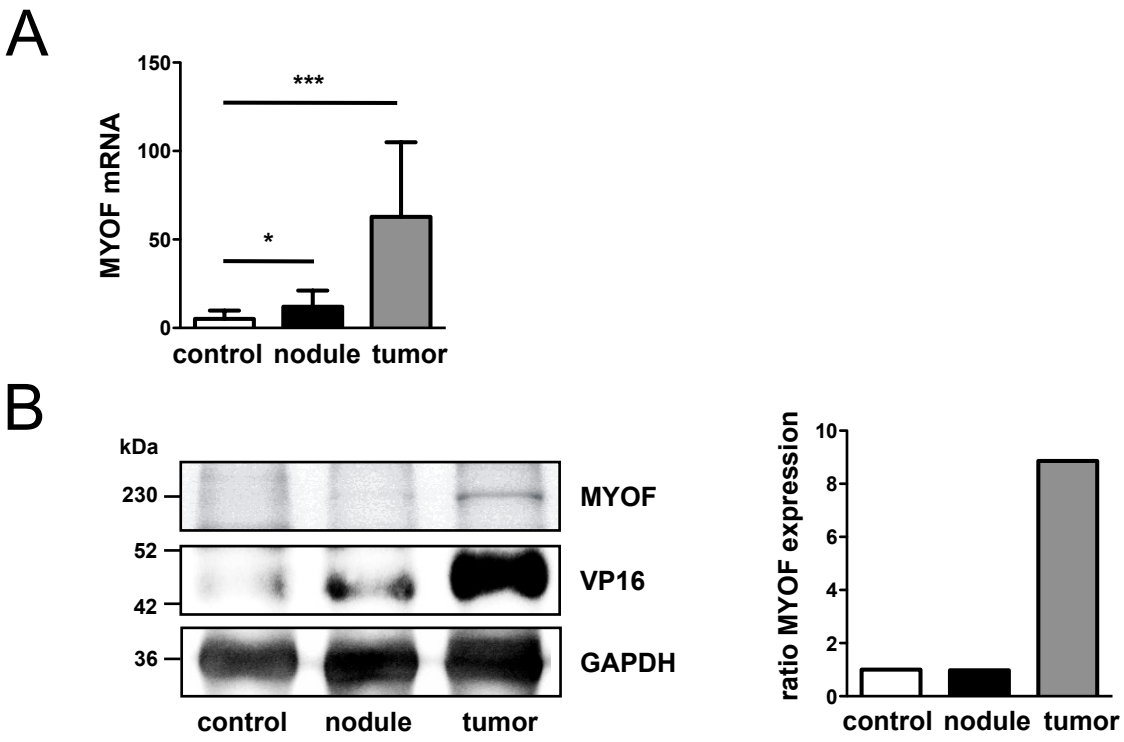

Figure 38: Myoferlin is upregulated in murine HCCs. MYOF mRNA **(A)** and protein **(B)** expression in control, premalignant nodule and tumor tissue was analysed by qRT-PCR with murine MYOF and 18S rRNA primers for normalization and immunoblotting with anti-MYOF, anti-VP16 and anti-GAPDH antibodies as loading control. The ratio of myoferlin protein expression was quantitated (right). Values are mean ± SD (n=6) *p<0.05, ***p<0.001.

6.3.3 Tumorigenic characteristics of myoferlin

Choosen MYOF as target gene of interest, we had to find out if MYOF is able to be the transducer of the MKL1/2 effects on tumorigenesis and oncogene-induced senescence. Beside its direct regulation and dependency on MKL1 and FLNa, we next investigated the role of MYOF on different essential tumorigenic properties, like proliferation and invasion of cells, hallmarks of nearly all cancer cells.

6.3.3.1 Myoferlin depletion leads to proliferation arrest

One characteristic property of tumor cells is their rapid proliferation for which reason we analysed the proliferation rate of HuH6 hepatocellular carcinoma cells transfected with negative control or MYOF siRNA, which displayed a knockdown efficiency of MYOF of over

90% (Fig. 39, right). Counting the cell number for 6 days we observed a significant decrease in proliferation upon MYOF depletion (Fig. 39), suggesting that the presence of MYOF seems to be important for aberrant cell proliferation.

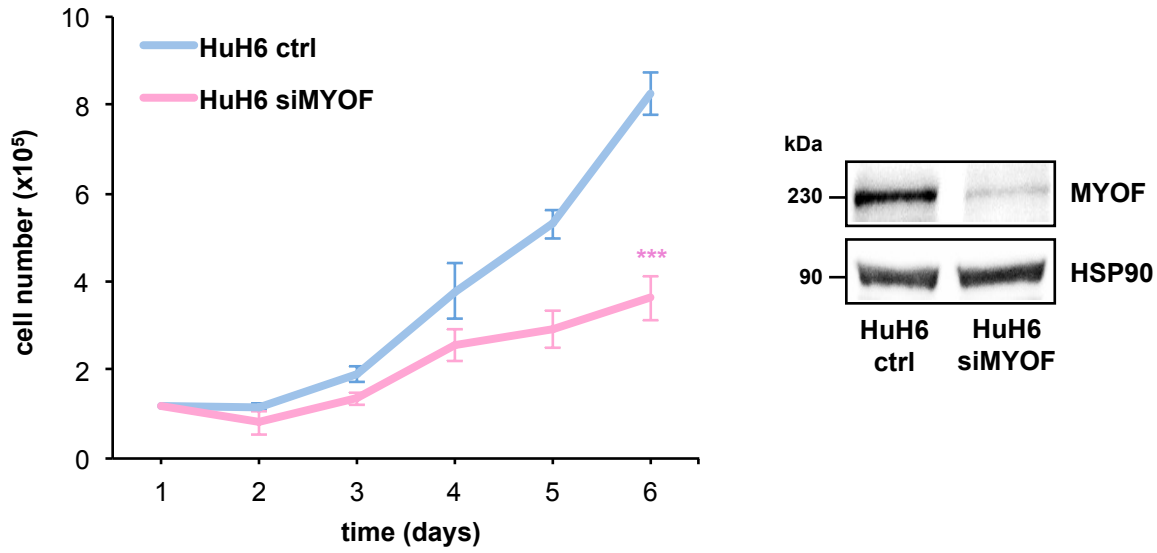

Figure 39: Proliferation arrest upon MYOF depletion. HuH6 cells were transfected with negative control or MYOF siRNA and counted daily for 6 days. Values are mean ± SD (n=3); ***p<0.001. Lysates of the HuH6 ctrl and HuH6 siMYOF cells were subjected to immunoblotting with anti-MYOF and anti-HSP90 antibodies as loading control.

6.3.3.2 Myoferlin depletion resulted in decreased invasion

As another important tumor cell specific property we analysed the invasive behavior of HuH6 cells transfected with negative control or MYOF siRNA and here we also got a knockdown efficiency of over 90% (Fig. 40, right). Performing a matrigel invasion assay and then counting the invaded cells after 24 h, a significant decrease of invasive cells due to MYOF depletion was observed concluding that MYOF is also required for cell invasion (Fig. 40).

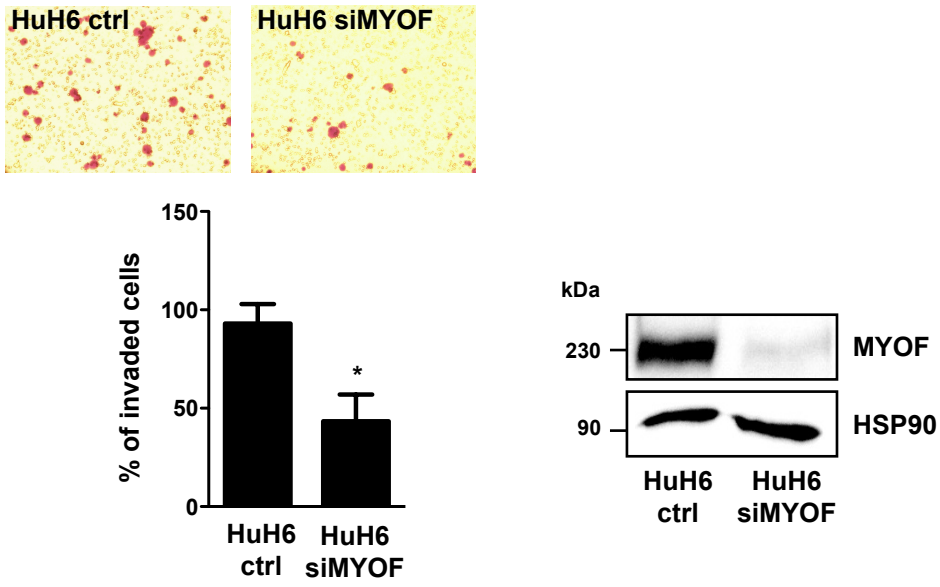

Figure 40: Decreased invasion upon MYOF depletion. HuH6 ctrl and HuH6 siMYOF cells were subjected to a three-dimensional matrigel invasion assay. Number of invaded cells after 24 h at 37 °C was counted. Values are mean ± SD (n=3); *p<0.05. Lysates of the HuH6 cells were immunoblotted with anti-MYOF and anti-HSP90 antibodies as loading control.

6.3.3.3 Myoferlin depletion induces senescence

Due to the findings above, the requirement of MYOF for cell proliferation and invasion, and the fact that MKL1/2 depletion inhibits HCC xenograft growth by inducing senescence, we also analysed the possibility of senescence induction by MYOF depletion. Therefore, a senescence associated β-galactosidase staining was performed and the blue cells in negative control and MYOF depleted HuH6 cells were counted. In HuH6 cells with MYOF knockdown we observed a significant induction of cellular senescence indicating a role for MYOF in senescence induction (Fig. 41).

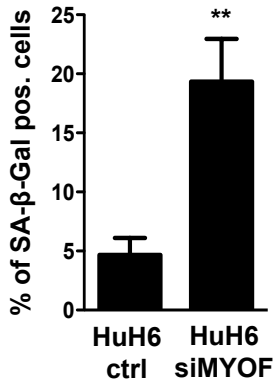

Figure 41: Induction of cellular senescence upon MYOF depletion. Senescence associated β-galactosidase staining was performed in HuH6 ctrl and HuH6 siMYOF cells. Numbers of SA-β-gal positive cells were counted. Values are mean ± SD (n=3); **p< 0.01.

All these results are conform with the fact that the examined HCC cells show characteristic features of tumor cells, like cell proliferation and invasion, while MYOF presence. These tumorigenic properties can be inhibited by MYOF depletion and may be due to the senescence-inducing strategy upon MYOF knockdown. Based on the given results, we can hypothesize that the target gene MYOF is able to transduce the known effects of MKL1/2 on evading tumorigenesis and tumor growth by inducing a senescence response.

6.3.4 Myoferlin depletion provokes phosphorylation of the EGFR

After characterizing MYOF presence as relevant for tumor cell specific behavior we focused on the mechanistic insights and the signaling pathways MYOF can act on. In a recent study, Turtoi and colleagues showed an effect of MYOF knockdown on the activation and phosphorylation of the EGF receptor (EGFR) in breast cancer cells (Turtoi et al., 2013). We therefore investigated the role of MYOF depletion on activation of the EGFR in HuH6 and HuH7 HCC cells. Our experiments also revealed a strong phosphorylation of the EGFR at tyrosin 1173 upon a stable MKL1/2 as well as a stable MYOF knockdown in HuH7 and a transient knockdown of MYOF in HuH6 cells (Fig. 42A). We could also show that the phosphorylation of the EGFR is a reversible process because the strong EGFR phosphorylation in HuH7 MKL1/2 knockdown cells was reverted by overexpression of MYOF in the MKL1/2 KD cells (Fig. 42B). These results indicate a direct effect of MYOF on the EGFR activation by phosphorylation. We wanted to verify this result also *in vivo* and found a

strongly phosphorylated EGFR in the HCC xenograft samples treated with MKL1+2 siRNA (Fig. 42C, top). In tumor tissue of SRF-VP16^{iHep} mice expressing high amounts of MYOF (Fig. 38) the EGFR is not phosphorylated compared to the control cells expressing no MYOF (Fig. 42C, bottom). Concluding, we found a strong upregulation of the EGFR phosphorylation in MYOF depleted hepatocellular carcinoma cells *in vitro* as well as *in vivo*.

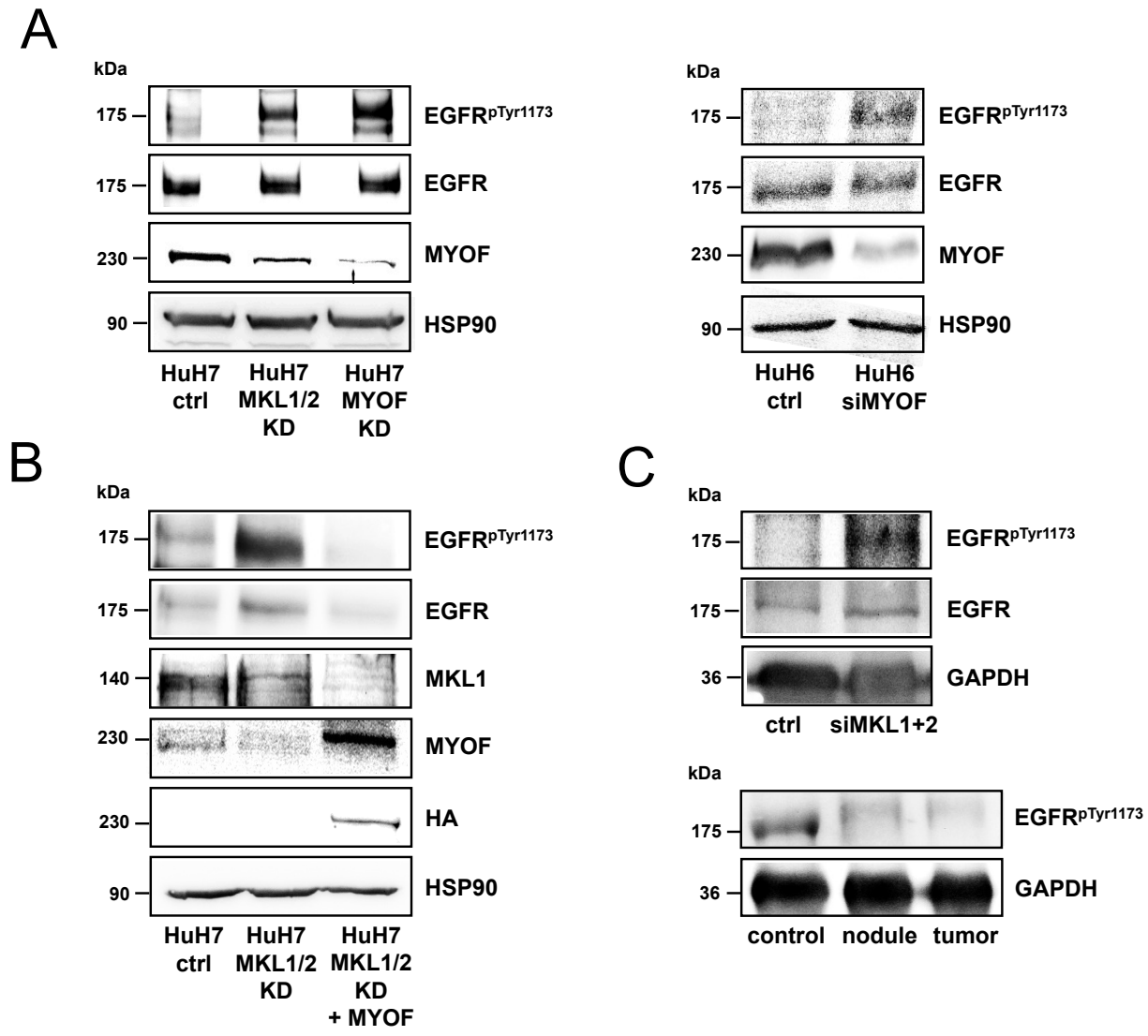

Figure 42: MYOF depletion leads to phosphorylation of the EGFR. (A) Lysates of HuH7 cells stably expressing negative control, MKL1/2 or MYOF shRNA (left; performed by V. Hampl) and lysates of HuH6 cells transfected with negative control or MYOF siRNA (right) were immunoblotted with anti-EGFR^{pTyr1173}, anti-EGFR, anti-MYOF and anti-HSP90 antibodies as loading control. **(B)** Immunoblotting of HuH7 cells stably expressing negative control or MKL1/2 shRNA with or without reconstitution of HA-tagged MYOF with the indicated antibodies (performed by V. Hampl). **(C)** Lysates of HCC xenografts after treatment with PEI/control siRNA or PEI/MKL1+2 siRNA were immunoblotted with anti-EGFR^{pTyr1173}, anti-EGFR and anti-GAPDH antibodies as loading control (top). Immunoblotting of control, premalignant nodule and tumor tissue of SRF-VP16^{iHep} mice with anti-EGFR^{pTyr1173} and anti-GAPDH antibodies (bottom).

Next, we investigated the role of MYOF in internalization of the EGFR in HuH7 cells by GFP-tagged EGFR transfection into HuH7 control and HuH7 siMYOF cells. In the HuH7 cells without MYOF distinct dots of EGFR are visible by immunofluorescence analysis in contrast to diffuse coloring of the cell in the control cells (Fig. 43). To test the mechanism underlying the degradation arrest of the EGFR upon MYOF knockdown we treated cells with negative control siRNA with the proteasome inhibitor MG132 and observed similar to the effects of MYOF depletion distinct dots of non-degraded EGFR (Fig. 43) suggesting that MYOF depletion leads to a degradation arrest of the EGFR internalization by blocking the proteasome.

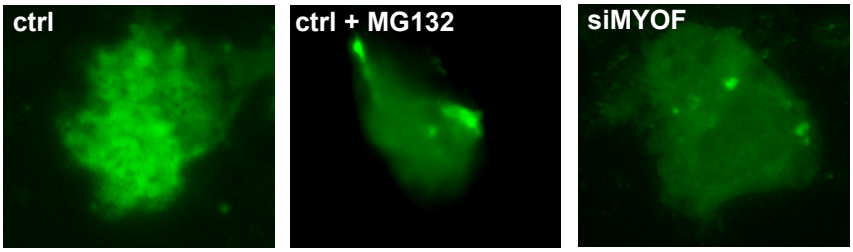

Figure 43: EGFR degradation is inhibited by MYOF depletion. HuH7 ctrl cells treated with or without 10 µM MG132 and HuH7 siMYOF cells were transfected with GFP-tagged EGFR and analysed by immunofluorescence. Representative images are shown.

6.3.5 Myoferlin depletion induces oncogene-induced senescence

After demonstrating an activating effect of MYOF depletion on the EGF receptor via EGFR phosphorylation and also a senescence-inducing strategy upon MYOF depletion revealed by β-galactosidase staining we tried to figure out if the knockdown of MYOF also leads to oncogene-induced senescence (OIS) as MKL1/2 depletion does (Hampl et al., 2013). We therefore focused our analyses shown in the following figures on established markers of OIS such as ERK1/2 phosphorylation, $p16^{Ink4a}$ activation, hypophosphorylation of Rb and the CXCL10 and TNFSF10 expression upon silencing of MYOF (Peeper et al., 1994; Weinberg, 1995; Alcorta et al., 1996; Cristofalo & Pignolo, 1996; Hara et al., 1996 and Serrano et al., 1997).

6.3.5.1 Myoferlin depletion causes Ras activation and ERK1/2 phosphorylation

Following the signal cascade of EGFR activation by autophosphorylation, the adaptor protein growth factor receptor-bound protein 2 (GRB2) binds to the phosphorylated tyrosine residues of the EGFR and also binds to the guanine nucleotide exchange factor son of sevenless (SOS) that becomes activated. This subsequently leads to the exchange of inactive GDP to active GTP of Ras. Activated Ras then activates via further kinase activities the extracellular signal-regulated kinase 1/2 (ERK1/2) by phosphorylation. Based on this known signaling pathway we looked for Ras and ERK1/2 activation upon MYOF depletion and found Ras in HuH7 cells transfected with MYOF or MKL1/2 siRNA strongly activated (Fig. 44A, top). ERK1/2 was also phosphorylated in HuH7 cells with stable MKL1/2 or MYOF knockdown (Fig. 44A, bottom) and HuH6 cells transfected with MYOF siRNA (Fig. 44B). Confirming that MYOF is the gene mediating the effect of MKL1/2 on Ras GTP loading we overexpressed MYOF in MKL1/2 depleted cells resulting in suppression of Ras activation (Fig. 44A, top). To further demonstrate that MYOF directly acts on the Ras/Raf/MEK/ERK pathway, we analysed the influence of cell treatment with a SOS SH3 domain inhibitor in combination with MYOF knockdown. Our results impressingly show a strong decrease of phosphorylated ERK1/2 (Fig. 44A, bottom) and also of induced senescence monitored by senescence associated β-galactosidase staining (Fig. 44C) after SOS inhibitor treatment of cells lacking MYOF or MKL1/2 expression.

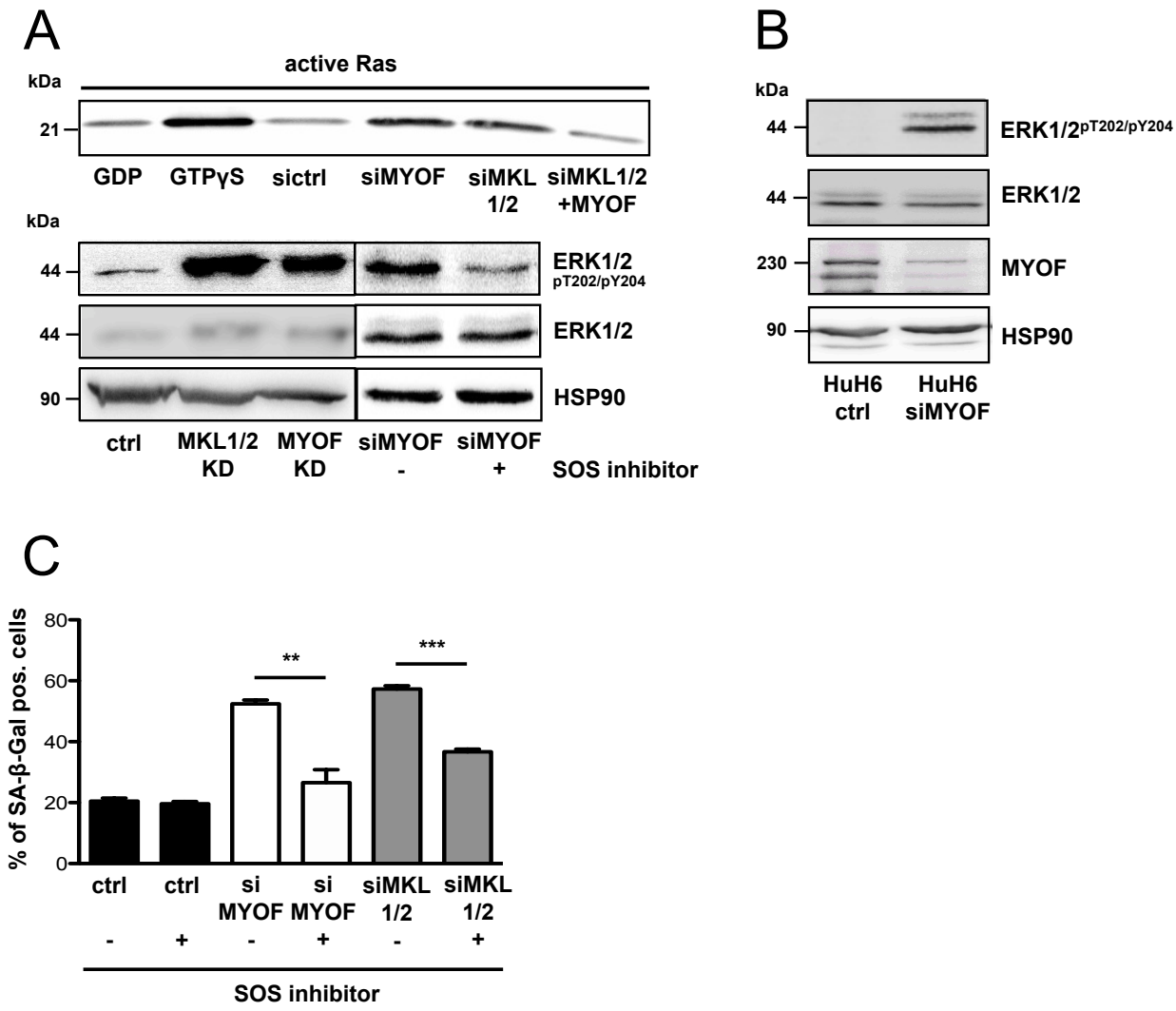

Figure 44: ERK1/2 phosphorylation upon MYOF depletion. (A) HuH7 cells transfected with control, MYOF, MKL1/2 or MKL1/2 siRNA reconstituted with HA-tagged MYOF and a negative (GDP) and positive (GTPγS) control were subjected to the active Ras detection kit. Eluates were immunoblotted with anti-Ras antibody (top). Immunoblotting of HuH7 cells stably expressing a negative control vector or MKL1/2 or MYOF shRNA and HuH7 cells transfected with MYOF siRNA treated with or without 20 µM SOS SH3 domain inhibitor using anti-ERK1/2$^{pT202/pY204}$, total anti-ERK1/2 and anti-HSP90 antibodies. **(B)** HuH6 ctrl and HuH6 siMYOF cells were immunoblotted with anti- ERK1/2$^{pT202/pY204}$, total anti-ERK1/2, anti-MYOF and anti-HSP90 antibodies. **(C)** Senescence associated β-galactosidase staining in HuH7 cells transfected with negative control, MYOF or MKL1/2 siRNA and treated as in (A). Numbers of SA-β-gal positive cells were counted. Values are mean ± SD (n=3); **p<0.01, ***p<0.001.

6.3.5.2 Activation of senescence markers upon Myoferlin depletion

Analysing more markers being characteristic for oncogene-induced senescence, we tested the effect of MYOF downregulation on the phosphorylation status of the retinoblastoma protein (Rb). Immunoblotting revealed a hypophosphorylation of Rb indicated by a strong decrease of phosphorylated Rb expression upon MYOF knockdown in HuH7 (Fig. 45A) and

HuH6 (Fig. 45B) cells. Treatment with SOS inhibitor reversed the MYOF induced effect and Rb gets phosphorylated (Fig. 45A) confirming the given results of SOS inhibitor treatment on reduced ERK1/2 phosphorylation and senescence induction described above. Demonstrating that MYOF depletion induced oncogene-induced senescence is mediated by the EGFR, we inhibited EGFR in parallel with MYOF siRNA in HuH7 cells and observed, as expected, a decline in senescence associated β-galactosidase activity and a potent inhibition of $p16^{Ink4a}$ expression compared to cells with a single MYOF knockdown (Fig. 45C, D).

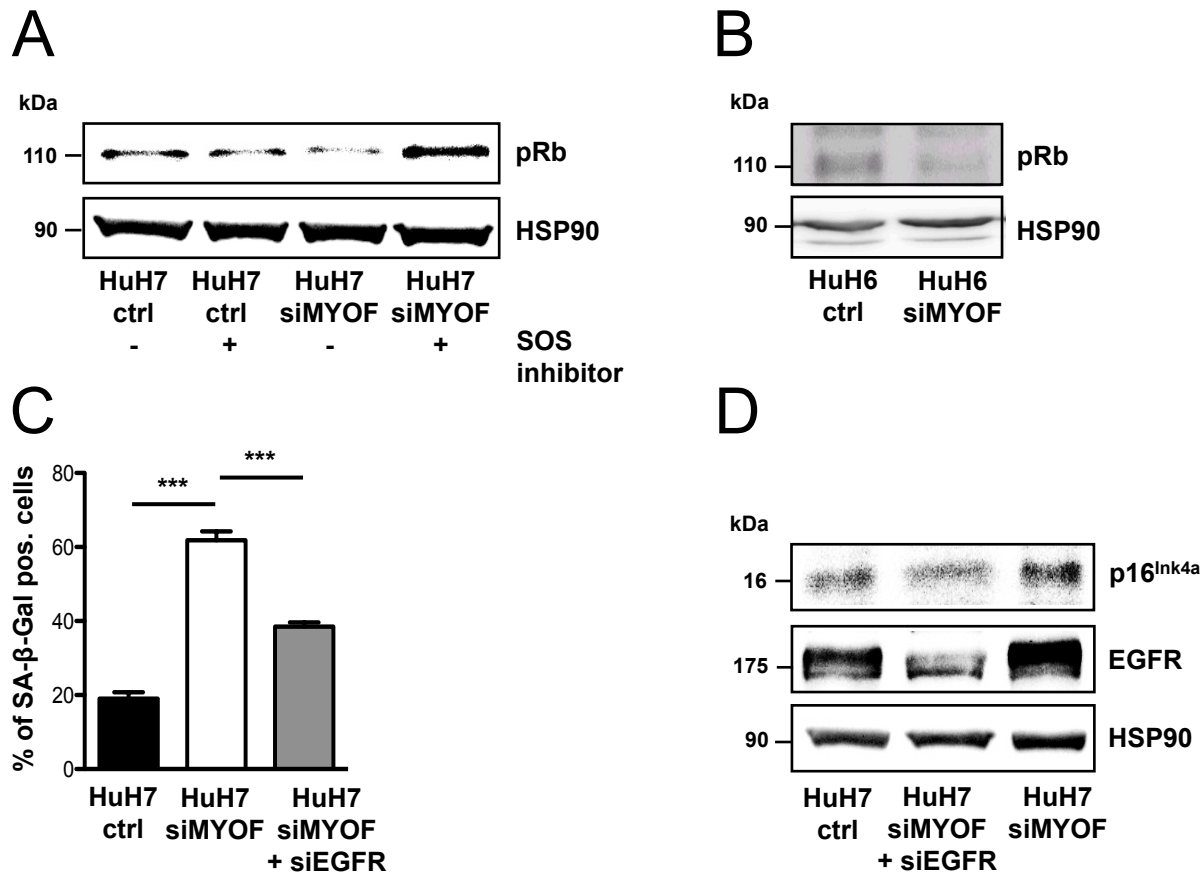

Figure 45: Hypophosphorylation of Rb upon MYOF depletion. (A) HuH7 ctrl or HuH7 siMYOF cells treated with or without 20 µM SOS SH3 domain inhibitor were immunoblotted with anti-pRb and anti-HSP90 antibodies. **(B)** Immunoblotting of HuH6 ctrl and HuH6 siMYOF cells as in (A). **(C)** Senescence associated β-galactosidase staining in HuH7 cells transfected with negative control, MYOF or MYOF+EGFR siRNAs. Numbers of SA-β-gal positive cells were counted. Values are mean ± SD (n=3); ***p<0.001. **(D)** HuH7 ctrl, HuH7 siMYOF+siEGFR and HuH7 siMYOF cells were immunoblotted with anti-$p16^{Ink4a}$, anti-EGFR and anti-HSP90 antibodies.

Additionally to the senescence inhibiting effect of the SOS inhibitor we wanted to investigate the potential role of the EGFR inhibitor Tyrphostin AG1478 on senescence induction. Therefore, we performed immunoblotting and β-galactosidase staining in HuH7 cells transfected with MYOF or MKL1/2 siRNA and treated them with AG1478 (Fig. 46A-B). A

strong EGFR inhibiting effect of AG1478 shown by decreased phosphorylation of the EGFR was observable (Fig. 46A, top) but no alteration in the $p16^{Ink4a}$ expression (Fig. 46A, bottom) or in the senescence induction (Fig. 46B) was detectable after addition of AG1478 to HuH7 MKL1 or MYOF knockdown cells.

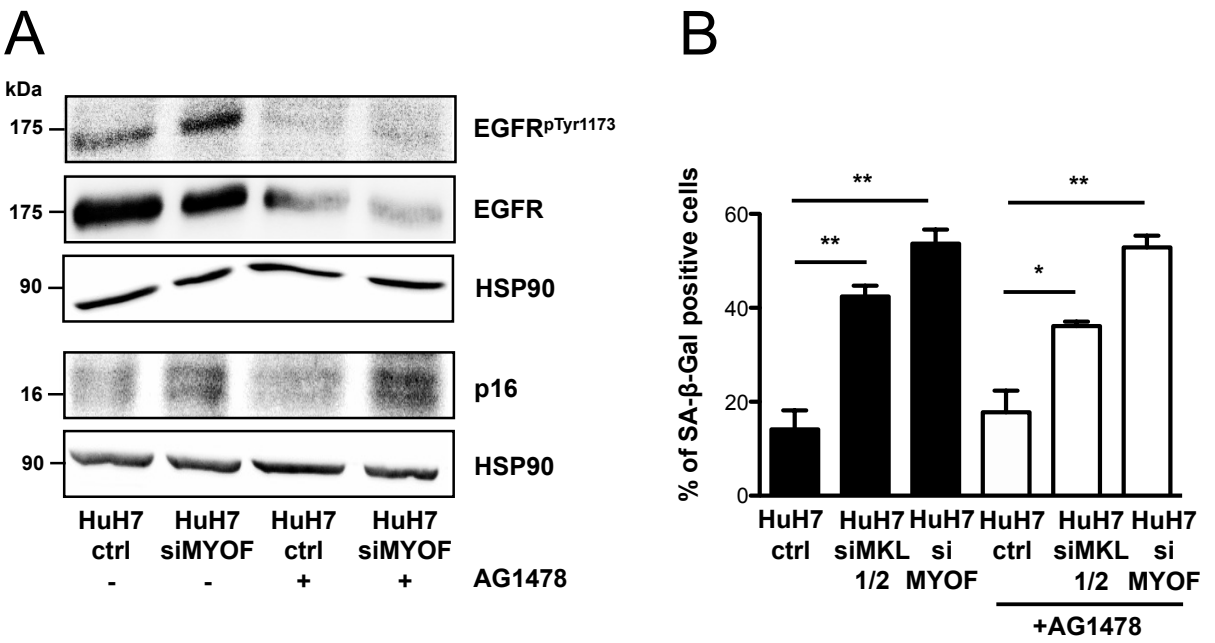

Figure 46: Inhibition of EGFR phosphorylation by AG1478. (A) HuH7 cells were transfected with negative control or MYOF siRNA and treated with or without 10 µM AG1478. Lysates were immunoblotted with anti-$EGFR^{pTyr1173}$, anti-EGFR, anti-$p16^{Ink4a}$ and anti-HSP90 antibodies as loading control. **(B)** HuH7 ctrl, HuH7 siMKL1/2 and HuH7 siMYOF cells were treated with or without 10 µM AG1478 and subjected to β-galactosidase staining. Numbers of SA-β-gal positive cells were counted. Values are mean ± SD (n=3); *p< 0.05, **p< 0.01.

To complete the markers for oncogene-induced senescence affected by MYOF knockdown we analysed the expression levels of the senescence messaging secretome (SMS) factors C-X-C motif chemokine 10 (CXCL10) and tumor necrosis factor superfamily member 10 (TNFSF10) (Fig. 47A-B). In HuH7 cells with a stable MYOF knockdown (Fig. 47A) as well as in HuH6 cells with a transient MYOF knockdown (Fig. 47B) TNFSF10 and CXCL10 (only in HuH7 cells) were significantly upregulated compared to the negative control cells.

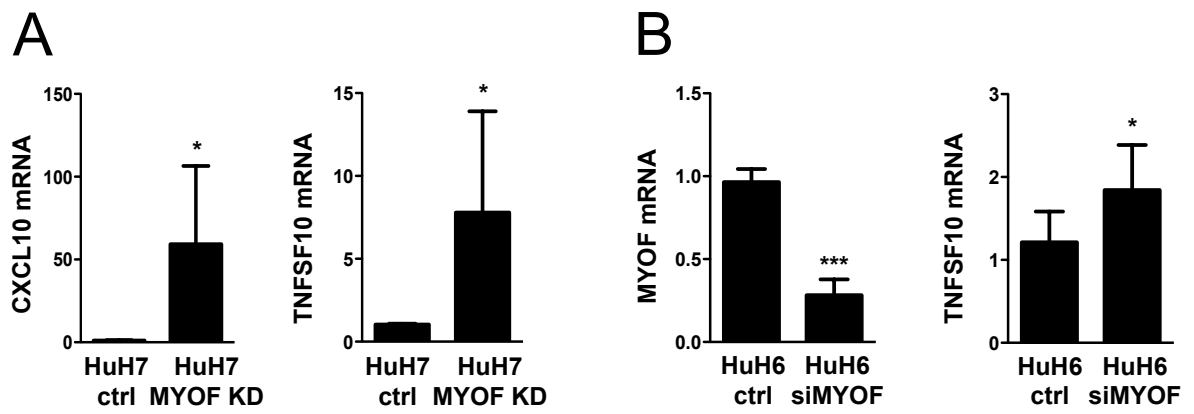

Figure 47: Upregulation of senescence markers upon MYOF depletion. (A) HuH7 cells transfected with negative control or MYOF shRNA were subjected to qRT-PCR with CXCL10, TNFSF10 and 18S rRNA primers for normalization. Values are mean ± SD (n=3); *p< 0.05. **(B)** HuH6 cells were transfected with negative control or MYOF siRNA. MYOF knockdown efficiency and TNFSF10 mRNA expression were analysed by qRT-PCR as in (A). Values are mean ± SD (n=3); *p< 0.05, ***p< 0.001.

In a further experiment, we treated HuH7 control cells and HuH7 cells with a stable MKL1/2 knockdown with the antitumor antibiotic Actinomycin D (ActD). MKL1 mRNA expression was strongly reduced after ActD treatment very similar to a stable knockdown of MKL1/2 (Fig. 48, top). The combination of MKL1/2 knockdown and ActD treatment of cells revealed an even stronger decrease of MKL1 expression compared to a single treatment of the cells (Fig. 48, top). Confirming the results described above we here also found decreased SRF expression but increased EGFR and TNFSF10 expression upon MKL1/2 knockdown (Fig. 48). After treatment with ActD we observed mRNA levels of SRF, EGFR and TNFSF10 strongly reduced in control as well as in MKL1/2 depleted HuH7 cells (Fig. 48). Since ActD inhibits the transcription of genes by binding to the DNA and thereby preventing the RNA elongation we can conclude that all the analysed genes are repressed on the transcriptional level.

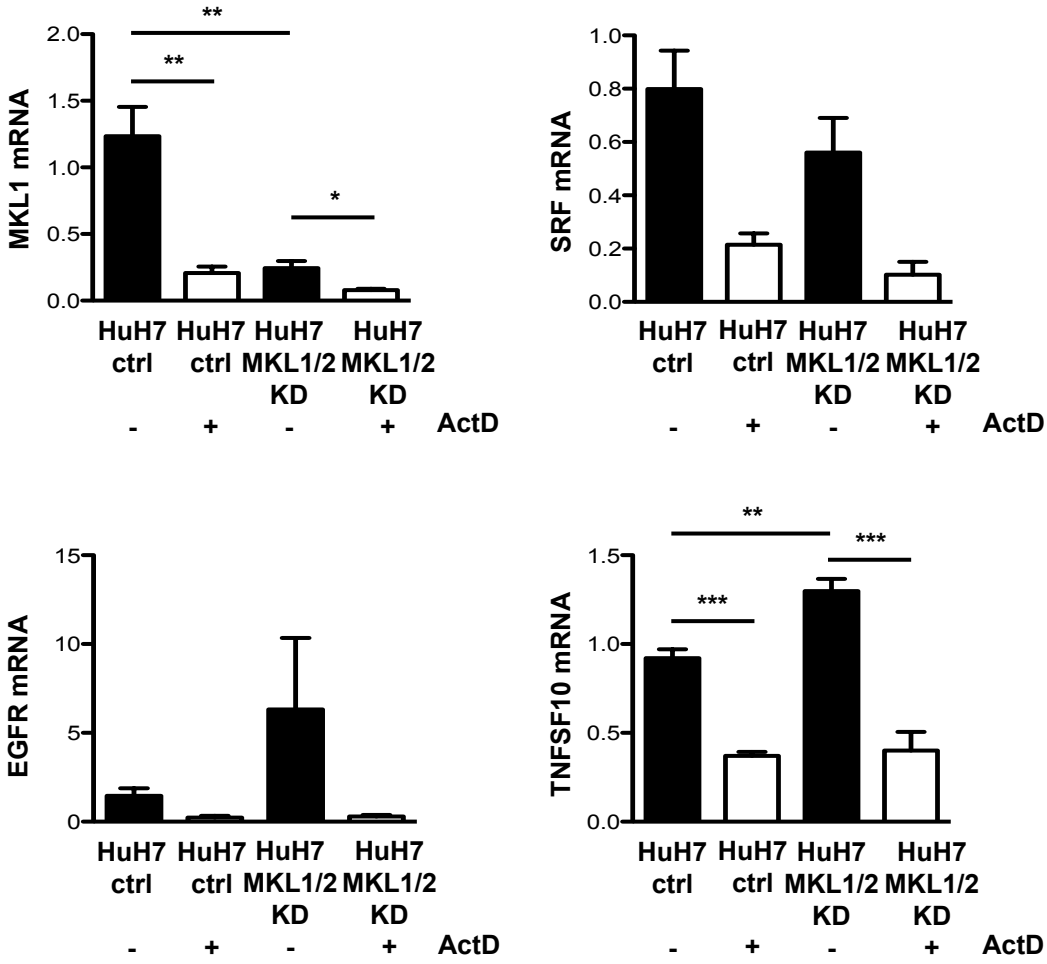

Figure 48: Downregulation of EGFR and TNFSF10 mRNA expression upon ActD treatment. HuH7 ctrl and MKL1/2 KD cells were treated with or without 1 µg/mL Actinomycin D (ActD) for 24 h. mRNA expression of MKL1, SRF, EGFR and TNFSF10 was measured by qRT-PCR with the gene specific and the 18S rRNA primers for normalization. Values are mean ± SD (n=2 for SRF and EGFR and n=3 for MKL1 and TNFSF10); *p< 0.05, **p< 0.01, ***p< 0.001.

All the results given in this chapter argue for a role of MYOF depletion in mediating the effect of MKL1/2 depletion on reduced tumorigenic cell properties by induction of oncogene-induced senescence. We could demonstrate that the senescence induction was accomplished by activation of the EGFR and subsequently activating the Ras/Raf-MEK-ERK pathway indicated by Rb hypophosphorylation, enhanced $p16^{Ink4a}$ and CXCL10 as well as TNFSF10 expression.

6.3.6 Mig6 shows no effect on oncogene-induced senescence

In further studies on inducing senescence mediating proteins we had a look at the tumor suppressor gene mitogen-inducible gene 6 (Mig6), an already known target gene of MKL1/2 and known effector of EGFR and ERK signaling (Descot et al., 2009 and Reschke et al., 2010). First, we verified the MKL1/2 dependency of Mig6 by qRT-PCR showing strongly decreased mRNA expression of Mig6 in HuH7 cells with a stable MKL1/2 knockdown (Fig. 49).

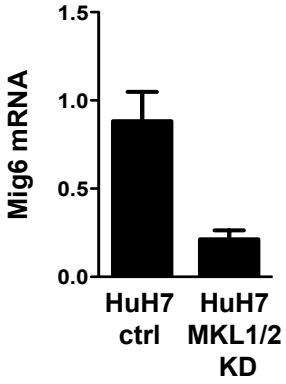

Figure 49: Downregulation of Mig6 upon MKL1/2 knockdown. Mig6 mRNA expression of HuH7 cells stably expressing control or MKL1/2 shRNA was analysed by qRT-PCR with Mig6 and 18S rRNA primers for normalization. Values are mean ± SD (n=2).

Firstly, we depleted Mig6 transiently in HuH7 cells and got a knockdown efficiency of around 60% (Fig. 50A, right). This HuH7 siMig6 cells showed no altered proliferation rate compared to the control cells while MKL1/2 depleted cells exerts strong inhibitory effects on cell proliferation serving as positive control for the performed proliferation assay (Fig. 50A). Confirming the result that Mig6 knockdown doesn't influence the proliferation rate, we additionally overexpressed Flag-tagged Mig6 into MKL1/2 depleted HuH7 cells and again no difference in cell growth compared to the MKL1/2 knockdown cells was observed (Fig. 50A) suggesting that Mig6 isn't involved in cell proliferation. Secondly, we investigated the role of Mig6 on oncogene-induced senescence and therefore analysed the expression levels of p16, CXCL10 and TNFSF10 in Mig6 depleted HuH7 cells by qRT-PCR. Neither p16 nor CXCL10 or TNSFSF10 were significantly upregulated by Mig6 knockdown (Fig. 50B) concluding that Mig6 in contrast to MYOF depletion isn't relevant for induction of oncogene-induced senescence. We refrained therefore from performing further analysis concerning Mig6

depletion or overexpression and found only MYOF as the suitable target gene mediating the effects of MKL1/2 on HCC avoiding strategies by oncogene-induced senescence induction.

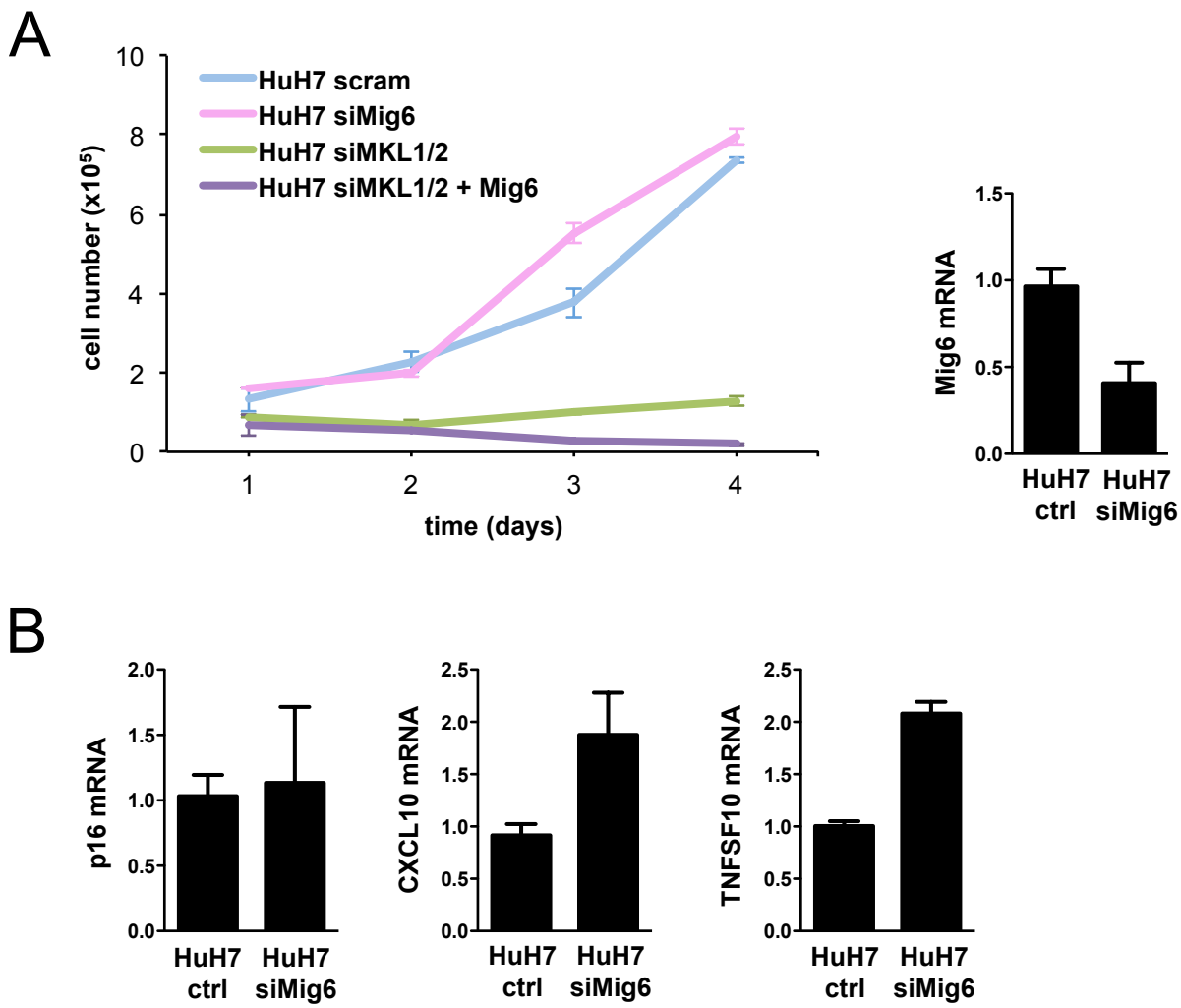

Figure 50: Knockdown of Mig6 doesn't provoke proliferation arrest or oncogene-induced senescence. (A) HuH7 cells were transfected with negative control, Mig6, MKL1/2 or MKL1/2 siRNA reconstituted with Flag-Mig6 and counted daily for 4 days (left). Mig6 knockdown efficiency was determined by qRT-PCR using Mig6 and 18S rRNA primers for normalization (right). Values are mean ± SD (n=2) **(B)** mRNA expression of p16, CXCL10 and TNFSF10 was measured by qRT-PCR with the gene specific primers. Values are mean ± SD (n=2).

6.3.7 *Ex vivo* evidence for oncogene-induced senescence by myoferlin depletion

After showing the pertinence of MYOF absence for anti-tumor effects by induction of oncogene-induced senescence *in vitro* we focused our attention on the same effects also in *ex vivo* experiments. We therefore used liver tumor cells, referred to LT cells in the following thesis, derived from HCCs developed in mice conditionally expressing SRF-VP16 (Ohrnberger et al., 2015). Transient MYOF knockdown mediated by RNAi in LT cells showed

a strong knockdown efficiency (Fig. 51A, right). By performing invasion assays LT cells lacking MYOF expression revealed a significantly lower invasive behavior into a three-dimensional matrigel than the control cells (Fig. 51A). We also observed in LT cells with MYOF knockdown a reduced proliferation rate (Fig. 51B) and significantly increased senescence induction monitored by senescence-associated β-galactosidase staining (Fig. 51C) indicating that MYOF depletion prevents also tumor cells from tumorigenic features by a senescence-inducing strategy.

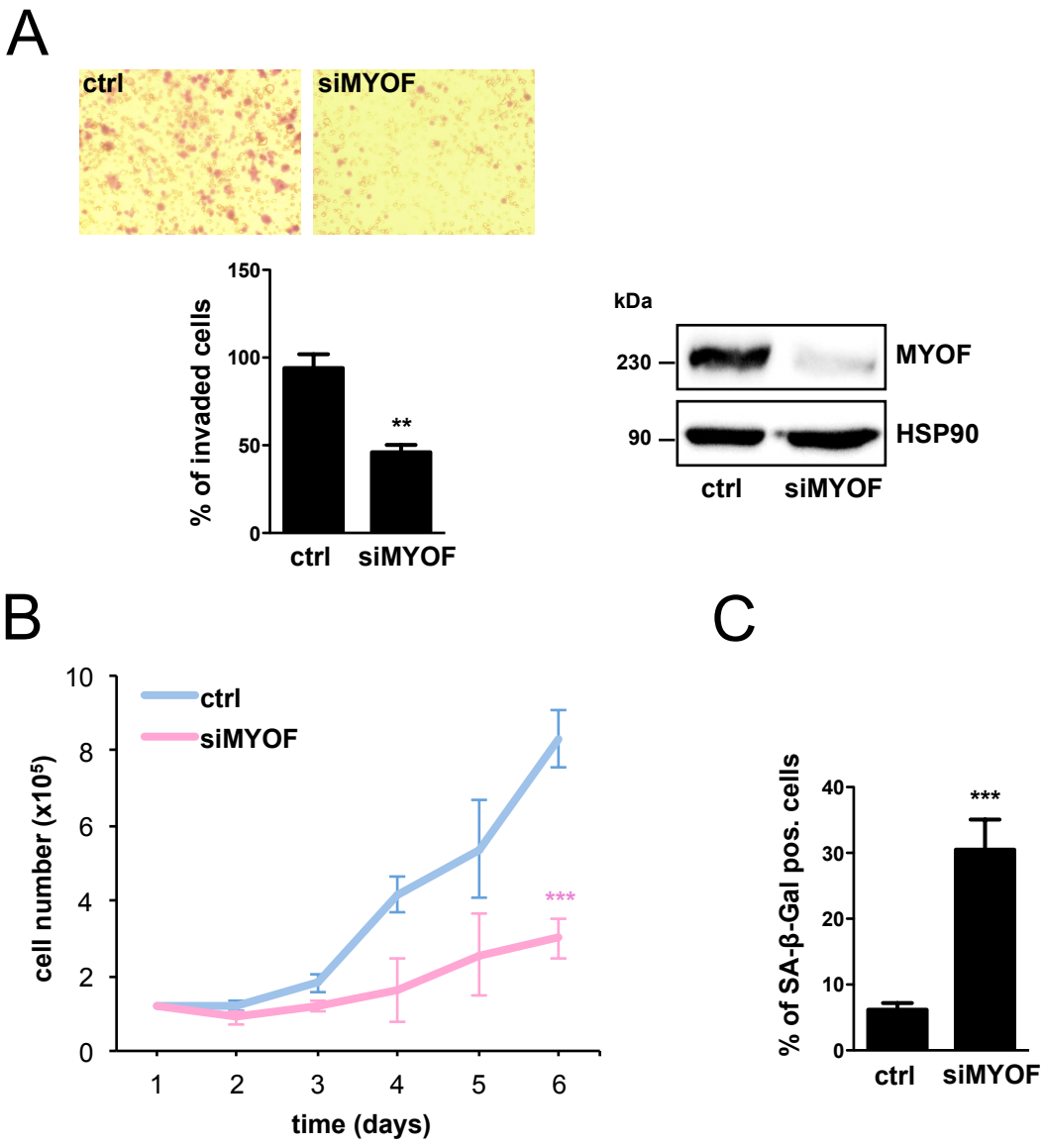

Figure 51: Downregulation of tumorigenic features upon MYOF depletion in murine liver tumor (LT) cells. **(A)** LT ctrl and LT siMYOF cells were subjected to a three-dimensional matrigel invasion assay. Number of invaded cells after 24 h at 37 °C was counted. Values are mean ± SD (n=3); **p< 0.01. Lysates of the LT cells were immunoblotted with anti-MYOF and anti-HSP90 antibodies. **(B)** LT cells were transfected with negative control or MYOF siRNA and counted daily for 6 days. Values are mean ± SD (n=3); ***p< 0.001. **(C)** Senescence associated β-galactosidase staining was performed in LT ctrl and LT siMYOF cells. Numbers of SA-β-gal positive cells were counted. Values are mean ± SD (n=3); ***p< 0.001.

Furthermore, we analysed the effect of MYOF knockdown on EGFR activation and found a strong phosphorylation of the EGFR in LT siMYOF cells (Fig. 52) contributing to senescence induction described above.

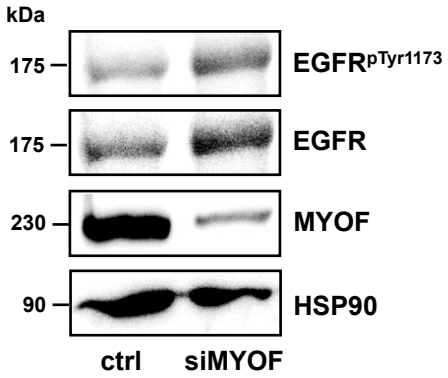

Figure 52: Phosphorylation of the EGFR upon MYOF depletion in LT cells. Lysates of LT ctrl and LT siMYOF were immunoblotted with anti-EGFR^{pTyr1173}, anti-EGFR, anti-MYOF and anti-HSP90 antibodies.

In additional experiments we checked for oncogene-induced senescence markers upregulated in MYOF depleted LT cells (Fig. 53). Our results obtained by immunoblotting and qRT-PCR demonstrate that MYOF depletion in LT cells leads to phosphorylation of ERK1/2 (Fig. 53A), to increased expression of p16^{Ink4a} (Fig. 53B) and to hypophosphorylation of Rb (Fig. 53C). We also observed an enhanced expression of the senescence messaging secretome factor TNFSF10 in the MYOF silenced LT cells (Fig. 53D). The described results in this chapter show a reduction of tumorigenic properties mediated by an oncogene-induced senescence response via phosphorylation of the EGFR and activation of the MEK/ERK signaling pathway in MYOF depleted murine liver tumor derived cells suggesting MYOF or the OIS induction as potential promising therapeutic target abolishing or preventing hepatocarcinogenesis.

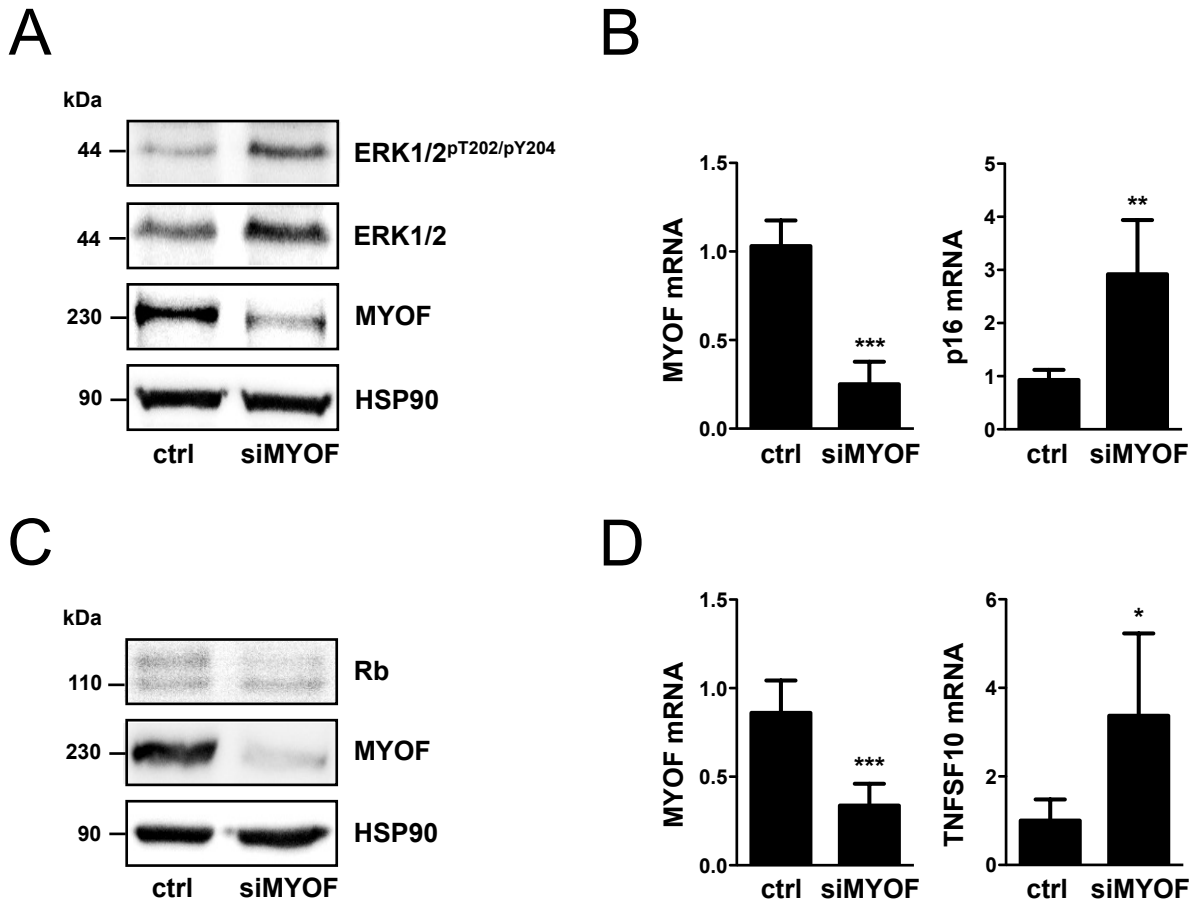

Figure 53: Induction of oncogene-induced senescence upon MYOF depletion. (A) Lysates of LT ctrl and LT siMYOF cells were immunoblotted with anti-ERK1/2$^{pT202/pY204}$, total anti-ERK1/2, anti-MYOF and anti-HSP90 antibodies. **(B)** MYOF knockdown efficiency and p16 mRNA expression was measured by qRT-PCR using MYOF, p16 and 18S rRNA primers for normalization. Values are mean ± SD (n=3); **p< 0.01, ***p< 0.001. **(C)** Immunoblotting of LT ctrl and LT siMYOF with anti-Rb, anti-MYOF and anti-HSP90 antibodies. **(D)** MYOF knockdown efficiency and mRNA expression of TNFSF10 were analysed by qRT-pCR with MYOF, TNFSF10 and 18S rRNA primers. Values are mean ± SD (n=3); *p< 0.05, ***p< 0.001.

7 Discussion

7.1 MKL1/2 target gene expression in HCC cells

7.1.1 MKL1 and/or MKL2 dependency of target genes

One aim of this thesis was the identification and validation of Megakaryoblastic Leukemia 1 and 2 (MKL1 and MKL2) dependent target genes and the discovery of one special target gene mediating the effects of MKL1 and/or MKL2 regarding their tumorigenic properties. Both proteins MKL1 and MKL2, acting as transcriptional coactivators of the transcription factor Serum Response Factor (SRF), are described to be involved in the activation of different target genes regulating processes being relevant for tumorigenesis of cells, such as cell growth, cell migration or cell differentiation (Pipes et al., 2006). The impact of MKL1 and MKL2 on cell migration and cell proliferation was demonstrated by Muehlich and colleagues by the finding that a depletion of MKL1/2 resulted in a reduced proliferation and migration rate of hepatocellular carcinoma (HCC) cells (Muehlich et al., 2012). By performing a microarray analysis by V. Hampl, the transcriptome of the HuH7 HCC cell line depleted of MKL1/2 in comparison to the HuH7 control cells was analyzed and thus several novel MKL1/2 dependent target genes were identified (Hermanns et al., 2017). The 8 genes with the strongest downregulation in the MKL1/2 knockdown cells compared to the control cells were smooth muscle protein 22 (SM22), glioma pathogenesis-related protein 1 (GLIPR1), calponin 1 (CNN1), myosin heavy chain (MYH9), transforming growth factor beta 1 (TGFß1), vestigial-like family member 3 (VGLL3), microtubule-associated protein 1B (MAP1B) and myoferlin (MYOF). These target genes, except for SM22, were then also validated *in vivo* in a HCC xenograft model treated with MKL1+2 siRNA (Hermanns et al., 2017). Confirming the microarray data also *in vitro*, we introduced a knockdown by RNAi of MKL1 or MKL2 alone or in combination and by a siRNA sequence directed against both sequences of MKL1 and MKL2 at the same time in hepatocellular carcinoma cells. We observed decreased mRNA as well as protein expressions of all 8 above mentioned target genes upon MKL1 and/or MKL2 depletion, except for TGFß1 whose expression was not reduced by a single MKL1 knockdown. This result illustrates the MKL1/2 dependency of the target genes and characterized GLIPR1, CNN1, VGLL3, MAP1B and MYOF the first time as novel MKL1 and MKL2 dependent target genes. The identified target genes SM22 and MYH9 were previously known as MKL1 dependent target genes, thus serving as a positive control of the validity of our microarray approach (Descot et al., 2009 and Medjkane et al., 2009). SM22 appeared to be regulated in NIH 3T3 fibroblasts by G-actin-MKL1 signaling, while it constitutes one of the

main components of differentiated smooth muscles and acts as regulator of the actin cytoskeleton (Gimona et al., 2003 and Descot et al., 2009). Its function as a tumor suppressor was also pointed out by the fact that breast, gut and prostate cancer cells lack an SM22 expression (Assinder et al., 2009). Contradictory to this finding, REF52 fibroblasts depleted of SM22 revealed a reduced cell migration, invasion and chemotaxis (Thompson et al., 2012). Given this discrepancy of cellular SM22 function, it may explain why the transient knockdown of MKL1+2 *in vitro* performed in this thesis resulted in reduced SM22 expression levels while the depletion of MKL1+2 in HCC xenografts *in vivo* revealed a strong increase in SM22 expression (Thompson et al., 2012 and Hermanns et al., 2017). MYH9, a component of the actomyosin contractile apparatus, showed an invasive behavior in tumor cells (Somlyo & Somlyo, 2003 and Betapudi et al., 2006). Supporting this involvement of MYH9, Medjkane and colleagues also revealed a contribution of MYH9 to metastasis and invasion in MDA-MB 231 breast cancer cells as well as in B16F2 melanoma cells by demonstrating that the depletion of MYH9 in MDA-MB 231 cells sequentially impaired the invasive growth significantly (Medjkane et al., 2009). GLIPR1 is described as proapoptotic tumor suppressor gene that is frequently downregulated in prostate cancer and also as potential target gene of p53 (Ren et al., 2002; Ren et al., 2004 and Ren et al., 2006). Besides its tumor inhibiting function, GLIPR1 exhibits also oncogenic properties exemplified by its specific expression in glioma and Wilms tumor (Murphy et al., 1995 and Chilukamarri et al., 2007). This way, the function of GLIPR1 on tumorigenesis seems to be cell-type specific. Despite its reduced expression in acute megakaryoblastic leukemia due to gene methylations in the GLIPR1 gene, GLIPR1 is not described in the context of MKL1/2 so far (Xiao et al., 2011). The smooth muscle protein CNN1 regulates the actin-myosin interaction and the smooth muscle contraction and is also known for binding actin to promote or sustain actin polymerization (Winder & Walsh, 1990; Wills et al., 1994 and Winder et al., 1998). Beside its function as modulator of the actomyosin contraction, CNN1 exhibits also tumor suppressive properties revealed by reduced CNN1 expression in tumor vessels in hepatocellular, melanoma and colon cancer (Sasaki et al., 2002; Koganehira et al., 2003 and Yanagisawa et al., 2008). The tumor suppressive effects of CNN1 were also observed by several research groups when they induced CNN1 expression into tumor cells (Kaneko et al., 2002 and Takeoka et al., 2002). The TGFß1 gene is known to be involved in epithelial-mesenchymal transition (EMT) of cells, a fundamental step in tumor cell progression from epithelial cells to invasive and migratory tumor cells (Thiery, 2002). In 2007, Morita and colleagues described for the first time a relation between TGFß1 and MKL1/2, when they demonstrated the requirement of MKL1/2 as critical mediators for the TGFß1-induced EMT (Morita et al., 2007). A structural microtubule-associated protein is MAP1B that is essential for the regulation of microtubule dynamics and their assembly as well as for the stability of neuronal cell cytoskeleton and the neuronal development and migration (Lu et al., 2004 and Tymanskyj et al., 2012). The last

target gene affected by MKL1/2 knockdown is represented by the transmembrane protein MYOF that is known to play a crucial role in cancer seen by a strong MYOF overexpression in a variety of different cancer cell lines and types, like breast, ovarian and liver cancer for example (Adam et al., 2003; Labhart et al., 2005 and Ponten et al., 2008) (see also the description under 2.3.2 in the introduction). The special role and involvement of MYOF in tumorigenesis, especially in hepatocellular carcinoma cells, will be discussed in more detail below in the following chapter under 7.3. The novel identified target genes have been shown to be downregulated upon MKL1/2 depletion in different HCC cell lines, such as HuH6, HuH7 and HepG2, indicating a high relevance of these genes for hepatocarcinogenesis. Further, almost all of the newly identified genes are involved in cancer and most of them exhibit tumorigenic properties, this way the novel target genes may potentially be involved in the MKL1/2 knockdown-mediated tumor growth regression and induction of OIS response and may be responsible for the repressed tumorigenic properties that arise due to MKL1/2 depletion (Muehlich et al., 2012).

7.1.2 Mutual dependence of MKL1 and MKL2 in HCC cell lines

While performing the target gene analysis with RNA interference (RNAi) experiments using MKL1, MKL2, MKL1/2 or a combination of both MKL1 and MKL2 siRNAs, we surprisingly found out that a single knockdown of MKL1 as well as a single knockdown of MKL2 in HCC cell lines reduced the mRNA expression level of target genes nearly in the same manner as a knockdown of both MKL1 and MKL2. This obtained result was not described in literature so far, rather in previous studies depletion of both MKL1 and MKL2 was required to inhibit the SRF target gene expression (Cen et al., 2003 and Medjkane et al., 2009). RNAi experiments in HeLa cells and MDA-MB 231 breast cancer cells showed that a single ablation of MKL1 or MKL2 was not sufficient for a reduced expression of immediate early genes (IEGs) (Cen et al., 2003 and Medjkane et al., 2009). Finding an explanation for the given phenomenon of the single MKL1 or MKL2 knockdown, we also observed a mutual dependence of MKL1 and MKL2, meaning that the introduction of MKL1 siRNA into HCC cells, like HuH6, HuH7 and HepG2 cells, resulted in strongly reduced MKL1 and also MKL2 expression as well as MKL2 siRNA inhibited MKL2 and additionally MKL1 expression. Contradictory to our findings, this mutual dependence was not observed in HeLa cells as well as in human primary tubular epithelial cells, where MKL1 siRNA only decreased the MKL1 expression level without affecting the MKL2 expression level and similarly the other way around (Cen et al., 2003 and Hermanns et al., 2017). This prompted us to declare the mutual dependence as a HCC specific phenomenon that remains to be determined also for other cancer types and tumor

cells. The fact that we achieved a reduced target gene expression only due to a single MKL1 or MKL2 knockdown may be a suitable explanation for the abolishment of HCC xenograft growth figured out by Hampl and colleagues (Hampl et al., 2013). In this study a knockdown of MKL1 was also sufficient for the tumor growth inhibition *in vivo* in which the HCC xenograft tumors in mice were significantly reduced due to the treatment with polyethylenimine (PEI)-complexed MKL1 siRNA comparable to the combinatory treatment of MKL1 and MKL2 siRNA (Hampl et al., 2013). Given the result that MKL1 or MKL2 silencing is sufficient for target gene inhibition this is also relevant for upcoming therapeutic approaches where only MKL1 or MKL2 siRNA is needed instead of a double knockdown of both MKL1 and MKL2.

7.1.3 Regulation of newly identified target genes upon stimulant or inhibitor treatment

Given that the transcriptional MKL1/SRF driven target gene expression is regulated via the RhoA-actin signaling, we investigated the effect of an alteration in this signaling pathway on the novel target genes using extracellular stimulating or inhibiting agents. Performing qRT-PCR analysis revealed a strong downregulation of MKL target genes including SRF upon treatment with the actin polymerization inhibitor latrunculin B (LatB). Because LatB inhibits the binding of adenosine triphosphate (ATP) to monomeric G-actin, it is unable to polymerize into filamentous F-actin and results in a repressive MKL1-G-actin complex (Yarmola et al, 2000; Miralles et al., 2003; Muehlich et al., 2008 and Kircher et al., 2015). The reduced target gene expression fits well to the MKL1 activation pathway and seems to be a result of the dissociated MKL1-FLNa complex due to LatB treatment that Kircher *et al.* recently found out (Miralles et al., 2003; Muehlich et al., 2008 and Kircher et al., 2015). On a molecular level, this blocked MKL1-FLNa complex formation in turn provokes a redistribution of MKL1 from the nucleus into the cytoplasm explaining the inhibitory effect of LatB on gene expression (Kircher et al., 2015). A result similar to ours was obtained by Medjkane and his group showing that LatB treatment in two different cancer cell lines inhibited the ability of MKL1 to activate an SRF reporter gene measured by luciferase activity illustrating a general effect of RhoA-actin signaling in cancer cell lines (Medjkane et al., 2009). As expected, experiments in NIH 3T3 fibroblasts and HepG2 hepatocellular carcinoma cells owing cytoplasmic MKL1 under physiological conditions showed strongly induced SRF and MKL target gene expression upon fetal bovine serum (FBS) treatment. Contrary to the inhibiting effect of LatB, serum/FBS activates RhoA and its signaling pathway by supporting the actin polymerization from G-actin into F-actin leading to an accumulation of MKL1 in the nucleus and therefore to the activation of SRF (Miralles et al., 2003). In the same way, lysophosphatidic acid (LPA) activates RhoA and thus enhances actin polymerization (Muehlich et al., 2004). Treatment of

HepG2 and MCF7 cells as well as human primary fibroblasts with LPA having cytoplasmic MKL1 in an unstimulated state revealed a strong induction of SRF and MKL target genes requiring the necessary translocation of MKL1 from the cytoplasm to the nucleus (Vartiainen et al., 2007 and Kircher et al., 2015). As cellular response to LPA, an enhanced association of MKL1 and FLNa in the nucleus was observed that subsequently resulted in the obtained MKL target gene activation (Kircher et al., 2015). This correlated well with the induction of the MKL target genes upon LPA treatment. Next, we also investigated the role of cytochalasin D (CytoD) on target gene expression and observed a strong induction of SRF and MKL target genes in cell lines having MKL1 in the cytoplasm under non-stimulated conditions, for instance NIH 3T3 fibroblasts, HepG2, HLF and MCF7 cancer cells, upon CytoD stimulation. While CytoD, an actin-binding drug, induces a dimerization of G-actin and promotes ATP hydrolysis, it disrupts the regulatory function of G-actin and reduces the inhibitory association of MKL1 and G-actin in the cytoplasm and therefore causes a release and accumulation of MKL1 in the nucleus (Sotiropoulos et al., 1999; Miralles et al., 2003 and Vartiainen et al., 2007). In a recent study of Muehlich and colleagues the stimulating effect of CytoD shown by CTGF induction due to an increased amount of nuclear MKL1 was reported (Muehlich et al., 2017). Consistent with all these findings, we did not observe a potent SRF or MKL target gene induction upon CytoD treatment in HuH7 and MDA-MB 468 cells having in common that they already constitute nuclear MKL1 in the unstimulated state. Contradictory to our observations, the stimulation with CytoD activates in a luciferase assay the SRF reporter gene mediated by MKL1/2 and SRF in MDA-MB 231 as well as in B16F2 cells, the former harboring nuclear MKL1 in the unstimulated state (Medjkane et al., 2009). At least, they found out that the activation of the SRF reporter gene and also the target gene activation is stronger in the B16F2 cells than in the MDA-MB 231 cells, being more suitable to our findings (Medjkane et al., 2009). The effect of cytochalasin D may act cell line specific and still remains to be more investigated. It is tempting to speculate that the induction or decline of target gene expression in response to the activating or inhibiting reagents is a result of the association or dissociation of the MKL1-FLNa complex. Because FLNa is an F-actin binding protein (Flanagan et al., 2001 and van der Flier & Sonnenberg, 2001) and the reagents have a strong effect on the actin polymerization status, it might be possible that the binding of FLNa to F-actin is also responsible for target gene induction and that actin itself becomes a part of an MKL1-FLNa-F-actin complex. Overall, we found that the expression of the novel identified target genes can be regulated and thus becomes activated or inhibited by extracellular reagents acting on the RhoA-actin signaling axis and verified thereby their dependency and intimate connection on MKL1's cellular localization.

7.2 The MKL1 binding protein Filamin A and its role in target gene expression

7.2.1 Characterization of FLNa expressing A7 cells and the effect of MKL1/2 in A7 cells

Filamin A (FLNa), belonging to the family of filamins, is an actin-binding protein being essential for actin filament crosslinking, stabilizing of orthogonal actin networks and linking them to cellular membranes (Flanagan et al., 2001; Stossel et al., 2001 and van der Flier & Sonnenberg, 2001). FLNa has also been described as multifunctional protein that is able to act on several different proteins and signaling pathways like binding to Rho family GTPases and therefore interacting with the Rho signaling cascade (Stossel et al., 2001). In a recent study of Kircher and colleagues FLNa was firstly characterized as novel MKL1 binding protein and interaction partner by a direct binding site on the MKL1 gene (Kircher et al., 2015). Given this knowledge about FLNa as an MKL1 interaction partner, one aim of this thesis was the evaluation of the impact of FLNa on the MKL1/2 target gene expression. Therefore, we further analysed the A7 melanoma cell line expressing FLNa. Additionally to the downregulation of FLNa itself in HuH7 cells with silenced MKL1/2, we observed a strong decrease in the mRNA expression of the novel MKL1/2 target genes upon MKL1/2 silencing in A7 cells in the same manner as a single MKL1 knockdown. These data show that silencing of only MKL1 and not the combination of MKL1 and MKL2 is also in melanoma cells sufficient for target gene downregulation and that the depletion of only one compound, MKL1 or FLNa, of the activating MKL1-FLNa complex suffices for reduced target gene expression. Here, a mutual dependence of MKL1 and MKL2 in the A7 melanoma cells was, additionally to the HCC cell lines described under 7.1.2, observable explaining the requirement of only MKL1 or MKL2 depletion for effects on target gene expression. Regarding this, the mutual dependence of MKL1 and MKL2 seems to be a phenomenon of cancer cells, at least shown in two different cancer types, the hepatocellular and the melanoma cancer. Furthermore, we found out that MKL1 and/or MKL2 downregulation in A7 cells resulted in a proliferation arrest of the melanoma cells and in a significant induction of cellular senescence, illustrated by β-galactosidase staining suggesting a broader significance for the proliferation arrest and the senescence induction due to MKL1/2 knockdown in different cancer cell lines like in both HCC and melanoma cells. In this context, it remains to be investigated whether a FLNa knockdown in cancer cell lines may also result in an increase in senescence induction and thus showing that FLNa acting as MKL1 binding partner might also be responsible for the tumorigenic properties arising from MKL1/2 and MYOF overexpression.

7.2.2 FLNa dependency of MKL1/2 target genes

In addition to the MKL1 dependency of the novel identified target genes described in 7.1.1, we verified their dependence on FLNa. Thus, we introduced FLNa siRNA into HepG2 hepatocellular carcinoma cells, MDA-MB 468 mammary carcinoma cells, A7 melanoma cells and NIH 3T3 fibroblasts and observed strongly reduced mRNA expression levels of the MKL1/2 target genes in all the different cell lines indicating the broad significance and relevance of the given result. The expression of all the novel MKL target genes as well as of the previously known target genes SM22 and MYH9 seems to be dependent on FLNa expression and thus, the interacting complex of MKL1 and FLNa is also essential for the regulation of the MKL gene expression. Regarding this result, only one compound of the MKL1-FLNa complex, MKL1 or FLNa, has to be downregulated for an effect on target gene expression.

7.2.3 Impact of FLNa on target gene expression and the influence of actin

Because the A7 melanoma cells show the same properties regarding the characteristics of tumor cells, like proliferation and senescence induction upon MKL1/2 knockdown, as the HuH6 and HuH7 hepatocellular carcinoma cells, we next focused our research concerning FLNa on the FLNa expressing A7 cells in comparison to the M2 cells lacking FLNa expression. Our aim was to figure out the impact of FLNa on the MKL1/2 dependent target gene expression and thus we overexpressed the MKL1 wildtype (wt) or the MKL1 S454A mutant in A7 control cells and additionally in A7 cells transfected with FLNa siRNA. qRT-PCR analyses revealed a strong upregulation of SRF and GLIPR1 expression in A7 cells overexpressing MKL1 wt and to a greater extend in A7 cells overexpressing the MKL1 S454A mutant compared to A7 cells endogenously expressing MKL1. This result perfectly corresponds to the study of Muehlich and colleagues generating the MKL1 S454A mutant being incapable of MKL1 phosphorylation due to its mutation at the phosphorylation site of MKL1 that enables MKL1 to enhanced nuclear accumulation and this way to activate SRF and its target genes (Miralles et al., 2003 and Muehlich et al., 2008). In contrast, overexpression of MKL1 wt and the MKL1 S454A mutant in A7 FLNa siRNA treated cells exhibited only modest effects on SRF and GLIPR1 induction and their expression is strongly reduced compared to the same MKL1 variants overexpression in FLNa expressing cells, whereas the SRF and GLIPR1 expression is also higher in cells transfected with the MKL1 S454A phosphorylation mutant than with MKL1 wt. Regarding these data, we can conclude that FLNa is essential for SRF activation and the subsequent target gene upregulation and

that an increased MKL1 expression cannot compensate the lacking FLNa existence. To further substantiate our observations, we next investigated the role of the constitutive active variant of MKL1, MKL1 N100, on target gene expression depending on the FLNa status of the cells. For the MKL1/2 target genes SM22 and GLIPR1 we found significantly increased mRNA expression levels in A7 control cells overexpressing the MKL1 N100 mutant compared to the MKL1 wt, whereas their expression with the MKL1 N100 overexpression in A7 cells depleted of FLNa was significantly reduced. Confirming the strong effect of FLNa on target gene expression, we also performed this experiment in M2 melanoma cells naturally lacking FLNa expression and observed, as expected, also a strong decrease in SM22 and GLIPR1 expression, very similar to the A7 cells with FLNa knockdown. The very strong induction of target gene expression upon MKL1 N100 mutant overexpression in A7 control cells can be explained by its structure: lacking the N-terminal 100 amino acids of MKL1 that contain the RPEL motifs being essential for actin binding abolishes the MKL1 binding to G-actin resulting in nuclear translocation and accumulation of the released MKL1, where it can now bind and activate SRF (Miralles et al., 2003 and Muehlich et al., 2008). The MKL1 N100 mutant has already been reported by Muehlich and colleagues to activate target genes, such as vinculin, and the luciferase activity serving as positive control of our approach (Muehlich et al., 2008). The only modest effects of MKL1 N100 expression in M2 cells and also in A7 cells with FLNa depletion on target gene expression illustrate again the importance of FLNa for the activation and induction of MKL1/2 target genes acting in concert with MKL1/2 and that constitutive active MKL1 is not sufficient for downstream gene expression in the absence of FLNa.

Suggesting that FLNa and MKL1 interact with each other by constituting a complex, we were interested in discovering the binding site of FLNa on MKL1 and therefore we used the MKL1 Δ301-342 mutant lacking the amino acids 301-342 for further investigations. qRT-PCR analysis revealed significantly reduced expression levels of SM22 and GLIPR1 in A7 cells overexpressing the MKL1 Δ301-342 mutant compared to the MKL1 wt indicating the existence of a potential FLNa binding site between the amino acids 301-342 of MKL1. Trying to identify a more precise binding site with a smaller amino acid range, we generated the MKL1 Δ301-310 mutant lacking only the amino acids 301-310 and observed the same strong decrease in target gene expression, exemplary shown for SM22 and CTGF, in A7 cells expressing the MKL1 Δ301-310 mutant in comparison to the MKL1 wt showing a great induction of gene expression. While narrowing down the binding site and pointing out that FLNa binds MKL1 between the amino acids 301-310, we focused our research on the deeper mechanism of FLNa acting on MKL1 activation and target gene expression. Performing chromatin immunoprecipitation (ChIP) assays, we observed an intense enrichment of CTGF and actin promoters from FLNa immunoprecipitates in A7 cells but not in M2 cells lacking FLNa expression demonstrating the direct recruitment of FLNa to the

CTGF and actin promoters leading to activation of their transcription. These data seem similar to the result obtained for the MYOF promoter in FLNa as well as in MKL1 immunoprecipitates described above suggesting a general role for FLNa on direct target gene activation by binding to the gene's promoter imaginable as MKL1-FLNa complex.
Regarding the direct regulation of actin by FLNa via binding to the actin promoter, it inspired us to further investigate the role of actin in the context of FLNa expression and target gene activation. Overexpression of FLNa wildtype (wt) in M2 cells revealed, not surprisingly, a very strong induction in FLNa and also a strong activation in GLIPR1 mRNA expression, whereas the overexpression of both FLNa wt and the formin mDiact showed a significant induction of GLIPR1 expression compared to the single FLNa wt overexpression. It is recently reported that mDiact, the constitutively active variant of mDia1 predominantly located in the nucleus, is a member of the formin family accelerating the actin nucleation and the formation of filamentous F-actin (Watanabe et al., 1999; Copeland et al., 2007 and Baarlink et al., 2013). This perfectly corresponds to the known mechanism of mDiact having a positive effect on MKL1/2 by enhancing actin polymerization from G-actin into F-actin consequently promoting MKL1/2's nuclear accumulation and therefore the activation of the MKL1/2 target genes (Staus et al., 2007 and Staus et al., 2014). The result that the target genes became more activated in the presence of mDiact and the simultaneous overexpression of FLNa proposes that the present actin status, such as monomeric G-actin or filamentous F-actin, is responsible for target gene expression. Our further observations in A7 cells exhibiting increased expression of SRF, SM22, GLIPR1 and CTGF upon mDiact expression are this way also in accordance with several published studies showing an effect of mDiact on different target genes and SRF activity that requires nuclear actin polymerization (Baarlink et al., 2013 and Staus et al., 2014). Kircher and colleagues also showed an effect on target genes upon mDiact overexpression only observable in A7 cells but not in M2 cells lacking FLNa expression suggesting that the presence of FLNa is required for the actin modulating activities (Kircher et al., 2015).

In this thesis, we could demonstrate that the newly identified MKL1 binding partner FLNa is additionally to the MKLs responsible for the novel MKL1/2 dependent target gene expression and that all these target genes are also FLNa dependent, shown in different cell lines. The requirement of FLNa for the induction of the target genes as well as for the modulating effects of actin attributes FLNa a very important role in carcinogenesis.

7.3 The target gene myoferlin and its role in hepatocarcinogenesis

7.3.1 Characterization of myoferlin as MKL and SRF dependent target gene

The main aim of this thesis was the characterization of the transmembrane protein myoferlin (MYOF) regarding its dependency on the MKLs, its tumorigenic properties and also its involvement in hepatocellular carcinoma. Beside the fact that we found several target genes depending on MKL1 and MKL2 we had to choose one of them for further investigations and had to show if this one is able to transduce the effects of MKL1 and MKL2 on tumor inhibition and induction of oncogene-induced senescence (Hampl et al., 2013). Based on the result of the Cancer Genome Atlas showing the highest coexpression with MKL1 and MKL2 compared to the other target genes and the recent study of Turtoi and colleagues demonstrating a strong impact of MYOF on breast cancer, we decided to choose MYOF as target gene of choice for further improvement (Cerami et al., 2012; Gao et al., 2013 and Turtoi et al., 2013).

Stimulation of HuH7 and MDA-MB 468 cancer cells with FBS, LPA, cytochalasin D and jasplakinolide revealed an induction of MYOF protein expression, in which the stimulation with CytoD showed only a very modest effect compared to the other reagents on the MYOF expression that matches well to the results discussed above under 7.1.3. Jasplakinolide enhances like LPA the actin polymerization and therefore binds and stabilizes the filamentous F-actin network (Bubb et al., 1994 and Bubb et al., 2000). The results also confirm a regulation of MYOF via the RhoA-actin signaling way and thus also an involvement of MKL1 and MKL2 acting on this pathway. To further review the direct dependency of MYOF on the MKLs we performed reporter gene assays with constitutive active variants of MKL1, the MKL1 N100, and SRF, the SRF-VP16 plasmid, and different promoter constructs of MYOF. This way, we found out that only the 900 bp promoter but not the 200 bp promoter was activated by SRF-VP16 and that the activity of this 900 bp promoter construct was also increased by MKL1 N100 expression. To narrow down the binding site of SRF and MKL1 on the MYOF promoter, we generated a deletion mutant lacking the basepairs 304-363 in whose region one of the MYOF promoter CArG boxes is located. Not surprisingly, the activity of the reporter genes and thus the deletion mutant promoter construct (Δ304-363) was not enhanced due to MKL1 N100 expression shown by a reporter gene assay. These findings illustrate the direct involvement of MKL1 and SRF as transcriptional regulators of MYOF by binding its CArG box in the MYOF promoter within the basepairs 304-363. Additionally to the results obtained by luciferase assays, we investigated the direct recruitment of MKL1 to the MYOF promoter by performing a chromatin immunoprecipitation (ChIP) assay and found a strong enrichment of the MYOF promoter due to an MKL1 pulldown. The GAPDH promoter

and an upstream site in the MYOF promoter (MYOF 1167) were not enriched by MKL1, while the promoter of the known MKL target gene α-smooth muscle actin (α-SMA) was amplified (Zhao et al., 2007), whereas the induction of the MYOF promoter was much stronger showing the intense occupancy by MKL1. Confirming the mentioned regulation of MYOF expression via the RhoA-actin signaling pathway, we also performed this ChIP assay with serum-starved cells and cells with LPA stimulation and found, as expected, an inducible enrichment of the MYOF promoter upon LPA treatment. Next, we also checked for a direct recruitment of FLNa, the novel identified MKL1 interaction partner (Kircher et al., 2015), to the MYOF promoter and observed a strong increase in MYOF promoter activity in FLNa expressing A7 cells compared to FLNa-deficient M2 cells, where no promoter enrichment was detectable. This data argue for a responsibility of MKL1 as well as of its interaction partner FLNa for the MYOF expression by a direct recruitment of MKL1 and FLNa to a CArG box that is located within the position 304-363 in the MYOF promoter and strengthens the requirement of the activating MKL1-FLNa complex for target gene expression in general, as also shown for the target gene CTGF described under 7.2.3.

While bringing to light that MYOF is directly dependent on MKL1 and MKL2 and thus MYOF may be the transducer of the effects arised by MKL1/2 and the fact that the induction of oncogene-induced senescence is reached by MKL1/2 downregulation as shown by Hampl and colleagues (Hampl et al., 2013), we asked for the tumorigenic properties of MYOF and if it mediates some characteristic features of cancer cells in order to be able to transduce the tumorigenic properties mediated by the MKLs.

7.3.2 Tumorigenic characteristics of myoferlin

Because previous studies pointed out oncogenic properties for activated, nuclear MKL1 and MKL2 and thus a strong decrease in cell proliferation, cell invasion and cell migration due to a depletion of MKL1/2 in tumor cells was shown (Medjkane et al., 2009, Muehlich et al., 2012 and Hampl et al., 2013), we investigated the role of MYOF regarding its possessing tumorigenic features. Here, we found a significant proliferation arrest in HuH6 hepatocellular carcinoma cells due to a knockdown of MYOF that is also shown in HuH7 cells in the study of Hermanns *et al.* (2017) and is similar to the result of an MKL1/2 depletion found by Hampl and colleagues (Hampl et al., 2013). We also observed strongly decreased invasive properties of HuH6 cells depleted of MYOF compared to the invasive control cells. In agreement with our data, Eisenberg and colleagues demonstrated also a reduced invasive capacity of MDA-MB 231 breast cancer cells upon MYOF ablation and another study of

Leung and his group revealed a decreased proliferation rate in MYOF depleted mouse Lewis Lung carcinoma (LCC) cells *in vitro* as well as in LCC tumors *in vivo* (Eisenberg et al., 2011 and Leung et al., 2013). The observed involvement of MYOF in regulating cancer cell invasion is additionally accompanied by a mesenchymal-epithelial transition (MET) in cells lacking MYOF and therefore they were converted from migratory and invasive cells into more epithelial like cells as shown by a correlation of the morphological changes as well as lower expression levels of mesenchymal EMT markers, such as fibronectin and vimentin (Kalluri & Weinberg, 2009 and Li et al., 2012). Because MYOF plays also a role in exocytosis of cells, it is not unattended that MYOF depletion alters the expression of matrix metalloproteinases (MMPs) being endopeptidases essential for degrading basement membrane and extracellular matrix (ECM) components and thus being targets of MYOF (Duffy et al., 2000; Cipta & Patel, 2009 and Li et al., 2012). A significant decrease in MMP production and secretion in breast cancer cells due to a MYOF knockdown is shown in several studies explaining the effects of MYOF on cell invasion because MMPs are known to play an important role in modulating the invasive properties of cells (Eisenberg et al., 2011 and Li et al., 2012). Summing up, MYOF seems to play an important role in promoting the proliferative and invasive behavior of cancer cells by inducing EMT and mediating endocytosis as well as exocytosis of cells and thus MYOF contributes to the characteristic features of cancer cells.

Because the described features occurring upon a MYOF depletion in cells, like the proliferation arrest, may possibly arise due to an induced apoptotic or senescent pathway of the cell as tumor evading strategy (Wyllie et al., 1980 and Wynford-Thomas, 1999), we next looked for an alteration of the cell's senescence level due to rendered MYOF expression. Therefore, we performed a β-galactosidase staining in MYOF depleted HuH6 cells serving as a well established marker for senescent cells *in vitro* as well as *in vivo* (Dimri et al., 1995 and Debacq-Chainiaux et al., 2009). In accordance to the result of an MKL1/2 knockdown depicted by Hampl and colleagues (Hampl et al., 2013), the MYOF lacking cells in our approach exhibited a significantly induced cellular senescence compared to the control cells. Since MKL1/2 and SRF are still described in the context of inducing senescence when they are downregulated in HCC cells, in murine smooth muscle cells (SMCs) and in mice muscles, MYOF is for the first time characterised as a modulator of proliferation and cellular senescence in HCC cells (Angstenberger et al., 2007; Lahoute et al., 2008 and Hampl et al., 2013). Indicating the cellular senescence as underlying mechanism for the observed proliferation arrest so far, we were next interested in this molecular mechanism of the induced senescence response upon MYOF depletion.

7.3.3 Induction of oncogene-induced senescence via EGFR phosphorylation due to myoferlin depletion

For clarifying the molecular mechanisms and the mechanistic insights underlying the cellular senescence induction upon MYOF depletion, we first focused on the effect of MYOF on the expression and activation of the epidermal growth factor receptor (EGFR). Since a recent study of Turtoi and colleagues demonstrated a significant increase in the activation and phosphorylation of the EGFR due to MYOF knockdown in breast cancer cells (Turtoi et al., 2013), we depleted MYOF as well as MKL1/2 in HuH6 and HuH7 HCC cells and also observed a strong phosphorylation of the EGFR at tyrosine 1173 both upon MYOF and MKL1/2 ablation. Showing that the induced EGFR phosphorylation due to the MKL1/2 depletion was strongly reduced upon additional MYOF overexpression, we can assume that the phosphorylation and dephosphorylation of the EGFR is a dynamic and reversible process depending on the MYOF expression level. Further, we examined the role of the EGFR activation also *in vivo* in the HCC xenograft samples treated with MKL1+2 siRNA and found the EGF receptor strongly phosphorylated. In accordance with these data, we observed no phosphorylation of the EGFR in the tumor tissue of SRF-VP16^{iHep} mice strongly expressing MYOF, but a strongly phosphorylated EGFR in the non-tumorous control tissue arguing for a prominent role of MYOF in modulating the phosphorylation state of the EGFR *in vitro* as well as *in vivo*. In an additional experiment, we checked for the reason of the sustained EGFR phosphorylation upon MKL1/2 and MYOF knockdown and performed an immunofluorescence staining in HuH7 control and HuH7 MYOF depleted cells transfected with GFP-tagged EGFR. In the MYOF lacking cells the EGFR was visible as distinct dots compared to a diffuse coloring of the EGFR in the control cells suggesting that MYOF depletion causes a degradation arrest and thus an accumulation of the EGFR in the cell, similar to the observations in the study of Turtoi and his group (Turtoi et al., 2013). To further verify this hypothesis, we also treated HuH7 cells with the proteasome inhibitor MG132 and observed the same result of EGFR accumulation as treated with MYOF siRNA, again confirming the result obtained by Turtoi and colleagues in breast cancer cells (Turtoi et al., 2013). Because MG132 is known as a peptide effectively inhibiting the proteolytic activity of the 26S proteasome, MYOF seems to be involved in the regulation of the internalization and degradation process of the EGF receptor and the regulation of the proteasome activity (Lee & Goldberg, 1998). Since the EGFR is localized to the caveolae and the phosphorylation of the EGFR results in a dissociation from the caveolae accompanied by a reduced binding of the phosphorylated EGFR and caveolin-1, the main structural component of caveolae, the EGFR also colocalizes with MYOF in breast cancer cells that in turn is also colocalized with caveolin (Smart et al., 1995; Agelaki et al., 2009 and Turtoi et al., 2013). These data demonstrate the important interaction of MYOF and caveolin being essential for

the organization of caveolae and the endocytosis of the phosphorylated EGFR and that there is a relationship between MYOF and the caveolae in the context of endocytosis (Bernatchez et al., 2009). It remains to be investigated how MYOF interacts with the caveolae in detail and what the role of MYOF in the underlying mechanism of EGFR degradation is. Our observations are also confirmed by several other studies demonstrating an impact of MYOF on the stabilization of different receptor tyrosine kinases (RTKs), such as vascular endothelial growth factor (VEGF) or insulin-like growth factor (IGF) receptors, and the modulation of receptor recycling or the degradation rate (Bernatchez et al., 2007; Demonbreun et al., 2010 and Eisenberg et al., 2011).

Following the known signaling cascade of activated EGFR, we next looked for the influence of MYOF on the important components of this downstream pathway. Here, we found that, beside the MKL1/2 knockdown, MYOF depletion strongly activated oncogenic Ras, shown by the increased expression level of GTP-bound Ras. The GTP load of Ras is a dynamic process in which MYOF seems to be involved, because the re-expression of MYOF in MKL1/2 depleted cells resulted in inactive GDP-bound Ras. In consequence of the activated Ras, the extracellular signal-regulated kinase 1/2 (ERK1/2) gets phosphorylated and thus activated upon MYOF silencing in HCC cells. Treatment of MYOF depleted cells with a SOS SH3 domain inhibitor revealed a strong decrease in the activation and phosphorylation of ERK1/2 as well as in the induction of cellular senescence, indicated by β-galactosidase staining, to nearly basal levels observed in the cells without MYOF knockdown. Because the SOS SH3 domain inhibitor blocks the interaction of the guanine nucleotide exchange factor son of sevenless (SOS) and the SH3 domain of the growth factor receptor-bound protein 2 (GRB2) bound to the phosphorylated EGFR, SOS is now unable to bind the inactive GDP-bound Ras and thus no exchange of GDP to active GTP can occur resulting in inactive Ras and no downstream signaling (Li et al., 1993; Vidal et al., 2003 and McKay & Morrison, 2007). Because the inhibitor acts on the interface of EGFR phosphorylation, Ras activation and senescence induction, whereas SOS itself links the RTKs, such as EGFR, to Ras signaling, and the fact that the inhibitor altered the MYOF-silenced-mediated ERK1/2 phosphorylation and the senescence induction we can assume that MYOF directly acts on the Ras/Raf/MEK/ERK pathway.

The Ras/Raf/MEK/ERK pathway downstream of Ras is described as the most relevant one for senescence induction and thus proliferation arrest (Lin et al., 1998 and Zhu et al., 1998). In this context, Serrano and colleagues postulated for the first time the existence of the premature or so-called oncogene-induced senescence (OIS) arising due to the activation of oncogenes in contrast to the so far known replicative senescence characterized by a finite number of cell doublings (Serrano et al., 1997). This by activated oncogenes triggered OIS response is described to function as a very efficient cellular failsafe and tumor suppression

mechanism reducing the transforming potential of sustained Ras signaling (Serrano et al., 1997; Lin et al., 1998 and Michaloglou et al. 2005). According to several studies showing that the OIS induction via the activation of the MAPK cascade is controlled by the two tumor suppressors $p16^{Ink4a}$ and p53, we observed an increased expression level of $p16^{Ink4a}$ upon MYOF deletion (Serrano et al., 1997 and Lin et al., 1998). In our recent study, we also demonstrated a strong phosphorylation and therefore activation of p53 on serine 15 in HuH7 HCC cells lacking MYOF expression (Hermanns et al., 2017). In contrast, the HuH7 control cells, endogenously expressing MYOF, revealed only very low expression levels of $p16^{Ink4a}$ and phosphorylated p53, corresponding to the results found in literature showing also a very low expression and a high mutation rate of $p16^{Ink4a}$ and p53 due to many genetic or epigenetic alterations in many different tumor cell lines arguing for their important role in tumor development (Hollstein et al., 1991; Hollstein et al., 1996; Ruas & Peters, 1998 and Bennett, 2003). The fact that MYOF depletion increased the $p16^{Ink4a}$ and p53 activity and that their expression levels are always raised in senescent cells underscores the impact of MYOF on the induction of the OIS response (Alcorta et al., 1996; Hara et al., 1996 and Braig et al., 2005). On the molecular level, the tumor suppressor protein p53 activates the cyclin dependent kinase (CDK) inhibitor p21 and this prevents proliferation and promotes a cell cycle arrest in response to cellular stress causing senescence (Waldmann et al., 1995 and Brown et al., 1997). The tumor suppressor and CDK inhibitor protein $p16^{Ink4a}$ inhibits the CDK4/6 activity and thus provokes a G1 cell cycle arrest consequently preventing the phosphorylation of the retinoblastoma (Rb) protein (Alcorta et al., 1996; Hara et al., 1996 and Serrano et al., 1997). This way, the Rb protein is maintained in its activated, hypophosphorylated state having a negative influence on the G1 to S phase cell cycle progression resulting in senescence induction (Peeper et al., 1994; Weinberg et al., 1995 and Chicas et al., 2010). Given this molecular background, we monitored the effect of MYOF silencing on the phosphorylation status of Rb and observed a strong decrease of the phosphorylated Rb (pRb) expression in HuH6 as well as in HuH7 cells lacking MYOF. This way, MYOF ablation leads to induction of the OIS response due to forcing the Rb protein into its hypophosphorylated form that is also indicated by the molecular shift of Rb from the phosphorylated form to the hypophosphorylated form in HuH7 MYOF depleted cells seen in gelelectrophoresis in our recent study (Hermanns et al., 2017). The existence of the hypophosphorylated Rb protein is consistent with the observed G1 arrest of MYOF silenced cells and their inhibited G1 to S phase transition in our novel study, that is revealed by FACS analysis (Hermanns et al., 2017). For a deeper elucidation of the contribution of MYOF and the EGFR on the mechanism of senescence induction, we performed several experiments with inhibition of the MYOF-mediated effect on tumor suppressor activation. Additionally to the experiments described above, we treated HuH7 MYOF depleted cells again with the SOS SH3 domain inhibitor and observed a strong increase of the phosphorylated form of Rb

compared to the hypophosphorylated Rb in HuH7 cells without SOS inhibitor treatment. Silencing of the EGFR in parallel with MYOF knockdown also revealed a significant decrease in $p16^{Ink4a}$ expression as well as a decline in senescence induction induced by a single MYOF loss demonstrating once again the importance of MYOF on the OIS response executed by the EGFR and the downstream Ras/Raf/MEK/ERK as well as the p16/Rb pathway. Contradictory to these findings, silencing of the EGFR with tyrphostin AG1478, a specific tyrosine kinase inhibitor of the EGFR, in HuH7 MYOF depleted cells showed no alteration in the expression of $p16^{Ink4a}$ and the senescence induction in comparison to the cells lacking MYOF, although the EGFR gets dephosphorylated and the total EGFR expression was also diminished. AG1478 functions by competitive binding to the ATP pocket of the EGFR resulting in inhibiting its activity and by increasing the formation of inactive EGFR dimers (Han et al., 1996 and Gan et al., 2007). In several studies AG1478 treatment was able to inhibit the growth of tumors overexpressing EGFR in combination with an antibody against the EGFR that prevents the ligand binding to the receptor or the AG1478 inhibited the proliferation rate and forced a cell cycle arrest in nasopharyngeal carcinoma (NPC) cells (Zhu et al., 2001 and Johns et al., 2003). Whereas Gao and colleagues found out that 1 µM AG1478 was sufficient to reduce the cadmium-induced phosphorylated ERK1/2 expression in human uterine leiomyoma (ht-UtLM) cells, Zhu and his group observed an inhibition of the downstream AKT and MAPK pathway in NPC cells only upon treatment with a minimum of 50 µM AG1478 although the EGFR phosphorylation was almost completely inhibited upon addition of only 1 µM AG1478 (Zhu et al., 2001 and Gao et al., 2015). The effect of AG1478 on the downstream targets of the EGFR and the Ras/Raf/MEK/ERK pathway seems to be dose-dependent and also cell type specific, thus explaining that there is no observable modification in the $p16^{Ink4a}$ and senescence induction upon treatment of 10 µM AG1478 in MYOF depleted cells in our approach. Another suitable explanation for this finding might also be the known redundant kinase activation mechanism, for example the activation of IGFR, VEGFR or PDGFR, as escaping strategy from EGFR inhibiting reagents (Luo et al., 2014). It might also be possible that the developed acquired resistance mechanism of HCC cells against antitumor drugs, such as AG1478, is responsible for the inefficient treatment of HuH7 HCC cells with AG1478 (Bagrodia et al., 2012 and Lackner et al., 2012).

Finally showing the direct contribution of MYOF knockdown on OIS induction, we analysed the expression of two additional OIS markers being beside the increased β-galactosidase activity and the activation of the MAPK and p16/Rb pathway a characteristic feature of senescent cells. Alterations in the extracellular matrix (ECM) associated factors and the change of the secretome of cells are key events during senescence induction and referred to as senescence-messaging secretome (SMS) (Cristofalo & Pignolo, 1996 and Kuilman & Peeper, 2009). This SMS induction contributes to senescence by upregulation of

several secretory factors, including inflammatory cytokines, chemokines, matrix remodeling factors or growth factors (Kuilman et al., 2008; Kuilman et al., 2010; Rodier & Campisi, 2011 and Ohtani & Hara, 2013). Our experiments revealed a significant increase in the expression of the SMS factors C-X-C motif chemokine ligand 10 (CXCL10) and tumor necrosis factor superfamily member 10 (TNFSF10) in both HuH6 and HuH7 HCC cells depleted of MYOF. These data and the fact that CXCL10 as well as TNFSF10 are secreted by senescent cells and that they force cancer cells into a senescence response give evidence to the concept of MYOF silenced-mediated and induced OIS (Dabrowska et al., 2011 and Braumuller et al., 2013).

Although we focused our research on the effects of the target gene myoferlin, we cannot exclude a partial contribution of other MKL1/2 target genes on senescence induction. In this context, we also checked for the known MKL target gene mitogen-inducible gene-6 (Mig6) that is reported to be a negative regulator of the EGFR family and the MAPK signaling cascade, especially in human hepatocellular carcinoma (Descot et al., 2009 and Reschke et al., 2010). Our performed experiments demonstrated also a dependency of Mig6 on MKL1/2, but we did not observe an alteration in the proliferative capacity of HuH7 cells either transfected with Mig6 siRNA compared to the control cells nor with an overexpression of Mig6 in MKL1/2 depleted cells in comparison to the cells with MKL1/2 knockdown. Downregulation of Mig6 mediated by RNAi showed also no effect on senescence induction, because there was no change in the expression levels of $p16^{Ink4a}$, CXCL10 and TNFSF10 observable. These data strongly argue against a potential role of Mig6 in the MKL1/2-mediated senescence response induction so that Mig6 can be excluded as tumor properties transmitting gene despite its function to negatively regulate the EGFR. However, other target genes, especially those identified in the MKL1/2 dependent microarray, may have an impact on the MAPK signaling pathway and the senescence induction. To figure out these potential genes and their involvement in the induction of the OIS response might be an aim for future experiments. So far, it has already been reported that the target gene MYH9 does not alter the cell cycle phase distribution of cancer cells and does not induce apoptosis, whereas MYH9 silencing resulted in decreased invasive and metastatic properties suggesting that MYH9 may also be involved in senescence induction due to its invasive behavior observed in different cell lines (Medjkane et al., 2009 and Derycke et al., 2011). Like MYH9, SM22 depleted fibroblasts also exhibit a reduced cell migration and invasion rate (Thompson et al., 2012) and the target gene TGFß1 is described to play a key role in the epithelial-mesenchymal transition (EMT), thus it forces cells into invasive and migratory tumor cells and it is shown to be involved in the expression of the EGFR and senescence induction in melanoma cells (Thiery, 2002; Morita et al., 2007 and Sun et al., 2014). In this context, one may assume that TGFß1 expression is also critical for inducing senescence in hepatocellular

carcinoma cells and that the described tumorigenic characteristics of HCC cells may be mediated by TGFß1 due to the EMT induction. This way, in addition to MYOF silencing (Kalluri & Weinberg, 2009 and Li et al., 2012), the downregulation of TGFß1 may be required for the MET, the reversion of the EMT, and consequently for HCC regression. Since some other target genes, like GLIPR1, exhibit besides its tumor suppressing features in some kind of cells also oncogenic properties exemplified by their specific expression in some tumors (Murphy et al., 1995 and Chilukamarri et al., 2007), there is a high variety of different MKL1 and MKL2 target genes possibly involved in executing the MKLs mediated activation of the MAPK signaling cascade and the induction of the oncogene-induced senescence response that remains to be elucidated.

After indicating the very important role of MYOF in senescence induction via the EGFR and activation of the Ras/Raf/MEK/ERK pathway *in vitro*, we assumed to verify also *ex vivo* the mechanism MYOF is acting on as illustrated in the model in Fig. 54. Thus, we used liver tumor (LT) cells, which were derived from developed HCCs in mice conditionally expressing SRF-VP16 (Ohrnberger et al., 2015). Also these LT cells transfected with MYOF siRNA showed strongly reduced invasive and proliferative capacities compared to the LT control cells and furthermore, the β-galactosidase activity and thus the senescence induction was increased in the MYOF depleted cells. These data also suggest an important role for MYOF in the mediation of tumorigenic features *ex vivo*. In additional experiments, we confirmed the contribution of MYOF depletion in LT cells on the EGFR as well as on ERK1/2 phosphorylation and on the hypophosphorylation of Rb, illustrated by western blotting. qRT-PCR analyses revealed also a strong induction of $p16^{Ink4a}$ expression and of the SMS factor TNFSF10 due to MYOF knockdown.

Taken together, all these results strikingly show for the first time the direct involvement of MYOF in the OIS response of HCC cells via phosphorylation of the EGFR and activation of the Ras/Raf/MEK/ERK signaling pathway due to silencing of MYOF explaining the reduced tumorigenic properties of HCC cells upon MYOF knockdown *in vitro* as well as *ex vivo*. This way, we identified MYOF as novel MKL1 and MKL2 dependent target gene and characterized it as the special gene being responsible and mediating the effects of MKL1/2 on tumor inhibition via OIS induction. Thus, MKL1, MKL2 or most notably MYOF serve as novel promising therapeutic target preventing or abolishing hepatocarcinogenesis.

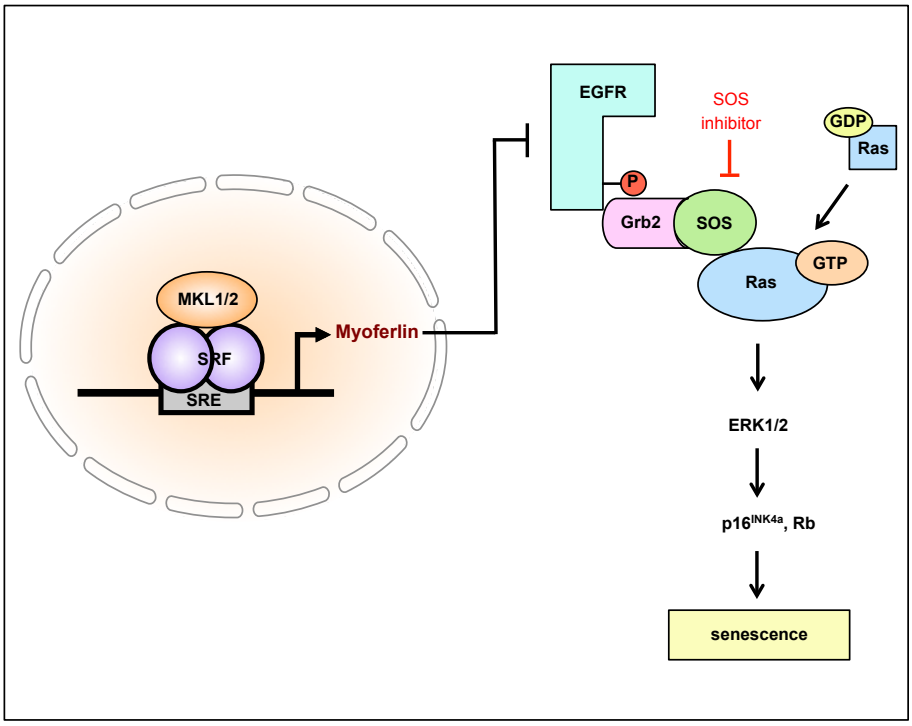

Figure 54: Oncogene-induced senescence response upon MYOF depletion. MYOF depletion leads to phosphorylation and therefore activation of the EGFR that in consequence activates Ras by GTP binding resulting in ERK1/2 phosphorylation, $p16^{Ink4a}$ activation, hypophosphorylation of Rb and finally in senescence induction.

7.4 Hepatocellular carcinoma and possible therapeutic approaches

The hepatocellular carcinoma (HCC), being the most common type of liver cancer, represents with 745 000 registered deaths per year the second cause of cancer related deaths in the world (Jemal et al., 2011 and Ferlay et al., 2015). Although the incidence of HCC is steadily rising, the underlying mechanisms and the formation of the hepatocellular carcinoma are only rarely understood so far and this way, it is a very important research goal for the upcoming years to figure out the mechanisms driving the HCC development and to give novel insights into the transformation of healthy hepatic cells into malignant hepatic tumor cells.

One already well known and documented signaling pathway involved in HCC formation and progression is the Ras/Raf/MEK/ERK pathway (Asati et al., 2016 and Wang et al., 2016). In this context it is reported that the aberrant activation of the Ras/Raf/MEK/ERK pathway is involved in cell proliferation, differentiation, motility and survival in general and thus in cancer growth and especially in HCC development (Yu et al., 2015; Asati et al., 2016 and Wang et al., 2016). More precisely, in 58 % of all HCCs MAPK/ERK signaling is activated and their corresponding genes are upregulated, demonstrated by MEK as well as ERK that are strongly overexpressed in hepatocirrhosis and HCC samples (Ho et al., 1998 and Liu et al., 2006). Also mutations that activate the small GTPase Ras occur in around 30 % of all cancers, whereas H-Ras is activated in around 94 % of HCC cases (Zuo et al., 2012). On a cellular level and serving as mechanism, the Ras/Raf/MEK/ERK pathway is activated amongst others via receptor tyrosine kinases (RTKs) and thus, 47.1 % of the HCCs are positive for the EGFR overexpression being also responsible for the recurrence and invasiveness of HCC (Tang et al., 1998). These findings perfectly resemble our results described above showing that the Ras/Raf/MEK/ERK pathway as well as its trigger EGFR is activated upon myoferlin depletion in HCC cells and thus plays an essential role in the development of cancer and especially of liver cancer. Contradictory to the results of the activated Ras/Raf/MEK/ERK signaling pathway in advanced HCC tissues, we figured out that the activation of Ras and its downstream targets leads to the induction of senescence and therefore to a reduced HCC growth. The existence of both opposed approaches may explain the bad outcome of a drug therapy directed against the members of the signaling pathway, like Ras or ERK1/2, for HCC patients because the senescence induction gets prevented by the drug administration and thus a tumor regression is difficult to achieve. With regard to this problem the role of the Ras/Raf/MEK/ERK pathway has to be more investigated in detail to elucidate the complete underlying mode of action also in the context of a promising cancer therapy. Given this high impact of the Ras/Raf/MEK/ERK pathway on hepatocarcinogenesis, it seems to be obvious looking for inhibitors of the different kinases and molecules of this

pathway. Great importance to such inhibitors is also attached because surgical resections of the tumors lead to an increased 5-year survival rate, but the long-term survival remains only low and the rate of recurrence and metastasis is still high (Kim et al., 2011 and Baek et al., 2012). Beside the well characterized therapeutic drug sorafenib, whose characteristics will be discussed below, the application of all other inhibitors ended up in preclinical or clinical studies without administration to patients with HCC so far. For example, the synthetic S-prenyl-cysteine analog Salirasib is a potent inhibitor of the active Ras protein by degrading all Ras isoforms and this way prevents the activation of the Ras dependent signaling cascades (Marom et al., 1995; Haklai et al., 1998 and McMahon et al., 2005). The farnesylthiosalicyclic acid Salirasib is reported to partially induce apoptosis and to inhibit the proliferation rate of HCC cells, and it reduced the tumor growth and prevented the development of hepatic tumors in xenograft models confirming its therapeutic potential *in vitro* and *in vivo* (Schneider-Merck et al., 2009 and Charette et al., 2010). In addition to the mentioned Ras inhibitor, the benzimidazole derivate Selumetinib that already entered the clinical trial phase inhibited the activation and phosphorylation of ERK1/2 in various cancer cell lines as well as in a xenograft model and showed an induction of apoptosis upon treatment (Davies et al., 2007; Huynh et al., 2007; Huynh et al., 2007a and Quan-Jun et al., 2017). However, Selumetinib was not able to reduce the progression time of advanced HCC cases (O'Neil et al., 2011). A secondary MEK inhibitor is the preclinical drug UO126 that also inhibits the phosphorylation of ERK1/2, but showed only a low bioavailability and solubility excluding this reagent as potential drug against HCC (Favata et al., 1998; Wiesenauer et al., 2004 and Montagut & Settleman, 2009). The only by the Food and Drug Administration (FDA) in 2007 approved drug therapy and most successful inhibitor against HCC is the agent Sorafenib strongly inhibiting a variety of kinases, especially several subtypes of the kinase Raf (Llovet et al., 2008). The importance of the Raf-1 suppression is given by the fact that this kinase is overexpressed in 91.2 % of patients with hepatocirrhosis and in 100 % of patients with HCC and that Raf-1 becomes activated by the HCV core protein when HCC is activated via hepatitis C virus infections (Gollob et al., 2006; Schmitz et al., 2008 and Nakamura et al., 2011). Sorafenib is reported to inhibit HCC cell proliferation as well as tumor growth and also to inhibit angiogenesis due to the altered Ras/RAF/MEK/ERK pathway by Raf-1 inhibition (Liu et al., 2006 and Gedaly et al., 2012). The kinase inhibitor has also been proven to significantly increase the survival time as well as the time to cancer progression in patients with advanced HCC, but the survival time was only around 3 months longer than that of the patients treated with placebos (Llovet et al., 2008 and Lee et al., 2015). The use of sorafenib against HCC progression is also hampered by adverse side effects, including the occurrence of diarrhea, hand-foot skin reactions or weight loss in patients treated with sorafenib (Wilhelm et al., 2006). Another important point challenging the treatment with sorafenib are the preclinical and also clinical observations showing that the drug has only a limited efficacy to

tumor regression due to primary resistance or the development of acquired resistance against the kinase inhibitor (Blivet-Van Eggelpoël et al., 2012 and Zhai & Sun 2013). On the one hand, one explanation for the poor treatment efficacy of HCC is its genetic heterogeneity causing the primary resistance, the fact that some patients are initially resistant to sorafenib (O'Connor et al., 2007 and Friemel et al., 2015). Since the exact mechanism is still unknown, some predictive biomarkers for this primary resistance are identified so far. These biomarkers are for example the existence of JNK and VEGFA (Hagiwara et al., 2012 and Llovet, 2014) as well as the EGFR status of the cell because it is reported that a high number of HCC patients exhibit a strong overexpression of the EGFR and its downstream ligands being able to inhibit the effects of sorafenib treatment (Ito et al., 2001; Blivet-Van Eggelpoël et al., 2012 and Ezzoukhry et al., 2012). Additionally, the cellular levels of pERK are also shown to be responsible for the inhibition of the antitumor effects of sorafenib because the downregulation of phosphorylated ERK seems to be associated with sorafenib resistance in HCC patients (Zhang et al., 2009). On the other hand, due to long-term exposure to antitumor drugs the so-called acquired resistance against kinase inhibitors can develop and negatively affect the sorafenib therapy. This acquired resistance provoking mechanisms involve the crosstalk of different signaling pathways, the induction of hypoxia, the epithelial-mesenchymal transition (EMT), etc. (Bagrodia et al., 2012 and Lackner et al., 2012). So far, it is known that an activation of the PI3K/Akt pathway and thus the increased expression of phosphorylated Akt and the subsequent phosphorylation of the downstream targets are associated with sorafenib resistance (Gedaly et al., 2010 and Chen et al., 2011). Also abnormal changes in the JAK/STAT pathway and this way the raised levels of phosphorylated STAT3, JAK1 and JAK2 contribute to the acquired resistance mechanism (Chen et al., 2012 and Tai et al., 2012). Another important key regulator participating in the acquired resistance to sorafenib in HCC is the EMT, one of the most important steps in the development of metastasis: the transition of epithelial cells into a mesenchymal phenotype of cells (Wang et al., 2010; van Malenstein et al., 2013 and Dazert et al., 2016). The process of EMT leads to the loss of cell polarity and the loss of cell-to-cell contacts as well as to an enhancement of tumor cell migration and invasion (Kalluri & Neilson, 2003; Kalluri & Weinberg, 2009 and Maheswaran & Rushbrook, 2012). These newly generated tumor cells then become more motile and insensitive to antitumor drugs (van Malenstein et al., 2013). In the context of the EMT process and the emerging evidence that the occurrence of EMT and its mediated anticancer drug resistance may restrict the therapeutic efficacy of the treatment, it might be relevant to identify and analyse the trigger of EMT (Huang et al., 2013 and van Malenstein et al., 2013). Regarding this, it is reported that the transcription factor serum response factor (SRF) plays a crucial role in tumor progression and also in EMT formation of cells (Psichari et al., 2002). In addition, Park and colleagues figured out that epithelial HCC cell lines exhibited only a minimal expression of SRF, while the cell lines

having undergone EMT show a high expression of SRF and of the mesenchymal marker vimentin (Park et al., 2007). In accordance with these data, an increase in the expression of mesenchymal markers like vimentin as well as N-cadherin and the simultaneous loss of endogenous E-cadherin expression due to SRF expression is reported arguing for an important role for SRF in the EMT process in HCCs (Park et al., 2007 and Bae et al., 2013). Consequently, the recent study of Bae *et al.* demonstrates that the induced sorafenib resistance caused by EMT is a result of SRF overexpression in the cells (Bae et al., 2013). The authors also showed the reduced responsiveness of SRF-expressing, mesenchymal-like cells to sorafenib-induced cell death and the fact that the depletion of SRF enhanced the apoptotic effect of sorafenib again (Bae et al., 2013). Because the process of EMT elicited by SRF is responsible for the development of cell's resistance to sorafenib in HCC and the finding that a modulation of the SRF expression can affect the sensitivity of HCC cells to sorafenib, the combinational administration of sorafenib and the reduction of SRF expression might be a potential therapeutic approach for a more efficient treatment of HCC. Results from our group also revealed a strong effect of MYOF on the cell proliferation and invasion of HCC cells comparable to those shown for SRF. Since MYOF is described as a direct SRF/MKL1/2 target gene it might be possible that the tumorigenic effects are mediated by MYOF and that the knockdown of MYOF may also increase the therapeutic potential of sorafenib in HCC patients during a combinatorial therapeutic approach. In this regard, there is recent evidence that MYOF has an effect on the malignant transformation of epithelial cells because Volakis and colleagues found out that the knockdown of MYOF can reverse the EMT and thus leads to a mesenchymal-epithelial transition (MET) of breast cancer cell lines (Volakis et al., 2014). This way, the decrease of MYOF expression in combination with sorafenib administration to HCC patients represents a very promising strategy to overcome the chemoresistance of sorafenib and other drugs in therapeutical approaches.

The described data of the low efficacy of chemo drugs such as sorafenib treatment suggest that more effective strategies for conquering the sorafenib resistance of cells and patients with advanced HCC are needed. In this regard, there are recently several ongoing clinical trials of two categories, whereas the first option is a combinatorial therapy combining sorafenib with other anticancer drugs like tegafur/uracil or octreotide (Hsu et al., 2010 and Prete et al., 2010). The second option is the use of other drugs as second line therapy in consequence of the failure of sorafenib treatment like sunitinib and tivantinib (Worns et al., 2010 and Santoro et al., 2013). Both variants are in the phase II clinical trial with good effects and promising results for the patients and this way let expect a better prognosis for patients with advanced HCC.

Because of the limited number of therapeutic approaches and the high significance of an effective HCC treatment it remains an important research goal to find new drugs for HCC therapy that do not underlie a resistance mechanism of the cell and that prevents the patients from recurrence of tumor development. Our research and the results of this thesis strongly accounts for a very promising role for MYOF in the context of HCC therapy and restriction of hepatocarcinogenesis. We could impressingly show that MYOF depletion resulted in reduced tumorigenic properties, like proliferation and invasion, and in the induction of oncogene-induced senescence of HCC cells *in vitro* as well as in liver tumor cells *ex vivo*. The particular relevance of MYOF in tumor regression is additionally substantiated by a very recent study of Blomme and colleagues indicating a prominent role for MYOF also in triple-negative breast cancer (TNBC) exhibiting poor prognosis for the patients (Blomme et al., 2017). The authors describe that MYOF depletion in TNBC cells reduced the tumor growth and metastatic progression due to a deregulation of the cellular metabolism. For the first time they pointed out a link between cancer progression, cancer cell metabolism and cellular vesicle traffic depending on the expression level of MYOF (Blomme et al., 2017).

In summary, the novel identified MKL1/2 target gene MYOF serves as very promising target for cancer therapy and especially for treatment in HCC patients to reduce the tumor growth and to decrease the metastatic potential of mesenchymal like cells and this way, further *in vivo* studies with MYOF depletion as therapeutical approach are required.

8 References

Adam, P. J., Boyd, R., Tyson, K. L., Fletcher, G. C., Stamps, A., Hudson, L., Poyser, H. R., Redpath, N., Griffiths, M., Steers, G., Harris, A. L., Patel, S., Berry, J., Loader, J. A., Townsend, R. R., Daviet, L., Legrain, P., Parekh, R., & Terrett, J. A. (2003). Comprehensive proteomic analysis of breast cancer cell membranes reveals unique proteins with potential roles in clinical cancer. *J Biol Chem, 278*(8), 6482-6489. doi:10.1074/jbc.M210184200

Agelaki, S., Spiliotaki, M., Markomanolaki, H., Kallergi, G., Mavroudis, D., Georgoulias, V., & Stournaras, C. (2009). Caveolin-1 regulates EGFR signaling in MCF-7 breast cancer cells and enhances gefitinib-induced tumor cell inhibition. *Cancer Biol Ther, 8*(15), 1470-1477.

Alcorta, D. A., Xiong, Y., Phelps, D., Hannon, G., Beach, D., & Barrett, J. C. (1996). Involvement of the cyclin-dependent kinase inhibitor p16 (INK4a) in replicative senescence of normal human fibroblasts. *Proc Natl Acad Sci U S A, 93*(24), 13742-13747.

Alimonti, A., Nardella, C., Chen, Z., Clohessy, J. G., Carracedo, A., Trotman, L. C., Cheng, K., Varmeh, S., Kozma, S. C., Thomas, G., Rosivatz, E., Woscholski, R., Cognetti, F., Scher, H. I., & Pandolfi, P. P. (2010). A novel type of cellular senescence that can be enhanced in mouse models and human tumor xenografts to suppress prostate tumorigenesis. *J Clin Invest, 120*(3), 681-693. doi:10.1172/JCI40535

Angstenberger, M., Wegener, J. W., Pichler, B. J., Judenhofer, M. S., Feil, S., Alberti, S., Feil, R., & Nordheim, A. (2007). Severe intestinal obstruction on induced smooth muscle-specific ablation of the transcription factor SRF in adult mice. *Gastroenterology, 133*(6), 1948-1959. doi:10.1053/j.gastro.2007.08.078

Aravind, L., & Koonin, E. V. (2000). SAP - a putative DNA-binding motif involved in chromosomal organization. *Trends Biochem Sci, 25*(3), 112-114.

Asati, V., Mahapatra, D. K., & Bharti, S. K. (2016). PI3K/Akt/mTOR and Ras/Raf/MEK/ERK signaling pathways inhibitors as anticancer agents: Structural and pharmacological perspectives. *Eur J Med Chem, 109*, 314-341. doi:10.1016/j.ejmech.2016.01.012

Assinder, S. J., Stanton, J. A., & Prasad, P. D. (2009). Transgelin: an actin-binding protein and tumour suppressor. *Int J Biochem Cell Biol, 41*(3), 482-486. doi:10.1016/j.biocel.2008.02.011

Baarlink, C., Wang, H., & Grosse, R. (2013). Nuclear actin network assembly by formins regulates the SRF coactivator MAL. *Science, 340*(6134), 864-867. doi:10.1126/science.1235038

Baba, A. I., & Catoi, C. (2007). In *Comparative Oncology*. Bucharest.

Bae, J. S., Noh, S. J., Kim, K. M., Jang, K. Y., Chung, M. J., Kim, D. G., & Moon, W. S. (2014). Serum response factor induces epithelial to mesenchymal transition with resistance to sorafenib in hepatocellular carcinoma. *Int J Oncol, 44*(1), 129-136. doi:10.3892/ijo.2013.2154

Baek, Y. H., Kim, K. T., Lee, S. W., Jeong, J. S., Park, B. H., Nam, K. J., Cho, J. H., Kim, Y. H., Roh, Y. H., Lee, H. S., Choi, Y. M., & Han, S. Y. (2012). Efficacy of hepatic arterial infusion chemotherapy in advanced hepatocellular carcinoma. *World J Gastroenterol, 18*(26), 3426-3434. doi:10.3748/wjg.v18.i26.3426

Bagrodia, S., Smeal, T., & Abraham, R. T. (2012). Mechanisms of intrinsic and acquired resistance to kinase-targeted therapies. *Pigment Cell Melanoma Res, 25*(6), 819-831. doi:10.1111/pcmr.12007

Ben-Porath, I., & Weinberg, R. A. (2005). The signals and pathways activating cellular senescence. *Int J Biochem Cell Biol, 37*(5), 961-976. doi:10.1016/j.biocel.2004.10.013

Bennett, D. C. (2003). Human melanocyte senescence and melanoma susceptibility genes. *Oncogene, 22*(20), 3063-3069. doi:10.1038/sj.onc.1206446

Bennett, J. P., Zaner, K. S., & Stossel, T. P. (1984). Isolation and some properties of macrophage alpha-actinin: evidence that it is not an actin gelling protein. *Biochemistry, 23*(21), 5081-5086.

Bernatchez, P. N., Acevedo, L., Fernandez-Hernando, C., Murata, T., Chalouni, C., Kim, J., Erdjument-Bromage, H., Shah, V., Gratton, J. P., McNally, E. M., Tempst, P., & Sessa, W. C. (2007). Myoferlin regulates vascular endothelial growth factor receptor-2 stability and function. *J Biol Chem, 282*(42), 30745-30753. doi:10.1074/jbc.M704798200

Bernatchez, P. N., Sharma, A., Kodaman, P., & Sessa, W. C. (2009). Myoferlin is critical for endocytosis in endothelial cells. *Am J Physiol Cell Physiol, 297*(3), C484-492. doi:10.1152/ajpcell.00498.2008

Berry, F. B., O'Neill, M. A., Coca-Prados, M., & Walter, M. A. (2005). FOXC1 transcriptional regulatory activity is impaired by PBX1 in a filamin A-mediated manner. *Mol Cell Biol, 25*(4), 1415-1424. doi:10.1128/MCB.25.4.1415-1424.2005

Betapudi, V., Licate, L. S., & Egelhoff, T. T. (2006). Distinct roles of nonmuscle myosin II isoforms in the regulation of MDA-MB-231 breast cancer cell spreading and migration. *Cancer Res, 66*(9), 4725-4733. doi:10.1158/0008-5472.CAN-05-4236

Binder-Foucard, F., Bossard, N., Delafosse, P., Belot, A., Woronoff, A. S., Remontet, L., & French network of cancer, r. (2014). Cancer incidence and mortality in France over the 1980-2012 period: solid tumors. *Rev Epidemiol Sante Publique, 62*(2), 95-108. doi:10.1016/j.respe.2013.11.073

Bishop, A. L., & Hall, A. (2000). Rho GTPases and their effector proteins. *Biochem J, 348 Pt 2*, 241-255.

Blivet-Van Eggelpoel, M. J., Chettouh, H., Fartoux, L., Aoudjehane, L., Barbu, V., Rey, C., Priam, S., Housset, C., Rosmorduc, O., & Desbois-Mouthon, C. (2012). Epidermal growth factor receptor and HER-3 restrict cell response to sorafenib in hepatocellular carcinoma cells. *J Hepatol, 57*(1), 108-115. doi:10.1016/j.jhep.2012.02.019

Blomme, A., Costanza, B., de Tullio, P., Thiry, M., Van Simaeys, G., Boutry, S., Doumont, G., Di Valentin, E., Hirano, T., Yokobori, T., Gofflot, S., Peulen, O., Bellahcene, A., Sherer, F., Le Goff, C., Cavalier, E., Mouithys-Mickalad, A., Jouret, F., Cusumano, P. G., Lifrange, E., Muller, R. N., Goldman, S., Delvenne, P., De Pauw, E., Nishiyama, M., Castronovo, V., & Turtoi, A. (2017). Myoferlin regulates cellular lipid metabolism and promotes metastases in triple-negative breast cancer. *Oncogene, 36*(15), 2116-2130. doi:10.1038/onc.2016.369

Bodnar, A. G., Ouellette, M., Frolkis, M., Holt, S. E., Chiu, C. P., Morin, G. B., Harley, C. B., Shay, J. W., Lichtsteiner, S., & Wright, W. E. (1998). Extension of life-span by introduction of telomerase into normal human cells. *Science, 279*(5349), 349-352.

Braig, M., Lee, S., Loddenkemper, C., Rudolph, C., Peters, A. H., Schlegelberger, B., Stein, H., Dorken, B., Jenuwein, T., & Schmitt, C. A. (2005). Oncogene-induced senescence as an initial barrier in lymphoma development. *Nature, 436*(7051), 660-665. doi:10.1038/nature03841

Braumuller, H., Wieder, T., Brenner, E., Assmann, S., Hahn, M., Alkhaled, M., Schilbach, K., Essmann, F., Kneilling, M., Griessinger, C., Ranta, F., Ullrich, S., Mocikat, R., Braungart, K., Mehra, T., Fehrenbacher, B., Berdel, J., Niessner, H., Meier, F., van den Broek, M., Haring, H. U., Handgretinger, R., Quintanilla-Martinez, L., Fend, F., Pesic, M., Bauer, J., Zender, L., Schaller, M., Schulze-Osthoff, K., & Rocken, M. (2013). T-helper-1-cell cytokines drive cancer into senescence. *Nature, 494*(7437), 361-365. doi:10.1038/nature11824

Brown, J. P., Wei, W., & Sedivy, J. M. (1997). Bypass of senescence after disruption of p21CIP1/WAF1 gene in normal diploid human fibroblasts. *Science, 277*(5327), 831-834.

Bubb, M. R., Senderowicz, A. M., Sausville, E. A., Duncan, K. L., & Korn, E. D. (1994). Jasplakinolide, a cytotoxic natural product, induces actin polymerization and competitively inhibits the binding of phalloidin to F-actin. *J Biol Chem, 269*(21), 14869-14871.

Bubb, M. R., Spector, I., Beyer, B. B., & Fosen, K. M. (2000). Effects of jasplakinolide on the kinetics of actin polymerization. An explanation for certain in vivo observations. *J Biol Chem, 275*(7), 5163-5170.

Burkhart, D. L., & Sage, J. (2008). Cellular mechanisms of tumour suppression by the retinoblastoma gene. *Nat Rev Cancer, 8*(9), 671-682. doi:10.1038/nrc2399

Campisi, J. (2005). Senescent cells, tumor suppression, and organismal aging: good citizens, bad neighbors. *Cell, 120*(4), 513-522. doi:10.1016/j.cell.2005.02.003

Campisi, J., & d'Adda di Fagagna, F. (2007). Cellular senescence: when bad things happen to good cells. *Nat Rev Mol Cell Biol, 8*(9), 729-740. doi:10.1038/nrm2233

Cen, B., Selvaraj, A., Burgess, R. C., Hitzler, J. K., Ma, Z., Morris, S. W., & Prywes, R. (2003). Megakaryoblastic leukemia 1, a potent transcriptional coactivator for serum response factor (SRF), is required for serum induction of SRF target genes. *Mol Cell Biol, 23*(18), 6597-6608.

Cerami, E., Gao, J., Dogrusoz, U., Gross, B. E., Sumer, S. O., Aksoy, B. A., Jacobsen, A., Byrne, C. J., Heuer, M. L., Larsson, E., Antipin, Y., Reva, B., Goldberg, A. P., Sander, C., & Schultz, N. (2012). The cBio cancer genomics portal: an open platform for exploring multidimensional cancer genomics data. *Cancer Discov, 2*(5), 401-404. doi:10.1158/2159-8290.CD-12-0095

Charette, N., De Saeger, C., Lannoy, V., Horsmans, Y., Leclercq, I., & Starkel, P. (2010). Salirasib inhibits the growth of hepatocarcinoma cell lines in vitro and tumor growth in vivo through ras and mTOR inhibition. *Mol Cancer, 9*, 256. doi:10.1186/1476-4598-9-256

Chen, K. F., Chen, H. L., Tai, W. T., Feng, W. C., Hsu, C. H., Chen, P. J., & Cheng, A. L. (2011). Activation of phosphatidylinositol 3-kinase/Akt signaling pathway mediates acquired resistance to sorafenib in hepatocellular carcinoma cells. *J Pharmacol Exp Ther, 337*(1), 155-161. doi:10.1124/jpet.110.175786

Chen, K. F., Tai, W. T., Hsu, C. Y., Huang, J. W., Liu, C. Y., Chen, P. J., Kim, I., & Shiau, C. W. (2012). Blockade of STAT3 activation by sorafenib derivatives through enhancing SHP-1 phosphatase activity. *Eur J Med Chem, 55*, 220-227. doi:10.1016/j.ejmech.2012.07.023

Chen, Z., Trotman, L. C., Shaffer, D., Lin, H. K., Dotan, Z. A., Niki, M., Koutcher, J. A., Scher, H. I., Ludwig, T., Gerald, W., Cordon-Cardo, C., & Pandolfi, P. P. (2005). Crucial role of p53-dependent cellular senescence in suppression of Pten-deficient tumorigenesis. *Nature, 436*(7051), 725-730. doi:10.1038/nature03918

Cheng, E. C., Luo, Q., Bruscia, E. M., Renda, M. J., Troy, J. A., Massaro, S. A., Tuck, D., Schulz, V., Mane, S. M., Berliner, N., Sun, Y., Morris, S. W., Qiu, C., & Krause, D. S. (2009). Role for MKL1 in megakaryocytic maturation. *Blood, 113*(12), 2826-2834. doi:10.1182/blood-2008-09-180596

Chicas, A., Wang, X., Zhang, C., McCurrach, M., Zhao, Z., Mert, O., Dickins, R. A., Narita, M., Zhang, M., & Lowe, S. W. (2010). Dissecting the unique role of the retinoblastoma tumor suppressor during cellular senescence. *Cancer Cell, 17*(4), 376-387. doi:10.1016/j.ccr.2010.01.023

Chilukamarri, L., Hancock, A. L., Malik, S., Zabkiewicz, J., Baker, J. A., Greenhough, A., Dallosso, A. R., Huang, T. H., Royer-Pokora, B., Brown, K. W., & Malik, K. (2007). Hypomethylation and aberrant expression of the glioma pathogenesis-related 1 gene in Wilms tumors. *Neoplasia, 9*(11), 970-978.

Cipta, S., & Patel, H. H. (2009). Molecular bandages: inside-out, outside-in repair of cellular membranes. Focus on "Myoferlin is critical for endocytosis in endothelial cells". *Am J Physiol Cell Physiol, 297*(3), C481-483. doi:10.1152/ajpcell.00288.2009

Clark, K. A., & Graves, B. J. (2014). Dual views of SRF: a genomic exposure. *Genes Dev, 28*(9), 926-928. doi:10.1101/gad.242420.114

Collado, M., Gil, J., Efeyan, A., Guerra, C., Schuhmacher, A. J., Barradas, M., Benguria, A., Zaballos, A., Flores, J. M., Barbacid, M., Beach, D., & Serrano, M. (2005). Tumour biology: senescence in premalignant tumours. *Nature, 436*(7051), 642. doi:10.1038/436642a

Collado, M., & Serrano, M. (2006). The power and the promise of oncogene-induced senescence markers. *Nat Rev Cancer, 6*(6), 472-476. doi:10.1038/nrc1884

Collado, M., & Serrano, M. (2010). Senescence in tumours: evidence from mice and humans. *Nat Rev Cancer, 10*(1), 51-57. doi:10.1038/nrc2772

Collins, K., & Mitchell, J. R. (2002). Telomerase in the human organism. *Oncogene, 21*(4), 564-579. doi:10.1038/sj.onc.1205083

Copeland, S. J., Green, B. J., Burchat, S., Papalia, G. A., Banner, D., & Copeland, J. W. (2007). The diaphanous inhibitory domain/diaphanous autoregulatory domain interaction is able to mediate heterodimerization between mDia1 and mDia2. *J Biol Chem, 282*(41), 30120-30130. doi:10.1074/jbc.M703834200

Cristofalo, V. J., & Pignolo, R. J. (1996). Molecular markers of senescence in fibroblast-like cultures. *Exp Gerontol, 31*(1-2), 111-123.

Cunningham, C. C. (1995). Actin polymerization and intracellular solvent flow in cell surface blebbing. *J Cell Biol, 129*(6), 1589-1599.

Cunningham, C. C., Gorlin, J. B., Kwiatkowski, D. J., Hartwig, J. H., Janmey, P. A., Byers, H. R., & Stossel, T. P. (1992). Actin-binding protein requirement for cortical stability and efficient locomotion. *Science, 255*(5042), 325-327.

d'Adda di Fagagna, F., Teo, S. H., & Jackson, S. P. (2004). Functional links between telomeres and proteins of the DNA-damage response. *Genes Dev, 18*(15), 1781-1799. doi:10.1101/gad.1214504

Dabrowska, M., Skoneczny, M., & Rode, W. (2011). Functional gene expression profile underlying methotrexate-induced senescence in human colon cancer cells. *Tumour Biol, 32*(5), 965-976. doi:10.1007/s13277-011-0198-x

Dai, J., & Sheetz, M. P. (1999). Membrane tether formation from blebbing cells. *Biophys J, 77*(6), 3363-3370. doi:10.1016/S0006-3495(99)77168-7

Davies, B. R., Logie, A., McKay, J. S., Martin, P., Steele, S., Jenkins, R., Cockerill, M., Cartlidge, S., & Smith, P. D. (2007). AZD6244 (ARRY-142886), a potent inhibitor of mitogen-activated protein kinase/extracellular signal-regulated kinase kinase 1/2

kinases: mechanism of action in vivo, pharmacokinetic/pharmacodynamic relationship, and potential for combination in preclinical models. *Mol Cancer Ther, 6*(8), 2209-2219. doi:10.1158/1535-7163.MCT-07-0231

Davis, D. B., Delmonte, A. J., Ly, C. T., & McNally, E. M. (2000). Myoferlin, a candidate gene and potential modifier of muscular dystrophy. *Hum Mol Genet, 9*(2), 217-226.

Davletov, B. A., & Sudhof, T. C. (1993). A single C2 domain from synaptotagmin I is sufficient for high affinity Ca2+/phospholipid binding. *J Biol Chem, 268*(35), 26386-26390.

Dazert, E., Colombi, M., Boldanova, T., Moes, S., Adametz, D., Quagliata, L., Roth, V., Terracciano, L., Heim, M. H., Jenoe, P., & Hall, M. N. (2016). Quantitative proteomics and phosphoproteomics on serial tumor biopsies from a sorafenib-treated HCC patient. *Proc Natl Acad Sci U S A, 113*(5), 1381-1386. doi:10.1073/pnas.1523434113

Debacq-Chainiaux, F., Erusalimsky, J. D., Campisi, J., & Toussaint, O. (2009). Protocols to detect senescence-associated beta-galactosidase (SA-betagal) activity, a biomarker of senescent cells in culture and in vivo. *Nat Protoc, 4*(12), 1798-1806. doi:10.1038/nprot.2009.191

Demonbreun, A. R., Posey, A. D., Heretis, K., Swaggart, K. A., Earley, J. U., Pytel, P., & McNally, E. M. (2010). Myoferlin is required for insulin-like growth factor response and muscle growth. *FASEB J, 24*(4), 1284-1295. doi:10.1096/fj.09-136309

Deng, W., Lopez-Camacho, C., Tang, J. Y., Mendoza-Villanueva, D., Maya-Mendoza, A., Jackson, D. A., & Shore, P. (2012). Cytoskeletal protein filamin A is a nucleolar protein that suppresses ribosomal RNA gene transcription. *Proc Natl Acad Sci U S A, 109*(5), 1524-1529. doi:10.1073/pnas.1107879109

Derycke, L., Stove, C., Vercoutter-Edouart, A. S., De Wever, O., Dolle, L., Colpaert, N., Depypere, H., Michalski, J. C., & Bracke, M. (2011). The role of non-muscle myosin IIA in aggregation and invasion of human MCF-7 breast cancer cells. *Int J Dev Biol, 55*(7-9), 835-840. doi:10.1387/ijdb.113336ld

Descot, A., Hoffmann, R., Shaposhnikov, D., Reschke, M., Ullrich, A., & Posern, G. (2009). Negative regulation of the EGFR-MAPK cascade by actin-MAL-mediated Mig6/Errfi-1 induction. *Mol Cell, 35*(3), 291-304. doi:10.1016/j.molcel.2009.07.015

Dimri, G. P., Lee, X., Basile, G., Acosta, M., Scott, G., Roskelley, C., Medrano, E. E., Linskens, M., Rubelj, I., Pereira-Smith, O., & et al. (1995). A biomarker that identifies senescent human cells in culture and in aging skin in vivo. *Proc Natl Acad Sci U S A, 92*(20), 9363-9367.

Doherty, K. R., Cave, A., Davis, D. B., Delmonte, A. J., Posey, A., Earley, J. U., Hadhazy, M., & McNally, E. M. (2005). Normal myoblast fusion requires myoferlin. *Development, 132*(24), 5565-5575. doi:10.1242/dev.02155

Du, K. L., Chen, M., Li, J., Lepore, J. J., Mericko, P., & Parmacek, M. S. (2004). Megakaryoblastic leukemia factor-1 transduces cytoskeletal signals and induces smooth muscle cell differentiation from undifferentiated embryonic stem cells. *J Biol Chem, 279*(17), 17578-17586. doi:10.1074/jbc.M400961200

Duffy, M. J., Maguire, T. M., Hill, A., McDermott, E., & O'Higgins, N. (2000). Metalloproteinases: role in breast carcinogenesis, invasion and metastasis. *Breast Cancer Res, 2*(4), 252-257.

Eisenberg, M. C., Kim, Y., Li, R., Ackerman, W. E., Kniss, D. A., & Friedman, A. (2011). Mechanistic modeling of the effects of myoferlin on tumor cell invasion. *Proc Natl Acad Sci U S A, 108*(50), 20078-20083. doi:10.1073/pnas.1116327108

Ezzoukhry, Z., Louandre, C., Trecherel, E., Godin, C., Chauffert, B., Dupont, S., Diouf, M., Barbare, J. C., Maziere, J. C., & Galmiche, A. (2012). EGFR activation is a potential

determinant of primary resistance of hepatocellular carcinoma cells to sorafenib. *Int J Cancer, 131*(12), 2961-2969. doi:10.1002/ijc.27604

Farazi, P. A., & DePinho, R. A. (2006). Hepatocellular carcinoma pathogenesis: from genes to environment. *Nat Rev Cancer, 6*(9), 674-687. doi:10.1038/nrc1934

Favata, M. F., Horiuchi, K. Y., Manos, E. J., Daulerio, A. J., Stradley, D. A., Feeser, W. S., Van Dyk, D. E., Pitts, W. J., Earl, R. A., Hobbs, F., Copeland, R. A., Magolda, R. L., Scherle, P. A., & Trzaskos, J. M. (1998). Identification of a novel inhibitor of mitogen-activated protein kinase kinase. *J Biol Chem, 273*(29), 18623-18632.

Ferlay, J., Soerjomataram, I., Dikshit, R., Eser, S., Mathers, C., Rebelo, M., Parkin, D. M., Forman, D., & Bray, F. (2015). Cancer incidence and mortality worldwide: sources, methods and major patterns in GLOBOCAN 2012. *Int J Cancer, 136*(5), E359-386. doi:10.1002/ijc.29210

Flanagan, L. A., Chou, J., Falet, H., Neujahr, R., Hartwig, J. H., & Stossel, T. P. (2001). Filamin A, the Arp2/3 complex, and the morphology and function of cortical actin filaments in human melanoma cells. *J Cell Biol, 155*(4), 511-517. doi:10.1083/jcb.200105148

Friemel, J., Rechsteiner, M., Frick, L., Bohm, F., Struckmann, K., Egger, M., Moch, H., Heikenwalder, M., & Weber, A. (2015). Intratumor heterogeneity in hepatocellular carcinoma. *Clin Cancer Res, 21*(8), 1951-1961. doi:10.1158/1078-0432.CCR-14-0122

Futreal, P. A., & Barrett, J. C. (1991). Failure of senescent cells to phosphorylate the RB protein. *Oncogene, 6*(7), 1109-1113.

Gan, H. K., Walker, F., Burgess, A. W., Rigopoulos, A., Scott, A. M., & Johns, T. G. (2007). The epidermal growth factor receptor (EGFR) tyrosine kinase inhibitor AG1478 increases the formation of inactive untethered EGFR dimers. Implications for combination therapy with monoclonal antibody 806. *J Biol Chem, 282*(5), 2840-2850. doi:10.1074/jbc.M605136200

Gao, J., Aksoy, B. A., Dogrusoz, U., Dresdner, G., Gross, B., Sumer, S. O., Sun, Y., Jacobsen, A., Sinha, R., Larsson, E., Cerami, E., Sander, C., & Schultz, N. (2013). Integrative analysis of complex cancer genomics and clinical profiles using the cBioPortal. *Sci Signal, 6*(269), pl1. doi:10.1126/scisignal.2004088

Gao, X., Yu, L., Moore, A. B., Kissling, G. E., Waalkes, M. P., & Dixon, D. (2015). Cadmium and proliferation in human uterine leiomyoma cells: evidence of a role for EGFR/MAPK pathways but not classical estrogen receptor pathways. *Environ Health Perspect, 123*(4), 331-336. doi:10.1289/ehp.1408234

Gedaly, R., Angulo, P., Hundley, J., Daily, M. F., Chen, C., & Evers, B. M. (2012). PKI-587 and sorafenib targeting PI3K/AKT/mTOR and Ras/Raf/MAPK pathways synergistically inhibit HCC cell proliferation. *J Surg Res, 176*(2), 542-548. doi:10.1016/j.jss.2011.10.045

Gedaly, R., Angulo, P., Hundley, J., Daily, M. F., Chen, C., Koch, A., & Evers, B. M. (2010). PI-103 and sorafenib inhibit hepatocellular carcinoma cell proliferation by blocking Ras/Raf/MAPK and PI3K/AKT/mTOR pathways. *Anticancer Res, 30*(12), 4951-4958.

Gimona, M., Kaverina, I., Resch, G. P., Vignal, E., & Burgstaller, G. (2003). Calponin repeats regulate actin filament stability and formation of podosomes in smooth muscle cells. *Mol Biol Cell, 14*(6), 2482-2491. doi:10.1091/mbc.E02-11-0743

Glogauer, M., Arora, P., Chou, D., Janmey, P. A., Downey, G. P., & McCulloch, C. A. (1998). The role of actin-binding protein 280 in integrin-dependent mechanoprotection. *J Biol Chem, 273*(3), 1689-1698.

Gollob, J. A., Wilhelm, S., Carter, C., & Kelley, S. L. (2006). Role of Raf kinase in cancer: therapeutic potential of targeting the Raf/MEK/ERK signal transduction pathway. *Semin Oncol, 33*(4), 392-406. doi:10.1053/j.seminoncol.2006.04.002

Gorgoulis, V. G., & Halazonetis, T. D. (2010). Oncogene-induced senescence: the bright and dark side of the response. *Curr Opin Cell Biol, 22*(6), 816-827. doi:10.1016/j.ceb.2010.07.013

Gorlin, J. B., Yamin, R., Egan, S., Stewart, M., Stossel, T. P., Kwiatkowski, D. J., & Hartwig, J. H. (1990). Human endothelial actin-binding protein (ABP-280, nonmuscle filamin): a molecular leaf spring. *J Cell Biol, 111*(3), 1089-1105.

Greider, C. W., & Blackburn, E. H. (1985). Identification of a specific telomere terminal transferase activity in Tetrahymena extracts. *Cell, 43*(2 Pt 1), 405-413.

Greider, C. W., & Blackburn, E. H. (1987). The telomere terminal transferase of Tetrahymena is a ribonucleoprotein enzyme with two kinds of primer specificity. *Cell, 51*(6), 887-898.

Hagiwara, S., Kudo, M., Nagai, T., Inoue, T., Ueshima, K., Nishida, N., Watanabe, T., & Sakurai, T. (2012). Activation of JNK and high expression level of CD133 predict a poor response to sorafenib in hepatocellular carcinoma. *Br J Cancer, 106*(12), 1997-2003. doi:10.1038/bjc.2012.145

Haklai, R., Weisz, M. G., Elad, G., Paz, A., Marciano, D., Egozi, Y., Ben-Baruch, G., & Kloog, Y. (1998). Dislodgment and accelerated degradation of Ras. *Biochemistry, 37*(5), 1306-1314. doi:10.1021/bi972032d

Hampl, V., Martin, C., Aigner, A., Hoebel, S., Singer, S., Frank, N., Sarikas, A., Ebert, O., Prywes, R., Gudermann, T., & Muehlich, S. (2013). Depletion of the transcriptional coactivators megakaryoblastic leukaemia 1 and 2 abolishes hepatocellular carcinoma xenograft growth by inducing oncogene-induced senescence. *EMBO Mol Med, 5*(9), 1367-1382. doi:10.1002/emmm.201202406

Han, Y., Caday, C. G., Nanda, A., Cavenee, W. K., & Huang, H. J. (1996). Tyrphostin AG 1478 preferentially inhibits human glioma cells expressing truncated rather than wild-type epidermal growth factor receptors. *Cancer Res, 56*(17), 3859-3861.

Hanahan, D., & Weinberg, R. A. (2000). The hallmarks of cancer. *Cell, 100*(1), 57-70.

Hanahan, D., & Weinberg, R. A. (2011). Hallmarks of cancer: the next generation. *Cell, 144*(5), 646-674. doi:10.1016/j.cell.2011.02.013

Hara, E., Smith, R., Parry, D., Tahara, H., Stone, S., & Peters, G. (1996). Regulation of p16CDKN2 expression and its implications for cell immortalization and senescence. *Mol Cell Biol, 16*(3), 859-867.

Harley, C. B. (1991). Telomere loss: mitotic clock or genetic time bomb? *Mutat Res, 256*(2-6), 271-282.

Harley, C. B., Futcher, A. B., & Greider, C. W. (1990). Telomeres shorten during ageing of human fibroblasts. *Nature, 345*(6274), 458-460. doi:10.1038/345458a0

Hartwig, H. G., Brisson, P., Lyncker, I., & Collin, J. P. (1980). Aminergic systems in pulmonate gastropod molluscs. III. Microspectrofluorometric characterization of the monoamines in the reproductive system. *Cell Tissue Res, 210*(2), 223-234.

Hatakeyama, M., & Weinberg, R. A. (1995). The role of RB in cell cycle control. *Prog Cell Cycle Res, 1*, 9-19.

Hayflick, L. (1964). Advances in Tissue Culture Methods Important to Viral Disease Problems. *Postgrad Med, 35*, 503-511.

Hayflick, L., & Moorhead, P. S. (1961). The serial cultivation of human diploid cell strains. *Exp Cell Res, 25*, 585-621.

He, W., Zeng, Q., Zheng, Y., Chen, M., Shen, J., Qiu, J., Chen, M., Zou, R., Liao, Y., Li, Q., Wu, X., Li, B., & Yuan, Y. (2015). The role of clinically significant portal hypertension in hepatic resection for hepatocellular carcinoma patients: a propensity score matching analysis. *BMC Cancer, 15*, 263. doi:10.1186/s12885-015-1280-3

Herbert, B. S., Wright, W. E., & Shay, J. W. (2002). p16(INK4a) inactivation is not required to immortalize human mammary epithelial cells. *Oncogene, 21*(51), 7897-7900. doi:10.1038/sj.onc.1205902

Hermanns, C., Hampl, V., Holzer, K., Aigner, A., Penkava, J., Frank, N., Martin, D. E., Maier, K. C., Waldburger, N., Roessler, S., Goppelt-Struebe, M., Akrap, I., Thavamani, A., Singer, S., Nordheim, A., Gudermann, T., & Muehlich, S. (2017). The novel MKL target gene myoferlin modulates expansion and senescence of hepatocellular carcinoma. *Oncogene, 36*(24), 3464-3476. doi:10.1038/onc.2016.496

Hill, C. S., Wynne, J., & Treisman, R. (1995). The Rho family GTPases RhoA, Rac1, and CDC42Hs regulate transcriptional activation by SRF. *Cell, 81*(7), 1159-1170.

Ho, S., Lau, W. Y., Leung, T. W., & Johnson, P. J. (1998). Internal radiation therapy for patients with primary or metastatic hepatic cancer: a review. *Cancer, 83*(9), 1894-1907.

Hollstein, M., Shomer, B., Greenblatt, M., Soussi, T., Hovig, E., Montesano, R., & Harris, C. C. (1996). Somatic point mutations in the p53 gene of human tumors and cell lines: updated compilation. *Nucleic Acids Res, 24*(1), 141-146.

Hollstein, M., Sidransky, D., Vogelstein, B., & Harris, C. C. (1991). p53 mutations in human cancers. *Science, 253*(5015), 49-53.

Hsu, C. H., Shen, Y. C., Lin, Z. Z., Chen, P. J., Shao, Y. Y., Ding, Y. H., Hsu, C., & Cheng, A. L. (2010). Phase II study of combining sorafenib with metronomic tegafur/uracil for advanced hepatocellular carcinoma. *J Hepatol, 53*(1), 126-131. doi:10.1016/j.jhep.2010.01.035

Huang, X. Y., Ke, A. W., Shi, G. M., Zhang, X., Zhang, C., Shi, Y. H., Wang, X. Y., Ding, Z. B., Xiao, Y. S., Yan, J., Qiu, S. J., Fan, J., & Zhou, J. (2013). alphaB-crystallin complexes with 14-3-3zeta to induce epithelial-mesenchymal transition and resistance to sorafenib in hepatocellular carcinoma. *Hepatology, 57*(6), 2235-2247. doi:10.1002/hep.26255

Huynh, H., Chow, P. K., & Soo, K. C. (2007). AZD6244 and doxorubicin induce growth suppression and apoptosis in mouse models of hepatocellular carcinoma. *Mol Cancer Ther, 6*(9), 2468-2476. doi:10.1158/1535-7163.MCT-07-0162

Huynh, H., Soo, K. C., Chow, P. K., & Tran, E. (2007). Targeted inhibition of the extracellular signal-regulated kinase kinase pathway with AZD6244 (ARRY-142886) in the treatment of hepatocellular carcinoma. *Mol Cancer Ther, 6*(1), 138-146. doi:10.1158/1535-7163.MCT-06-0436

Ito, T., Suzuki, A., & Stossel, T. P. (1992). Regulation of water flow by actin-binding protein-induced actin gelatin. *Biophys J, 61*(5), 1301-1305. doi:10.1016/S0006-3495(92)81938-0

Ito, Y., Takeda, T., Sakon, M., Tsujimoto, M., Higashiyama, S., Noda, K., Miyoshi, E., Monden, M., & Matsuura, N. (2001). Expression and clinical significance of erb-B receptor family in hepatocellular carcinoma. *Br J Cancer, 84*(10), 1377-1383. doi:10.1054/bjoc.2000.1580

Janknecht, R., & Nordheim, A. (1993). Gene regulation by Ets proteins. *Biochim Biophys Acta, 1155*(3), 346-356.

Jemal, A., Bray, F., Center, M. M., Ferlay, J., Ward, E., & Forman, D. (2011). Global cancer statistics. *CA Cancer J Clin, 61*(2), 69-90. doi:10.3322/caac.20107

Johns, T. G., Luwor, R. B., Murone, C., Walker, F., Weinstock, J., Vitali, A. A., Perera, R. M., Jungbluth, A. A., Stockert, E., Old, L. J., Nice, E. C., Burgess, A. W., & Scott, A. M. (2003). Antitumor efficacy of cytotoxic drugs and the monoclonal antibody 806 is enhanced by the EGF receptor inhibitor AG1478. *Proc Natl Acad Sci U S A, 100*(26), 15871-15876. doi:10.1073/pnas.2036503100

Kalluri, R., & Neilson, E. G. (2003). Epithelial-mesenchymal transition and its implications for fibrosis. *J Clin Invest, 112*(12), 1776-1784. doi:10.1172/JCI20530

Kalluri, R., & Weinberg, R. A. (2009). The basics of epithelial-mesenchymal transition. *J Clin Invest, 119*(6), 1420-1428. doi:10.1172/JCI39104

Kaneko, M., Takeoka, M., Oguchi, M., Koganehira, Y., Murata, H., Ehara, T., Tozuka, M., Saida, T., & Taniguchi, S. (2002). Calponin h1 suppresses tumor growth of Src-induced transformed 3Y1 cells in association with a decrease in angiogenesis. *Jpn J Cancer Res, 93*(8), 935-943.

Kim, S. H., Choi, S. B., Lee, J. G., Kim, S. U., Park, M. S., Kim, D. Y., Choi, J. S., & Kim, K. S. (2011). Prognostic factors and 10-year survival in patients with hepatocellular carcinoma after curative hepatectomy. *J Gastrointest Surg, 15*(4), 598-607. doi:10.1007/s11605-011-1452-7

Kim, W. Y., & Sharpless, N. E. (2006). The regulation of INK4/ARF in cancer and aging. *Cell, 127*(2), 265-275. doi:10.1016/j.cell.2006.10.003

Kipling, D., & Cooke, H. J. (1990). Hypervariable ultra-long telomeres in mice. *Nature, 347*(6291), 400-402. doi:10.1038/347400a0

Kircher, P., Hermanns, C., Nossek, M., Drexler, M. K., Grosse, R., Fischer, M., Sarikas, A., Penkava, J., Lewis, T., Prywes, R., Gudermann, T., & Muehlich, S. (2015). Filamin A interacts with the coactivator MKL1 to promote the activity of the transcription factor SRF and cell migration. *Sci Signal, 8*(402), ra112. doi:10.1126/scisignal.aad2959

Knoll, B., & Nordheim, A. (2009). Functional versatility of transcription factors in the nervous system: the SRF paradigm. *Trends Neurosci, 32*(8), 432-442. doi:10.1016/j.tins.2009.05.004

Koganehira, Y., Takeoka, M., Ehara, T., Sasaki, K., Murata, H., Saida, T., & Taniguchi, S. (2003). Reduced expression of actin-binding proteins, h-caldesmon and calponin h1, in the vascular smooth muscle inside melanoma lesions: an adverse prognostic factor for malignant melanoma. *Br J Dermatol, 148*(5), 971-980.

Kohno, M., & Pouyssegur, J. (2006). Targeting the ERK signaling pathway in cancer therapy. *Ann Med, 38*(3), 200-211. doi:10.1080/07853890600551037

Krishnamurthy, J., Torrice, C., Ramsey, M. R., Kovalev, G. I., Al-Regaiey, K., Su, L., & Sharpless, N. E. (2004). Ink4a/Arf expression is a biomarker of aging. *J Clin Invest, 114*(9), 1299-1307. doi:10.1172/JCI22475

Kuilman, T., Michaloglou, C., Mooi, W. J., & Peeper, D. S. (2010). The essence of senescence. *Genes Dev, 24*(22), 2463-2479. doi:10.1101/gad.1971610

Kuilman, T., Michaloglou, C., Vredeveld, L. C., Douma, S., van Doorn, R., Desmet, C. J., Aarden, L. A., Mooi, W. J., & Peeper, D. S. (2008). Oncogene-induced senescence relayed by an interleukin-dependent inflammatory network. *Cell, 133*(6), 1019-1031. doi:10.1016/j.cell.2008.03.039

Kuilman, T., & Peeper, D. S. (2009). Senescence-messaging secretome: SMS-ing cellular stress. *Nat Rev Cancer, 9*(2), 81-94. doi:10.1038/nrc2560

Labhart, P., Karmakar, S., Salicru, E. M., Egan, B. S., Alexiadis, V., O'Malley, B. W., & Smith, C. L. (2005). Identification of target genes in breast cancer cells directly regulated by the SRC-3/AIB1 coactivator. *Proc Natl Acad Sci U S A, 102*(5), 1339-1344. doi:10.1073/pnas.0409578102

Lackner, M. R., Wilson, T. R., & Settleman, J. (2012). Mechanisms of acquired resistance to targeted cancer therapies. *Future Oncol, 8*(8), 999-1014. doi:10.2217/fon.12.86

Lahoute, C., Sotiropoulos, A., Favier, M., Guillet-Deniau, I., Charvet, C., Ferry, A., Butler-Browne, G., Metzger, D., Tuil, D., & Daegelen, D. (2008). Premature aging in skeletal muscle lacking serum response factor. *PLoS One, 3*(12), e3910. doi:10.1371/journal.pone.0003910

Lai, C. K., Mitchell, J. R., & Collins, K. (2001). RNA binding domain of telomerase reverse transcriptase. *Mol Cell Biol, 21*(4), 990-1000. doi:10.1128/MCB.21.4.990-1000.2001

Lee, D. H., & Goldberg, A. L. (1998). Proteasome inhibitors: valuable new tools for cell biologists. *Trends Cell Biol, 8*(10), 397-403.

Lee, S. H., Song, I. H., Noh, R., Kang, H. Y., Kim, S. B., Ko, S. Y., Lee, E. S., Kim, S. H., Lee, B. S., Kim, A. N., Chae, H. B., Kim, H. S., Lee, T. H., Kang, Y. W., Lee, J. D., & Lee, H. Y. (2015). Clinical outcomes of patients with advanced hepatocellular carcinoma treated with sorafenib: a retrospective study of routine clinical practice in multi-institutions. *BMC Cancer, 15*, 236. doi:10.1186/s12885-015-1273-2

Leitner, L., Shaposhnikov, D., Mengel, A., Descot, A., Julien, S., Hoffmann, R., & Posern, G. (2011). MAL/MRTF-A controls migration of non-invasive cells by upregulation of cytoskeleton-associated proteins. *J Cell Sci, 124*(Pt 24), 4318-4331. doi:10.1242/jcs.092791

Leung, C., Yu, C., Lin, M. I., Tognon, C., & Bernatchez, P. (2013). Expression of myoferlin in human and murine carcinoma tumors: role in membrane repair, cell proliferation, and tumorigenesis. *Am J Pathol, 182*(5), 1900-1909. doi:10.1016/j.ajpath.2013.01.041

Levine, A. J., & Oren, M. (2009). The first 30 years of p53: growing ever more complex. *Nat Rev Cancer, 9*(10), 749-758. doi:10.1038/nrc2723

Li, N., Batzer, A., Daly, R., Yajnik, V., Skolnik, E., Chardin, P., Bar-Sagi, D., Margolis, B., & Schlessinger, J. (1993). Guanine-nucleotide-releasing factor hSos1 binds to Grb2 and links receptor tyrosine kinases to Ras signalling. *Nature, 363*(6424), 85-88. doi:10.1038/363085a0

Li, R., Ackerman, W. E. t., Mihai, C., Volakis, L. I., Ghadiali, S., & Kniss, D. A. (2012). Myoferlin depletion in breast cancer cells promotes mesenchymal to epithelial shape change and stalls invasion. *PLoS One, 7*(6), e39766. doi:10.1371/journal.pone.0039766

Li, S., Chang, S., Qi, X., Richardson, J. A., & Olson, E. N. (2006). Requirement of a myocardin-related transcription factor for development of mammary myoepithelial cells. *Mol Cell Biol, 26*(15), 5797-5808. doi:10.1128/MCB.00211-06

Lin, A. W., Barradas, M., Stone, J. C., van Aelst, L., Serrano, M., & Lowe, S. W. (1998). Premature senescence involving p53 and p16 is activated in response to constitutive MEK/MAPK mitogenic signaling. *Genes Dev, 12*(19), 3008-3019.

Lin, M. E., Herr, D. R., & Chun, J. (2010). Lysophosphatidic acid (LPA) receptors: signaling properties and disease relevance. *Prostaglandins Other Lipid Mediat, 91*(3-4), 130-138. doi:10.1016/j.prostaglandins.2009.02.002

Lingner, J., Hughes, T. R., Shevchenko, A., Mann, M., Lundblad, V., & Cech, T. R. (1997). Reverse transcriptase motifs in the catalytic subunit of telomerase. *Science, 276*(5312), 561-567.

Liu, J., Aoki, M., Illa, I., Wu, C., Fardeau, M., Angelini, C., Serrano, C., Urtizberea, J. A., Hentati, F., Hamida, M. B., Bohlega, S., Culper, E. J., Amato, A. A., Bossie, K., Oeltjen, J., Bejaoui, K., McKenna-Yasek, D., Hosler, B. A., Schurr, E., Arahata, K., de Jong, P. J., & Brown, R. H., Jr. (1998). Dysferlin, a novel skeletal muscle gene, is

mutated in Miyoshi myopathy and limb girdle muscular dystrophy. *Nat Genet, 20*(1), 31-36. doi:10.1038/1682

Liu, L., Cao, Y., Chen, C., Zhang, X., McNabola, A., Wilkie, D., Wilhelm, S., Lynch, M., & Carter, C. (2006). Sorafenib blocks the RAF/MEK/ERK pathway, inhibits tumor angiogenesis, and induces tumor cell apoptosis in hepatocellular carcinoma model PLC/PRF/5. *Cancer Res, 66*(24), 11851-11858. doi:10.1158/0008-5472.CAN-06-1377

Llovet, J. M. (2014). Focal gains of VEGFA: candidate predictors of sorafenib response in hepatocellular carcinoma. *Cancer Cell, 25*(5), 560-562. doi:10.1016/j.ccr.2014.04.019

Llovet, J. M., Ricci, S., Mazzaferro, V., Hilgard, P., Gane, E., Blanc, J. F., de Oliveira, A. C., Santoro, A., Raoul, J. L., Forner, A., Schwartz, M., Porta, C., Zeuzem, S., Bolondi, L., Greten, T. F., Galle, P. R., Seitz, J. F., Borbath, I., Haussinger, D., Giannaris, T., Shan, M., Moscovici, M., Voliotis, D., Bruix, J., & Group, S. I. S. (2008). Sorafenib in advanced hepatocellular carcinoma. *N Engl J Med, 359*(4), 378-390. doi:10.1056/NEJMoa0708857

Loo, D. T., Fuquay, J. I., Rawson, C. L., & Barnes, D. W. (1987). Extended culture of mouse embryo cells without senescence: inhibition by serum. *Science, 236*(4798), 200-202.

Lowe, S. W., Cepero, E., & Evan, G. (2004). Intrinsic tumour suppression. *Nature, 432*(7015), 307-315. doi:10.1038/nature03098

Lowe, S. W., & Lin, A. W. (2000). Apoptosis in cancer. *Carcinogenesis, 21*(3), 485-495.

Lu, R., Wang, H., Liang, Z., Ku, L., O'Donnell W, T., Li, W., Warren, S. T., & Feng, Y. (2004). The fragile X protein controls microtubule-associated protein 1B translation and microtubule stability in brain neuron development. *Proc Natl Acad Sci U S A, 101*(42), 15201-15206. doi:10.1073/pnas.0404995101

Luo, M., & Fu, L. W. (2014). Redundant kinase activation and resistance of EGFR-tyrosine kinase inhibitors. *Am J Cancer Res, 4*(6), 608-628.

Ma, L., Chua, M. S., Andrisani, O., & So, S. (2014). Epigenetics in hepatocellular carcinoma: an update and future therapy perspectives. *World J Gastroenterol, 20*(2), 333-345. doi:10.3748/wjg.v20.i2.333

Maheswaran, T., & Rushbrook, S. M. (2012). Epithelial-mesenchymal transition and the liver: role in hepatocellular carcinoma and liver fibrosis. *J Gastroenterol Hepatol, 27*(3), 418-420. doi:10.1111/j.1440-1746.2012.07060.x

Marom, M., Haklai, R., Ben-Baruch, G., Marciano, D., Egozi, Y., & Kloog, Y. (1995). Selective inhibition of Ras-dependent cell growth by farnesylthiosalisylic acid. *J Biol Chem, 270*(38), 22263-22270.

Mathon, N. F., Malcolm, D. S., Harrisingh, M. C., Cheng, L., & Lloyd, A. C. (2001). Lack of replicative senescence in normal rodent glia. *Science, 291*(5505), 872-875. doi:10.1126/science.1056782

McKay, M. M., & Morrison, D. K. (2007). Integrating signals from RTKs to ERK/MAPK. *Oncogene, 26*(22), 3113-3121. doi:10.1038/sj.onc.1210394

McMahon, L. P., Yue, W., Santen, R. J., & Lawrence, J. C., Jr. (2005). Farnesylthiosalicylic acid inhibits mammalian target of rapamycin (mTOR) activity both in cells and in vitro by promoting dissociation of the mTOR-raptor complex. *Mol Endocrinol, 19*(1), 175-183. doi:10.1210/me.2004-0305

Medjkane, S., Perez-Sanchez, C., Gaggioli, C., Sahai, E., & Treisman, R. (2009). Myocardin-related transcription factors and SRF are required for cytoskeletal dynamics and experimental metastasis. *Nat Cell Biol, 11*(3), 257-268. doi:10.1038/ncb1833

Michaloglou, C., Vredeveld, L. C., Soengas, M. S., Denoyelle, C., Kuilman, T., van der Horst, C. M., Majoor, D. M., Shay, J. W., Mooi, W. J., & Peeper, D. S. (2005). BRAFE600-

associated senescence-like cell cycle arrest of human naevi. *Nature, 436*(7051), 720-724. doi:10.1038/nature03890

Miralles, F., Posern, G., Zaromytidou, A. I., & Treisman, R. (2003). Actin dynamics control SRF activity by regulation of its coactivator MAL. *Cell, 113*(3), 329-342.

Montagut, C., & Settleman, J. (2009). Targeting the RAF-MEK-ERK pathway in cancer therapy. *Cancer Lett, 283*(2), 125-134. doi:10.1016/j.canlet.2009.01.022

Morita, T., Mayanagi, T., & Sobue, K. (2007). Dual roles of myocardin-related transcription factors in epithelial mesenchymal transition via slug induction and actin remodeling. *J Cell Biol, 179*(5), 1027-1042. doi:10.1083/jcb.200708174

Muehlich, S., Cicha, I., Garlichs, C. D., Krueger, B., Posern, G., & Goppelt-Struebe, M. (2007). Actin-dependent regulation of connective tissue growth factor. *Am J Physiol Cell Physiol, 292*(5), C1732-1738. doi:10.1152/ajpcell.00552.2006

Muehlich, S., Hampl, V., Khalid, S., Singer, S., Frank, N., Breuhahn, K., Gudermann, T., & Prywes, R. (2012). The transcriptional coactivators megakaryoblastic leukemia 1/2 mediate the effects of loss of the tumor suppressor deleted in liver cancer 1. *Oncogene, 31*(35), 3913-3923. doi:10.1038/onc.2011.560

Muehlich, S., Rehm, M., Ebenau, A., & Goppelt-Struebe, M. (2017). Synergistic induction of CTGF by cytochalasin D and TGFbeta-1 in primary human renal epithelial cells: Role of transcriptional regulators MKL1, YAP/TAZ and Smad2/3. *Cell Signal, 29*, 31-40. doi:10.1016/j.cellsig.2016.10.002

Muehlich, S., Schneider, N., Hinkmann, F., Garlichs, C. D., & Goppelt-Struebe, M. (2004). Induction of connective tissue growth factor (CTGF) in human endothelial cells by lysophosphatidic acid, sphingosine-1-phosphate, and platelets. *Atherosclerosis, 175*(2), 261-268. doi:10.1016/j.atherosclerosis.2004.04.011

Muehlich, S., Wang, R., Lee, S. M., Lewis, T. C., Dai, C., & Prywes, R. (2008). Serum-induced phosphorylation of the serum response factor coactivator MKL1 by the extracellular signal-regulated kinase 1/2 pathway inhibits its nuclear localization. *Mol Cell Biol, 28*(20), 6302-6313. doi:10.1128/MCB.00427-08

Murphy, E. V., Zhang, Y., Zhu, W., & Biggs, J. (1995). The human glioma pathogenesis-related protein is structurally related to plant pathogenesis-related proteins and its gene is expressed specifically in brain tumors. *Gene, 159*(1), 131-135.

Nakamura, H., Aoki, H., Hino, O., & Moriyama, M. (2011). HCV core protein promotes heparin binding EGF-like growth factor expression and activates Akt. *Hepatol Res, 41*(5), 455-462. doi:10.1111/j.1872-034X.2011.00792.x

Niu, Z., Li, A., Zhang, S. X., & Schwartz, R. J. (2007). Serum response factor micromanaging cardiogenesis. *Curr Opin Cell Biol, 19*(6), 618-627. doi:10.1016/j.ceb.2007.09.013

O'Connor, R., Clynes, M., Dowling, P., O'Donovan, N., & O'Driscoll, L. (2007). Drug resistance in cancer - searching for mechanisms, markers and therapeutic agents. *Expert Opin Drug Metab Toxicol, 3*(6), 805-817. doi:10.1517/17425255.3.6.805

O'Neil, B. H., Goff, L. W., Kauh, J. S., Strosberg, J. R., Bekaii-Saab, T. S., Lee, R. M., Kazi, A., Moore, D. T., Learoyd, M., Lush, R. M., Sebti, S. M., & Sullivan, D. M. (2011). Phase II study of the mitogen-activated protein kinase 1/2 inhibitor selumetinib in patients with advanced hepatocellular carcinoma. *J Clin Oncol, 29*(17), 2350-2356. doi:10.1200/JCO.2010.33.9432

Oh, J., Richardson, J. A., & Olson, E. N. (2005). Requirement of myocardin-related transcription factor-B for remodeling of branchial arch arteries and smooth muscle differentiation. *Proc Natl Acad Sci U S A, 102*(42), 15122-15127. doi:10.1073/pnas.0507346102

Ohrnberger, S., Thavamani, A., Braeuning, A., Lipka, D. B., Kirilov, M., Geffers, R., Autenrieth, S. E., Romer, M., Zell, A., Bonin, M., Schwarz, M., Schutz, G., Schirmacher, P., Plass, C., Longerich, T., & Nordheim, A. (2015). Dysregulated serum response factor triggers formation of hepatocellular carcinoma. *Hepatology, 61*(3), 979-989. doi:10.1002/hep.27539

Ohtani, N., & Hara, E. (2013). Roles and mechanisms of cellular senescence in regulation of tissue homeostasis. *Cancer Sci, 104*(5), 525-530. doi:10.1111/cas.12118

Olson, E. N., & Nordheim, A. (2010). Linking actin dynamics and gene transcription to drive cellular motile functions. *Nat Rev Mol Cell Biol, 11*(5), 353-365. doi:10.1038/nrm2890

Packer, L., & Fuehr, K. (1977). Low oxygen concentration extends the lifespan of cultured human diploid cells. *Nature, 267*(5610), 423-425.

Park, M. Y., Kim, K. R., Park, H. S., Park, B. H., Choi, H. N., Jang, K. Y., Chung, M. J., Kang, M. J., Lee, D. G., & Moon, W. S. (2007). Expression of the serum response factor in hepatocellular carcinoma: implications for epithelial-mesenchymal transition. *Int J Oncol, 31*(6), 1309-1315.

Parrinello, S., Samper, E., Krtolica, A., Goldstein, J., Melov, S., & Campisi, J. (2003). Oxygen sensitivity severely limits the replicative lifespan of murine fibroblasts. *Nat Cell Biol, 5*(8), 741-747. doi:10.1038/ncb1024

Peeper, D. S., van der Eb, A. J., & Zantema, A. (1994). The G1/S cell-cycle checkpoint in eukaryotic cells. *Biochim Biophys Acta, 1198*(2-3), 215-230.

Pellegrini, L., Tan, S., & Richmond, T. J. (1995). Structure of serum response factor core bound to DNA. *Nature, 376*(6540), 490-498. doi:10.1038/376490a0

Pipes, G. C., Creemers, E. E., & Olson, E. N. (2006). The myocardin family of transcriptional coactivators: versatile regulators of cell growth, migration, and myogenesis. *Genes Dev, 20*(12), 1545-1556. doi:10.1101/gad.1428006

Ponten, F., Jirstrom, K., & Uhlen, M. (2008). The Human Protein Atlas--a tool for pathology. *J Pathol, 216*(4), 387-393. doi:10.1002/path.2440

Posern, G., Miralles, F., Guettler, S., & Treisman, R. (2004). Mutant actins that stabilise F-actin use distinct mechanisms to activate the SRF coactivator MAL. *EMBO J, 23*(20), 3973-3983. doi:10.1038/sj.emboj.7600404

Posern, G., & Treisman, R. (2006). Actin' together: serum response factor, its cofactors and the link to signal transduction. *Trends Cell Biol, 16*(11), 588-596. doi:10.1016/j.tcb.2006.09.008

Prete, S. D., Montella, L., Caraglia, M., Maiorino, L., Cennamo, G., Montesarchio, V., Piai, G., Febbraro, A., Tarantino, L., Capasso, E., Palmieri, G., Guarrasi, R., Bianco, M., Mamone, R., Savastano, C., Pisano, A., Vincenzi, B., Sabia, A., D'Agostino, A., Faiola, V., & Addeo, R. (2010). Sorafenib plus octreotide is an effective and safe treatment in advanced hepatocellular carcinoma: multicenter phase II So.LAR. study. *Cancer Chemother Pharmacol, 66*(5), 837-844. doi:10.1007/s00280-009-1226-z

Prowse, K. R., & Greider, C. W. (1995). Developmental and tissue-specific regulation of mouse telomerase and telomere length. *Proc Natl Acad Sci U S A, 92*(11), 4818-4822.

Psichari, E., Balmain, A., Plows, D., Zoumpourlis, V., & Pintzas, A. (2002). High activity of serum response factor in the mesenchymal transition of epithelial tumor cells is regulated by RhoA signaling. *J Biol Chem, 277*(33), 29490-29495. doi:10.1074/jbc.M112368200

Quan-Jun, Y., Yan, H., Yong-Long, H., Li-Li, W., Jie, L., Jin-Lu, H., Jin, L., Peng-Guo, C., Run, G., & Cheng, G. (2017). Selumetinib Attenuates Skeletal Muscle Wasting in

Murine Cachexia Model through ERK Inhibition and AKT Activation. *Mol Cancer Ther, 16*(2), 334-343. doi:10.1158/1535-7163.MCT-16-0324

Ramirez, R. D., Morales, C. P., Herbert, B. S., Rohde, J. M., Passons, C., Shay, J. W., & Wright, W. E. (2001). Putative telomere-independent mechanisms of replicative aging reflect inadequate growth conditions. *Genes Dev, 15*(4), 398-403. doi:10.1101/gad.859201

Reeves, H. L., Zaki, M. Y., & Day, C. P. (2016). Hepatocellular Carcinoma in Obesity, Type 2 Diabetes, and NAFLD. *Dig Dis Sci, 61*(5), 1234-1245. doi:10.1007/s10620-016-4085-6

Ren, C., Li, L., Goltsov, A. A., Timme, T. L., Tahir, S. A., Wang, J., Garza, L., Chinault, A. C., & Thompson, T. C. (2002). mRTVP-1, a novel p53 target gene with proapoptotic activities. *Mol Cell Biol, 22*(10), 3345-3357.

Ren, C., Li, L., Yang, G., Timme, T. L., Goltsov, A., Ren, C., Ji, X., Addai, J., Luo, H., Ittmann, M. M., & Thompson, T. C. (2004). RTVP-1, a tumor suppressor inactivated by methylation in prostate cancer. *Cancer Res, 64*(3), 969-976.

Ren, C., Ren, C. H., Li, L., Goltsov, A. A., & Thompson, T. C. (2006). Identification and characterization of RTVP1/GLIPR1-like genes, a novel p53 target gene cluster. *Genomics, 88*(2), 163-172. doi:10.1016/j.ygeno.2006.03.021

Reschke, M., Ferby, I., Stepniak, E., Seitzer, N., Horst, D., Wagner, E. F., & Ullrich, A. (2010). Mitogen-inducible gene-6 is a negative regulator of epidermal growth factor receptor signaling in hepatocytes and human hepatocellular carcinoma. *Hepatology, 51*(4), 1383-1390. doi:10.1002/hep.23428

Rodier, F., & Campisi, J. (2011). Four faces of cellular senescence. *J Cell Biol, 192*(4), 547-556. doi:10.1083/jcb.201009094

Ruas, M., & Peters, G. (1998). The p16INK4a/CDKN2A tumor suppressor and its relatives. *Biochim Biophys Acta, 1378*(2), F115-177.

Santoro, A., Simonelli, M., Rodriguez-Lope, C., Zucali, P., Camacho, L. H., Granito, A., Senzer, N., Rimassa, L., Abbadessa, G., Schwartz, B., Lamar, M., Savage, R. E., & Bruix, J. (2013). A Phase-1b study of tivantinib (ARQ 197) in adult patients with hepatocellular carcinoma and cirrhosis. *Br J Cancer, 108*(1), 21-24. doi:10.1038/bjc.2012.556

Sasaki, A., Masuda, Y., Ohta, Y., Ikeda, K., & Watanabe, K. (2001). Filamin associates with Smads and regulates transforming growth factor-beta signaling. *J Biol Chem, 276*(21), 17871-17877. doi:10.1074/jbc.M008422200

Sasaki, Y., Yamamura, H., Kawakami, Y., Yamada, T., Hiratsuka, M., Kameyama, M., Ohigashi, H., Ishikawa, O., Imaoka, S., Ishiguro, S., & Takahashi, K. (2002). Expression of smooth muscle calponin in tumor vessels of human hepatocellular carcinoma and its possible association with prognosis. *Cancer, 94*(6), 1777-1786.

Schmitz, K. J., Wohlschlaeger, J., Lang, H., Sotiropoulos, G. C., Malago, M., Steveling, K., Reis, H., Cicinnati, V. R., Schmid, K. W., & Baba, H. A. (2008). Activation of the ERK and AKT signalling pathway predicts poor prognosis in hepatocellular carcinoma and ERK activation in cancer tissue is associated with hepatitis C virus infection. *J Hepatol, 48*(1), 83-90. doi:10.1016/j.jhep.2007.08.018

Schneider-Merck, T., Borbath, I., Charette, N., De Saeger, C., Abarca, J., Leclercq, I., Horsmans, Y., & Starkel, P. (2009). The Ras inhibitor farnesylthiosalicyclic acid (FTS) prevents nodule formation and development of preneoplastic foci of altered hepatocytes in rats. *Eur J Cancer, 45*(11), 2050-2060. doi:10.1016/j.ejca.2009.04.014

Selvaraj, A., & Prywes, R. (2003). Megakaryoblastic leukemia-1/2, a transcriptional co-activator of serum response factor, is required for skeletal myogenic differentiation. *J Biol Chem, 278*(43), 41977-41987. doi:10.1074/jbc.M305679200

Serrano, M., Lin, A. W., McCurrach, M. E., Beach, D., & Lowe, S. W. (1997). Oncogenic ras provokes premature cell senescence associated with accumulation of p53 and p16INK4a. *Cell, 88*(5), 593-602.

Sharma, A., Yu, C., Leung, C., Trane, A., Lau, M., Utokaparch, S., Shaheen, F., Sheibani, N., & Bernatchez, P. (2010). A new role for the muscle repair protein dysferlin in endothelial cell adhesion and angiogenesis. *Arterioscler Thromb Vasc Biol, 30*(11), 2196-2204. doi:10.1161/ATVBAHA.110.208108

Shaw, P. E., Schroter, H., & Nordheim, A. (1989). The ability of a ternary complex to form over the serum response element correlates with serum inducibility of the human c-fos promoter. *Cell, 56*(4), 563-572.

Shay, J. W., & Bacchetti, S. (1997). A survey of telomerase activity in human cancer. *Eur J Cancer, 33*(5), 787-791. doi:10.1016/S0959-8049(97)00062-2

Sherr, C. J., & DePinho, R. A. (2000). Cellular senescence: mitotic clock or culture shock? *Cell, 102*(4), 407-410.

Shore, P., & Sharrocks, A. D. (1995). The MADS-box family of transcription factors. *Eur J Biochem, 229*(1), 1-13.

Small, J. V., Stradal, T., Vignal, E., & Rottner, K. (2002). The lamellipodium: where motility begins. *Trends Cell Biol, 12*(3), 112-120.

Smart, E. J., Ying, Y. S., Mineo, C., & Anderson, R. G. (1995). A detergent-free method for purifying caveolae membrane from tissue culture cells. *Proc Natl Acad Sci U S A, 92*(22), 10104-10108.

Smith, E. C., Thon, J. N., Devine, M. T., Lin, S., Schulz, V. P., Guo, Y., Massaro, S. A., Halene, S., Gallagher, P., Italiano, J. E., Jr., & Krause, D. S. (2012). MKL1 and MKL2 play redundant and crucial roles in megakaryocyte maturation and platelet formation. *Blood, 120*(11), 2317-2329. doi:10.1182/blood-2012-04-420828

Somlyo, A. P., & Somlyo, A. V. (2003). Ca2+ sensitivity of smooth muscle and nonmuscle myosin II: modulated by G proteins, kinases, and myosin phosphatase. *Physiol Rev, 83*(4), 1325-1358. doi:10.1152/physrev.00023.2003

Sotiropoulos, A., Gineitis, D., Copeland, J., & Treisman, R. (1999). Signal-regulated activation of serum response factor is mediated by changes in actin dynamics. *Cell, 98*(2), 159-169.

Staus, D. P., Blaker, A. L., Taylor, J. M., & Mack, C. P. (2007). Diaphanous 1 and 2 regulate smooth muscle cell differentiation by activating the myocardin-related transcription factors. *Arterioscler Thromb Vasc Biol, 27*(3), 478-486. doi:10.1161/01.ATV.0000255559.77687.c1

Staus, D. P., Weise-Cross, L., Mangum, K. D., Medlin, M. D., Mangiante, L., Taylor, J. M., & Mack, C. P. (2014). Nuclear RhoA signaling regulates MRTF-dependent SMC-specific transcription. *Am J Physiol Heart Circ Physiol, 307*(3), H379-390. doi:10.1152/ajpheart.01002.2013

Stossel, T. P., Condeelis, J., Cooley, L., Hartwig, J. H., Noegel, A., Schleicher, M., & Shapiro, S. S. (2001). Filamins as integrators of cell mechanics and signalling. *Nat Rev Mol Cell Biol, 2*(2), 138-145. doi:10.1038/35052082

Sun, C., Wang, L., Huang, S., Heynen, G. J., Prahallad, A., Robert, C., Haanen, J., Blank, C., Wesseling, J., Willems, S. M., Zecchin, D., Hobor, S., Bajpe, P. K., Lieftink, C., Mateus, C., Vagner, S., Grernrum, W., Hofland, I., Schlicker, A., Wessels, L. F., Beijersbergen, R. L., Bardelli, A., Di Nicolantonio, F., Eggermont, A. M., & Bernards,

R. (2014). Reversible and adaptive resistance to BRAF(V600E) inhibition in melanoma. *Nature, 508*(7494), 118-122. doi:10.1038/nature13121

Sun, Q., Chen, G., Streb, J. W., Long, X., Yang, Y., Stoeckert, C. J., Jr., & Miano, J. M. (2006). Defining the mammalian CArGome. *Genome Res, 16*(2), 197-207. doi:10.1101/gr.4108706

Sun, Y., Boyd, K., Xu, W., Ma, J., Jackson, C. W., Fu, A., Shillingford, J. M., Robinson, G. W., Hennighausen, L., Hitzler, J. K., Ma, Z., & Morris, S. W. (2006a). Acute myeloid leukemia-associated Mkl1 (Mrtf-a) is a key regulator of mammary gland function. *Mol Cell Biol, 26*(15), 5809-5826. doi:10.1128/MCB.00024-06

Tahara, H., Sato, E., Noda, A., & Ide, T. (1995). Increase in expression level of p21sdi1/cip1/waf1 with increasing division age in both normal and SV40-transformed human fibroblasts. *Oncogene, 10*(5), 835-840.

Takeoka, M., Ehara, T., Sagara, J., Hashimoto, S., & Taniguchi, S. (2002). Calponin h1 induced a flattened morphology and suppressed the growth of human fibrosarcoma HT1080 cells. *Eur J Cancer, 38*(3), 436-442.

Tang, D. G., Tokumoto, Y. M., Apperly, J. A., Lloyd, A. C., & Raff, M. C. (2001). Lack of replicative senescence in cultured rat oligodendrocyte precursor cells. *Science, 291*(5505), 868-871. doi:10.1126/science.1056780

Tang, Z., Qin, L., Wang, X., Zhou, G., Liao, Y., Weng, Y., Jiang, X., Lin, Z., Liu, K., & Ye, S. (1998). Alterations of oncogenes, tumor suppressor genes and growth factors in hepatocellular carcinoma: with relation to tumor size and invasiveness. *Chin Med J (Engl), 111*(4), 313-318.

Thiery, J. P. (2002). Epithelial-mesenchymal transitions in tumour progression. *Nat Rev Cancer, 2*(6), 442-454. doi:10.1038/nrc822

Thompson, O., Moghraby, J. S., Ayscough, K. R., & Winder, S. J. (2012). Depletion of the actin bundling protein SM22/transgelin increases actin dynamics and enhances the tumourigenic phenotypes of cells. *BMC Cell Biol, 13*, 1. doi:10.1186/1471-2121-13-1

Treisman, R. (1986). Identification of a protein-binding site that mediates transcriptional response of the c-fos gene to serum factors. *Cell, 46*(4), 567-574.

Treisman, R. (1994). Ternary complex factors: growth factor regulated transcriptional activators. *Curr Opin Genet Dev, 4*(1), 96-101.

Treisman, R. (1995). Journey to the surface of the cell: Fos regulation and the SRE. *EMBO J, 14*(20), 4905-4913.

Trojan, J., Zangos, S., & Schnitzbauer, A. A. (2016). Diagnostics and Treatment of Hepatocellular Carcinoma in 2016: Standards and Developments. *Visc Med, 32*(2), 116-120. doi:10.1159/000445730

Turtoi, A., Blomme, A., Bellahcene, A., Gilles, C., Hennequiere, V., Peixoto, P., Bianchi, E., Noel, A., De Pauw, E., Lifrange, E., Delvenne, P., & Castronovo, V. (2013). Myoferlin is a key regulator of EGFR activity in breast cancer. *Cancer Res, 73*(17), 5438-5448. doi:10.1158/0008-5472.CAN-13-1142

Tymanskyj, S. R., Scales, T. M., & Gordon-Weeks, P. R. (2012). MAP1B enhances microtubule assembly rates and axon extension rates in developing neurons. *Mol Cell Neurosci, 49*(2), 110-119. doi:10.1016/j.mcn.2011.10.003

van der Flier, A., & Sonnenberg, A. (2001). Structural and functional aspects of filamins. *Biochim Biophys Acta, 1538*(2-3), 99-117.

van Malenstein, H., Dekervel, J., Verslype, C., Van Cutsem, E., Windmolders, P., Nevens, F., & van Pelt, J. (2013). Long-term exposure to sorafenib of liver cancer cells induces resistance with epithelial-to-mesenchymal transition, increased invasion and risk of rebound growth. *Cancer Lett, 329*(1), 74-83. doi:10.1016/j.canlet.2012.10.021

Vartiainen, M. K., Guettler, S., Larijani, B., & Treisman, R. (2007). Nuclear actin regulates dynamic subcellular localization and activity of the SRF cofactor MAL. *Science, 316*(5832), 1749-1752. doi:10.1126/science.1141084

Vidal, M., Liu, W. Q., Lenoir, C., Salzmann, J., Gresh, N., & Garbay, C. (2004). Design of peptoid analogue dimers and measure of their affinity for Grb2 SH3 domains. *Biochemistry, 43*(23), 7336-7344. doi:10.1021/bi030252n

Volakis, L. I., Li, R., Ackerman, W. E. t., Mihai, C., Bechel, M., Summerfield, T. L., Ahn, C. S., Powell, H. M., Zielinski, R., Rosol, T. J., Ghadiali, S. N., & Kniss, D. A. (2014). Loss of myoferlin redirects breast cancer cell motility towards collective migration. *PLoS One, 9*(2), e86110. doi:10.1371/journal.pone.0086110

Waldman, T., Kinzler, K. W., & Vogelstein, B. (1995). p21 is necessary for the p53-mediated G1 arrest in human cancer cells. *Cancer Res, 55*(22), 5187-5190.

Wang, D., Chang, P. S., Wang, Z., Sutherland, L., Richardson, J. A., Small, E., Krieg, P. A., & Olson, E. N. (2001). Activation of cardiac gene expression by myocardin, a transcriptional cofactor for serum response factor. *Cell, 105*(7), 851-862.

Wang, D. Z., Li, S., Hockemeyer, D., Sutherland, L., Wang, Z., Schratt, G., Richardson, J. A., Nordheim, A., & Olson, E. N. (2002). Potentiation of serum response factor activity by a family of myocardin-related transcription factors. *Proc Natl Acad Sci U S A, 99*(23), 14855-14860. doi:10.1073/pnas.222561499

Wang, D. Z., & Olson, E. N. (2004). Control of smooth muscle development by the myocardin family of transcriptional coactivators. *Curr Opin Genet Dev, 14*(5), 558-566. doi:10.1016/j.gde.2004.08.003

Wang, Y., Nie, H., Zhao, X., Qin, Y., & Gong, X. (2016). Bicyclol induces cell cycle arrest and autophagy in HepG2 human hepatocellular carcinoma cells through the PI3K/AKT and Ras/Raf/MEK/ERK pathways. *BMC Cancer, 16*(1), 742. doi:10.1186/s12885-016-2767-2

Wang, Z., Li, Y., Ahmad, A., Azmi, A. S., Kong, D., Banerjee, S., & Sarkar, F. H. (2010). Targeting miRNAs involved in cancer stem cell and EMT regulation: An emerging concept in overcoming drug resistance. *Drug Resist Updat, 13*(4-5), 109-118. doi:10.1016/j.drup.2010.07.001

Watanabe, N., Kato, T., Fujita, A., Ishizaki, T., & Narumiya, S. (1999). Cooperation between mDia1 and ROCK in Rho-induced actin reorganization. *Nat Cell Biol, 1*(3), 136-143. doi:10.1038/11056

Wei, S., Wei, S., & Sedivy, J. M. (1999). Expression of catalytically active telomerase does not prevent premature senescence caused by overexpression of oncogenic Ha-Ras in normal human fibroblasts. *Cancer Res, 59*(7), 1539-1543.

Weiler, T., Bashir, R., Anderson, L. V., Davison, K., Moss, J. A., Britton, S., Nylen, E., Keers, S., Vafiadaki, E., Greenberg, C. R., Bushby, C. R., & Wrogemann, K. (1999). Identical mutation in patients with limb girdle muscular dystrophy type 2B or Miyoshi myopathy suggests a role for modifier gene(s). *Hum Mol Genet, 8*(5), 871-877.

Weinberg, R. A. (1995). The retinoblastoma protein and cell cycle control. *Cell, 81*(3), 323-330.

Whitmarsh, A. J., Yang, S. H., Su, M. S., Sharrocks, A. D., & Davis, R. J. (1997). Role of p38 and JNK mitogen-activated protein kinases in the activation of ternary complex factors. *Mol Cell Biol, 17*(5), 2360-2371.

Wiesenauer, C. A., Yip-Schneider, M. T., Wang, Y., & Schmidt, C. M. (2004). Multiple anticancer effects of blocking MEK-ERK signaling in hepatocellular carcinoma. *J Am Coll Surg, 198*(3), 410-421. doi:10.1016/j.jamcollsurg.2003.10.004

Wilhelm, S., Carter, C., Lynch, M., Lowinger, T., Dumas, J., Smith, R. A., Schwartz, B., Simantov, R., & Kelley, S. (2006). Discovery and development of sorafenib: a multikinase inhibitor for treating cancer. *Nat Rev Drug Discov, 5*(10), 835-844. doi:10.1038/nrd2130

Wills, F. L., McCubbin, W. D., & Kay, C. M. (1994). Smooth muscle calponin-caltropin interaction: effect on biological activity and stability of calponin. *Biochemistry, 33*(18), 5562-5569.

Winder, S. J., Allen, B. G., Clement-Chomienne, O., & Walsh, M. P. (1998). Regulation of smooth muscle actin-myosin interaction and force by calponin. *Acta Physiol Scand, 164*(4), 415-426.

Winder, S. J., & Walsh, M. P. (1990). Smooth muscle calponin. Inhibition of actomyosin MgATPase and regulation by phosphorylation. *J Biol Chem, 265*(17), 10148-10155.

Winkles, J. A. (1998). Serum- and polypeptide growth factor-inducible gene expression in mouse fibroblasts. *Prog Nucleic Acid Res Mol Biol, 58*, 41-78.

Worns, M. A., Schuchmann, M., Duber, C., Otto, G., Galle, P. R., & Weinmann, A. (2010). Sunitinib in patients with advanced hepatocellular carcinoma after progression under sorafenib treatment. *Oncology, 79*(1-2), 85-92. doi:10.1159/000320363

Wright, W. E., Piatyszek, M. A., Rainey, W. E., Byrd, W., & Shay, J. W. (1996). Telomerase activity in human germline and embryonic tissues and cells. *Dev Genet, 18*(2), 173-179. doi:10.1002/(SICI)1520-6408(1996)18:2<173::AID-DVG10>3.0.CO;2-3

Wyllie, A. H., Kerr, J. F., & Currie, A. R. (1980). Cell death: the significance of apoptosis. *Int Rev Cytol, 68*, 251-306.

Wynford-Thomas, D. (1999). Cellular senescence and cancer. *J Pathol, 187*(1), 100-111. doi:10.1002/(SICI)1096-9896(199901)187:1<100::AID-PATH236>3.0.CO;2-T

Xiao, Y. H., Li, X. H., Tan, T., Liang, T., Yi, H., Li, M. Y., Zeng, G. Q., Wan, X. X., Qu, J. Q., He, Q. Y., Li, J. H., Chen, Y., & Xiao, Z. Q. (2011). Identification of GLIPR1 tumor suppressor as methylation-silenced gene in acute myeloid leukemia by microarray analysis. *J Cancer Res Clin Oncol, 137*(12), 1831-1840. doi:10.1007/s00432-011-1065-2

Yanagisawa, Y., Takeoka, M., Ehara, T., Itano, N., Miyagawa, S., & Taniguchi, S. (2008). Reduction of Calponin h1 expression in human colon cancer blood vessels. *Eur J Surg Oncol, 34*(5), 531-537. doi:10.1016/j.ejso.2007.05.010

Yang, N., Ekanem, N. R., Sakyi, C. A., & Ray, S. D. (2015). Hepatocellular carcinoma and microRNA: new perspectives on therapeutics and diagnostics. *Adv Drug Deliv Rev, 81*, 62-74. doi:10.1016/j.addr.2014.10.029

Yarmola, E. G., Somasundaram, T., Boring, T. A., Spector, I., & Bubb, M. R. (2000). Actin-latrunculin A structure and function. Differential modulation of actin-binding protein function by latrunculin A. *J Biol Chem, 275*(36), 28120-28127. doi:10.1074/jbc.M004253200

Young, A. P., Schlisio, S., Minamishima, Y. A., Zhang, Q., Li, L., Grisanzio, C., Signoretti, S., & Kaelin, W. G., Jr. (2008). VHL loss actuates a HIF-independent senescence programme mediated by Rb and p400. *Nat Cell Biol, 10*(3), 361-369. doi:10.1038/ncb1699

Yu, C., Sharma, A., Trane, A., Utokaparch, S., Leung, C., & Bernatchez, P. (2011). Myoferlin gene silencing decreases Tie-2 expression in vitro and angiogenesis in vivo. *Vascul Pharmacol, 55*(1-3), 26-33. doi:10.1016/j.vph.2011.04.001

Yu, H., Rosen, M. K., Shin, T. B., Seidel-Dugan, C., Brugge, J. S., & Schreiber, S. L. (1992). Solution structure of the SH3 domain of Src and identification of its ligand-binding site. *Science, 258*(5088), 1665-1668.

Yu, P., Ye, L., Wang, H., Du, G., Zhang, J., Zhang, J., & Tian, J. (2015). NSK-01105 inhibits proliferation and induces apoptosis of prostate cancer cells by blocking the Raf/MEK/ERK and PI3K/Akt/mTOR signal pathways. *Tumour Biol, 36*(3), 2143-2153. doi:10.1007/s13277-014-2824-x

Yuan, H., Kaneko, T., & Matsuo, M. (1995). Relevance of oxidative stress to the limited replicative capacity of cultured human diploid cells: the limit of cumulative population doublings increases under low concentrations of oxygen and decreases in response to aminotriazole. *Mech Ageing Dev, 81*(2-3), 159-168.

Yuan, Y., & Shen, Z. (2001). Interaction with BRCA2 suggests a role for filamin-1 (hsFLNa) in DNA damage response. *J Biol Chem, 276*(51), 48318-48324. doi:10.1074/jbc.M102557200

Zhai, B., & Sun, X. Y. (2013). Mechanisms of resistance to sorafenib and the corresponding strategies in hepatocellular carcinoma. *World J Hepatol, 5*(7), 345-352. doi:10.4254/wjh.v5.i7.345

Zhang, Z., Zhou, X., Shen, H., Wang, D., & Wang, Y. (2009). Phosphorylated ERK is a potential predictor of sensitivity to sorafenib when treating hepatocellular carcinoma: evidence from an in vitro study. *BMC Med, 7*, 41. doi:10.1186/1741-7015-7-41

Zhao, X. H., Laschinger, C., Arora, P., Szaszi, K., Kapus, A., & McCulloch, C. A. (2007). Force activates smooth muscle alpha-actin promoter activity through the Rho signaling pathway. *J Cell Sci, 120*(Pt 10), 1801-1809. doi:10.1242/jcs.001586

Zhu, J., Woods, D., McMahon, M., & Bishop, J. M. (1998). Senescence of human fibroblasts induced by oncogenic Raf. *Genes Dev, 12*(19), 2997-3007.

Zhu, X. F., Liu, Z. C., Xie, B. F., Li, Z. M., Feng, G. K., Yang, D., & Zeng, Y. X. (2001). EGFR tyrosine kinase inhibitor AG1478 inhibits cell proliferation and arrests cell cycle in nasopharyngeal carcinoma cells. *Cancer Lett, 169*(1), 27-32.

Zuo, Q., Huang, H., Shi, M., Zhang, F., Sun, J., Bin, J., Liao, Y., & Liao, W. (2012). Multivariate analysis of several molecular markers and clinicopathological features in postoperative prognosis of hepatocellular carcinoma. *Anat Rec (Hoboken), 295*(3), 423-431. doi:10.1002/ar.21531

II Abbreviation index

aa	amino acids
ActD	actinomycin D
APS	ammonium persulfate
ATP	adenosine triphosphate
bp	base pairs
BSA	bovine serum albumin
CaCl_2	calcium chloride
cDNA	complementary DNA
CDK	cyclin dependent kinase
ChIP	chromatin immunoprecipitation
CNN1	calponin 1
CO_2	carbon dioxide
CTGF	connective tissue growth factor
CXCL10	C-X-C motif chemokine 10
CytoD	cytochalasin D
DEPC	diethyl dicarbonate
DLC1	deleted in liver cancer 1
DMEM	Dulbecco's modified Eagle medium
DMF	*N*,*N*-dimethylformamide
DMSO	Dimethyl sulfoxide
DNA	deoxyribonucleic acid
dNTP	deoxynucleoside triphosphate
DTT	dithiothreitol
***E**.coli*	*Escherichia coli*
EBS	Ets binding site
ECL	enhanced chemiluminescence
ECM	extracellular matrix
EDTA	ethylenediaminetetraacetic acid
EGFR	epidermal growth factor receptor
EMT	epithelial-mesenchymal transition
ERK1/2	extracellular signal-related kinase 1/2

FACS	fluorescence activated cell sorting
F-actin	filamentous actin
FBS	fetal bovine serum
FDA	Food and Drug Administration
FER1L3	Fer-1-like protein 3 (synonym for myoferlin)
FHL2	four and a half LIM domains 2
FLNa	Filamin A
fw	forward
G-actin	globular actin
GAP	GTPase activating protein
GAPDH	glyceraldehyde 3-phosphate dehydrogenase
GDP	guanosine diphosphate
GEF	guanine nucleotide exchange factor
GFP	green fluorescent protein
GLIPR1	glioma pathogenesis-related protein 1
GRB2	growth factor receptor-bound protein 2
GTP	guanosine triphosphate
h	hour(s)
H_2O	water
HBS	HEPES buffered saline
HCC	hepatocellular carcinoma
HCl	hydrochloric acid
HEPES	4-(2-hydroxyethyl)-1-piperazineethanesulfonic acid
HRP	horseradish peroxidase
HSP90	heat shock protein 90
IEG	immediate early genes
IGFR	insulin growth factor receptor
Itga5	integrin alpha-5
JAK	Janus kinase
JNK	c-Jun N-terminal kinase
KCl	potassium chloride
kDa	kilo Dalton
KH_2PO_4	potassium dehydrogen phosphatase

LatB	latrunculin B
LiCl	lithium chloride
LLC	Lewis lung carcinoma
LPA	lysophosphatidic acid
LT cells	liver tumor cells
LZ	leucine zipper
M	molar
mA	milliampere
MADS-Box	MCM1, Agamous, Deficiens, SRF-Box
MAL	megakaryocytic acute leukemia
MAP	mitogen-activated protein
MAP1B	microtubule-associated protein 1B
MAPK	mitogen-activated protein kinase
MEF	mouse embryonic fibroblast
MEM	minimum essential medium
MET	mesenchymal-epithelial transition
mg	milligram
Mig6	mitogen-inducible gene 6
min	minute(s)
MKL1	megakaryoblastic Leukemia 1
MKL2	megakaryoblastic Leukemia 2
mL	milliliter
mM	millimolar
MMP	matrix metalloproteinase
MRTF-A	myocardin-related transcription factor A
MRTF-B	myocardin-related transcription factor B
MYH9	myosin heavy chain 9
MYL9	myosin light chain 9
MYOF	myoferlin
Na_2HPO_4	sodium hydrogen phosphate
NaCl	sodium chloride
NAFLD	non-alcoholic fatty liver disease
$NaHCO_3$	sodium hydrogen carbonate
NaOH	sodium hydroxide
NF1	neurofibromin 1
nm	nanometer

NPC	nasopharyngeal carcinoma
OIS	oncogene-induced senescence
PAGE	polyacrylamide gel electrophoresis
PBS	phosphate buffered saline
PCR	polymerase chain reaction
PDGFR	platelet derived growth factor receptor
pEGFR	phosphorylated epidermal growth factor receptor
PEI	polyethylenimine
pERK	phosphorylated extracellular signal-related kinase 1/2
PFA	paraformaldehyde
PI	protease inhibitor
PIPES	piperazine-N,N′-bis(2-ethanesulfonic acid)
PMSF	phenylmethylsulfonyl fluoride
pRb	phosphorylated retinoblastoma protein
PTEN	phosphatase and tensin homolog
PVDF	polyvinylidene fluoride
Ras	rat sarcoma
Rb	retinoblastoma protein
rev	reverse
RNA	ribonucleic acid
RNAi	RNA interference
rpm	rounds per minute
RPMI	Roswell Park Memorial Institute
rRNA	ribosomal RNA
RT	room temperature
RTK	receptor tyrosine kinase
RT-PCR	real-time polymerase chain reaction
SA-β-Gal	senescence-associated β-galactosidase
SAP	SAF-A/B, Acinus and Pias
SD	standard deviation
SDS	sodium dodecyl sulfate
sec	second(s)
shRNA	short hairpin ribonucleic acid
SIPS	stress-induced premature senescence

siRNA	small interfering ribonucleic acid
SM22	smooth muscle protein 22
SMA	smooth muscle actin
SMC	smooth muscle cell
SMS	senescence-messaging secretome
SOS	son of sevenless
SRE	serum response element
SRF	serum response factor
STAT	signal transducers and activators of transcription
TAD	transcription activation domain
TAGLN	smooth muscle protein 22 (synonym for SM22)
TBS	tris-buffered saline
TBS-T	tris-buffered saline with Tween 20
TCF	ternary complex factor
TEMED	N,N,N',N'-tetramethylethylenediamine
TGFβ1	transforming growth factor β1
TM	transmembrane
TNBC	triple-negative breast cancer
TNFSF10	tumor necrosis factor superfamily member 10
Tris	tris(hydroxymethyl)aminomethane
Tween 20	polysorbate 20
VEGFA	vascular endothelial growth factor A
VEGFR	vascular endothelial growth factor receptor
VGLL3	vestigial like 3
VHL	von Hippel-Lindau
v/v	volume to volume
wt	wildtype
X-Gal	5-bromo-4-chloro-3-indolyl-β-D-galactopyranoside
µg	microgram
µL	microliter
µM	micromolar

III Index of figures

IV Index of tables

V Publications

Parts of the results of this thesis are published in the following scientific peer-reviewed journals:

1. **Hermanns C**, Hampl V, Holzer K, Aigner A, Penkava J, Frank N, Martin DE, Maier KC, Waldburger N, Roessler S, Goppelt-Struebe M, Akrap I, Thavamani A, Singer S, Nordheim A, Gudermann T, Muehlich S.

   The novel MKL target gene myoferlin modulates expansion and senescence of hepatocallular carcinoma.
   Oncogene, 2017 Jun 15; 36 (24): 3464-3476. doi: 10.1038/onc.2016.496.

2. Muehlich S, **Hermanns C**, Meier MA, Kircher P, Gudermann T.

   Unravelling a new mechanism linking actin polymerization and gene transcription.
   Nucleus, 2016 Apr 25; 7 (2): 121-5. doi: 10.1080/19491034.2016.1171433.

3. Kircher P, **Hermanns C**, Nossek M, Drexler MK, Grosse R, Fischer M, Sarikas A, Penkava J, Lewis T, Prywes R, Gudermann T, Muehlich S.

   Filamin A interacts with the coactivator MKL1 to promote the activity of the transcription factor SRF and cell migration.
   Science Signaling, 2015 Nov 10; 8 (402): ra112. doi: 10.1126/ scisignal.aad2959.

Results of another project worked on in my PhD are published in the following journal:

4. Romagnani A, Vettore V, Rezzonico-Jost T, Hampe S, Rottoli E, Nadolni W, Perotti M, Meier MA, **Hermanns C**, Geiger S, Wennemuth G, Recordati C, Matsushita M, Muehlich S, Proietti M, Chubanov V, Gudermann T, Grassi F, Zierler S.

   The kinase activity of the TRPM7 channel-enzyme is essential for gut colonization by T cells and graft-versus-host reaction.
   Nature Communications, 2017 Dec 4; 8(1):1917. doi: 10.1038/s41467-017-01960-z.

Posters and talks

Parts of the results were presented at poster sessions or in short talks at the following congresses:

- **Hermanns C**, Hampl V, Aigner A, Singer S, Thavamani A, Nordheim A, Gudermann T, Muehlich S.

  The novel MKL target gene MYOF (myoferlin) modulates expansion and senescence of hepatocellular carcinoma.

  1. German Pharm-Tox Summit / 82. Annual Meeting of the German Society of Pharmacology and Toxicology, Berlin 2016

- **Hermanns C**, Hampl V, Aigner A, Frank N, Martin D, Maier K, Gudermann T, Muehlich S.

  Expression profiling of novel MKL target genes involved in HCC growth identifies Myoferlin as the mediator of the MKL-associated senescence response.

  81. Annual Meeting of the German Society of Pharmacology and Toxicology, Kiel 2015

- Kircher P, Nossek M, Drexler MK, Chinchilla P, Grosse R, **Hermanns C**, Lewis T, Prywes R, Gudermann T, Muehlich S.

  Filamin A interacts with Megakaryoblastic Leukemia 1 (MKL1) to regulate transcriptional activity of the Serum Response Factor (SRF) cofactor.

  80. Annual Meeting of the German Society of Pharmacology and Toxicology, Hannover 2014

VI Acknowledgements

First of all, I would like to thank Dr. Susanne Mühlich for giving me the opportunity to perform my PhD thesis in her group and for providing me this very interesting research topic. Many thanks for being a great scientific supervisor and for your enthusiastic encouragement, motivation and constant support with all the discussions!

I also want to thank Prof. Dr. Thomas Gudermann for being my doctor father and for all his ideas, nice suggestions and scientific input concerning my projects and doctoral thesis.

I am very thankful to PD Dr. Dietmar Martin for being my external representative of this thesis at the faculty of chemistry and pharmacy and for his great interest in my project and all the helpful advise, especially regarding the ChIP assay method.

Additionally, I would like to thank Prof. Dr. Karl-Klaus Conzelmann, Prof. Dr. Julian Stingele, Prof. Dr. Klaus Förstemann and Prof. Dr. Karl-Peter Hopfner for their willingness to be a member of my examination board.

Furthermore, I would like to thank all the previous and present members of my group, the Mühlich lab, for their nice support over the last years: especially Clara-Mae Beer for her technical support and all her help and assistance; Philipp Kircher, Melanie Meier, Katharina Wörther, Laura Schreyer, Josef Penkava and in particular Sandra Voringer for being nice colleagues and for the common coffee breaks and all the nice talks with scientific as well as non scientific topics… Thank you all for your helpfulness and the friendly and cheerful atmosphere in the lab!

My special gratitude goes to my family: I have to thank my parents for their great support and encouragement throughout the time of my PhD and the whole time of my life and also my sister for always supporting me. Thank you so much for always being there for me and making everything possible!

Last but not least, I am very thankful to Lorenz for thoroughly proofreading this thesis, his patience and everlasting support. Many thanks for making me laugh, for being there for me all the time and your love! I am really grateful for having you in my life!